

NOVEL APPROACH TO COAL LIQUEFACTION
UTILIZING HYDROGEN SULFIDE AND CARBON MONOXIDE

Mahmoud B. Abdel-Baset and Charles T. Ratcliffe

Allied Chemical Corporation, Corporate Research Center
P. O. Box 1021-R, Morristown, NJ 07960

INTRODUCTION

All coal liquefaction processes involve thermal cracking of weak bonds in coal to form radical fragments which are stabilized by abstracting hydrogen atoms from a donor solvent. The activity of the hydrogen donor solvent is maintained by further hydrogenation of a recycled fraction. Thus, the costs of hydrogen comprise a major expense in any liquefaction process especially if pure H_2 is used. Hydrogen sulfide, a by-product of a negative value from the cleaning of natural gas, crude oil or coal, has been demonstrated to be a potential hydrogen source for a few chemical processes, such as selective reduction of NO_x to hydroxyl amine [1] and reduction of nitroaromatics to amines [2]. The effect of H_2S on coal liquefaction in the presence of hydrogen donor solvents and under H_2 atmosphere has been reported to increase the coal conversion to soluble products [3,4]. Hydrogen sulfide in these latter cases was not the main source of hydrogen but acted as a promoter in the presence of hydrogen donors and elemental H_2 . In order to utilize the inherent hydrogen value of hydrogen sulfide, we studied the effect of H_2S and CO on coal liquefaction in the absence of other hydrogen sources. A more detailed study of this chemistry was achieved by the use of coal tar, a material that contains many of the basic structural features of coal itself. The objective of this study has been to utilize low grade industrial hydrogen streams, particularly those produced via coal gasification which contain a large variety of impurities including H_2S , CO, CO_2 , COS and NH_3 . Utilization of the H_2S/CO from such dirty streams in the first stage of coal liquefaction will alleviate a number of expensive process steps in the cleaning of syngas.

EXPERIMENTAL

1. The coal liquefaction experiments were carried out in a 316 SS, 300 mL Magnedrive, packless, stirred autoclave (Autoclave Engineer, Inc.), fitted with a 1200 watt heating jacket. The coal was pulverized to -60 mesh and dried under nitrogen in a vacuum oven at 100°C. The coal sample (20 g), solvent (80 g of 1-methylnaphthalene or tetralin) and a catalyst (2 g), if required, were charged into the autoclave. The autoclave was flushed and pressure tested with nitrogen, then charged with 1655 kPa of H_2S (about 4.5 g) and to 6894 kPa with CO. The reaction was carried out at 400°C for 2 hours while stirring, then quenched utilizing a cold water cooling coil. The contents of the reactor were transferred into an extraction thimble and extracted with ethyl acetate for 24 hours. The thimble was dried in a vacuum oven and the weight of the residue

was determined. Conversion is defined as the percentage of the organic matter in coal that was converted to ethyl acetate-solubles and gases on a dry ash-free basis. The extract was stripped of ethyl acetate and the asphaltenes were precipitated by adding 800 mL of pentane. The sulfur contents of the asphaltenes were determined by Eschka method (ASTM D-271).

2. Coal tar treatment with H_2S and CO was carried out in the same manner as the coal liquefaction but without any solvents to avoid complications with the analytical procedure. Coal tar (80 g) was mixed with 5% presulfided Harshaw HT-400E catalyst ($Co-Mo-\gamma Al_2O_3$) and loaded into the autoclave prior to charging with H_2S (1655 kPa) and CO (6894 kPa). The autoclave was then heated at 400°C for 2 hours while stirring. Small aliquots of the product mixture were dissolved in $CDCl_3$, filtered, then subjected to both 1H -nmr and ^{13}C -nmr analysis. One experiment was carried out using 60% enriched ^{13}CO in a microreactor consisting of a 30 mL stainless steel vessel (Hoke) connected to a manifold and fitted with a magnetic stirrer and a heating jacket. The reaction was carried out at 350°C, 1655 kPa of H_2S and 5515 kPa of ^{13}CO for 6 hours. The contents of the vessel were extracted with $CDCl_3$, filtered and subjected to ^{13}C nmr. During the course of the coal tar treatment any hydrogen-containing solvents were carefully excluded.

3. Catalyst Preparation. A commercial sample of 13% MoO_3 and 3% CoO on γ -alumina was obtained from The Harshaw Chemical Company, Beachwood, Ohio. The pellets were ground to -60 mesh, heated to 500°C in a nitrogen stream, and then sulfided at 400°C with a 40% stream of H_2S in N_2 for one hour.

RESULTS

Utilization of the waste components from a coal cleaning process in the liquefaction of coal can only be achieved if H_2S , with other components, hydrogenates or serves as a radical trap during coal pyrolysis. The inherent hydrogen in hydrogen sulfide has now been shown to be capable of supplying the main source of hydrogen necessary for coal liquefaction. The coals were dried to avoid water that may act as a hydrogen source through the water-gas shift reaction. 1-Methylnaphthalene was used as a non-hydrogen donor dispersing medium. Catalysts used with certain runs were sulfided samples of $Co-Mo$ on $\gamma-Al_2O_3$ (Harshaw HT-400E). Liquefaction results of Illinois No. 6 Dean Mitchell coal are shown in Table 1. A comparison of the blank run in which coal was heated in 1-methylnaphthalene under nitrogen at 400°C and with H_2S treatment showed slight increase in conversion to ethyl acetate soluble products of 18% vs. 12.5% for the blank run indicating partial liquefaction using only H_2S . The sulfur content of the asphaltene fraction increased from 3.36% for the reaction under nitrogen to 6.34% when H_2S was used. The use of a mixture of H_2S and CO caused a threefold increase in conversion from 12.5% (Run 1) to 38.2% (Run 3). Sulfur content showed only a slight increase from 3.36% to 4.33%. Although the use of catalysts such as

sulfided Co-Mo on γ - Al_2O_3 (Run 4) or ammonium molybdate (impregnated on the coal, Run 5) did not cause significant change in conversion, it did decrease the sulfur content slightly. When a large excess of H_2S was used with the same amount of CO, a higher conversion was achieved with a slight increase in the sulfur content (Run 7).

Liquefaction of coal has been studied with mixtures of CO and H_2O by several groups with the main effort now involved in the COSTEAM process [5]. A comparison of $\text{H}_2\text{S}/\text{CO}$ versus $\text{H}_2\text{O}/\text{CO}$ was carried out. In the absence of a hydrogen donor solvent, $\text{H}_2\text{S}/\text{CO}$ was found to be more effective for coal liquefaction (38.2%) than $\text{H}_2\text{O}/\text{CO}$ (28%) under the same conditions (Runs 3 and 8).

The results of liquefying Illinois No. 6 Delta Mine coal in the presence of either an inert solvent (1-methylnaphthalene) or a hydrogen donor solvent (tetralin) are shown in Table 2. In agreement with previous data, the liquefaction in the presence of H_2S and CO in an inert solvent increased the conversion to 59.5% (Run 10) relative to a blank experiment (38.5% conversion, Run 9). The use of catalyst did not influence the conversion or the sulfur content. This indicated that the reaction of $\text{H}_2\text{S}/\text{CO}$ was either noncatalytic or catalyzed by the inorganic minerals in coal. The use of a hydrogen donor solvent gave a higher conversion and slightly lower sulfur content than the use of an inert solvent (Run 12 vs. Run 9). Furthermore, the use of $\text{H}_2\text{S}/\text{CO}$ enhanced the coal liquefaction in the presence of a hydrogen donor as evident from the results in Table 2.

Coal tar was used as a coal-like material in order to examine the nature of $\text{H}_2\text{S}/\text{CO}$ interaction on coal linkages. Although we do not imply that coal tar is a model for coal, it does contain many of the structural components in the original coal and has the added advantage of greater solubility in chloroform.

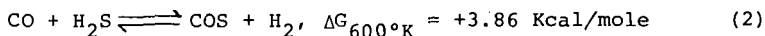
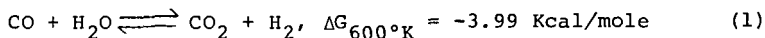
Coal tar samples were treated with $\text{H}_2\text{S}/\text{CO}$ in the presence of sulfided Co-Mo on Al_2O_3 catalysts under similar liquefaction conditions. Both ^1H and ^{13}C -nmr were used to evaluate the gross change in hydrogen and carbon distribution in coal tar as a result of $\text{H}_2\text{S}/\text{CO}$ treatment. Examination of the results in Table 3 demonstrated a substantial increase in the content of the aliphatic protons from 5.3% for the tar heated under nitrogen to 15.9% for the tar treated with $\text{H}_2\text{S}/\text{CO}$. A similar increase in the aliphatic carbon content from 4.4% to 6.6% was observed. The ^1H -nmr spectra of both nitrogen- and $\text{H}_2\text{S}/\text{CO}$ -treated coal indicated that the major change in the aliphatic hydrogen was due to functional aryl-methyl groups (singlets at δ 2.33-2.5 ppm) and the generation of ethylenic linkages between aromatic rings (singlets at δ 3.3 ppm) such as acenaphthene or dihydrophenanthrene structures. The appearance of aryl-methyl groups was quite intriguing since it indicated the possibility of methylating coal tar or coal using a mixture of $\text{H}_2\text{S}/\text{CO}$. The ^{13}C -nmr has substantiated this observation by indicating the appearance of singlet peaks around δ 22.0 and 30.3 ppm due to aryl-methyl and dihydrophenanthrene structures. The use of ^{13}CO and H_2S clearly showed the incorporation of $^{13}\text{CH}_3$ groups

as evident from the substantial increase in the aliphatic carbon₃ from 6.6% to 12.1% when CO or ¹³CO was used respectively. The ¹³C-nmr also indicated a major increase in the region of δ18.5-22 ppm indicative of aryl-methyl groups as a result of treating coal tar with ¹³CO/H₂S.

DISCUSSION

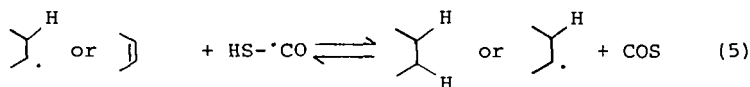
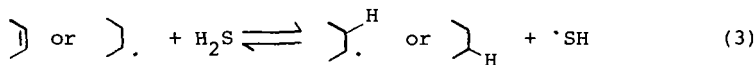
The above results show that the presence of CO with H₂S is required to achieve substantial hydrogenation and/or methylation of coal with H₂S. Hydrogen transfer to coal may involve nascent hydrogen or other similar intermediates that have been considered in CO/H₂O reduction of coal. The weaker bond energy of H-S bonds in H₂S versus H-O bonds in H₂O undoubtedly provides one advantage for hydrogen transfer from H₂S. One must also consider a shift type reaction which can occur with H₂S/CO over sulfided catalysts to produce elemental H₂ [6].

While H₂S has a much lower heat of formation than water, a shift reaction for H₂S/CO is highly unfavorable as compared to the shift reaction for H₂O/CO.



A more likely mechanism for hydrogen transfer involves splitting of H₂S to give a hydrogen atom or abstraction of hydrogen atom from H₂S by the coal radical fragments followed by trapping the thiyl radical with CO to form a thioformyl radical. The latter is a better hydrogen donor than H₂S itself resulting in the formation of COS.

Scheme I



The ability of H₂S/CO to methylate aromatics only in the presence of a sulfided catalyst surface may also involve a thioformyl intermediate. We currently feel that thioformyl cations or radicals on an active metal sulfide surface attack aromatic rings which are electron rich. Subsequent hydrogenation of the thioformyl group appears to lead to the aryl-methyl product in a coal or coal tar. While methylation with H₂S/CO probably bears

resemblance to the formate mechanisms proposed earlier by Friedman, et al [7], further investigation of this area is necessary to make any accurate conclusions.

CONCLUSIONS

This investigation has shown that treatment of coal with a mixture of H₂S and CO allows the liquefaction of coal to an ethyl acetate soluble material. The interaction of H₂S/CO with coal results in both hydrogenation and methylation of coal fragments. While the mechanism has not been fully established, the ability of this reagent to solubilize coal in the absence of hydrogen and/or a donor solvent will allow reduction in the raw material cost of hydrogen in future liquefaction processes.

ACKNOWLEDGMENTS

The authors wish to acknowledge Mr. F. Worden for technical assistance and Mr. G. Babbitt for nmr analysis. We also acknowledge Professor M.J.S. Dewar for valuable discussions.

REFERENCES

1. C.T. Ratcliffe, U.S. Patent No. 4,115,523 (1979).
2. C.T. Ratcliffe and Geza Pap, submitted to J.C.S. Chem. Commun.
3. J.G. Gatsis, U.S. Patent No. 3,503,863 (1970).
4. R. Bearden, Jr. and C.L. Aldridge, U.S. Patents Nos. 4,077,867 (1978), 4,094,765 (1978) and 4,149,959 (1979).
5. H.R. Appell, E.C. Moroni and R.D. Miller, ACS Fuel Chem. Div. Preprints, Vol. 20, No. 1, 58 (1975).
6. K. Fukuda, M. Dokiya, T. Kameyama and Y. Kotera, J. Catal., 49, 379 (1977).
7. S. Friedman, H.H. Ginsberg, I. Wender and P.M. Yavorsky, "Continuous Processing of Urban Refuse to Oil Utilizing Carbon Monoxide"; The 3rd Mineral Waste Utilization Symposium, IIT, Chicago, IL, March 14-16, 1972.

TABLE 1. Dean Mitchell Coal Solubilization with H₂S, CO at 400°C for 2 hours

Run	Solvent	Reactants, Catalyst	Conversion (% daf)	Sulfur ^(a)
1	1-methylnaphthalene	N ₂	12.5	3.36
2	"	H ₂ S/N ₂	18.0	6.34
3	"	H ₂ S/CO	38.2	4.33
4	"	H ₂ S/CO, Co/Mo ^(b)	37.1	3.86
5	"	H ₂ S/CO, (NH ₄) ₂ MoO ₄ ^(c)	41.8	3.92
6	"	H ₂ S/CO, Co/Mo/K ₂ CO ₃ ^(b)	32.5	4.4
7	"	H ₂ S(25 g)/CO, Co/Mo ^(b)	46.6	4.85
8	"	H ₂ O/CO ^(d)	28.0	4.03

(a) Total sulfur in asphaltene.

(b) Sulfided Harshaw HT-400E. 3% Co, 12% Mo oxides on Al₂O₃.

(c) Wet impregnated on the coal followed by vacuum drying.

(d) H₂O quantity was 2.4 g, to provide same molar quantity as 4.25 g of H₂S. Pressure at ambient temperature was brought to 6894 kPa with CO.

TABLE 2. Delta Mine, Illinois No. 6 Coal Solubilization at 400°C for 2 hours

Run	Solvent	Reactants, Catalyst	Conversion (% daf)	Sulfur ^(a)
9	1-methylnaphthalene	N ₂	38.5	2.73
10	"	H ₂ S/CO	59.5	2.78
11	"	H ₂ S/CO, Co/Mo/K ₂ CO ₃ ^(b)	58.5	2.70
12	tetralin	N ₂	73.5	2.53
13	"	H ₂ S/CO, Co/Mo/K ₂ CO ₃ ^(b)	83.0	2.48

(a) Total sulfur in asphaltene.

(b) Sulfided Harshaw HT-400E. 3% Co, 12% Mo oxides on Al₂O₃.

TABLE 3. NMR Data of Coal Tar Reaction with
H₂S/CO

<u>Reactants</u>	<u>Aliphatic</u>		<u>Aromatic</u>	
	<u>H</u>	<u>C</u>	<u>H</u>	<u>C</u>
Coal tar, N ₂ (a)	5.3	4.4	94.74	95.6
Coal tar, H ₂ S, CO (a)	15.9	6.6	84.09	93.4
Coal tar, H ₂ S, ¹³ CO (b)	12.7	12.1	87.17	87.9

(a) Reaction was carried out in 300 mL autoclave at 400°C, 6894 kPa ambient pressure for 2 hours in the presence of 5% Harshaw HT-400E sulfided catalyst.

(b) Reaction was carried out in 30 mL microreactor at 400°C, 5515 kPa ambient pressure for 6 hours in the presence of 5% Harshaw HT-400E sulfided catalyst.

PILOT UNIT EVALUATION OF EXXON DONOR SOLVENT (EDS) PROGRAM COALS. G. H. Anderson,
S. J. Hsia and K. L. Trachte. Exxon Research and Engineering Company, P. O. Box
4255, Baytown, Texas 77520.

Two Recycle Coal Liquefaction Units (RCLU's) are employed as a research and development tool to evaluate the performance of the Exxon Donor Solvent (EDS) coal liquefaction process with various program coals. These small (50 pounds-per-day and 100 pounds-per-day) integrated, continuous flow units with solvent recycle are used to evaluate new coals, investigate process modifications and conduct process variable studies. The RCLU's have been used to generate data for overall process yields and to provide information on operability trends for a variety of coals ranging in rank from lignitic through subbituminous to bituminous. We have found that the EDS process can be operated successfully throughout this range of coal rank. Optimum yields, and the conditions at which these yields are achieved, are strongly dependent on the specific coal. Recent process improvement operations have shown significant improvements in total liquid yield, as well as a lighter liquid product slate may be achieved. Operability trends are related to coal rank, with generally better operability obtained with higher rank coals. Yield and operability information from the RCLU's are used to select preferred operating conditions for the larger (one ton-per-day and 250 ton-per-day) pilot plants in preparation for future commercial operation.

EFFECTS OF SOLVENT HYDROGEN CONTENT IN THE SRC PROCESS. Ronald W. Skinner and Edwin N. Givens, Corporate Research and Development Department, Air Products and Chemicals, Inc., P. O. Box 538, Allentown, PA 18105.

Five coal-derived solvents containing between 6.2 and 9.5% hydrogen were compared as once-through SRC process solvents in a continuous flow unit equipped with a stirred tank reactor (CSTR). Gaseous hydrogen consumption varied inversely with the solvent hydrogen content. Coal conversion to pyridine soluble products was insensitive to solvent hydrogen; but the yield of toluene solubles decreased significantly with hydrogen-deficient solvents. The yields of liquid products and hydrocarbon gases were also reduced with hydrogen-deficient solvent. The approach to solvent equilibrium was examined in solvent recycle experiments using 8.7% H and 6.2% H starting solvents. After five passes, the recovered solvents had not reached equilibrium, as determined by differences in hydrogen content, fraction aromatic hydrogen, and average ring number. However, these differences in solvent composition did not affect the product yields.

CONTINUOUS HYDROLIQUEFACTION TESTS OF AUSTRALIAN BROWN COAL

N.V.P. Kelvin, B.P.K. Lim and P.W. Fredrickson

Australian Coal Industry Research Laboratories Ltd.,
P.O. Box 83, North Ryde. N.S.W. 2113. Australia.

INTRODUCTION

The Australian state of Victoria possesses huge proven reserves (66.7×10^9 tonnes) of brown coal which have been shown (1-3) to be highly suitable for hydrogenation to liquid fuels. Previous ACIRL (3) batch autoclave tests on Victorian brown coal gave toluene-soluble liquid yields of 61% when hydrogenated in tetralin at 400°C for 4 hours at hydrogen pressure of around 21 MPa. Moreover, high yields of oil have been reported (4) for the hydrogenation of German brown coals (similar to the Victorian variety) in large-scale continuous operations.

Hydroliquefaction tests on a Victorian brown coal in ACIRL's 1 kg/hr continuous reactor unit are reported here. The unit and supporting equipment have been described earlier (5) with reference to black coal hydrogenation tests.

CONTINUOUS REACTOR OPERATIONS

The brown coal sample was from a steam-dried batch of run-of-mine brown coal then exposed to ambient room conditions for several hours. The coal was then crushed and screened to pass .075 mm and stored in polyethylene bags until required. Equilibrated moisture contents determined by the Dean and Stark (boiling toluene) method were in the range 11-16%.

The conditions under which these tests were run were -

Slurry solvent/coal ratio	1.68 - 2.0	: 1
Slurry feed rate	0.7 - 1.0	kg/hr
Hydrogen feed rate	88 - 92	g/h
Catalyst % Coal	0 - 4.3	
Temperatures:		
Preheater	25	- 450 C
Reactor	25	- 430 C
Preheater tube dimensions	6 - 25 m long	x 6 mm I.D. x 9.5mm O.D.
Reactor volume		3.5 L

Table 1 gives further run details.

The reactor internal configuration is shown in the figure. The reactor has been divided into three stirred compartments in an effort to increase the number of CSTR stages with minimal interstage backmixing, and thus to approach plug flow which is known to be more effective for a given reactor volume.

OPERABILITY

Feed slurry solvent/coal ratios were limited to above 1.68 : 1 as thicker slurries could not be pumped satisfactorily. At larger scales of operation it is likely that thicker slurries could more readily be handled. Accordingly, the data obtained at this small scale may be affected by the low feed slurry coal concentrations that could be achieved.

Product slurry let-down valves operating with pressure drops of up to 21 MPa down to atmospheric have survived longer (over 200 hours) in brown coal service than in black coal runs (50-100 hours). This is most likely the result of lower ash contents and lower percentages of hard macerals in brown coal.

Preheater tube blockages have been encountered in every run with brown coal. We observed that high temperatures tended to accelerate deposition of mineral matter and coke on the preheater wall. Deposition of solid coke-salt materials in preheaters also appears to be a problem for other workers in brown coal and lignite

hydrogenation. High levels of calcium have been qualitatively observed in some of our preheater solids. However the original deposit that eventually caused a blockage could not always be found because preheater contents tended to coke along the whole length when flow stopped. The original high-calcium deposit was then only locatable by laboriously cutting the whole preheater into many sections and examining each one individually.

RESULTS

Observed mass balances and oil yields are presented in Tables 2 and 3. Yield data corrected to 100% recovery for operationally stable runs 33, 44 and 45 are presented in Table 4. Overall recoveries for these runs were 95- 96%.

Because of the small scale of operations perfect mass balances were very difficult to achieve. Overall mass balances varied from 82% to 97%, the poorer mass balances being partly attributable to operational problems such as leaks, necessarily hasty remedial action to clear blockages in the feed slurry circulating system, and losses when discharging material in process in order to replace a blocked preheater. Distillation mass balances (i.e. recovery of water, light oil, middle and vacuum distillates and distillation residue) were 95 - 98% of product slurry fed to the distillation equipment. Observed oil yields were corrected by assuming perfect recovery. Thus, observed oil yields in the range 31 - 44% for overall 95 - 96% recoveries are estimated to be in the range 42 - 55% assuming 100% recovery. We believe that the downside error is unlikely to be greater than 5%, that is the above oil yield range is unlikely to be less than 26 - 39%.

Observed distillate yields for runs with poor overall recoveries are unfortunately suspect. However, some conclusions can be drawn with reasonable certainty, namely:

- (a) Distillate oil yields of up to 55% can be obtained from this coal at conditions attainable in this bench unit.
- (b) Oil yields were higher when reactants flowed through both preheater and reactor (both at above 400°C) than through either alone. Some negative oil yields were observed probably as the result of degradation of solvent in the hot preheater.
- (c) Solids building up in the preheater tended to reduce liquid yields probably due to decreasing reaction volume.
- (d) Preheater deposits tended to form more rapidly at higher temperatures.
- (e) Added red mud and sulfur improved liquid yields slightly. Further verification of this effect is under way.

PRODUCT CHARACTERISTICS

Light oils (IBP - 200°C) were found to contain 19-37% paraffins, 19-27% naftenes, 26-50% aromatic hydrocarbons, and 9-14% oxygenated compounds, mainly phenols and ketones. This would suggest that substantial extraction and/or catalytic hydro-treatment would be required to produce a suitable feedstock for gasoline. By comparison light oils derived from black coals generally contain about half as much oxygenated compounds.

The heavier oils from which aliquots are used as recycle oil, contained substantial concentrations of heteroatoms of which phenolic hydroxyl groups accounted for 70-90% of the oxygen present. The concentration of saturated hydrocarbons increased up to 10% with succeeding recycle passes while aromatics and simple polar compounds remained approximately constant. Branched hydrocarbons were present in only very small amounts. After about 400 hours total operation, indications were that 30-40% of the original starting solvent components remained. In other words, the original starting solvent (mildly hydrogenated creosote) is fairly stable at these hydrogenation conditions and thus it merely becomes diluted with every succeeding recycle pass.

CONCLUSION

It is important to recognise that these data were generated on a small bench unit and are indicative of trends and likely ranges of oil yields. These runs have provided valuable experience enabling us to better plan future improvements to improve mass balances and yields. However, we believe that at this small scale the best recoveries achievable are 98% on feed slurry, that is 95-96% on feed coal.

ACKNOWLEDGEMENTS

Support was provided under the National Energy Research, Development and Demonstration Program administered by the Commonwealth Department of National Development and the Victorian Brown Coal Council. Permission by Mr. A.H. Hams, ACIRL's General Manager and Director of Research to present this paper is gratefully acknowledged. The assistance of J.F. Cudmore, R.E. Guyot, P.A. Bennett, R. Staker and co-operating ACIRL staff is also gratefully acknowledged.

TABLE 1.
Run Conditions

Runs	Duration h	Brown Coal feed kg	Starting Solvent	Solvent/ Coal Ratio	Catalyst % coal
33	98	25	100% MHC	1.68 : 1	4.3
34-36	311	85	100% MHC then RS from previous runs	1.78 - 2.0 : 1	0 - 1.2
44A, B	100	30	49% MHC 51% RS from previous runs	1.80 : 1	4.0
45	106	35	100% RS from Run 44	1.80 : 1	4.0

MHC = mildly hydrogenated creosote
RS = recycle solvent
Catalyst = 75% red mud + 25% elemental sulfur.

TABLE 2.
Unit Configuration and Preheater Behaviour

Runs	Preheater			Reactor	
	Temperature C	Status	Time to block, h	Temperature C	Status
33	450	In	71	425	In
34A	450	In	-	-	Out
34B	450	In	89	425	In
35A	450	In	53	425	In
35B	450	In	26	-	Out
36A	450	In	-	-	Out
36B	450	In	50	370	In
36C	-	Out	-	425	In
44A	435	In	59	430	In
44B	410	In	-	430	In
45	410	In	86*	430	In

* Blockage cleared by imposed excess pressure drop.
All other blocked preheaters could not be cleared
and were therefore replaced.

TABLE 3.
Mass Balances and Yields

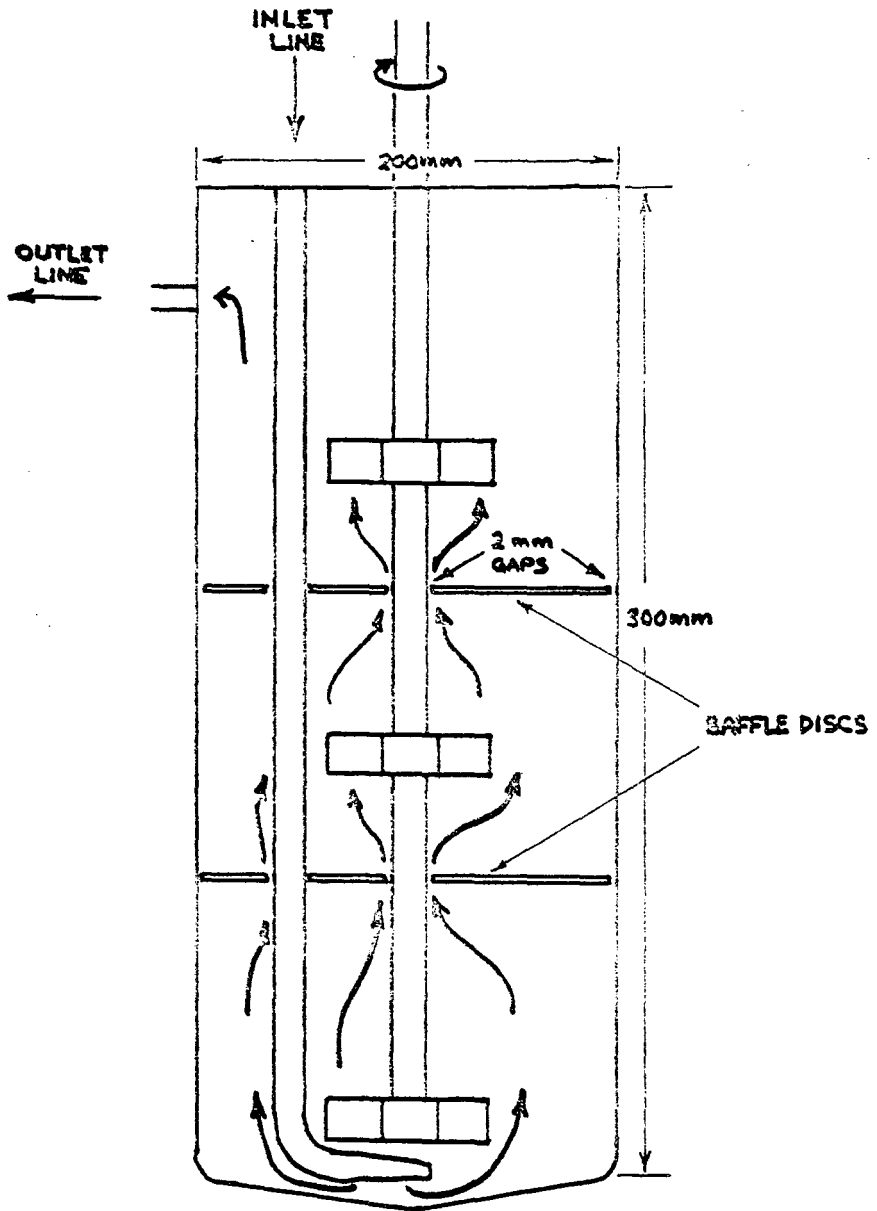
Run	Mass Balance Closure on Total Feeds (%)			Observed Distillate Yield % d.a.f. Coal
	Continuous Reactor	Distillation	Overall	
33	100.1	94.7	95	44
34A	85	97.9	83	-16
34B	84	97.6	82	- 5
35A	89	96.5	86	- 2
35B	95	98.7	94	3
36A	101.4	98.6	97	-11
36B	98.0	97.2	95	- 7
36C	89	98.2	87	11
44A	97.4	97.4	95	31
44B	97.6	97.4	95	38
45	98.3	97.8	96	32

TABLE 4.
Yields Corrected to 100% Recovery

Run	33	44A	44B	45
<u>IN</u>				
Coal (d.a.f.)	100	100	100	100
Hydrogen consumed	6	10	12	7
	<u>106</u>	<u>110</u>	<u>112</u>	<u>107</u>
<u>OUT</u>				
C ₁ - C ₄ hydrocarbons	13	17	13	11
CO, CO ₂	12	17	14	15
Heterogases	2	1	1	3
Generated Water	12	13	12	15
Light Oil (IBP - 200°C)	10	13	10	10
Middle Distillate (200 - 320°C)	28	25	29	22
Vacuum Distillate (320 - 550°C)	17	7	13	10
Distillation Residue (d.a.f.)	12	17	20	21
	<u>106</u>	<u>110</u>	<u>112</u>	<u>107</u>
Net distillate Oil Yield, % d.a.f. coal	55	45	52	42

REFERENCES

1. SINNATT, F.S., and G.E. BARAGWANATH (1938) "The Hydrogenation of Victorian Brown Coals" State Electricity Commission of Victoria (2nd Edition, 1974)
2. GUYOT, R.E. (1976) "Production of Synthetic Oil and Chemicals from Coal - Part 3 - Relationships between Coal Properties and Hydroliquefaction Potential" ACIRL Report P.R. 76-8.
3. GUYOT, R.E. (1978) "Influence of Coal Characteristics on the Yields and Properties of Hydrogenation Products" ACIRL Report P.R. 78-8.
4. KRÖNIG, W. (1977) "Kohlehydrierung (Erzeugen von Kohlenwasserstoffen durch Direkthydrierung)" Ch. 4 Georg Thieme, Stuttgart, 1977.
5. KELVIN, N.V.P. (1979) "Hydroliquefaction of Australian Coals" A.C.S. Div. Fuel Chem. Sept. 1979, Washington D.C.



Internal Configuration of Stirred Reactor

Disposable Catalysts for Coal Liquefaction

Eneo C. Moroni and Ronald H. Fischer, U.S. Department of Energy, Office of Fossil Fuel Programs, Division of Fossil Fuel Processing, Mail Stop E338/Gtwn, Washington, DC

The objective of DOE's Disposable Catalyst Program is to utilize the mineral matter in coal or other inexpensive naturally occurring ores as coal liquefaction catalysts which will substantially reduce hydrogen consumption and increase selectivity to liquids. Fundamental and applied research work performed in several laboratories has been coordinated into an integrated program. Research in the area of coal minerals has shown that pyrites and pyrrhotites are active and effective catalysts for the hydroliquefaction of coals exhibiting both hydrocracking and hydrogenation functionalities. Batch experiments have shown that pyrite or pyrrhotite addition improves coal conversion as well as product selectivity, i.e., a 5 wt% pyrite addition increases the conversion of coal to benzene solubles product equivalent to 25° C operating temperature increase and to distillate product equivalent to 20° C operating temperature increase.

Pyrites from various coals provide different levels of catalytic activity which are attributed to differences in morphologies of the pyrites and/or are related to different inherent surface area of the pyrites.

Pyrites from mineral deposits show in general lower catalytic activity than coal-extracted pyrites.

The catalytic role of coal mineral clays and their effect on the pyrite-pyrrhotite catalytic system is being studied.

THE MECHANISM OF HYDROGEN TRANSFER FROM DIALIN DONORS, D.H. Bass and P.S. Virk,
Department of Chemical Engineering, Massachusetts Institute of Technology, Cambridge,
MA 02139

We report experiments concerning the transfer of hydrogen from the two dihydronaphthalene isomers, namely Δ^1 -dialin and Δ^2 -dialin, to two polynuclear hydrocarbon acceptors, namely anthracene and phenanthrene. These substrates were chosen both to model some of the hydrocarbon moieties involved in coal liquefaction as well as to test our hypothesis that the hydrogen transfer occurs by a concerted pericyclic reaction. The Woodward-Hoffmann rules for orbital symmetry conservation then suggest that hydrogen transfer to anthracene should be thermally-allowed from Δ^2 -dialin but forbidden from Δ^1 -dialin; however hydrogen transfer to phenanthrene should be thermally-allowed from Δ^1 -dialin but forbidden from Δ^2 -dialin. The experiments were conducted in tubing bomb reactors in the temperature range 240 C to 430 C, at times from 5 to 960 minutes and donor-to-acceptor mol ratios from 0.25 to 16. Reactions were essentially first order in each of donor and acceptor, with second order rate constants, $\log_{10}k$ (liter/mol s) tabulated below:

Acceptor +	Donor +	Δ^1 -dialin	Δ^2 -dialin	tetralin
Anthracene	300 C	-5.1	-3.0	-6.1
Phenanthrene	400 C	-4.0	-5.5	-5.7

The experimental results evidently accord with the theoretical predictions for a pericyclic hydrogen-transfer.

COMPARISON OF METHODS FOR THE DETERMINATION OF
ASPHALTENES, OILS AND INSOLUBLES - PART II

Hyman Schultz and Margaret J. Mima

U. S. Department of Energy
Pittsburgh Energy Technology Center
4800 Forbes Avenue, Pittsburgh, PA 15213

INTRODUCTION

According to Sternberg et al., asphaltenes are high molecular weight compounds which affect the viscosity of products from coal conversion processes (10) and may be the intermediaries in the formation of oil from coal (3, 6, 12). Asphaltenes have traditionally been defined by their solubility properties. A knowledge of the concentration of asphaltenes in coal-derived oil is often helpful to the engineer in evaluating hydrotreating processes. Studies of coal hydrogenation at DOE's Pittsburgh Energy Technology Center (formerly Pittsburgh Energy Research Center, Bureau of Mines) over the years often depended on the determination of asphaltenes (5, 11, 12). However, there is no standard method for the determination of asphaltenes in the products from coal conversion, nor is there any known relationship between asphaltene values produced by the analytical methods currently in use. Therefore, one cannot with any degree of confidence compare the asphaltene content of coal derived liquid fuels that are analyzed by different methods. At present, every laboratory has developed its own procedure for determining asphaltenes in coal-derived materials.

In order to ascertain if the different methods used to determine asphaltenes in coal-derived materials produce significantly different results, a study was initiated at the Pittsburgh Energy Technology Center aimed at objectively comparing five different methods currently used to analyze such

materials for asphaltenes, oils and insolubles. Part I of the study involved the use of a hydroliquefaction product of intermediate asphaltene content as a test material and was reported previously (7). Part II of the study is reported herein and involves the use of a high asphaltene containing substance as the test material.

EXPERIMENTAL

The experimental methods used were the same as those employed in Part I (7). A solid product from the Solvent Refined Coal (SRC) plant of Fort Lewis, Washington was chosen for the "standard" material. A large sample of the SRC was provided by the Combustion Division at PETC and was subsequently ground to pass through a 60-mesh screen. After thorough mixing, the SRC was divided into five portions which were stored under nitrogen in sealed, dark glass bottles until used.

The analytical procedures used were outlined previously (7) and will be described in greater detail in a future publication.

Method A has been in use by the Analytical Chemistry Branch at PETC for years for routine, high volume work and requires only inexpensive equipment (5). No attempt is made to keep the sample or the various fractions from contact with the air since chemical characterization of the fractions was not a consideration in the design or use of this method.

Method B was developed in the Molecular Spectroscopy Branch at PETC to give rapid results with a small number of samples and to produce fractions for further study (8).

Method C was designed in the Process Sciences Division at PETC as a means of studying the conditions for precipitation of asphaltenes and for preparing fractions for further study (2, 9).

Method D was developed at ARCO as a means of preparing fractions for further study (4).

Method E was designed at EXXON Research and Engineering Company as a preparative method (1). Due to the limited amount of sample available and after consultations with the originators of the method, a 25 gram sample size was employed instead of the 50 gram sample originally specified.

RESULTS AND DISCUSSION

The results of the study are shown in Table 1. After replicating method C a number of times it became apparent that the results varied so widely that the method was not working well enough to warrant continued replication. It was concluded that the probable cause of the observed variation was the passing of fine particles through the extraction thimble in a non-reproducible way. The results for method C were therefore left out of Table 1.

The averages vary over almost a factor of 2 for insolubles and asphaltenes and almost a factor of 15 for the oils. The ranges for the relative standard deviations were 4 to 9% for the insolubles, 6 to 15% for the asphaltenes and 4 to 40% for the oils.

The sums of the average values of insolubles, asphaltenes and oils for methods B, D and E (the oils are calculated by difference in method A) add up to more than 100%. While the difference between the sums of the average values and 100% are not statistically significant at the 95% confidence interval for methods B and D (it is for method E), the fact that all three methods show sums of greater than 100% can be interpreted as evidence of solvent retention in the fractions (the use of nitrogen in these methods would make oxidation an unlikely explanation).

In order to determine in an objective manner if significant differences exist between the results obtained from the various methods, Student's "t" test was applied. The results obtained with methods A, B, D and E were compared two at a time and in all cases statistically significant differences were found.

Based on the experience gained during this study the analysts involved made estimates for each method of the elapsed time and man-hours necessary to complete a determination and of the expected production rate. They concluded that in all cases these were not as favorable as those for the medium asphaltene material in Part I of the study (7). The differences were mainly due to the difficulties encountered in removing solvents from the insoluble material and, in some cases, the oils.

CONCLUSIONS

This study has shown that materials high in asphaltenes are more difficult to analyze for their asphaltene content than materials of moderate asphaltene content. Indeed, one of the test methods failed completely to work with the test sample. As authors of the method report (9) successfully applying the method to an SRC-I material, it was concluded that our results were caused by either of two things. First, although the specifications spelled out in the method were met, the Soxhlet thimbles were obtained from a different manufacturer than used by the originators and therefore may have been of a different porosity allowing fine particles through. Second, the SRC used was different than that reported on and may have been ground to a different average particle size.

Four of the methods worked but were less precise, required more effort and produced analyses at a lower rate than they did with the more tractable medium asphaltene material. In spite of all the above, methods A, B, D and

E could be used to analyze high asphaltene materials but each will produce different results with the same material. Clearly a standard method is called for but whether one method can be devised that will be usable with coal derived materials of widely varying asphaltene content is problematical.

REFERENCES

1. Aczel, T., R. B. Williams, R. J. Pancirov, and J. H. Karchmer. Chemical Properties of SYNTHOIL Products and Feeds, Anal. Proj. Rept. BRD.1BA.76, EXXON Research and Engineering Company, Baytown, Texas.
2. Bockrath, B. C. PETC/DOE, personal communication, May 1977.
3. Husack, R. and C. Golumbic. J. Am. Chem. Soc. 73, 1567 (1951).
4. Kutta, H. W. and E. H. Burk. Investigations on the Nature of Preasphaltenes Derived From Solvent Refined Coal Conversion Products, Atlantic Richfield Company, Harvey Technical Center, 400 E. Sibley Boulevard, Harvey, Illinois.
5. Mima, M. J., H. Schultz, and W. E. McKinstry. Method for the Determination of Benzene Insolubles, Asphaltenes, and Oils in Coal-Derived Liquids, PERC/RI-76/6.
6. Pelipetz, M. G., E. M. Kuhn, S. Friedman, and H. H. Storch. Ind. & Eng. Chem. 40, 1259 (1948).
7. Schultz, H. and M. J. Mima. American Chemical Society, Division of Fuel Chemistry, Preprints of papers presented at Anaheim, California, March 12-17, 1978, Volume 23, No. 2, pp. 76-78.
8. Schweighardt, F. K. PETC/DOE, personal communication, January 1977.
9. Steffgen, F. W., K. T. Schroeder, and B. C. Bockrath. Anal. Chem 51, 1164 (1979).
10. Sternberg, H. W., R. Raymond, and F. K. Schweighardt, Science 188, 49 (1975).
11. Weller, S., M. G. Pelipetz, and S. Friedman. Ind. & Eng. Chem. 43, 1572 (1951).
12. Weller, S., op.cit., pp. 1575-79.

Table 1. Average of 20 replicate analyses of a sample of SRC.

<u>Method</u>	<u>% Insolubles</u> <u>± 1S</u>	<u>% Asphaltenes</u> <u>± 1S</u>	<u>% Oils</u> <u>± 1S</u>
A	37 ± 3	52 ± 3	12 ± 2
B	58 ± 5	43 ± 6	1.5 ± 0.6
C	<u>See Text</u>		
D	64 ± 3	27 ± 4	14 ± 2
E	49 ± 2	34 ± 2	22.0 ± 0.8

The Composition of Liquids from Coals of Different Rank

G. P. Sturm, Jr., J. E. Dooley, J. S. Thomson,
P. W. Woodward, and J. W. Vogh

U.S. Department of Energy, Bartlesville Energy
Technology Center, P. O. Box 1398
Bartlesville, Oklahoma 74003

INTRODUCTION

Eight coal liquids prepared from six coals (9,10) of widely differing rank were characterized by procedures previously developed for petroleum (3,4,7) and by ASTM methods. The liquids were prepared and upgraded by hydrogenation in a batch autoclave under conditions intended to minimize cracking of the hydrocarbons (especially those of cyclic and aromatic structure) and yet produce most of the liquid hydrocarbons potentially obtainable from a given coal. The extent of the hydrogenation/hydrogenolysis (henceforth referred to as hydrogenation) of the raw coal liquids was adjusted as required to decrease the nitrogen content to about 0.2 to 0.3 weight-percent with the additional intent of providing a predominantly hydrocarbon liquid for analysis. Details of the coal liquid preparations have been reported previously (9,10). This report covers the characterization of the coal liquids and possible implications in relation to refining.

Among the many reports in the literature on coal liquefaction, several indicate a relationship between the rank of the coal and the complexity of the hydrocarbon groups in the coal and in its liquefaction products. This subject was reviewed in some detail in our previous reports (9,10) and will only be summarized and updated here. Early German work indicated that the lower-rank brown coals (lignite) were more reactive, requiring less hydrogen pressure, and produced smaller polynuclear hydrocarbon units (18) than bituminous coals. Also, the asphaltene content of the coal liquids decreased with the coal rank to a minimum for sub-bituminous coals. Early work by the U.S. Bureau of Mines produced similar results (14). Low rank coals were found to be so reactive that, at a reaction temperature of 430° C, high hydrogen pressure was required to prevent repolymerization of reactive fragments to coke. More recent studies have shown that the product from the liquefaction of a Utah sub-bituminous coal with hydrogen donor solvent (6) contained less benzene insoluble material than that from Pittsburgh bituminous coal.

Although the literature suggests that the complexity of hydrocarbon groups in coal and coal liquefaction products can differ substantially with the rank of the coal, specific data are sketchy and sometimes appear to be contradictory. A recent report on the comparison of solvent-refined lignite and solvent-refined sub-bituminous and bituminous coals (2) indicates hardly any difference among the products in terms of gross combustion analysis, acid and basic titres, molecular weight, and nuclear magnetic resonance, ultraviolet and electron spin resonance spectra. Only the nitrogen content of the coal was reflected in the solvent-refined products. However, in another recent study of a lignite, a bituminous coal, and an anthracite coal, analysis of the organic compounds trapped in the coals and contained in the products of selective oxidation indicated an increased condensation of aromatic rings with increasing rank (8). Analysis was performed by gas chromatography/time-of-flight mass

spectrometry and high resolution mass spectrometry. Furthermore, an extensive, detailed study revealed compositional differences in the pyridine extracts of three coals of different rank and also in their liquefaction products produced by the Synthoil process (1). For example, larger quantities of saturates and higher percentages of lower ring number saturate compound types were observed in the two higher rank coal extracts. However, the ring distributions of the aromatic fractions from the coal extracts indicated slightly higher average ring numbers for the higher rank coals.

Similar results were obtained in a study characterizing liquid products obtained from six coals of different rank by treatment of the coals with NaOH-alcohol for one hour at 300° to 350° C (11). Characterization by elemental analysis, molecular weight determination, and proton NMR indicated that the younger (lower-rank) coals gave simpler products with primarily tetralin-type nuclei and more abundant ether linkages than the higher rank bituminous coals which yielded products with five to six rings, about two of which were naphthenic. Similarly, in Japanese studies of pyridine extracts of coals of different rank (17), analysis by proton NMR indicated more condensed aromatic rings with less substitution and shorter aliphatic chains in the higher rank coal extracts. Extracts from bituminous coals contained an average of four or five aromatic rings with side chains averaging three or four carbons in length, whereas a lignite extract had an average of one or two aromatic rings with seven- or eight-carbon, aliphatic side chains. Finally, a study using carbon-13 NMR to characterize a hard-coal-tar pitch and a brown-coal-tar pitch indicated a predominance of fused aromatic ring systems with small amounts of methyl and hydroaromatic methylene groups for the hard-coal-tar pitch (5). The results for the brown-coal-tar pitch indicated primarily long, straight-chain aliphatics estimated at 25 to 40 carbon atoms in length.

The coal liquids characterized at the Bartlesville Energy Technology Center to date have come from different projects in which the primary objective was the development of a specific process. This precluded a systematic study of the relationship of coal rank to coal liquid composition, which is the objective of this study.

EXPERIMENTAL PROCEDURES

The upgraded coal liquids were distilled with a metal-mesh-spinning-band still under vacuum to produce cuts at 200°, 325°, and 425° C. Asphaltenes were then precipitated from each >425° C residuum dissolved in benzene by addition of 50 volumes of normal pentane (12). Further distillations on the asphaltene-free materials, at 202° C and 4 micron pressure using a wiped-wall molecular still, produced 425°-540° C distillate cuts and residua fractions. After removal of acids and bases from the <200° C distillates by extraction methods (16), an additional chromatographic separation with silica gel provided a check for the presence of olefins. No olefins were detected; thus, the acid- and base-free distillates were analyzed by ASTM D2789-71, Standard Method of Test for Hydrocarbon Types in Low Olefinic Gasoline by Mass Spectrometry.

The higher-boiling distillates were characterized by methods adapted from the characterization of heavy ends of petroleum (3,7). A schematic of the procedure is depicted in Figure 1. Details of the procedures have been reported previously (3,7,15,16). Analyses of subfractions of aromatic concentrates separated by gel-permeation chromatography (GPC) were performed on a low-resolution CEC 21-103 C

mass spectrometer (MS) using low-ionizing energy electrons to produce predominantly molecular ions. Compound-type assignments were made by means of previously established GPC-MS correlations and high-resolution mass spectral data for selected fractions. High-resolution, 70 eV, mass spectra were obtained on an AEI MS 3074 mass spectrometer. High- and low-resolution field-ionization spectra of selected fractions, primarily polyaromatic-polar concentrates, were obtained at Oklahoma State University on a CEC Model 21-110 B mass spectrometer fitted with a razor blade source (13).

RESULTS

Descriptions and analyses of the six coal samples used to prepare the coal liquids are summarized in Table 1. Physical and chemical property data for the eight coal liquids prepared from the six coals are summarized in Table 2. Included in Table 2 are data for repeat runs on Illinois No. 6 and Wyodak coals. The repeat run for the Illinois No. 6 coal was made because of changes in the procedure instituted during the first liquefaction run, Illinois No. 6 run 1. The changes involved a switch from CoMo to NiMo catalyst and a decrease in the maximum temperature from 425° to 400° C (9). Also, upgrading of the first Illinois crude liquid fell short of the targeted value of 0.2 to 0.3 percent nitrogen. The second Wyodak coal liquid was prepared from the same crude liquid as the first by upgrading according to the time-temperature profile used for the Illinois No. 6 run 2 liquid. It was noted previously, that the lower-rank coals reacted more readily and under milder conditions than those of higher rank for both the initial liquefaction and the upgrading of the raw coal liquids (9). Thus, the second Wyodak run was made to determine possible effects of the extent of upgrading upon liquefaction-product composition.

Distillation results for the upgraded coal liquids are also summarized in Table 2. The results showed no large differences for the liquids, except for the extensively upgraded second Wyodak liquid which had a higher percentage of low-boiling material. Asphaltene content of the six "normally" upgraded liquids ranged from about 1 to 7 percent. Inclusion of the second Wyodak and first Illinois liquids extended the ranges of asphaltene content from 0.1 to 14 percent. The asphaltene content correlated with the nitrogen content of the liquids, thus supporting the use of nitrogen content to monitor the extent of coal-liquid upgrading.

Table 3 lists the specific gravity, nitrogen content, and sulfur content of the various distillation fractions obtained from each of the eight coal liquids. Nitrogen content increased for the higher-boiling distillates as expected. All sulfur values were low as expected. Nitrogen contents of the asphaltenes from the bituminous-coal liquids were higher than those from the lower-rank-coal liquids.

Results from the dual silica-gel/alumina-gel adsorption chromatography separations of the 200°-325° C, 325°-425° C, and 425°-540° C coal-liquid distillates are summarized in Table 4. Data for the acid and base extracts of the polyaromatic-polar adsorption fractions are also included in Table 4. Detailed results from the analyses of the saturate concentrates and the fractions from the GPC separations of the aromatic concentrates are not reported here but will be published elsewhere. Compound type assignments and the quantitative results for selected fractions from the GPC separations were checked by high-resolution electron-impact MS and by high- and

low-resolution FI/MS. The results were consistent except for the indication of very small amounts of additional compound types containing S, NO, NO₂, and O₂.

The characterization results from all fractions for each coal liquid were combined and expressed in terms of compound types containing the same number of total rings (aromatic and naphthenic). This scheme was chosen because of the different degree of saturation of aromatic rings in the upgrading of the crude liquids from different coals, and the fact that liquefaction and upgrading reaction conditions were chosen to minimize hydrocarbon ring cracking reactions. The results are summarized in Tables 5 and 6.

DISCUSSION

Examination of the data in Table 5 shows the coal liquids to be more alike than different with regard to distribution by ring number. Differences among the liquids from the several coals doubtless were minimized because the upgrading was adjusted to eliminate heteroatoms to about the same level in most of the liquids. The greater reactivity of the lower-rank coals and the lesser required upgrading of their crude liquids was clear from the previously reported preparations (9). Some scatter in compositional data could be expected because of the variation of details of individual preparations. However, since conditions generally were such as to avoid cracking of hydrocarbons, especially hydrocarbon ring structures, differences or similarities in basic hydrocarbon structures should be valid. One of the largest uncertainties, is the extent of hydrogenation of aromatic hydrocarbon rings originally present in the coal. Total consumption of hydrogen was approximately constant, independent of coal rank (9), so that hydrogen consumed by reaction with high-combined oxygen in lower rank coals was counterbalanced by increased saturation of aromatic rings in the coals of higher rank. With the catalyst and conditions used, many of the polynuclear aromatic structures originally present could be expected to hydrogenate partially to yield hydroaromatics in the upgraded liquids. The uncertainty in the extent of hydrogenation of aromatics is circumvented in part by counting total rings per molecule in the several distillate fractions.

Comparison of the data from the two Illinois No. 6 liquefaction and upgrading runs summarized in Table 6 indicate very little difference in the products in terms of ring number distributions especially in the lower-ring-number compounds. The largest effect in switching from CoMo to NiMo catalyst and decreasing the maximum reaction temperature from 425° to 400° C appears in the compound types containing four or more rings and in the asphaltene content. The second Illinois run with NiMo at 400° C maximum temperature produced more >4-ring compound-type material at the expense of the asphaltenes.

As seen in Table 6, the ring-number data for the two Wyodak runs show that the extent of upgrading was an important factor in final product composition. The more extensive upgrading (Wyodak run 2) produced considerably higher yields of low-ring-number compound types. This was due only in part to more complete conversion of heteroatomic-ring compounds to hydrocarbons. Beyond that, some hydrocarbon cracking must have occurred.

Comparison of the data for the Illinois run 2 and Wyodak run 2 shows significantly higher yields of low-ring-number compound types for the liquid from the lower-rank Wyodak coal. However, since the

Wyodak coal was more reactive, the extent of upgrading as seen in the nitrogen contents was much greater for the Wyodak coal even though the same upgrading temperature-time profile was followed in each case. These differences were in contrast to the data from the six coal liquids in Table 5 which were upgraded to about the same nitrogen content, and for which no clear trend in terms of yields of compounds of equal ring number as a function of coal rank was evident.

CONCLUSIONS

On the whole, the compositional studies showed the coal liquids upgraded to about the same level of nitrogen removal were much more alike than different. There was some scatter in the compositions in terms of number of rings per molecule but no consistent trend with the rank of coal. Although the ranks of the coals used in this study covered the full range of practical interest for liquefaction, selection of additional coal samples covering an even greater range of coal rank might be of value in determining any possible dependence of coal liquid composition upon coal rank.

The extent of upgrading influenced the ring-number distribution for liquids from a given coal. More extensive upgrading produced larger amounts of low-ring-number compound types, due in part to greater removal of heteroatoms and to additional cracking of alkyl linkages between ring systems.

Finally, taking the results of this compositional study in conjunction with the results of the preparation of the coal liquids, liquids from lower-rank coals were more easily upgraded and somewhat more cracking to lower molecular weight components occurred at a given severity of upgrading.

ACKNOWLEDGMENTS

We are indebted to Dr. John B. Green and Steve Holmes for assistance in preparation of the coal liquids, and Janet Porter, Lois Karasa, Bob Vrana, Faye Cotton and Ed Zagula for their assistance in acquisition and reduction of the mass spectral data. We thank Dr. W. C. Lanning for discussions helpful in interpretation of the data. Also, we gratefully acknowledge the assistance of Drs. Q. Grindstaff and S. E. Scheppele of Oklahoma State University for providing the field-ionization mass spectra of selected fractions.

REFERENCES

1. Aczel, T., R. B. Williams, R. J. Pancirov, and J. H. Karchmer, Final Report to U.S. Department of Energy, MERC-8007-1 (Pt. 1) (1976).
2. Baltisberger, R. J., R. A. Kaba, K. J. Klabunde, K. Saita, W. Sukalski, V. I. Stenber, and N. F. Woolsey, *Fuel*, 57, 529 (1978).
3. Coleman, H. J., J. E. Dooley, D. E. Hirsch, and C. J. Thompson, *Anal. Chem.*, 45 (9), 1724 (1973).
4. Dooley, J. E., D. E. Hirsch, C. J. Thompson, and C. C. Ward, *Hydrocarbon Processing*, 53 (11), 187 (1974).
5. Fischer, P., J. W. Standelhofer, and M. Zander, *Fuel*, 57 (6), 345 (1978).
6. Gorin, E., C. J. Kulik, and H. E. Lebowitz, *ACS Div. Fuel Chem. Preprints*, 20 (1), 79 (1975).

7. Haines, W. E., and C. J. Thompson, U.S. ERDA, LERC/RI-75/5-BERC/RI-75/2 (1975).
8. Hayatsu, R., R. E. Winans, R. G. Scott, L. P. Moore, and M. H. Studier, *Fuel*, 57, 541 (1978).
9. Lanning, W. C., J. B. Green, and J. E. Dooley, U.S. Department of Energy, BETC/RI-78/10 (1978).
10. Lanning, W. C., J. B. Green, and J. E. Dooley, ACS Div. Fuel Chem. Preprints, 23 (1), 62 (1978).
11. Makabe, M., and K. Ouchi, *Fuel*, 58 (1), 43 (1979).
12. Mima, M. J., H. Schultz, and W. E. McKinstry, U.S. ERDA, PERC/RI-76/6 (1976).
13. Scheppele, S. E., P. L. Grizzle, G. J. Greenwood, T. D. Marriott, and N. Perreira, *Anal. Chem.*, 48, 2105 (1976).
14. Storch, H. H., C. H. Fisher, C. O. Hawk, and A. Eisner, U.S. BuMines, Tech. Paper 654 (1943).
15. Sturm, G. P., Jr., P. W. Woodward, J. W. Vogh, S. A. Holmes, and J. E. Dooley, U.S. Department of Energy, BERC/RI-78/4 (1978).
16. Sturm, G. P., Jr., P. W. Woodward, J. W. Vogh, S. A. Holmes, and J. E. Dooley, U.S. ERDA BERC/RI-75/12 (1975).
17. Takeya, G., *Pure and Appl. Chem.*, 50, 1099 (1978).
18. Wu, W. R. K., and H. H. Storch, U.S. BuMines Bull. 633 (1968).

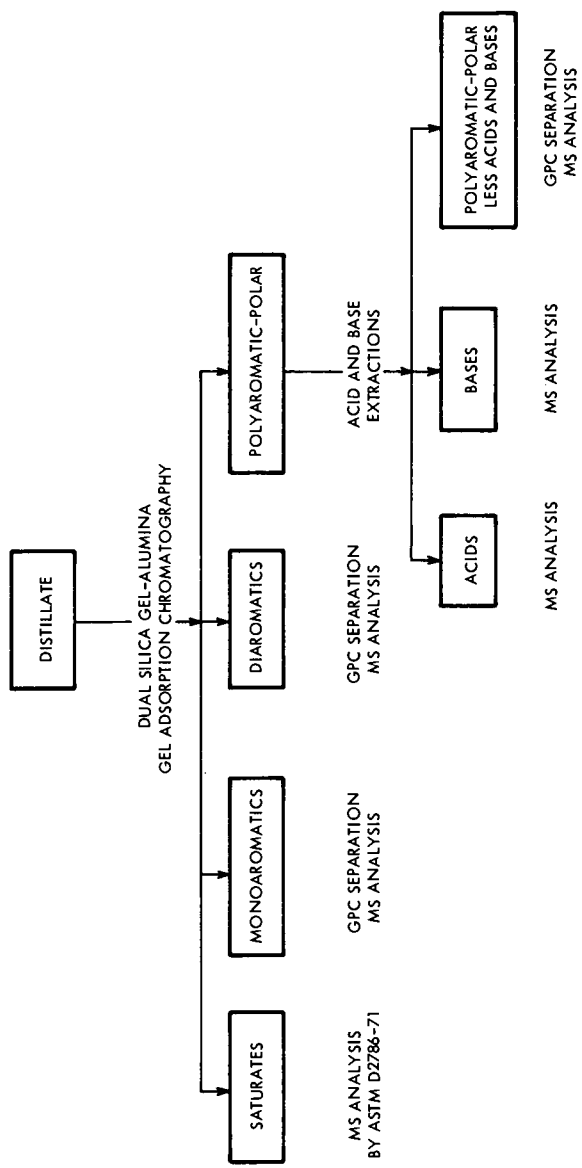


FIGURE 1. - Characterization scheme for 200-325° C, 325-425° C, and asphaltene-free 425-540° C coal liquid distillates.

TABLE I. - Analysis of coals, (weight percent)

Source Seam Rank	PA-WV Pittsburgh hvb A	Illinois No. 6 hvb B/C	W. KY -- hvb B/C	Montana (Colstrip) Rosebud subb. A	Wyoming (Wyodak) Lower subb. C	N. Dakota Beulah Std. II Lignite
Proximate analysis, (as received)						
Moisture.....	1.7	7.8	2.9	4.2	10.9	28.0
Volatile matter	35.9	34.2	38.4	34.4	39.5	31.0
Fixed carbon ..	55.1	51.4	48.8	48.5	42.7	33.3
Ash.....	7.3	6.6	9.9	12.9	6.9	7.7
Ultimate analysis, (moisture free)						
Hydrogen.....	5.1	4.9	4.9	4.3	4.8	4.5
Carbon.....	76.9	75.2	70.2	65.2	66.8	63.5
Nitrogen.....	1.5	1.6	1.4	0.6	1.0	0.9
Sulfur.....	1.6	1.5	4.3	1.8	0.5	1.3
Oxygen (diff) .	7.6	9.7	8.8	14.5	19.2	19.1
Ash.....	7.4	7.1	10.2	13.5	7.8	10.7

hvb B/C -- high volatile bituminous B or C
subb. -- subbituminous

TABLE 2. - Properties of crude and upgraded coal liquids

Coal	Illinois No. 6		Illinois No. 6		W. Ky.	Colstrip		Wyodak	Lignite
	Pittsburgh	Run 1	Run 2	Run 2		Crude Liquids	Run 1		
Nitrogen, wt-pct.....	0.44	1.45	1.10	1.28	0.64	0.48	0.43		
Oxygen, wt-pct.....	.59	-	1.34	2.09	1.61	1.08	1.55		
Sulfur, wt-pct.....	<.01	0.17	<0.01	0.02	<0.01	<0.01	<0.01		
Spec. gr. @ 60/60° F....	0.993	1.006	0.992	0.989	0.987	0.955	0.922		
SSU vis. @ 100° F....	441	129	126	89	263	96	56		181
SSU vis. @ 130° F....	189	65	86	-	123	-	-		123
Pour point, ° F.....	+5	<+5	<+5	<+5	+20	+70	+65		+45
Carbon, wt-pct.....	89.2	90.1	88.6	88.2	88.1	88.9	88.0		89.0
Hydrogen, wt-pct.....	10.8	9.9	10.3	10.7	10.6	11.0	11.9		10.8
Sulfur, wt-pct.....	<0.01	0.03	0.02	0.02	<0.01	<0.01	<0.01		<0.01
Nitrogen, wt-pct.....	.20	.444	.250	.287	.192	.095	.008		.250
Oxygen, wt-pct.....	.28	.50	.19	.32	.34	.17	.04		.61
Distillation, wt-pct:									
<200° C	10.0	12.3	11.4	16.6	11.5	13.9	18.3		12.3
200°-325° C	21.7	27.3	27.9	26.1	21.5	26.7	30.3		24.0
325°-425° C	20.3	20.7	22.5	22.8	21.1	21.3	19.1		20.7
425°-540° C ^a	26.6	19.1	23.7	19.7	20.9	25.2	25.3		21.0
>540° C ^b	16.2	6.4	7.5	9.3	18.4	11.2	6.3		15.0
Asphaltenes, wt-pct ...	4.7	14.3	6.8	5.2	6.6	1.2	0.1		6.7

¹ Upgraded on same temperature-time program as Illinois No. 6 Run 2.

^a Asphaltenes removed from >425° C residuum.

TABLE 3. - Distillation fractions of upgraded coal liquids

Coal	Pittsburgh	Illinois No. 6 Run 1	Illinois No. 6 Run 2	W. Ky.	Colstrip	Wyodak Run 1	Wyodak Run 2	Lignite
<200° C distillate:								
Spec. gr.	0.829	0.825	0.827	0.832	0.822	0.819	0.810	0.822
Sulfur, wt-pct.	<.01	.02	<.01	<.01	<.01	<.01	<.01	<.01
Nitrogen, wt-pct.003	.068	.001	.096	.023	.003	<.001	.007
200°-325° C:								
Spec. gr.915	.937	.926	.919	.918	.909	.897	.916
Sulfur, wt-pct.	<.01	.03	<.01	.02	<.01	<.01	<.01	<.01
Nitrogen, wt-pct.016	.102	.021	.062	.030	.012	.002	.104
325°-425° C:								
Spec. gr.983	1.018	1.001	.993	.982	.972	.952	.983
Sulfur, wt-pct.	<.01	0.01	<0.01	.02	<.01	<.01	<.01	<.01
Nitrogen, wt-pct.076	.396	.159	.200	.119	.072	.004	.304
425°-540° C ¹ :								
Spec. gr.	1.045	1.079	1.061	1.049	1.032	1.026	1.001	1.032
Sulfur, wt-pct.	<0.01	<0.01	<0.01	<0.01	<0.01	<0.01	<0.01	<0.01
Nitrogen, wt-pct.272	.594	.415	.415	.233	.176	.029	.412
>540° C resid ¹ :								
Nitrogen, wt-pct.420	.709	.576	.565	.348	.275	.052	.518
Asphaltenes:								
Nitrogen, wt-pct.722	1.104	1.004	1.036	.579	.393	.194	.714
>425° C resid:								
Sulfur, wt-pct.	<0.01	.01	<.01	0.04	.02	<.01	<.01	<.01
Nitrogen, wt-pct.374	.829	.56	.573	.332	.219	.024	.501
Asphaltenes, wt-pct.	9.9	35.9	17.9	15.3	14.3	3.3	.4	15.7

¹ Asphaltene-free.

TABLE 4. - Fraction yields from adsorption chromatography and acid-base separations (weight percent)

Cool Liquid Fraction	Pittsburgh		Illinois No. 6 Run 1		Illinois No. 6 Run 2		Western Kentucky	
	Crude	Distillate	Crude	Distillate	Crude	Distillate	Crude	Distillate
200 - 325° C Distillate								
Saturates	11.91	54.9	7.92	29.0	11.75	42.1	11.82	45.3
Monoaromatics	7.77	35.8	15.02	55.0	13.81	49.5	12.01	46.0
Diaromatics	1.36	6.3	2.37	8.7	1.54	5.5	1.31	5.0
Polyaromatic-Polar	.36	1.7	2.00	7.3	.80	2.9	.65	2.5
Loss	.30	1.3	0.0	0.0	0.0	0.0	.31	1.2
325 - 425° C Distillate								
Saturates	5.44	26.8	2.11	10.2	3.87	17.2	4.92	21.6
Monoaromatics	10.17	50.1	6.91	33.4	9.70	43.1	9.46	41.5
Diaromatics	2.52	12.4	6.42	31.0	5.09	22.6	4.47	19.6
Polyaromatic-Polar	2.13	10.5	5.26	25.4	3.67	16.3	3.97	17.4
PAP Hydrocarbons	1.93	9.53	4.82	23.3	3.40	15.10	3.58	15.7
PAP Acids	.11	.56	.11	.51	.11	.47	.11	.47
PAP Bases	.05	.24	.14	.66	.10	.43	.09	.38
Loss	.08	.40	.19	.90	.23	1.10	.17	.80
425 - 540° C Distillate								
Saturates	2.26	8.8	.53	3.2	.80	3.6	2.17	11.8
Monoaromatics	5.76	22.4	1.30	7.9	1.80	8.1	2.36	12.8
Diaromatics	5.78	22.5	3.60	21.8	4.82	21.7	4.36	23.7
Polyaromatic-Polar	11.87	46.2	11.06	67.0	14.79	66.6	9.27	50.4
PAP Hydrocarbons	11.77	45.8	10.91	66.1	14.54	65.5	9.05	49.2
PAP Acids	.07	.29	.08	.50	.13	.59	.10	.55
PAP Bases	.05	.18	.07	.40	.10	.45	.04	.21
Loss	.01	.03	.01	.10	.01	-	.32	1.7

Cool Liquid Fraction	Calstrip		Wyodak Run 1		Wyodak Run 2		Lignite	
	Crude	Distillate	Crude	Distillate	Crude	Distillate	Crude	Distillate
200 - 325° C Distillate								
Saturates	10.75	50.0	15.06	56.4	22.73	75.0	11.71	48.8
Monoaromatics	8.92	41.5	10.12	37.9	6.24	20.6	10.13	42.2
Diaromatics	1.01	4.7	1.01	3.8	.51	1.7	1.02	4.2
Polyaromatic-Polar	.77	3.6	.51	1.9	.48	1.6	1.15	4.8
Loss	.05	.2	0.0	0.0	.34	1.1	0.0	0.0
325 - 425° C Distillate								
Saturates	5.84	27.7	6.99	32.8	11.77	61.6	5.22	25.2
Monoaromatics	8.52	40.4	8.48	39.8	4.22	22.1	7.87	38.0
Diaromatics	3.19	15.1	3.11	14.6	1.64	8.6	3.29	15.9
Polyaromatic-Polar	3.42	16.2	2.73	12.8	1.47	7.7	4.06	19.6
PAP Hydrocarbons	3.17	15.0	2.56	12.0	1.34	7.0	3.62	17.5
PAP Acids	.09	.41	.08	.37	.10	.52	.16	.76
PAP Bases	.08	.37	.03	.13	.01	.03	.18	.88
Loss	.21	1.0	.05	.25	.02	.15	.36	1.7
425 - 540° C Distillate								
Saturates	3.15	15.6	4.96	19.7	8.86	35.0	2.70	13.8
Monoaromatics	3.47	17.2	4.96	19.7	5.46	21.6	2.88	14.7
Diaromatics	4.38	21.7	4.79	19.0	3.74	14.8	3.49	17.8
Polyaromatic-Polar	9.19	45.5	10.48	41.6	7.24	28.6	10.29	52.5
PAP Hydrocarbons	8.79	43.5	10.21	40.5	6.93	27.4	10.09	51.5
PAP Acids	.12	.59	.09	.34	.14	.55	.11	.58
PAP Bases	.03	.14	.03	.11	.02	.06	.11	.54
Loss	.26	1.2	.16	.63	.15	.60	.22	1.1

TABLE 5. - Comparison of six coal liquids based on ring number, and asphaltene and residuum content (weight percent - total coal liquid basis)

No. of Rings \ Coal Liquid	Pittsburgh	Illinois No. 6 Run 2	Western Kentucky	Colstrip	Wyodak Run 1	Lignite
0	1.8	1.9	4.8	4.4	5.7	3.6
1	12.1	12.2	15.7	11.7	16.9	14.4
2	12.9	17.4	16.9	13.8	17.0	15.0
3	15.2	17.1	15.8	14.8	15.6	15.3
Sum 0 to 3	42.0	48.6	53.2	44.7	55.2	48.3
>4	32.2	31.9	27.9	27.6	29.6	24.5
Asphaltenes	4.7	6.8	5.2	6.6	1.2	6.7
>540° C Resid	16.2	7.5	9.3	18.4	11.2	15.0
Acids	.2	.2	.2	.2	.2	.3
Bases	.1	.2	.1	.1	.1	.3
Other ¹	4.6	4.8	4.1	2.4	2.5	4.9

¹ Includes unknowns, material not analyzed due to insufficient sample, and material lost in separations.

TABLE 6. - Ring number distributions for coal liquids produced from Illinois No. 6 and Wyodak coal using different processing conditions

No. of Rings \ Coal Liquid	Illinois No. 6 Run 1	Illinois No. 6 Run-2	Wyodak Run 1	Wyodak Run 2
0	2.1	1.9	5.7	6.2
1	11.4	12.2	16.9	21.6
2	16.1	17.4	17.0	20.1
3	17.3	17.1	15.6	16.9
>4	27.0	31.9	29.6	26.4
Asphaltenes	14.3	6.8	1.2	.1
>540° C Resid	6.4	7.5	11.2	6.3
Acids	.2	.2	.2	.2
Bases	.2	.2	.1	tr
Unknown and Losses	5.0	4.8	2.5	2.2

CHEMICAL COMPOSITION OF RAW AND UPGRADED
ANTHRACENE OIL AND THE CHEMISTRY OF COAL
LIQUIDS UPGRADING(1)

S. E. Scheppele(2)*, G. J. Greenwood*,
R. J. Pancirov**, and T. R. Ashe**

Department of Chemistry*, Oklahoma State University, Stillwater, OK 74074
and Exxon Research and Engineering Co.**, Linden, NJ 07036

INTRODUCTION

Anthracene oil was hydrotreated using flow-through trickle-bed reactors containing Co-Mo-alumina catalysts (3). The conditions are specified in Table I. Samples of the feedstock and four reaction mixtures were separated using cation, anion, and complexation chromatography (4). The compound types and the weight percents of the individual homologs present in the acid, base, neutral nitrogen, and hydrocarbon + ether (neutral) fractions were determined from high- and low-resolutions FI/MS and high-resolution 70-eV EI/MS. The basic and neutral fractions were subjected to GC/MS analysis.

RESULTS AND DISCUSSION

The salient results are summarized. Hydrocarbons containing three aromatic rings account for ca. 40% of the feedstock. The parent member of the -18(H)Z series ($C_{14}H_{10}$) was preparatively isolated using GC and identified as $\geq 98\%$ phenanthrene. The dominance of phenanthrene over anthracene in both high- and low-temperature coal tars has been previously noted (5-10). Thus, phenanthrene and assumably its alkylated homologs comprise the -18(H)Z series and account for 15.6% of the feedstock.

The data in Table II demonstrate the occurrence of extensive phenol deoxygenation. The reactivity of -18(O) through -22(O) and -18(O₂) and -22(O₂) compounds is indicated to be independent of the experimental conditions. However, the weight percents for the lower -Z(O) and -Z(O₂) series reveal that the increased reaction time did not overcome the effect of a decrease in temperature upon reactivity. Comparison of the data in columns 6 and 7 with those in columns 3 and 4 indicates a very small net effect of decreases in both H₂ pressure and space time and catalyst change on deoxygenation.

The acid fraction contains significant amounts of -Z(N) compound types. These compounds and also the ones present in the neutral-nitrogen-containing fraction are indicated to contain the pyrrole nucleus based upon the chemistry associated with the separation and both the molecular weights and formulas for the first homolog observed

for each compound type. For example, as seen in Table III, the carbon number for the first homolog in the -9(N), -15(N), and -21(N) series are those expected for indoles, carbazoles, and benzocarbazoles, respectively. Comparison of the weight percents in columns 4 through 7 with the ones in column 3 of Table III reveal a net nonreactivity for compounds containing the pyrrole nucleus under the specified conditions.

The base fraction from the feed was found to contain -5(N) through -23(N) and -27(N) compound types. These specific -Z series are indicated to be principally composed of compounds possessing the pyridine nucleus based upon the chemistry associated with the separation, the formulas for the first homolog observed in each series, and GC/MS analysis. The -17(N) series ranging from $C_{13}H_9N$ to $C_{18}H_{19}N$ is the most abundant one, accounting for 28.8% of the base fraction. The principal components are assumably isomeric azaphenanthrenes and variously alkylated homologs possessing up to 5 alkyl carbons.

The -11(N) series ranging from C_9H_7N to $C_{16}H_{21}N$ is the second most abundant one, accounting for ca. 23.5% of the base fraction. The first members of this series, quinoline and isoquinoline by GC/MS, account for 0.9 percent of the feedstock. It is interesting to note that isoquinoline accounts for 1/2 to 2/3 of this total.

The feedstock base fraction also contains -11(NO), -19(NO), and -21(NO) compound types. The molecular formulas correspond to compounds containing both furan and pyridine nuclei. It is interesting to note that this fraction contains in excess of 40 heterocyclic compounds containing two nitrogen atoms (11). This appears to be the first report of numerous $C_N H_{2N+Z} (N_2)_2$ compounds in coal liquids and only the second instance (12) in which dinitrogen compounds have been observed in these materials.

The mass spectral and the GC/MS data demonstrate that the complexity of the base fractions is significantly increased under all conditions used (see Table I) in hydrotreating the anthracene oil. Table IV presents mole data for the reactant and product bases comprising the 129-139 molecular-weight series. The moles of quinoline (I) and isoquinoline (II) in the feed are ca. 2.2×10^{-3} and 4.4×10^{-3} , respectively, by GC/MS. In addition, GC/MS reveals the absence of II in the reactor bases. In regard to $C_9H_{11}N$, GC/MS indicates the presence of 1,2,3,4-tetrahydroquinoline (IIIa) and the absence of both 5,6,7,8-tetrahydroquinoline (IIIb) and tetrahydroisoquinolines (IV). Finally, the GC/MS analyses confirm the presence of minor and significant amounts of 2-propylaniline (V) in the feedstock and reactor-1 bases, respectively. These results are at least qualitatively consistent with those obtained from reaction of I with H_2 a) in a batch reactor

using MoS_2 as the catalyst (13) and b) in a high-pressure/high-temperature liquid-phase reactor using a variety of metal catalysts (14) and from the MoS_2 catalyzed reaction of II with H_2 (13).

As shown in Scheme 1 (14), rapid catalytic addition of H_2 to I produces IIIa and IIIb. The apparent presence of IIIa and the apparent absence of IIIb in the products is at least qualitatively consistent with the considerably greater reactivity of the latter compared to the former (14). Structure-reactivity relationships provide a preference for hydrogenolysis of the N-C(2) bond rather than the C(8a)-N bond in IIIa producing V rather than 3-phenylpropylamine. Both IIIa and IIIb are converted to decahydroquinoline (VI), mass 139; the rate constant for the latter conversion is significantly greater than the one for the former (14). The absence of significant amounts of VI in the products is consistent with its facile conversion to hydrocarbons and NH_3 (13,14).

The only nitrogen containing compounds observed from the MoS_2 catalyzed reaction of H_2 and II were IV and decahydroisoquinoline (VII) (14). VII is a minor product. As shown in Scheme 2, II reacts with H_2 producing either IVa or IVb. Hydrogenolysis of either the N-C(3) bond or the N-C(2) bond in IVa produces either 2-ethylbenzylamine (VIII) or 2-(2-methylphenyl)ethylamine (IX), respectively. Since VIII and IX contain a benzylic and aliphatic NH_2 group, respectively, their denitrogenation should be facile. In contrast, the NH_2 group in V, see Scheme 1, is aromatic and, hence, as observed would be expected to undergo hydrogenolysis less readily. Alternatively, hydrogenation of IVa and IVb produces VII which in turn suffers hydrogenolysis producing hydrocarbons plus NH_3 .

Table V lists the furan- and thiophene-compound types present in the neutral fractions from the feed and the products. Dibenzofurans and dibenzothiophenes were identified by GC/MS. Carbon-number distributions for these compound types in the feed and in selected reactor samples are also given in Table V. Table VI presents carbon-number distributions for the hydrocarbons in the feed and reactor sample 1.

The weight percents in Table V indicate that the furans were markedly resistant to both hydrogenation and hydrogenolysis under the experimental conditions. It should be noted that on a 100g basis the moles at C-16 and C-17 in the -22(0) series are 2.8×10^{-3} and 1.8×10^{-3} less in product 1 than in the feed. However, this decrease approximates the increase of 1.8×10^{-3} and 1×10^{-3} moles of C-16 and C-17 homologs in the -18(0) series in product 1. Similar results are observed for reactor-sample 3. This result suggests the hydrogenation of benzonaphthenofurans produces tetrahydroderivatives. The apparent unreactivity of the furans towards at least hydrogenation appears surprising.

The weight presents in Table V demonstrate that the thiophenes were very reactive toward sulfur removal under all experimental conditions. The absence of partially hydrogenated thiophenes in the products is consistent with the mechanism of dibenzothiophene desulfurization(15).

Comparison of the carbon-number distributions for the feedstock and reactor-sample 1 in Table VI reveals that the hydrotreating process significantly a) reduced the amount of aromatic and b) increased the quantity of hydroaromatic hydrocarbons. The occurrence of compound crossover in a number of these series, e.g., -14(H), -18(H), and -20(H), does not negate this conclusion although it complicates data interpretation. However, the following examples illustrate the qualitative information which can be deduced concerning the chemical processes occurring during hydrotreating. Dihydrophenanthrene ($C_{14}H_{12}$), tetrahydrophenanthrene ($C_{14}H_{14}$), and octahydrophenanthrene ($C_{14}H_{18}$) which are produced in chromia-alumina hydrotreating of phenanthrene(16) were identified in the product mixtures. Other C-14 compounds (16) involved in this process are 2-ethylbiphenyl, -14(H), 2-butylnaphthalene, -12(H), and 6-butyltetralin, -8(H). Reactor-sample 1 contains ca. 0.03 more moles of C-14 compounds in the -8(H) through -16(H) series than does the feed on a 100g basis. The former contains 0.018 fewer moles of phenanthrene than does the latter. This result suggests that the mechanism for hydrogenation of phenanthrene over chromia-alumina is at least qualitatively applicable to the conditions specified in Table I and that other compounds must contribute to the C-14 pool. In this regard, phenanthrene is a product in the hydrocracking of pyrene(17).

By GC/MS, acenaphthene and biphenyl account for 94% and 6% and 43% and 17% of the $C_{12}H_{10}$ hydrocarbons in the feed and reactor-sample 1, respectively. On a 100g basis, these values combined with the weight percents in Table VI result in a decrease of 14 millimoles in acenaphthene and an increase of 16 millimoles in tetrahydroacenaphthene between feed and products. This surprisingly good agreement suggests that the former is hydrogenated to the latter. Furthermore, the product mixture contains ca. 6 millimoles more biphenyl than does the feed. This result is not inconsistent with the expected formation of 4 millimoles from desulfurization(15) of dibenzothiophene.

Finally, the increase in the weight percent of the -8(H) Z-series from 0.4 in the feedstock to 7.0 in reactor-sample 1 and the distributions of weight percents across both the -8(H) and -12(H) series cannot be entirely explained by hydrogenation in the naphthalene family(17). Rather these results point to hydrogenation/hydrogenolysis of higher-molecular-weight hydrocarbons and/or heteroatom-containing compounds.

REFERENCES

1. Research at Oklahoma State University supported by the Department of Energy, Contract Number EX-76-C-01-2011.
2. Present address: U.S. Department of Energy, Bartlesville Energy Technology Center, Bartlesville, Oklahoma.
3. M. M. Ahmed and B. L. Crynes, PREPRINTS, Div. Petrol. Chem., Am. Chem. Soc., 22(3), 971(1977).
4. D. M. Jewell, J. H. Weber, J. W. Bunger, H. Plancher, and D. R. Latham, Anal. Chem., 44, 1391(1972).
5. E. Proksch, Z. Analyt. Chem., 233, 23(1966).
6. C. Karr, Jr., P. A. Estep, T. C. L. Chang, and J. R. Comberiat, Bull. U.S. Bureau of Mines, No. 637 (1967).
7. H. Pichler, P. Hennenberger, and G. Schwarz, Brennst.-Chem., 49, 175 (1968).
8. H. Pichler, W. Ripperger, and G. Schwarz, Erdoel Kohle, Erdgas, Petrochem, 23, 91 (1970).
9. K. D. Bartle, Rev. Pure Appl. Chem., 22, 79 (1972).
10. Private communication from T. Aczel and A. G. Sharkey, Jr.
11. R. D. Grigsby, L. R. Schronk, Q. Grindstaff, S. E. Scheppele, and T. Aczel, 27th Annual Conference on Mass Spectrometry and Allied Topics, 1979, in press.
12. A. Marzec, D. Bodzek, and T. Krzyzanowska, in "Organic Chemistry of Coal", J. W. Larsen, Ed., ACS Symposium Series 71, American Chemical Society, Washington, 1978.
13. S. Landa, Z. Kafka, V. Galik, and M. Safar, Collect. Czech. Chem. Comm., 34, 3967 (1967).
14. S. S. Shih, J. R. Katzer, H. Kwart, and A. B. Stiles, PREPRINTS, Div. Petrol. Chem., Am. Chem. Soc., 22(3), 919 (1977).
15. M. Houalla, D. Broderick, V. H. J. deBeer, B. C. Gates, and H. Kwart, PREPRINTS, Div. Petrol. Chem., Am. Chem. Soc., 22(3), 941 (1977).
16. W. L. Wu and H. W. Haynes, Jr., in "Hydrocracking and Hydrotreating", J. W. Ward and S. A. Qader, Ed., ACS Symposium Series 71, American Chemical Society, Washington, 1975.
17. S. A. Qader, J. Inst. Petrol., 59, 178 (1973).

TABLE I
CONDITIONS FOR HYDROTREATING ANTHRACENE OIL

	REACTOR-SAMPLE			
	1	2	3	4
Reactor Temperature (°F)	700	600	700	700
Reactor Pressure (psig)	1000	1000	1020	507
Space time (hrs)	1.48	2.50	0.75	0.75
Catalyst	Nalco Sphericat 474		Harshaw HT 400	

TABLE II
SUMMARY DATA FOR OXYGEN-CONTAINING ACIDS IN
FEEDSTOCK AND UPGRADED ANTHRACENE OIL

-Z	Parent Formula	Feedstock	Weight Percent in			
			Reactor-Samples			
			1	2	3	4
6(0)	C ₆ H ₆ O	4.0	0.1	0.9	0.3	0.8
8(0)	C ₉ H ₁₀	0.5	0.2	0.5	0.4	0.2
12(0)	C ₁₀ H ₈ O	1.0	< 0.0	< 0.1	0.0	0.0
14(0)	C ₁₂ H ₁₀ O	1.5	< 0.1	0.5	0.3	0.3
16(0)	C ₁₃ H ₁₀ O	1.2	0.1	0.5	0.3	0.3
18(0)	C ₁₄ H ₁₀ O	0.3	0.0	< 0.1	0.0	0.0
20(0)	C ₁₆ H ₁₂ O	0.4	0.0	0.2	0.1	0.2
22(0)	C ₁₆ H ₁₀ O	0.1	0.0	0.1	0.1	< 0.1
16(O ₂)	C ₁₂ H ₈ O ₂	2.8	0.0	0.4	0.0	< 0.1
18(O ₂)	C ₁₄ H ₁₀ O ₂	0.1	0.0	0.0	0.0	0.0
22(O ₂)	C ₁₆ H ₁₀ O ₂	0.1	0.0	0.0	0.0	0.0

TABLE III
 SUMMARY DATA FOR $C_N H_{2N+Z(N)} N$ COMPOUNDS
 IN THE ACID AND NEUTRAL-NITROGEN FRACTIONS FROM
 FEEDSTOCK AND HYDROTREATED ANTHRACENE OIL

-Z(N)	Parent Formula	Range In ^a N	Feedstock	Weight Percent			
				Reactor-Sample ^b			
				1	2	3	4
9	$C_8 H_7 N$	9-12	0.2	< 0.1	0.1	0.1	0.1
15	$C_{11} H_7 N$	12-16	1.8	1.6	1.4	1.9	1.6
17	$C_{13} H_9 N$	14-17	0.2	0.2	0.2	0.4	0.1
19	$C_{13} H_{11} N$	14-18	0.2	0.2	0.1	0.1	0.1
21	$C_{15} H_9 N$	16-17	0.3	0.3	0.2	0.2	0.1

^aValues for feedstock. ^bConditions specified in Table I.

TABLE IV
 MOLES OF BASES AT MOLECULAR WEIGHTS 129-135
 IN FEED AND REACTOR-SAMPLE 1

Mass	Formula	Moles ^a $\times 10^3$ In	
		Feedstock	Reactor Sample 1 ^b
129	$C_9 H_7 N$	6.6	0.4
133	$C_9 H_{11} N$	0.2	1.1
135	$C_9 H_{13} N$	0.2	1.8
139	$C_9 H_{17} N$	-	0.006
TOTAL		7.0	3.3

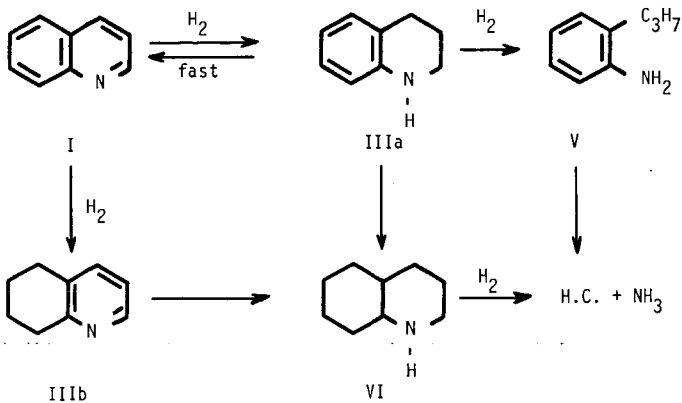
^aCalculated per 100g of feed. ^bConditions specified in Table I.

TABLE VI
CARBON-NUMBER DISTRIBUTIONS FOR THE HYDROCARBONS IN THE FEEDS AND IN REACTOR-SAMPLE 1

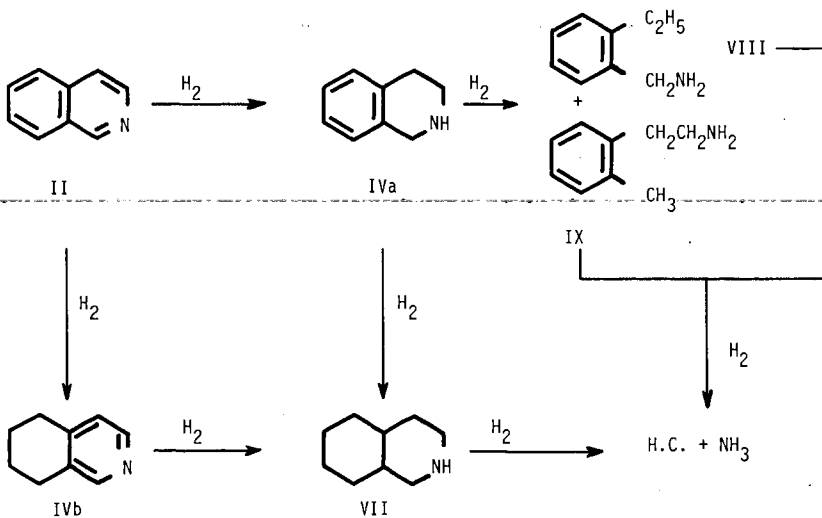
-Z(H)	Parent Formula	Sample ^a	Weight Percents at Carbon Number																	Total
			8	9	10	11	12	13	14	15	16	17	18	19	20					
6	C ₆ H ₆	F	0.1	0.04																0.1
		RI	0.2	0.2	0.1	0.1														0.6
8	C ₉ H ₁₀	F	0.2	0.1	0.1															0.4
		RI	0.5	3.2	1.4	1.1	0.6	0.2												7.0
10	C ₉ H ₈	F	-	-	-	-	-	-												0.0
		RI				3.0	1.0	1.5	0.5	0.2										6.2
12	C ₁₀ H ₈	F	4.8	2.3	1.3	0.6	0.2	0.03												9.2
		RI	3.9	2.2	1.4	0.7	0.3	0.2	1.2											9.9
14	C ₁₂ H ₁₀	F	5.3	1.8	1.4	0.4	0.4	0.3												9.3
		RI	3.5	1.4	3.3	0.9	0.6	0.3	0.1	0.05										10.1
16	C ₁₂ H ₈	F	2.6	1.8	0.7	0.3	0.1	0.05												5.6
		RI	2.7	3.7	1.2	1.6	0.5	0.3	0.1											10.1
18	C ₁₄ H ₁₀	F	10.4	3.2	1.3	0.4	0.1													15.4
		RI	7.2	2.4	3.9	1.2	0.7	0.2	0.1											15.7
20	C ₁₅ H ₁₀	F	1.4	2.4	0.9	0.3	0.3													5.3
		RI	0.9	2.7	0.8	1.0	0.2	0.2												5.8
22	C ₁₆ H ₁₀	F	12.1	2.7	1.6	0.3	0.2													16.9
		RI	6.1	1.3	0.9	0.3	0.3													8.9
24	C ₁₈ H ₁₂	F																		2.2
		RI																		2.2
26	C ₁₈ H ₁₀	F																		0.9
		RI																		0.4
28	C ₂₀ H ₁₂	F																		0.5
		RI																		0.1

^aF=Feedstock; RI=Reactor-Sample 1, Conditions specified in Table I.

SCHEME 1



SCHEME 2



Liquid Sulfur Dioxide - As An Agent
for Upgrading Coal Liquid

C. V. Philip[†], Ralph A. Zingaro^{*} and
Rayford G. Anthony[†]

Departments Chemical Engineering[†] and Chemistry^{*}
Texas A&M University
College Station, Texas 77843

INTRODUCTION

An approach to processing coal-derived liquid is to utilize advanced petroleum refining technology. Physical and chemical characteristics of the coal liquid currently produced from the pilot plants is different from that of petroleum crude. Although various coals may appear different, there is a striking similarity in the nature of major chemical species present in the coal liquids from different sources. Analytical data (1 to 7) on various coal liquids and various distillation cuts show that coal liquids are composed of bulk species such as straight chain hydrocarbons, 'asphaltenes', one or two ring alkylated aromatics (such as alkylated benzenes, indans and naphthalenes), phenols (alkylated phenols, indanols and naphthols). Straight chain hydrocarbons include slightly branched hydrocarbons such as pristene and phytane and long chain monoolefins. The concept of using sulfur dioxide for upgrading coal liquid is very attractive due to the fact that sulfur is going to be one of the large byproducts of any coal conversion technology. Liquid sulfur dioxide is a very good solvent for most of the bulk species in any coal liquid except for saturated hydrocarbons. Now the coal liquefaction technology is very costly due to several factors including consumption of large quantities of hydrogen to liquefy coal. The recovery of saturated hydrocarbon, the hydrogen rich fraction, from the coal liquid has great economic interest.

EXPERIMENTAL

Since liquid sulfur dioxide boils at -10°C , the extraction can be conducted at atmospheric conditions. The liquid sulfur dioxide is obtained by cooling the gas from the cylinder using Dry Ice-acetone mixture. When a coal liquid (usually in a waxy state) is treated with liquid sulfur dioxide, the insolubles remain with the minerals and the coal fragments as a solid residue. The SO_2 -solubles are separated from the insolubles by filtration. The filtrate is degased² to remove SO_2 from the SO_2 -solubles. The hydrocarbons in the SO_2 -insoluble residue are separated from the minerals and coal fragments by soxhlet extraction with tetrahydrofuran (THF-additive free). Both SO_2 -solubles and the THF extract of SO_2 -insolubles were separated by GPC. The details of GPC separation technique is published elsewhere⁽⁷⁾. The GPC system uses four 100A $\mu\text{Styragel}$ columns (total length: 120 cm.) and THF (dry, additive free) as the liquid mobile phase. Two hundred μl of 50% THF solutions of the SO_2 -solubles were separated into four fraction by GPC. Since the preliminary tests revealed that the THF extract of the SO_2 -insolubles are mostly saturated hydrocarbons and other major bulk species are absent, the GPC did not play a significant role in the separation except to remove the gc-nonvolatiles from the sample, as they belong to larger linear molecular size. The GPC fractions 1 and 2 of SO_2 -solubles are gc-nonvolatiles and they can not be analyzed by GC-MS. All other fractions were analyzed by GC-MS. Proton nmr and ir gave some qualitative information on the nonvolatiles.

RESULTS AND DISCUSSION

Liquid sulfur dioxide was used to separate two coal liquids produced from West Virginia subbituminous coal and North Dakota lignite. The samples were obtained from the pilot plant at Pittsburgh Energy Technology Center where SRC I process was used for the liquefaction. Since the liquid sulfur dioxide separation of saturated hydrocarbons from the coal liquid worked equally well for both coal liquids only the separation of SRC from West Virginia subbituminous coal is discussed in detail for the analytical evaluation of the SO₂ separation. Figure 1 is the GPC of SRC from the subbituminous coal. The components of the coal liquid are separated in the order of decreasing linear molecular size⁽¹⁰⁾. For analytical convenience the effluents from the GPC were collected as four fractions. Fraction 1 is composed of high molecular weight species which are nonvolatiles for gc separations. Fraction 2 is composed of saturated hydrocarbons, which could be separated and identified by GC-MS and 'asphaltenes' (9)-a mixture of high molecular weight species which have comparable linear molecular size to straight chain alkanes in the range n C₁₄H₃₈ to n C₄₄H₉₀. Vacuum distillation separates the nonvolatile asphaltenes from the volatile alkanes. Fraction 3 is composed mostly of phenols which have an 'effective linear molecular size' of normal alkanes ranging from C₇H₁₆ to C₁₃H₂₈. Each molecule of phenol has a tendency to hydrogen bond with one molecule of THF to result in an increase in effective linear molecular size by 3 to 4 linear carbon units (propane to butane size). Fraction 4 is mostly aromatics. In a non hydrogen bonding system such as toluene both phenols and aromatics will have similar molecular size and hence they could not be separated by GPC using toluene as the mobile liquid phase.

Figure 2 is the GPC of SO₂-solubles of SRC from subbituminous coal. As in the case of the sample in Figure 1, the GPC effluent was collected as four fractions. After SO₂ treatment the GPC areas of fraction 1 and 2 have decreased and the analysis of fraction 2 of SO₂-solubles does not show any alkanes. Elemental analysis of Fraction 2 after evaporating all the THF shows the following composition

C	H	S	N	O
83.79%	7.39%	3.96%	1.64%	3.22%(by diff.)

The proton nmr spectra of fraction 2 of SO₂-solubles resembles the nmr of asphaltenes reported by other workers⁽¹⁾. The elemental composition and the GPC size distribution agrees with the published values for coal derived asphaltenes^(1,3). Fractions 3 and 4 of SO₂-solubles were separated and identified by GC-MS (see figure 4 and 5). These fractions contain only a small amount of alkanes. The components are listed in Table I and II.

Figure 3 shows the GPC of the THF extract of the SO₂-insolubles. The GC-MS of the THF extract is shown in figure 6 and the components are listed in Table III. The THF extract is free of any phenols or aromatics and contains only straight chain hydrocarbons showing the insolubility of straight chain hydrocarbons as well as branched saturated hydrocarbons in liquid SO₂ even after stirring the sample in SO₂ for several hours.

When SRL produced from North Dakota lignite was treated with liquid sulfur dioxide, the bulk of the coal liquid dissolved except the saturated hydrocarbons and the mineral rich residue. The SO₂-soluble part did not contain any saturated hydrocarbons. The THF extract of the insolubles were mostly alkanes ranging from n-dodecane (C₁₂H₂₆) to n-tetratetracontane (C₄₄H₉₀).

Since most of the coal liquids are composed of more or less similar major species, may differ in composition, liquid sulfur dioxide can be used to extract all the aromatic species of the coal liquid, which is free of saturated hydrocarbons and ash precursors. After degasing SO₂, distillation under reduced pressure can yield all the phenols and aromatics from the SO₂-solubles of the coal liquid. The residue which is more or less identical to GPC-Fraction 2 of SO₂-solubles can be called coal asphaltenes. The

average molecular size of coal asphaltenes (linear molecular size is more precise since it is derived from GPC data) is smaller than that of petroleum derived asphaltenes.

ACKNOWLEDGMENTS

The financial support of the Texas Engineering Experiment Station, the Texas A&M University Center for Energy and Mineral Resources and Dow Chemical Co., The Alcoa Foundation, Pittsburgh, PA., Department of Chemical Engineering, and the Gulf Oil Company. Mrs. Argentina Vindiola assisted in collecting some of the data.

REFERENCES

1. Azel, T., Williams, R. B., Pancirov, R. J., and Karchmer, J. H., "Chemical Properties of Synthoil Products and Feeds," Report prepared for U.S. Energy Research and Development Administration, FE8007, 1976.
2. White, C. M., Shultz, J. L., and Sharkey, Jr. A. C., *Nature* 268, 620 (1977).
3. Bockrath, B. C., Delle Donne, C. L., and Schweighardt, F. K., *Fuel*, 57, (4), 1978.
4. Philip, C. V., and Anthony, R. G., *TEES PUBLICATIONS, TECH BN.*, 78-2, 10 (1978).
5. Philip, C. V., and Anthony, R. G., "Organic Chemistry of Coal," *ACS Symposium Series*, 258, (1978).
6. Philip, C. V., and Anthony, R. G., *Preprints ACE Fuel Div. 24 No. 4*, 196, Miami, (1978).
7. Philip, C. V., and Anthony, R. G., *Preprints ACE Fuel Div., 24 No 3*, 204, Washington, (1979).
8. Our unpublished GC-MS data on various coal liquids and distillation cuts.
9. The term 'asphaltene' is used for the coal liquid fraction which is nonvolatile but soluble in tetrahydrofuran (THF) and SO₂ currently.
10. GPC is used for molecular weight determinations as well as for molecular size determinations. Our unpublished GPC data on a number of compounds such as normal alkanes, amines, alcohols, multi-ring aromatics and etc. shows that the retention volume is a function of the length of the molecule rather than molecular volume or any other molecular size parameters. Therefore, authors think that it is quite appropriate to say that GPC separations are on the basis of linear molecular size rather than just molecular size.

Table I Phenolic Fraction (GPC Fraction #3 From SO₂ - Solubles)

Retention Time (min)	Compound	Retention Time (min)	Compound
4.5	Phenol	21.7	C ₄ -Alkylphenol
6.7	o-Cresol	22.3	C ₄ -Alkylphenol
7.7	p-Cresol + m-Cresol	23.2	C ₅ -Alkylphenol + Methyl Indanol
9.9	C ₂ -Alkylphenol		
11.0	C ₂ -Alkylphenol	24.3	C ₅ -Alkylphenol + n C ₁₃ H ₂₈ + Methyl Indanol
11.6	C ₂ -Alkylphenol		
12.1	C ₂ -Alkylphenol	24.8	Methyl Indanol
13.0	C ₃ -Alkylphenol	25.7	C ₅ -Alkylphenol
13.5	C ₃ -Alkylphenol	26.2	C ₅ -Alkylphenol
14.1	C ₃ -Alkylphenol	26.6	C ₅ -Alkylphenol
14.6	C ₃ -Alkylphenol	27.1	C ₅ -Alkylphenol
15.5	C ₃ -Alkylphenol	27.7	C ₂ -Indanol + C ₅ Alkylphenol
16.2	C ₃ -Alkylphenol	28.3	C ₅ -Alkylphenol + Dimethyl Indanol
16.7	C ₃ -Alkylphenol	29.1	
17.3	C ₃ -Alkylphenol	30.2	C ₆ -Alkylphenol + n C ₁₄ H ₃₀ (trace)
18.0	C ₃ -Alkylphenol	31.7	C ₂ -Alkylindanol + C ₆ Alkylphenol
18.5	C ₄ -Alkylphenol + n Dodecane (trace)	32.6	C ₂ -Alkylindanol + C ₆ Alkylphenol
		33.7	C ₆ -Alkylphenol + C ₂ Alkyl Naphthol
19.3	C ₄ -Alkylphenol	34.4	C ₆ -Alkylphenol + C ₂ Alkyl Naphthol
19.6	C ₄ -Alkylphenol	36.0	C ₃ -Alkylindanol
20.1	C ₄ -Alkylphenol	36.5	C ₃ -Alkylindanol
20.5	C ₄ -Alkylphenol	37.2	C ₃ -Alkylindanol
		38.2	C ₁ -Alkyl naphthol + C ₃ Alkylindanol

Table II Aromatic Fraction (GPC fraction #4 From SO₂ - Solubles)

Retention Time (min.)	Compound	Retention Time (min.)	Compound
3.6	Phenol	18.9	C ₁ -Alkyl naphthalene + C ₃ Alkylindan
4.6	C ₃ -Alkylbenzene		
5.4	o-Cresol	19.5	C ₃ -Alkylindan
6.2	p-Cresol	20.2	C ₃ -Alkylindan
7.3	m-Cresol	21.5	C ₄ -Alkylindan
8.0	C ₂ -Alkylphenol	22.6	C ₄ -Alkylindan
8.8	C ₂ -Alkylphenol	23.4	C ₄ -Alkylindan
9.4	C ₂ -Alkylphenol	24.2	C ₂ -Alkyl naphthalene + C ₄ -Alkylindane
9.9	C ₂ -Alkylphenol + Methyl Indan +	24.6	C ₄ -Alkylindane + C ₂ -Alkyl naphthalene
10.3	Methyl Indan		
11.2	C ₁ -Alkylindan	25.0	C ₄ -Alkylindane + C ₂ -Alkyl naphthalene
12.1	Naphthalene		
12.8	C ₂ -Alkyl Indan	25.5	C ₄ -Alkylindane + C ₂ -Alkyl naphthalene
13.4	C ₂ -Alkylindan		
14.5	C ₂ -Alkylindan	26.7	C ₂ -Alkyl naphthalene
15.5	C ₂ -Alkylindan	27.5	C ₂ -Alkyl naphthalene
16.3	C ₂ -Alkylindan	28.1	C ₁ -Alkylindan
17.0	C ₂ -Alkylindan	28.7	C ₃ -Alkyl naphthalene
17.1	C ₁ -Alkyl naphthalene	30.0	C ₃ -Alkyl naphthalene
18.2	C ₃ -Alkylindan + C ₁ -Alkyl naphthalene	31.7	C ₃ -Alkyl naphthalene

Table III Hydrocarbon Chains Separated from THF Extract of SO_2 - Insolubles

Retention Time (min.)	Compound	Retention Time (min.)	Compound
12.9	Tridecane	31.0	Eicosane
13.6	Tetradecane	33.4	Heneicosane
15.4	$C_{14}H_{30}$	35.9	Docosane
16.7	Pentadecane	38.2	Tricosane
19.7	Hexadecane	40.4	Tetracosane
21.0	$C_{16}H_{34}$	42.6	Pentacosane
22.7	Heptadecane + Pristine	44.7	Hexacosane
25.6	Octadecane	46.7	Heptacosane
28.4	Nonadecane		

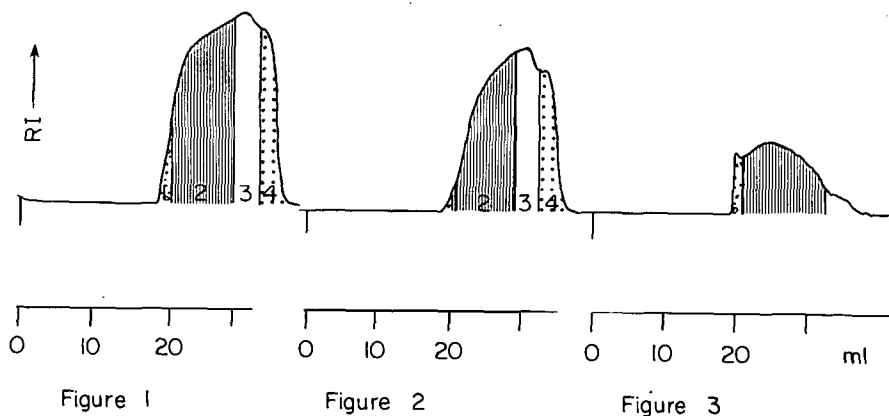


Figure 1. GPC separation of SRC from West Virginia subbituminous coal. The GPC system consisted of four 100 Å Styragel columns and the THF flow rate of 1 ml/min.

Figure 2. GPC separation of SO_2 -solubles of SRC from West Virginia subbituminous coal. Fraction 3 and 4 are identified by GC-MS (see figures 4 and 5 as well as Table I and II).

Figure 3. GPC of the THF extract of SO_2 -insolubles of SRC from West Virginia subbituminous coal. See figure 6 for the GC-MS of the extract and Table III for the identification of the components.

Figure 4

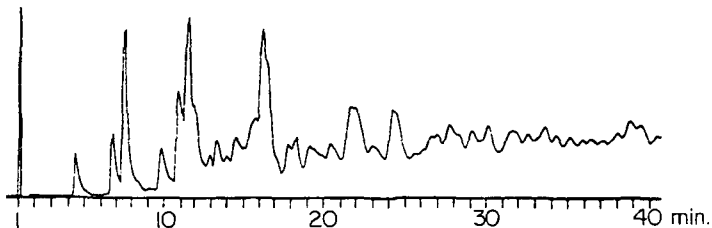


Figure 5

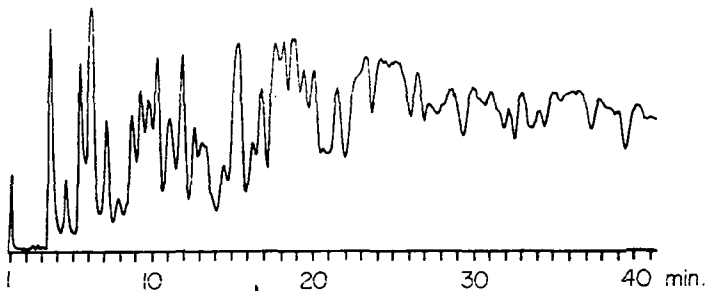


Figure 6

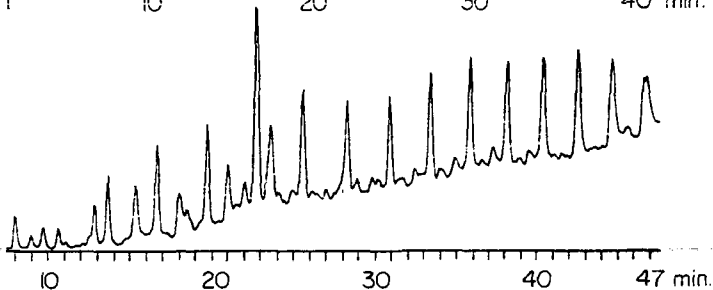


Figure 4. Total ion gas chromatogram of GPC fraction 3 of SO_2 -solubles (Figure 2). Column: 5% Dexsil 300 on 100/120 Chromosorb H-WP, 1/8 in. od \times 8 ft., Carrier gas: 20 ml helium/min., temperature program: 80-270°C at 2°C/min. for 40 min. followed by 4°C/min. See Table I for peak identification.

Figure 5. Total ion gas chromatogram of GPC fraction 4 of SO_2 -solubles (figure 2). Same GC condition as in figure 4. See Table III for peak identification.

Figure 6. Total ion gas chromatogram of the THF extract of SO_2 -insoluble of SRC from West Virginia subbituminous coal. GC conditions were same as in figure 4 except the temperature program of 80 to 270°C at 4°C/min. see Table III for peak identification.

HYDRODESULFURIZATION OF DIBENZOTHIOPHENE CATALYZED BY
SULFIDED $\text{CoO-MoO}_3/\gamma\text{-Al}_2\text{O}_3$: THE REACTION KINETICS

D. H. Broderick and B. C. Gates

Center for Catalytic Science and Technology
Department of Chemical Engineering
University of Delaware
Newark, Delaware 19711

INTRODUCTION

A renewed interest in hydrodesulfurization has come about largely as a result of the need to process more and heavier feedstocks, including synfuels. It has been recognized that model compounds like thiophene are not representative of the least reactive sulfur-containing constituents of these feedstocks. More representative compounds are dibenzothiophenes and benzonaphthothiophenes, which are present in high concentrations in heavy oils (and especially in coal-derived liquids) and are one to two orders of magnitude less reactive than thiophene (1,2).

There is a need for quantitative kinetics characterizing hydroprocessing of these relatively unreactive compounds at temperatures and pressures representative of commercial operation. The goal of this research was to determine detailed kinetics of dibenzothiophene hydrodesulfurization using a high-pressure flow microreactor (3). Earlier work had established the reaction network in dibenzothiophene hydrodesulfurization catalyzed by a commercial presulfided $\text{CoO-MoO}_3/\gamma\text{-Al}_2\text{O}_3$ (4). Early kinetics studies of dibenzothiophene hydrodesulfurization (5,6) fail to account for the complete reaction network and are lacking in experimental detail. Recent kinetics studies (7,8) of dibenzothiophene hydrodesulfurization also fail to provide sufficient detail of the reaction network, and the range of hydrogen partial pressures applied was so low and not all the parameters in the rate equations could be determined from the data.

In the present study rates of the two primary reactions of dibenzothiophene with hydrogen were measured independently, and the full set of data was analyzed and summarized in the form of Langmuir-Hinshelwood rate equations. The data allowed precise estimation of all the kinetics parameters at three temperatures.

EXPERIMENTAL

Materials

The catalyst was a commercial $\text{CoO-MoO}_3/\gamma\text{-Al}_2\text{O}_3$ (American Cyanamid HDS 16A) which was crushed and sieved to 149-178 μm (80-100 mesh) particle size and sulfided in situ. Catalyst compositions are given elsewhere (4). Dibenzothiophene (Eastman, reagent grade) was dissolved in n-hexadecane (Humphrey Chemical Co., specially distilled Lots No. 2270375 and 4090577), and the solution was filtered through a 0.5 μm filter element (Milipore). Biphenyl (Eastman, reagent grade) was used as supplied. Hydrogen was obtained from Linde as 3500 psi grade and treated as described below to remove traces of moisture and oxygen. H_2S was supplied by Linde in custom mixtures with hydrogen in concentrations of 0.5 to 10 mole% H_2S . Alundum "RR" (Fisher

Scientific, Blue Label) was sieved to 90 mesh and used as an inert reactor packing.

A high-pressure flow microreactor, described in detail by Eliezer *et al.* (3), was modified to allow for saturation of the feed mixture with a predetermined H_2S partial pressure (9). The catalyst (6.5×10^{-5} to 1.2×10^{-4} kg) was mixed with alundum (2.31×10^{-4} to 4.25×10^{-4} kg) to give the range of bed volumes [$(2.0-3.6) \times 10^{-7}$ m³] and bed heights [$(2.5-4.5) \times 10^{-2}$ m]. The catalyst was presulfided in the reactor for two hours in a 5.0×10^{-7} to 8×10^{-7} m³/s flow of 10 vol% hydrogen sulfide in hydrogen at atmospheric pressure and 673°K.

Reactant solutions containing 0.3-4.9 mole% dibenzothiophene in *n*-hexadecane or 1.24 mole% dibenzothiophene and 0.6 or 2.9 mole% biphenyl in *n*-hexadecane were prepared. After the solution (5×10^{-4} to 7×10^{-4} m³) had been loaded into a stirred autoclave, it was saturated with hydrogen or hydrogen plus H_2S at predetermined partial pressures after the mixture had been purged for 2 hr with the gas mixture. H_2S partial pressures were varied from 0 to 1 atm, and hydrogen partial pressures were varied between 34 and 150 atm. Low-pressure gas solubility data served as a basis for extrapolation to high saturation pressures, as described elsewhere (9), for calculating hydrogen and H_2S concentrations in the reactor. Reactant concentrations used to correlate the reaction rate data were calculated for the liquid density at the temperature and pressure of the reactor.

Immediately after sulfiding of the catalyst, the reactor was cooled to 573°K, and flow of reactant mixture was initiated. The pressure in the reactor was maintained at 178 ± 7 atm to ensure against formation of a gas phase inside the reactor. A catalyst break-in period of 50 to 72 hr was allowed, after which the reactor was run with differential conversion of dibenzothiophene to obtain reaction rate data. Over an extended period, hydrogen and H_2S partial pressures were varied, and solutions with the above-mentioned dibenzothiophene concentrations were each investigated at 548, 573 and 598°K. Throughout each run, the rate of reaction was repeatedly measured at the standard condition of 573°K, 96 atm hydrogen partial pressure, 1.24 mole% dibenzothiophene, and 0 or 0.16 atm H_2S partial pressure; these data demonstrated the lack of significant catalyst deactivation.

At each run condition, four to eight liquid product samples were collected and analyzed by glc. An Antek 462 gas chromatograph equipped with a flame ionization detector and an electronic integrator was used. The column was a 3.4 m stainless steel column having a 2.3×10^{-3} m ID and packed with 3% SP-2100 DB (methyl silicone fluid--the basic sites were deactivated) on 100-200 mesh Supelcoport (Supelco) at 423°K with a helium carrier-gas flow rate of about 5×10^{-7} m³/s. Gaseous products, such as H_2S and any light cracking products, were not collected. In the routine analysis, dibenzothiophene, biphenyl, cyclohexylbenzene, and 1,2,3,4-tetrahydrodibenzothiophene were determined quantitatively. Another product formed in equilibrium with 1,2,3,4-tetrahydrodibenzothiophene, i.e., 1,2,3,4,10,11-hexahydrodibenzothiophene (4), was masked by the solvent.

Using a wall-coated open tubular column (Perkin-Elmer OV-101) in a Perkin-Elmer 3920 B gas chromatograph, a sufficient number of samples were reanalyzed to establish the equilibrium constant for the reaction $\{1,2,3,4\text{-tetrahydrodibenzothiophene} + H_2 \rightleftharpoons 1,2,3,4,10,11\text{-}$

hexahydrodibenzothiophene] at the three temperatures studied. Equilibrium constants are given in Table 1. The concentration of 1,2,3,4,10,11-hexahydrodibenzothiophene was then calculated for each sample from the equilibrium constant and the known concentration of hydrogen and 1,2,3,4-tetrahydrodibenzothiophene. Total aromatic carbon in the product stream was typically 98 to 99% of the amount of dibenzothiophene in the feed mixture.

RESULTS

Preliminary experiments reported earlier (4) showed that the reactor filled with alundum alone had negligible activity for dibenzothiophene hydrodesulfurization, and intraparticle and extraparticle mass transfer resistances were negligible.

Addition of 0.02 mole of H_2S /liter of reactant solution was necessary to stabilize the catalyst (10). With constant catalytic activity, rates were determined from differential conversions for a wide range of reactant and product concentrations at 548, 573, and 578°K; detailed data are given elsewhere (9). Concentrations and temperatures were changed randomly throughout, with periodic activity checks at the standard conditions.

Data were plotted as fractional conversion to cyclohexylbenzene, to biphenyl, and to cyclohexylbenzene plus 1,2,3,4-tetrahydrodibenzothiophene plus 1,2,3,4,10,11-hexahydrodibenzothiophene (9). The plots show a linear dependence of conversion on WHSV, and the first set of data falls near a curve that approaches the origin with near-zero slope. These results are consistent with the reaction network proposed for dibenzothiophene hydrodesulfurization by Houalla *et al.* (4). This network indicates two primary reactions: Hydrogenation of one aromatic ring gives an equilibrium mixture of 1,2,3,4-tetrahydrodibenzothiophene and 1,2,3,4,10,11-hexahydrodibenzothiophene; hydrodesulfurization of these two intermediates occurs rapidly to give cyclohexylbenzene. This combination of reactions is referred to as the hydrogenation route, and this combination of products determined rates of hydrogenation of dibenzothiophene. The second reaction was direct hydrodesulfurization of dibenzothiophene to give biphenyl, which is referred to as the hydrogenolysis reaction. Biphenyl also reacted with hydrogen to give cyclohexylbenzene, but this reaction was typically two orders of magnitude slower than the rate of dibenzothiophene hydrogenolysis (11).

In summary, the reactant and product concentration data give the overall rate of dibenzothiophene disappearance and also the rates of the two primary reactions of dibenzothiophene, one aromatic ring hydrogenation, and the other hydrogenolysis.

There was a consistent discrepancy in the results indicated by lack of closure of the mass balance on carbon. The sum of the hydrogenation and hydrogenolysis rates was on the average 80-85% of the rate of dibenzothiophene disappearance. The cause of this imbalance could not be determined, but it appears most likely to have been the result of some cracking to volatiles lost in sample collection; it is possible that some heavier products were formed, but the lack of catalyst deactivation suggests that the former possibility is more likely. The rate of unobserved product formation was virtually independent of reaction conditions, and the lack of closure of the

mass balance therefore did not prevent meaningful measurement of the reaction rates.

Representative plots of some of the rate data are given in Figures 1-3. A Langmuir dependence of rate on dibenzothiophene concentration is suggested for each reaction. The rate of hydrogenation is linearly dependent on hydrogen concentration, and the rate of hydrogenolysis shows a Langmuir dependence on hydrogen concentration. Inhibition by hydrogen sulfide was observed for dibenzothiophene hydrogenolysis, but a striking and surprising absence of hydrogen sulfide inhibition is noted for hydrogenation. The effect of biphenyl concentration on the overall rate of dibenzothiophene conversion was negligible at the lower temperatures; a small inhibition effect was observed at 598°K.

DISCUSSION

A number of rate equations, both purely empirical equations and equations corresponding to Langmuir-Hinshelwood models, were evaluated in terms of their ability to represent the data for dibenzothiophene hydrogenation and hydrogenolysis. An independent set of equations was considered for each of the two reactions. The full set of equations is considered elsewhere (9), and here we consider only the equations giving the best fits to the data.

A non-linear least-squares regression analysis was used with each equation in Tables 2 and 3 to determine the best equations for representing the data. A library program, NLLS (1977), from the University of Delaware Computing Center (based on the Marquardt regression technique) was used. The output of the program includes the parameter values giving the best fit as determined by the routine and several statistical measures of the goodness of fit. These are (1) ϕ_{\min} , the minimized sum of the squares of the differences between the observed and predicted rates for each condition, (2) a correlation matrix representing the degree of independence of each of the equation parameters from the other parameters, and (3) non-linear 95% confidence limits given as an upper and lower bound on the value of each of the parameters. Summarized in Tables 2 and 3 are the parameter values, the largest difference between the parameter value and the upper or lower bound, and the calculated ϕ_{\min} values. The full sets of equations evaluated for each reaction are given in Broderick's thesis (9).

In addition to the statistical criteria of goodness of fit, there are several criteria determining whether an equation has physical meaning: (1) The estimated rate constant and adsorption constants should be positive or include positive values within their error bounds; (2) a plot of the logarithm of the rate constant versus reciprocal absolute temperature (Arrhenius plot) should be linear with a negative slope; (3) a plot of the logarithm of each adsorption equilibrium constant versus reciprocal absolute temperature (van't Hoff plot) should be linear with a positive slope except when chemisorption is endothermic; and (4) a visual comparison between experimentally measured trends and predicted curves should show satisfactory agreement.

The six best equations for the hydrogenolysis reaction data are given in Table 2. Of these, the first four can be derived from the Langmuir-Hinshelwood model assuming various forms of competitive and noncompetitive adsorption, dissociative or undissociative. The last

two equations are similar in form but do not correspond to any simple Langmuir-Hinshelwood model.

Equations (HS-3), (HS-5), and (HS-6) were found to satisfy all the physical and statistical criteria enumerated above. If, in addition, an equation of Langmuir-Hinshelwood formulation is preferred, Eq. (HS-3) is the only acceptable choice. Eq. (HS-1) gives a poorer fit, judging by the magnitude of ϕ_{\min} . Eqs. (HS-2) and (HS-4) showed strong parameter correlation and relatively large deviations from linearity of the Arrhenius plot.

Eq. (HS-5) differs from Eq. (HS-3) only in the half power on the term K_5C_5 in the denominator. That same power on K_5C_5 in Eq. (HS-6) is largely responsible for the good fit observed for this equation as well. The half power on K_5C_5 in Eq. (HS-5) might be interpreted as a suggestion that adsorption of H_2S may occur dissociatively. This suggestion is not unprecedented (12), but it is considered speculative if based only on kinetics data.

Eq. (HS-3) is recommended as the best equation resting on a Langmuir-Hinshelwood model for representing the data for hydrogenolysis at all conditions studied. From the Arrhenius plot for this equation, the activation energy, determined from the temperature dependence of k/K_5 is 30 kcal/gmole. Following the Langmuir-Hinshelwood model, the heats of adsorption for dibenzothiophene, H_2S , and hydrogen were calculated to be -4.5, -5.3, and 8.4 kcal/gmole, respectively. The positive value for the heat of adsorption of hydrogen was observed for all of the equations tested and is perhaps an anomaly associated with the imprecision in the data; the 90% confidence limits on the heat of adsorption are large and include negative values.

Data for the rate of dibenzothiophene hydrogenation were best represented by the equations in Table 3; other equations are considered in Broderick's thesis (9). Differences in goodness of fit among these four equations are relatively small. Eq. (HN-1) is recommended for its goodness of fit, its simple form, and its low parameter correlation and error bounds relative to the other equations. Eqs. (HN-2) and (HN-3) have high error bounds on K_H , and Eqs. (HN-2) and (HN-4) show large deviations from linear Arrhenius plots. Differences in ϕ_{\min} are not significant when compared with the standard deviations of the data. The temperature dependence of k' (defined as k/K_D) and K_D were calculated from Arrhenius and van't Hoff plots. An activation energy of 27.6 kcal/gmole and a heat of adsorption for dibenzothiophene of -1.4 kcal/gmole resulted.

The literature on hydrogenolysis reaction kinetics in hydrodesulfurization of thiophenic compounds catalyzed by Co-Mo/ γ - Al_2O_3 is in general agreement with the results for dibenzothiophene. Much of the work has concerned thiophene (13-16) and benzothiophene (17) at pressures near atmospheric and for narrow ranges of hydrogen partial pressure. There is much evidence that the principal reaction for both compounds is hydrogenolysis. There is strong agreement that the dependence of rate on the concentrations of thiophenic reactant and of H_2S is the same as shown in Eq. (HS-3). The dependence of rate on hydrogen partial pressure has typically been represented as first order at low partial pressures (13-14,16), although data have been meager. One of the contributions of the present kinetics study was

therefore the clear determination of the dependence of rate on hydrogen concentration under conditions more typical of commercial processes.

The results of previous kinetics studies of dibenzothiophene differ somewhat from the kinetics for hydrogenolysis reported here. For conditions similar to those applied here but for a maximum hydrogen partial pressure of 31 atm, Espino *et al.* (7) and Mahoney *et al.* (8) reported a rate equation with a power of 1 on the denominator term for adsorption of H₂S and dibenzothiophene. Mahoney *et al.* observed a first order dependence of rate on hydrogen partial pressure. In neither study was the rate of hydrogenation distinguished from the rate of hydrogenolysis, and we infer that under the reported reaction conditions, both reactions contributed to the measured rates of dibenzothiophene conversion. Thus the reported kinetics do not represent hydrogenolysis alone, but correlate all reaction rates. They are in good agreement with the sum of the equations for hydrogenolysis and hydrogenation determined in this work (9).

Reported activation energies for hydrogenolysis of thiophene and benzothiophene range from 4 to 20 kcal/gmole (9) compared with approximately 30 kcal/gmole for hydrogenolysis of the less reactive dibenzothiophene. If we interpret the Langmuir-Hinshelwood rate equation literally (which is surely an oversimplification), we can infer values of the heats of adsorption from the slopes of the van't Hoff plots. The heat of adsorption calculated for H₂S implied by the hydrogenolysis rate equation falls within the range reported in the literature (5-20 kcal/gmole), and the value for dibenzothiophene (4.5 kcal/gmole) is lower than those for thiophene and benzothiophene (12-24 kcal/gmole).

Literature on the hydrogenation reaction of dibenzothiophene consists of the work by Houalla *et al.* (4) and Bhide (18), who used large excesses of hydrogen and accurately approximated the rate of dibenzothiophene disappearance by hydrogenation as a pseudo first-order reaction. Hydrogenations of other heteroaromatics, such as quinoline and pyridine, and of aromatics such as biphenyl, naphthalene, and benzene catalyzed by presulfided Co-Mo/ γ -Al₂O₃ have been studied, and limited kinetics data have been reported. For biphenyl, Espino *et al.* (7) represented rate data with a Langmuir-Hinshelwood equation indicating competitive adsorption of biphenyl and cyclohexylbenzene on one kind of site and of hydrogen on another. No measure of inhibition by H₂S was determined. Few details were given concerning the data and the criteria for selection of the rate equation. For pyridine (19) and quinoline (18,20) the rate of hydrogenation of the aromatic ring (or rings) was approximated as first order in heteroaromatic, but the rate constant decreased with increasing reactant concentration, suggesting self inhibition of reaction. The order of reaction in hydrogen partial pressure ranged from 1 to 1.5 for pyridine, and from 0.5 to 1 for quinoline. The effect of H₂S on the rate of hydrogenation of quinoline was negligible, and for pyridine, H₂S was an inhibitor when <2 mole% H₂S was present, and otherwise the rate was independent of H₂S concentration. For the most part, these kinetics results for hydrogenation reactions of nitrogen-containing aromatics are in agreement with the dibenzothiophene hydrogenation kinetics represented by Eq. (HN-1). These results suggest a rather wide application of Eq. (HN-1) for hydrogenation of aromatics and heteroaromatics.

Studying the hydrodesulfurization kinetics of dibenzothiophene has provided a unique opportunity to examine carbon-sulfur bond hydrogenolysis reactions and aromatic ring hydrogenation under identical conditions. Both reactions are of major importance in hydroprocessing. The kinetics results provide some insight into the mechanisms of the catalytic mechanisms, on one hand, and suggestions for tailoring the catalyst and process conditions to the desired product selectivity, on the other.

Comparison of Figures 1 and 2 and Eqs. (HS-3) and (HN-1) suggests that for sulfided CoO-Mo/ γ -Al₂O₃ catalyst, the reaction mechanism and catalytic sites differ for hydrogenation and hydrogenolysis. The literature supports the proposal of two different kinds of sites for hydrogenation and hydrogenolysis. The evidence is provided by results of poisoning (14,21,22) and kinetics (13,14,17,18) studies. One kind of site is strongly poisoned by bases such as pyridine and quinoline, and the other is less acidic and less sensitive to such poisons. The former sites are associated with hydrogenation activity and the latter with C-S bond scission activity, although some overlap is expected. From Equation (HN-1), it is inferred that the hydrogenation sites do not bond strongly to hydrogen or H₂S, but they do bond strongly to dibenzothiophene. In contrast, H₂S does compete strongly with dibenzothiophene for hydrogenolysis sites, as follows from Eq. (HS-3). The form of this equation suggests the hydrogen adsorbs on still another type of site, as is expected from the known formation of -SH groups on the surface.

The structure of dibenzothiophene adsorbed on the catalyst surface is unknown, but the extensive hydrogenation of the benzenoid rings suggests considerable ring interaction with the surface. Dibenzothiophene, being a planar molecule, is believed to adsorb in a plane parallel to the catalyst surface favorable to metal-ring interactions at anion vacancies on the surface. Proposals for adsorption via π -complex formation (23,24) or multi-point bonding (25) are strengthened by these results.

A well-recognized concern in hydroprocessing is the consumption of expensive hydrogen. Considering quantitatively the marked differences in the kinetics reported here for hydrogenation and hydrogenolysis of dibenzothiophene, we recognize two important processing variables for minimizing the hydrogen consumption in hydrodesulfurization. Decreased H₂S concentrations (obtainable by recycle gas scrubbing) favor hydrogenolysis. The change in selectivity is dramatic for H₂S concentrations between about zero and 0.1 gmole/liter. Temperature also strongly influences the relative rates of hydrogenation and hydrogenolysis. As the temperature is raised, the relative rate of hydrogenolysis increases sharply. The selectivity for dibenzothiophene hydrogenolysis also increases with increasing concentration of quinoline, an inhibitor of both hydrogenation and hydrogenolysis reactions (18). It is important to remember that, in general, competition between the sulfur-containing reactant and other feed components may alter the kinetics and selectivity. Recognizing this limitation, we recommend the kinetics presented here for qualitative guidance in process design and suggest that the form of the rate equation (modified to account for the presence of various inhibitors) could be of use in reaction engineering models for process simulation.

ACKNOWLEDGMENT

This research was supported by the Department of Energy.

REFERENCES

- (1) Houalla, M., D. Broderick, V. H. J. de Beer, B. C. Gates, and H. Kwart, Preprints, ACS Div. Petrol. Chem., 22, 941 (1977).
- (2) Nag, N. K., A. V. Sapre, D. H. Broderick, and B. C. Gates, J. Catal., 57, 509 (1979).
- (3) Eliezer, K. F., M. Bhide, M. Houalla, D. H. Broderick, B. C. Gates, J. R. Katzer, and J. H. Olson, Ind. Eng. Chem. Fundamentals, 16, 380 (1977).
- (4) Houalla, M., N. K. Nag, A. V. Sapre, D. H. Broderick, and B. C. Gates, AIChE J., 24, 1015 (1978).
- (5) Obolentsev, R. D., and A. V. Mashkina, Doklady Akad. Nauk SSSR, 119, 1187 (1958).
- (6) Obolentsev, R. D., and A. V. Mashkina, Khim. Seraorganicheskikh Soedinenii Soderzh v Neft'yakh i Nefteprod Akad. Nauk SSSR, 2, 228 (1959).
- (7) Espino, R. L., J. E. Sobel, G. H. Singhal, and G. A. Huff, Jr., Preprints, ACS Div. Petrol. Chem., 23 (1), 46 (1978).
- (8) Mahoney, J. A., K. K. Robinson, and E. C. Myers, Chemtech, 8, 758 (1978).
- (9) Broderick, D. H., Ph.D. Thesis, University of Delaware, 1980.
- (10) Broderick, D. H., Schuit, G. C. A., and Gates, B. C., J. Catal., 54, 94 (1978).
- (11) Sapre, A. V., and B. C. Gates, Preprints, ACS Div. Fuel Chem., in press.
- (12) Massoth, F. E., J. Catal., 36, 164 (1975).
- (13) Satterfield, C. N., and G. W. Roberts, AIChE J., 14 (1), 159 (1968).
- (14) Lee, H. C., and J. B. Butt, J. Catal., 49, 320 (1977).
- (15) Phillipson, J. J., AIChE Meeting, Houston, 1971.
- (16) Morooka, S., and C. E. Hamrin, Chem. Eng. Sci., 32, 125 (1977).
- (17) Kilanowski, D. R., and B. C. Gates, J. Catal., in press.
- (18) Bhide, M. V., Ph.D. Thesis, University of Delaware (1979).
- (19) Goudriaan, F., Ph.D. Thesis, Twente Institute of Technology, The Netherlands (1974).
- (20) Shih, S. S., J. R. Katzer, H. Kwart, and A. B. Stiles, Preprints, ACS Div. Petrol. Chem., 22, 919 (1977).
- (21) Desikan, P., and C. H. Amberg, Can. J. Chem., 42, 843 (1964).

- (22) Urimoto, H., and N. Sakikawa, Sekiyu Gakkaishi, 15 (11), 926 (1972).
- (23) Cowley, S. W., Ph.D. Thesis, Southern Illinois University, Carbondale (1975).
- (24) Singhal, G. H., and R. L. Espino, Preprints, ACS Div. Petrol. Chem., 23 (1), 36 (1978).
- (25) Kwart, H., G. C. A. Schuit, and B. C. Gates, J. Catal., in press.

NOMENCLATURE

C_i	Concentration of Species "i"	k'	Intrinsic Rate Constant (= $k/K_0/K_H$)
D	Dibenzothiophene	K_i	Adsorption Equilibrium Constant of Species i
H	Hydrogen (H_2)	S	Hydrogen Sulfide (H_2S)
HHD	Hexahydrodibenzothiophene	THD	Tetrahydrodibenzothiophene
k	Observed Rate Constant		

TABLE 1

Temperature Dependence of the
Equilibrium Constant K_X

Temp., $^{\circ}K$	K_X^a
548	5.76 ± 0.29^b
573	3.45 ± 0.33
598	2.05 ± 0.17

$$K_X \approx \text{EXP}(-\Delta G^{\circ}/RT),$$

$$\Delta G^{\circ} = 13,400 - T(^{\circ}K) \times 10.55 \text{ cal/gmole}$$

^a K_X is defined as $X_{HHD}/X_H X_{THD}$ where X_i is the mole fraction of species i.

^b K_X was calculated for various X_H and averaged. Error bound is standard deviation.

TABLE 2

Rate Equations Best Fitting Dibenzothiophene Hydrogenolysis Kinetic Data

Rate Equation	Temp., °C.	$10^6 \times k, \text{ liter}^2$ mole \cdot g. of catalyst \cdot hr.	k_D , liter mole	k_H , liter mole	k_S , liter mole	$10^{16} \times \phi_{\text{min}}$ ($\frac{\text{mole}}{\text{mole}} \cdot \text{sec.}$) 2
(HS-1) $\frac{k C_D C_H}{(1+k_D C_D + k_S C_S)^2}$	275 300 325	11.4 \pm 1.3 39.9 \pm 4.3 130 \pm 15	10.3 \pm 3.0 7.2 \pm 2.5 6.6 \pm 2.6	-- -- --	86 \pm 16 74 \pm 12 59 \pm 11	0.366 6.81 82.3
(HS-2) $\frac{k C_D C_H}{(1+k_D C_D + k_S C_S + k_H C_H)^2}$	275 300 325	30.1 \pm 3.9 200 \pm 22 439 \pm 53	18.1 \pm 5.8 18.5 \pm 6.1 14.5 \pm 5.0	2.9 \pm 1.3 6.0 \pm 1.4 4.1 \pm 1.2	137 \pm 31 161 \pm 27 103 \pm 21	0.342 5.39 63.3
(HS-3) $\frac{k C_D C_H}{(1+k_D C_D + k_S C_S)^2 (1+k_H C_H)}$	275 300 325	15.7 \pm 2.0 69.3 \pm 7.5 215 \pm 26	11.5 \pm 3.5 8.7 \pm 2.7 8.2 \pm 2.8	1.6 \pm 1.0 3.2 \pm 1.1 2.9 \pm 1.2	86 \pm 19 75 \pm 12 58 \pm 12	0.341 5.36 63.4
(HS-4) $\frac{k C_D C_H}{(1+k_D C_D + k_S C_S)^2 [1 + (k_H C_H)^{1/2}]^2}$	275 300 325	20.3 106.3 315	11.4 8.5 8.1	0.46 1.72 1.40	86.5 76.9 58.1	0.361 5.41 64.6
(HS-5) $\frac{k C_D C_H}{[1 + k_D C_D + (k_S C_S)^{1/2}]^2 (1 + k_H C_H)}$	275 300 325	59.9 \pm 4.7 205 \pm 14 503 \pm 33	23.9 \pm 3.8 16.4 \pm 2.7 13.3 \pm 2.2	1.77 \pm 0.59 3.20 \pm 0.61 2.96 \pm 0.60	868 \pm 144 518 \pm 72 256 \pm 38	0.122 1.99 18.7
(HS-6) $\frac{k C_D C_H}{(1 + k_D C_D + k_H C_H)^2 [1 + (k_S C_S)^{1/2}]^2}$	275 300 325	25.1 \pm 1.9 111.0 \pm 7.4 323 \pm 21	5.2 \pm 1.2 4.7 \pm 1.0 5.0 \pm 0.9	0.89 \pm 0.28 1.44 \pm 0.27 1.38 \pm 0.27	270 \pm 42 221 \pm 29 127 \pm 17	0.122 1.98 18.3

TABLE 3
Rate Equations Best Fitting Dibenzothiophene Hydrogenation Kinetics Data

Rate Equation	Temp., °C	$10^6 \times k,$ $\frac{\text{liter}^2}{\text{gmole} \cdot \text{g of catalyst} \cdot \text{sec}}$	K_D $\frac{\text{liter}}{\text{gmole}}$	$K_H,$ $\frac{\text{liter}}{\text{gmole}}$	$K_S,$ $\frac{\text{liter}}{\text{gmole}}$	$10^{17} \times \phi_{\text{min}},$ $\left(\frac{\text{gmole}}{\text{g of catalyst} \cdot \text{sec}}\right)^2$
(HN-1) $k \frac{C_D C_H}{(1+K_D C_D)}$	275 300 325	2.78 ± 0.11 8.11 ± 0.24 20.9 ± 0.57	7.39 ± 0.89 7.70 ± 0.72 6.61 ± 0.55	-- -- --	--	1.30 7.14 24.3
(HN-2) $k \frac{C_D C_H}{(1+K_D C_D)(1+K_H C_H)}$	275 300 325	2.95 ± 0.14 8.60 ± 0.30 21.6 ± 0.7	7.6 ± 1.07 7.92 ± 0.85 6.73 ± 0.67	0.25 ± 0.25 0.26 ± 0.19 0.14 ± 0.16	-- -- --	1.26 6.78 23.7
(HN-3) $k \frac{C_D C_H}{(1+K_D C_D + K_H C_H)}$	275 300 325	2.98 ± 0.14 8.69 ± 0.30 21.7 ± 0.66	8.0 ± 1.1 8.4 ± 0.9 6.9 ± 0.7	0.31 ± 0.35 0.32 ± 0.26 0.16 ± 0.22	-- -- --	1.26 6.80 23.7
(HN-4) $k \frac{C_D C_H}{[1+(K_D C_D)^{\frac{1}{2}}]^2 (1+K_H C_H)}$	275 300 325	4.34 ± 0.18 12.6 ± 0.4 30.2 ± 0.74	3.78 ± 0.50 3.91 ± 0.41 2.81 ± 0.25	0.27 ± 0.22 0.27 ± 0.17 0.16 ± 0.13	-- -- --	0.987 5.73 16.0

FIGURE 1

REACTION RATES IN DIBENZOTHIOPHENE
HYDRODESULFURIZATION AS A FUNCTION OF
HYDROGEN CONCENTRATION AT 300°C

Curves are Predicted by Fitted Rate
Equations Described in the Text

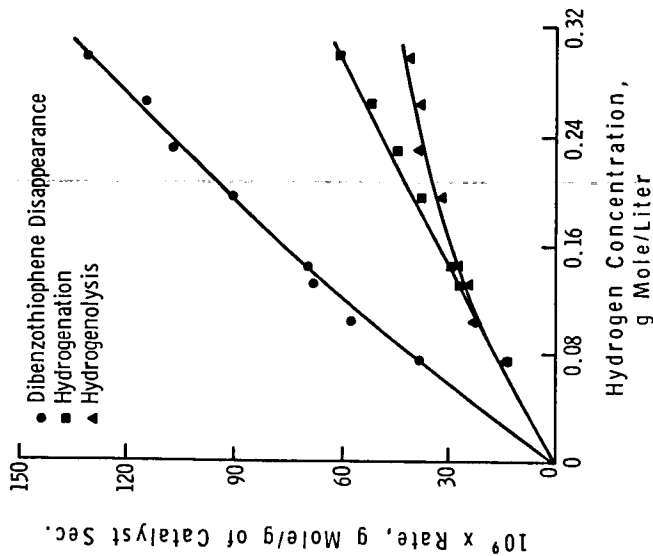


FIGURE 2

REACTION RATES IN DIBENZOTHIOPHENE
HYDRODESULFURIZATION AS A FUNCTION OF
DIBENZOTHIOPHENE CONCENTRATION AT 300°C

Curves are Predicted by Fitted Rate
Equations Described in the Text

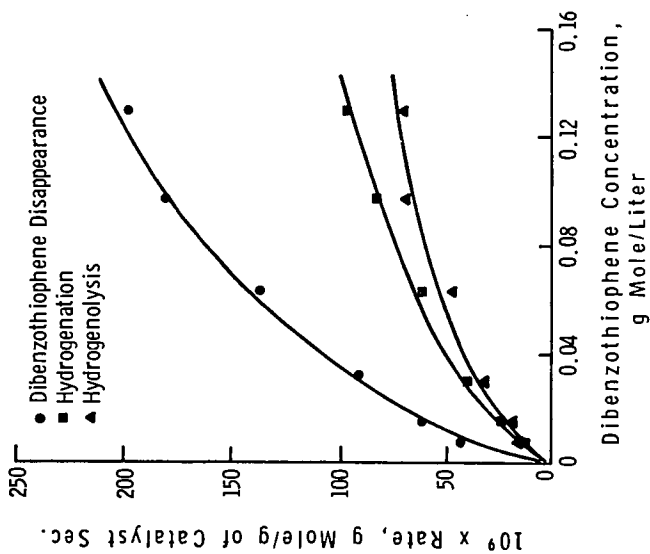
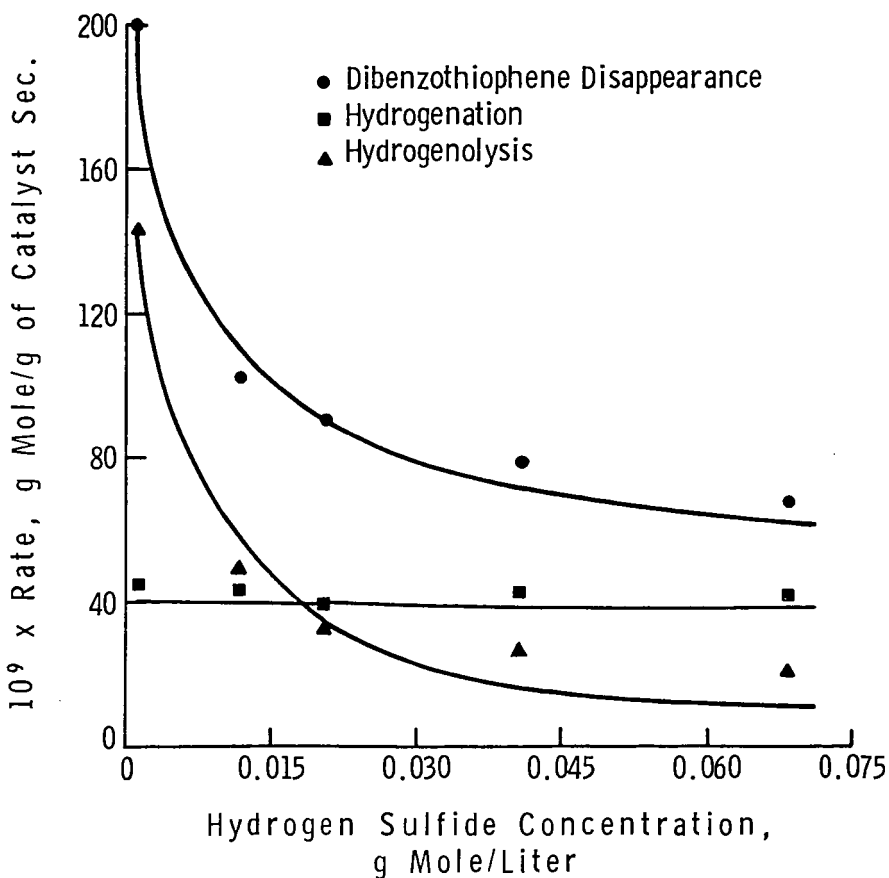


FIGURE 3
 REACTION RATES IN DIBENZOTHIOPHENE
 HYDRODESULFURIZATION AS A FUNCTION OF
 HYDROGEN SULFIDE CONCENTRATION AT 300°C

Curves are Predicted by the Fitted Rate
 Equations Described in the Text



Hydrogenation of Aromatic Hydrocarbons
Catalyzed by Sulfided $\text{CoO-MoO}_3/\gamma\text{-Al}_2\text{O}_3$:
Reactivities, Reaction Networks, and Kinetics

A. V. Sapre and B. C. Gates

Center for Catalytic Science and Technology
Department of Chemical Engineering
University of Delaware
Newark, Delaware 19711

INTRODUCTION

Accompanying the recent emphasis on new energy sources, there has been a surge of development work on processes for upgrading heavy fossil fuels, including coal liquids, shale oil, tar sands, and petroleum residua. Upgrading is normally effected by hydrotreating in the presence of catalysts like "cobalt molybdate" or "nickel molybdate" at 50-250 atm and 300-450°C (1). In these applications, the principal catalytic reactions are hydrodesulfurization, hydrodenitrogenation, hydrodeoxygenation, hydrocracking, and hydrogenation of aromatics. Among the slowest of these reactions are the aromatic hydrogenations, which take on great importance because hydrodenitrogenation of polycyclic aromatics does not take place until ring saturation has occurred (2). It therefore appears that with the best available catalysts, hydrogenation of aromatics is the class of hydroprocessing reactions most deserving of careful study.

Hydrogenation of aromatics is also important in developing coal liquefaction technology exemplified by the donor solvent process and some forms of the solvent refined coal process (3); in these processes the product liquid undergoes catalytic hydrogenation and is then recycled to the liquefaction reactor, where it transfers hydrogen to the liquefying coal (4).

The literature of catalytic hydroprocessing provides only fragmentary information about the reaction networks, reactivities, and kinetics in aromatic hydrogenation, most of the work having been done with unpromoted catalysts at conditions far removed from those of industrial interest (5). The reported kinetics data for hydrogenation of aromatics in the presence of promoted sulfided catalyst like "cobalt molybdate" are limited to benzene, cyclohexene, toluene, phenanthrene, and naphthalene (6-11).

The experiments reported here were carried out to establish the reactivities and reaction networks for hydrogenation of benzene, biphenyl, naphthalene, and 2-phenylnaphthalene as well as detailed kinetics of biphenyl hydrogenation in the presence of a commercial catalyst (sulfided "cobalt molybdate," $\text{CoO-MoO}_3/\gamma\text{-Al}_2\text{O}_3$). The relative reactivities and reaction networks were determined at a pressure (75 atm), and temperature (325°C) representative of industrial conditions. The biphenyl kinetics experiments were done over a pressure range of 64-200 atm and a temperature range of 300-375°C.

Biphenyl and 2-phenylnaphthalene were chosen as model reactants in part because they are the principal aromatic products formed in the hydrodesulfurization of dibenzothiophene and of benzo[b]naphtho[2,3-d]-

thiophene, respectively (12,13). The latter two compounds are typical of the least reactive sulfur-containing compounds found in the heavier petroleum residua and coal-derived liquids. Naphthalene was chosen because upon hydrogenation it forms tetralin, the most widely used model compound used as a hydrogen donor in coal liquefaction experiments.

EXPERIMENTAL

The experiments designed to determine relative reactivities were carried out in a commercial one-liter batch reactor (Autoclave Engineers). The design of the autoclave allowed charging of the catalyst after the reactants had been brought to reaction temperature, thereby virtually eliminating any heat-up period which would prevent elucidation of isothermal kinetics from the conversion data (14). The catalyst was particles ($\sim 150\mu\text{m}$) of $\text{CoO-MoO}_3/\gamma\text{-Al}_2\text{O}_3$ (American Cyanamid HDS 16A), 2g of which were externally sulfided at 400°C with 10 vol% H_2S in H_2 at atmospheric pressure for two hours prior to being charged to the reactor. The reactant solution (375 ml) contained roughly 0.75 mole% of the hydrocarbon reactant in *n*-hexadecane (Humphrey Chemical Co., redistilled). The solution was saturated with hydrogen at the reaction temperature, providing a large stoichiometric excess of this reactant. The reactor was operated at 75 ± 2 atm and $325 \pm 1^\circ\text{C}$ in all the experiments. Carbon disulfide, 0.1 mole%, was added to the reaction mixture. It was found that this source of sulfur in the reactant was essential to maintain the activity of the catalyst by maintaining it in the sulfided form (15). The CS_2 was almost instantaneously converted into H_2S under the reaction conditions, the rate of the hydrogenolysis reaction



being at least 8000 times greater than that of the aromatic hydrogenation reactions.

The biphenyl kinetics studies were carried out using a high-pressure flow microreactor, the design and operation of which are described elsewhere (16). The reactor operated with solid particles of catalyst and a liquid reactant phase saturated with hydrogen.

The operating conditions of the flow reactor used for the kinetics experiments are summarized in Table 1.

TABLE 1. Operating conditions for the flow reactor

Catalyst: commercial $\text{CoO-MoO}_3/\gamma\text{-Al}_2\text{O}_3$ (American Cyanamid HDS 16A)
 mass: 0.025-0.050g diluted with particles of alundum
 particle size: $150\mu\text{m}$
 volume of catalyst bed: 0.325 cm^3
 length of bed: 4.0 cm
 Catalyst pretreatment: sulfided in situ with 10% H_2S in H_2 for two hours at 400°C
 Reactor pressure: 64-200 atm
 Temperature: $300\text{-}375^\circ\text{C}$
 Biphenyl concentration: $5\text{-}25 \times 10^{-3}$ gmoles/liter
 Cyclohexylbenzene concentration: $0\text{-}13 \times 10^{-3}$ gmoles/liter
 Carbon disulfide concentration: $4\text{-}18 \times 10^{-3}$ gmoles/liter
 Hydrogen concentration: $100\text{-}450 \times 10^{-3}$ gmoles/liter
 Liquid flow rate: $0.2\text{-}60\text{ cm}^3/\text{hr}$.
 Solvent (carrier oil): *n*-hexadecane.

Materials:

The reagents naphthalene (>99%) and benzene (>99%) were supplied by Fisher; bicyclohexyl (>98%), cyclohexylbenzene (>98%), and tetralin (>99%) by Aldrich; biphenyl (>98%) by Eastman; and 2-phenylnaphthalene (>98%) by ICN Pharmaceuticals. All these reagents were used without further purification.

Product analysis:

The product samples from the flow reactor were analyzed with an Antek 440L gas chromatograph equipped with a flame ionization detector. The column was packed with methylsilicone on 100-200 mesh Supelcoport (GP 3% SP-2100 DB) operated at 140°C.

The product samples drawn periodically from the batch reactor were analyzed with a Perkin-Elmer 3920 B gas chromatograph equipped with a flame ionization detector and a 0.8 mm-O.D. X 0.025 mm-I.D. X 100-m-long wall-coated open tubular column (the liquid phase was OV-101, Perkin Elmer) with an all-glass splitter injector. The column temperature was varied depending on the reactant compound, and temperature programming was used to improve peak resolution.

Principal reaction products formed from benzene, biphenyl, and naphthalene were identified by comparing glc retention times of the known compounds with retention times of components of the product mixtures. For identification of the primary products of 2-phenylnaphthalene hydrogenation, tricarbonylchromium complexes of the products were synthesized using chromium hexacarbonyl (17). The tricarbonyl chromium complexes which were formed were separated by the column chromatography technique on an alumina (4% water) column. The hydrocarbon solvent and uncomplexed material were eluted with n-pentane. The separation of the complexes on the column was achieved by using different proportions of n-pentane and methylene chloride. The structures of the recrystallized complexes were determined by proton NMR spectroscopy; details of this technique are given elsewhere (13).

From these product analyses, conversion-time data were obtained for each set of reactants and products in the batch reactor experiments. In the flow reactor, differential conversions were measured to determine rate data directly. The rate data were obtained over a wide range of independent variables; mixed feeds were used, including the reaction products in widely varied concentrations.

RESULTS AND DISCUSSION

Figure 1 shows the principal products and the reaction networks for the aromatic compounds studied in the batch reactor. In all these experiments, mass balances obtained from the unconverted reactant and the products were good. Naphthalene analysis was extremely good, and mass balance of more than 98% was observed for all the samples.

In the flow-reactor experiments a linear relation between conversion and inverse space velocity was observed up to about 15% biphenyl conversion, demonstrating that all the data reported here represented differential conversions. These low-conversion data always showed more than 99% mass balance.

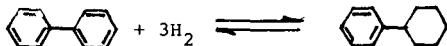
Blank experiments performed in the batch reactor with hydrogen and biphenyl and with hydrogen and cyclohexylbenzene confirmed that there was no observable conversion of these reactants even under more severe conditions (400°C and 100 atm), indicating that all the observed reactions were catalytic. These results are consistent with the thermochemical calculations reported by Ross et al. (20), showing the extreme stability of the C-C bond towards homolysis and free radical formation in the molecules like biphenyl and naphthalene.

In batch experiments with benzene, cyclohexane was observed as the only primary product. The concentration-time profiles for the benzene reaction are shown in Fig. 2. The unidentified hydrocarbon indicated in the benzene reaction network (Fig. 1) was not separated in the glc analysis. The benzene-cyclohexane reaction is reversible and is well documented in the literature (5), and so experiments with cyclohexane as a reactant were not done.

The most thorough set of experiments was carried out with biphenyl, which reacted with hydrogen to give cyclohexylbenzene as a primary product. Cyclohexylbenzene was subsequently converted into bicyclohexyl. The concentration-time plots for the biphenyl reaction network are shown in Fig. 3; the data clearly show that bicyclohexyl is a secondary product, since the slope of the curve at zero time is zero.

Three unidentified hydrocarbon products having very nearly equal retention times on the glc column were also observed in small quantity (in total, about 10% at the maximum conversion). Hydrogenation experiments carried out with cyclohexylbenzene and with bicyclohexyl as the reactants showed that these hydrocarbons were formed as primary products from cyclohexylbenzene, but not from bicyclohexyl. The comparison of the glc retention times of these products with those of several possible products obtained from ring opening (substituted benzene or cyclohexane) and substituted indane and tetralin suggest that these products were not obtained by cracking of biphenyl or by C-C bond cleavage followed by ring closure. Urimoto et al. (18) performed dibenzothiophene hydrodesulfurization experiments and observed 3-methylcyclopentylcyclohexane and 3-3'-dimethyldicyclopentyl products using a catalyst and reaction conditions similar to those used in this work, which indicates the occurrence of isomerization reactions. During hydroprocessing reactions, isomerization of cyclohexane to methylcyclopentane and of tetralin to methyl indane is reported in the literature (5,19). This information suggests that the three unidentified products could be isomerized products formed from cyclohexylbenzene--for example, methylcyclopentylbenzene.

These three products together are represented as hydrocarbons in the reaction network shown in Fig. 1. In experiments with hydrogen and cyclohexylbenzene as reactants, biphenyl was formed, indicating that the primary hydrogenation reaction,



is reversible. The experiments in the flow reactor were designed to determine the nonlinear rate expression for this primary hydrogenation-dehydrogenation reaction. Fig. 4 shows a typical set of data obtained at 350°C. The differential conversion experiments were done at 300, 325, 350 and 375°C; the full set of rate data was fitted with a non-

linear least squares technique (21). The following rate expression represents the data with a high degree of accuracy, but several other equations (similar in form) provide comparable fits. Work on discrimination of the equations is continuing; this rate expression should be considered tentative:

$$r = \frac{k K_{\text{BPH}} K_{\text{H}_2}^3 (C_{\text{BPH}} C_{\text{H}_2}^3 - \frac{1}{K_E} C_{\text{CHB}})}{(1.0 + K_{\text{BPH}} C_{\text{BPH}} + K_{\text{H}_2} C_{\text{H}_2})^2 (1.0 + K_{\text{H}_2} C_{\text{H}_2})^2} \quad (2)$$

$$k = 8 \times 10^7 \exp\left(-\frac{32,000}{RT}\right)$$

$$K_{\text{BPH}} = 4.5 \times 10^{-5} \exp\left(\frac{14,000}{RT}\right)$$

$$K_{\text{H}_2\text{S}} = 1.6 \times 10^{-4} \exp\left(\frac{13,000}{RT}\right)$$

$$K_{\text{H}_2} = 4.25 \exp\left(\frac{4,000}{RT}\right)$$

$$K_E = 2.2 \times 10^{-3} \exp\left(\frac{16,500}{RT}\right)$$

BPH = biphenyl, H₂ = hydrogen, CHB = cyclohexylbenzene

The smooth lines in Fig. 4 are the predictions based on the above equation. It is clear that this equation fits the data well.

In batch experiments, naphthalene was hydrogenated to give 1,2,3,4-tetrahydronaphthalene (tetralin) as a primary product. Tetralin was further hydrogenated to give cis- and trans-decahydronaphthalene (decalin). Time-concentration profiles for naphthalene and its reaction products are presented in Fig. 5. From these data, it is evident that equilibrium is approached between tetralin and naphthalene.

In experiments with hydrogen and tetralin as reactants, naphthalene was formed, indicating that the primary hydrogenation reaction is reversible. Trans-decalin was the predominant isomer of decalin. No other hydrocarbon products were detected.

Hydrogenation of 2-phenylnaphthalene gave two primary products, 2-phenyltetralin and 6-phenyltetralin, each of which experienced further hydrogenation. The concentration-time profiles are presented in Fig. 6. The secondary products are represented together as hydrocarbons in this analysis, consisting chiefly of phenyl-substituted decalins. 2-Phenyltetralin or 6-phenyltetralin are not commercially available, and experiments were not performed with these as reactants to demonstrate whether the primary hydrogenation reactions were reversible. But on the basis of the experience with biphenyl and naphthalene, it was assumed that the primary hydrogenation reactions are reversible. It can be seen from the data presented in Fig. 6 that equilibrium is approached between 2-phenylnaphthalene and its two primary products, 2-phenyltetralin and 6-phenyltetralin.

In contrast to these hydrogenation reactions, hydrodesulfurization reactions are practically irreversible, and the conversion data for the individual sulfur-containing compounds follow pseudo-first order behavior (23). As the primary hydrogenation reactions studied here are reversible, a deviation from the pseudo-first order behavior was observed as equilibrium was approached. The pseudo-first order rate constants for the overall disappearance of the component, determined from the low conversion data, are summarized in Table 2. For the determination of rate constants to represent the reaction networks from the high conversion data, it was assumed that each reaction in the network was pseudo-first order in the organic reactant. All the reversibilities were taken into account in representing quantitative kinetics for the complete reaction networks. The pseudo-first order rate constants were estimated from the full set of data determined in the experiments with each organic reactant, as follows: (1) In the case of benzene and biphenyl, raw concentration versus time data were smoothed by fitting spline functions using the IMSL subroutine ICSMOU (24); this program performs one dimensional data smoothing by error detection and is highly effective in smoothing a data set only mildly contaminated with isolated errors; (2) the smoothed data were used with equal weighting in the Carlton 2 program (25) to determine best values of the individual rate constants. The values of the rate constants for the individual reactions in the networks are shown in Fig. 1. The lines in Figs. 2,3,5,6 represent the model predictions from the estimated pseudo first-order rate constants based on the individual reaction networks shown in Fig. 1.

TABLE 2. Pseudo-first order rate constants for hydrogenation catalyzed by sulfided CoO-MoO₃/γ-Al₂O₃ at 325°C and 75 atm.

Reactant	Concentration, mole%	10 ⁶ X Pseudo-first order rate constant m ³ /kg of catalyst·sec ^a
Benzene	0.65	2.8 ± 0.1
Biphenyl	0.80	3.0 ± 0.2
Naphthalene	0.85	58.9 ± 3.6
2-Phenyl-naphthalene	0.75	61.4 ± 5.3

^aData are reported with 95% confidence limits.

The final conversion levels for naphthalene and 2-phenyl-naphthalene were of the order of 99%, whereas biphenyl and benzene were only about 75% converted after completion of the experiments. Experiments were carried out for long periods so that good estimates of the equilibrium constants could be obtained from the conversion data. The equilibrium constant for the biphenyl hydrogenation, $K_E = [CCHB/CBPH \cdot CH_2^3]_{\text{equil.}} = 365$, obtained from the above analysis of the kinetics, agrees fairly well with Frye's (26) gas-phase equilibrium experiments. At 325°C his data indicate K_E to be equal to 485.

From these networks, it can be seen that primary products obtained by aromatic hydrogenation are hydroaromatics, potential hydrogen donors which can readily be dehydrogenated in the presence of liquefying coal. The relative hydrogen-donor capacity of several

hydroaromatics was determined by Doyle (22), his results showing that tetralin or substituted tetralins are much better hydrogen donors than cyclohexylbenzene.

Liquefaction of coal has been shown to occur almost instantaneously upon reaching a high temperature in the presence of a hydrogen-donor solvent (27). Thus the slow steps in the hydrogenation/liquefaction process may be the hydrogenation of the recycle solvent to replenish hydrogen donor species (28). One of the objectives in the solvent hydrogenation is to maximize the yield of hydroaromatics. The reactions leading to consumption of hydroaromatic (for example, further hydrogenation of tetralin to decalins or isomerization of hydroaromatics) are undesirable, as they result in a solvent of reduced hydrogen-donor capacity. From Fig. 1 it is evident that these undesirable side reactions are relatively slow compared with the primary hydrogenation reactions. Under the experimental conditions of this study, the hydrogenation-dehydrogenation equilibrium was favorable towards higher yields of hydroaromatics. The biphenyl kinetics indicates that at higher temperatures dehydrogenation reactions are more significant, which suggests a strategy of maximizing yields of hydroaromatics by applying lower temperatures and high hydrogen partial pressures. The catalyst would also play an important role; the ideal catalyst would have moderate hydrogenation activity to hydrogenate the solvent to constituents like tetralin. But it should not have excessive activity to over-hydrogenate and form poor hydrogen donors like decalin, the formation of which would also represent excessive consumption of the costly hydrogen.

Ahuja et al. (7) ascribed the isomerization of cyclohexane to methylcyclopentane to the acidity of the support, and it follows from their suggestion that the isomerization of hydroaromatics would be less if less acidic catalyst supports (like SiO_2) were used. The isomerization reactions are significantly inhibited by nitrogen-containing compounds (7), hence the feeds with higher concentrations of nitrogen-containing compounds might seem to be favorable--except that nitrogen-containing compounds also strongly inhibit the hydrogenation reactions (2).

The results of Table 1 show that benzene and biphenyl have nearly the same reactivity; naphthalene and 2-phenylnaphthalene have nearly equal reactivities, one order of magnitude less than that of benzene. The high-pressure, high-temperature hydrogenation of benzene and naphthalene reported to occur in the presence of unsupported MoS_2 and WS_2 catalysts, indicates a 17-fold higher reactivity of naphthalene in comparison with benzene (5), which agrees well with the results reported in Table 1.

Naphthalene has a resonance energy of 75 kcal/mole, which is less than twice that of benzene's 42 kcal/mole (29), i.e., the rings in naphthalene are less aromatic in character than that of benzene and so more easily reduced, which explains the higher reactivity of naphthalene.

REFERENCES

- (1) Gates, B. C., Katzer, J. R., and Schuit, G. C. A., "Chemistry of Catalytic Processes," Chap. 5, McGraw-Hill, New York (1979).
- (2) Bhide, M. V., Ph.D. thesis, University of Delaware (1979).
- (3) National Academy of Sciences, Assessment of Technology for Liquefaction of Coal, Washington, D.C., 1977.
- (4) Furlong, L. E., Effron, E., Vernon, L. W., and Wilson, E. L., Chem. Eng. Progr., 72 (8), 69 (1976).
- (5) Weisser, O., and Landa, S., "Sulphide Catalysts, Their Properties and Applications," Pergamon, New York, 1973.
- (6) Voorhoeve, R. J. H., and Stuiver, J. C. M., J. Catal., 23, 228 (1971).
- (7) Ahuja, S. P., Derrien, M. L., and LePage, J. F., Ind. Eng. Chem. Prod. Res. Develop., 9, 272 (1970).
- (8) Huang, C. S., M.S. thesis, University of Mississippi (1976).
- (9) Rollmann, L. D., J. Catal., 46, 243 (1977).
- (10) de Beer, V. H. J., Dahlmans, J. G. S., and Smeets, J. G. M., J. Catal., 42, 467 (1976).
- (11) Hagenbach, G., Courty, Ph., and Delmon, B., J. Catal., 23, 295 (1971).
- (12) Houalla, M., Nag, N. K., Sapre, A. V., Broderick, D. H., and Gates, B. C., AIChE J., 24, 1015 (1978).
- (13) Sapre, A. V., Broderick, D. H., Fraenkel, D., Gates, B. C., and Nag, N. K., AIChE J., in press.
- (14) Shih, S. S., Katzer, J. R., Kwart, H., and Stiles, A. B., Preprints, ACS Div. Petrol. Chem., 22, 919 (1977).
- (15) Sapre, A. V., Ph.D. Thesis, University of Delaware, in preparation.
- (16) Eliezer, K. F., Bhide, M., Houalla, M., Broderick, D. H., Gates, B. C., Katzer, J. R., and Olson, J. H., Ind. Eng. Chem. Fundam., 16, 380 (1977).
- (17) Nicholls, B., and Whiting, M., J. Chem. Soc. (London), 551 (1959).
- (18) Urimoto, H., and Sakikawa, N., Sekiyu Gakkaiishi, 15, 926 (1972).
- (19) Cronauer, D. C., Jewell, D. M., Shah, Y. T., and Kueser, K. A., Ind. Eng. Chem. Fundam., 17 (4), 291 (1978).

- (20) Ross, D. S. and Blessing, J. E., Prepr. ACS Div. Fuel Chem. 24, 129 (1979).
- (21) NLLS program, University of Delaware Computing Center.
- (22) Doyle, G., Prepr. ACS Div. Petrol. Chem., 21, 165 (1975).
- (23) Nag, N. K., Sapre, A. V., Broderick, D. H., and Gates, B. C., J. Catal., 57, 509 (1979).
- (24) ICSSMOU, computer subroutine, International Mathematical and Statistical Library.
- (25) Himmelblau, D. M., Jones, C. R., and Bischoff, K. B., Ind. Eng. Chem. Fundam., 6, 539 (1967).
- (26) Frye, C. G., J. Chem. Eng. Data, 7, 592 (1962).
- (27) Whitehurst, D. D., and Mitchell, T. D., Prepr. ACS Div. of Fuel Chem., 21 (5), 127 (1976).
- (28) Guin, J. A., Tarrer, A. R., Lee, J. M., Lo, L., and Curtis, C. W., Ind. Eng. Chem. Proc. Des. Dev., 18, 371 (1979).
- (29) Pauling, L., "The Nature of The Chemical Bond," Cornell University Press, 1967.

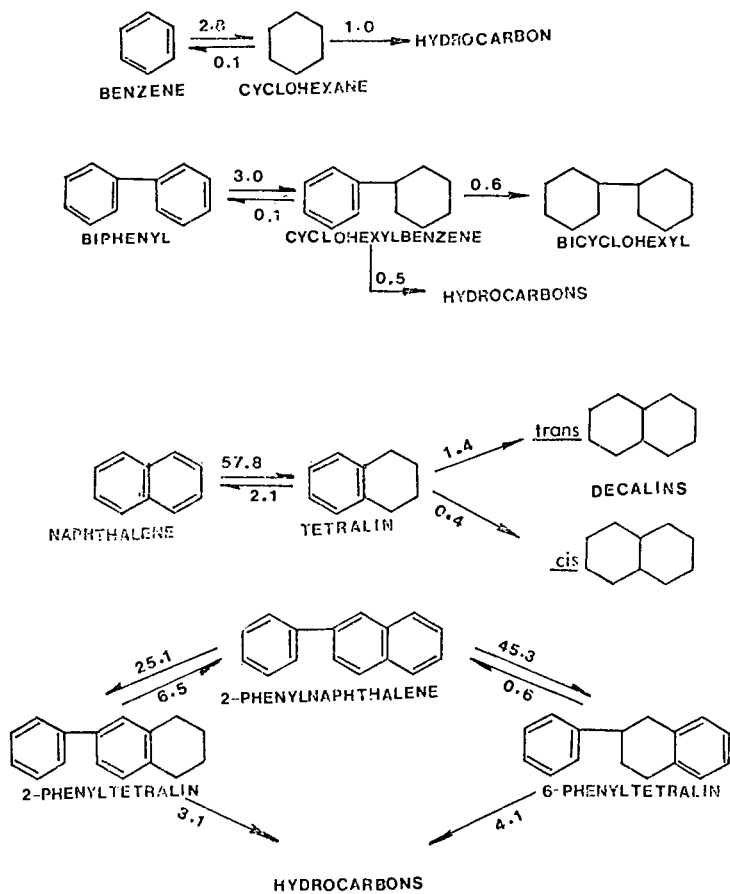


Fig. 1: Reaction networks for hydrogenation of benzene, biphenyl, naphthalene, and 2-phenylnaphthalene in the presence of sulfided $\text{CO-MoO}_3/\gamma\text{-Al}_2\text{O}_3$ at 325°C and 75 atm. Each reaction is approximated as first order in the organic reactant; the numbers next to the arrows are the pseudo first order rate constants in $10^9 \times$ cubic meters per kilogram of catalyst per second.

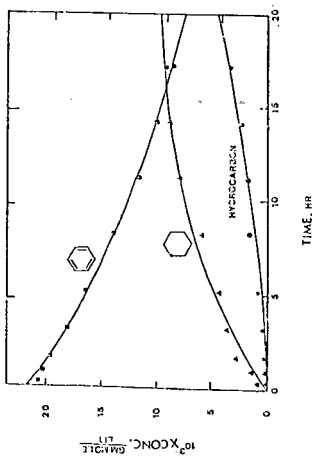


Fig. 2: Conversion of benzene and H_2 in the presence of sulfided $CoO-MoO_3/\gamma-Al_2O_3$ in a batch reactor at $325^\circ C$ and 75 atm. The curves are the predictions of the reaction network model of Fig. 1.

Fig. 3: Conversion of biphenyl and H_2 in the presence of sulfided $CoO-MoO_3/\gamma-Al_2O_3$ in a batch reactor at $325^\circ C$ and 75 atm. The curves are the predictions of the reaction network model of Fig. 1.

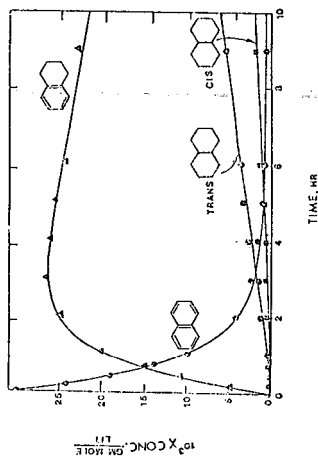
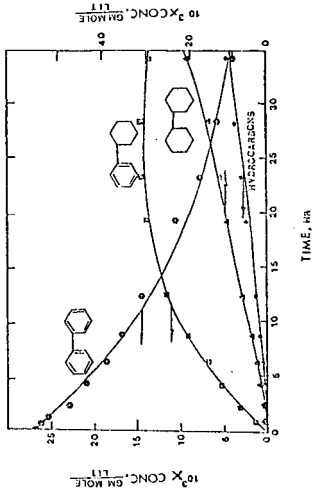


Fig. 5: Conversion of naphthalene and H_2 in the presence of sulfided $CoO-MoO_3/\gamma-Al_2O_3$ in a batch reactor at $325^\circ C$ and 75 atm. The curves are the predictions of the reaction network model of Fig. 1.

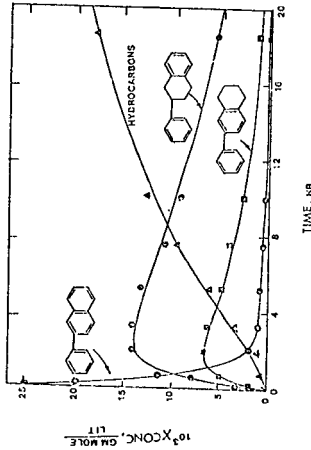


Fig. 6: Conversion of 2-phenylnaphthalene and H_2 in the presence of sulfided $CoO-MoO_3/\gamma-Al_2O_3$ in a batch reactor at $325^\circ C$ and 75 atm. The curves are the predictions of the reaction network model of Fig. 1.

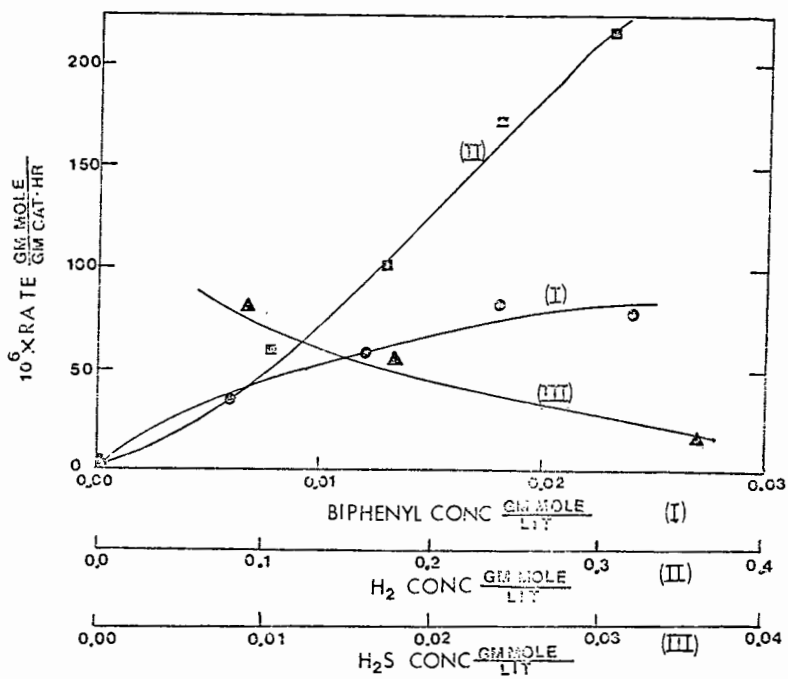


Fig. 4: Rate of biphenyl hydrogenation as a function of hydrogen, H_2S , and biphenyl concentrations at 350°C . The curves are cubic spline fits through individual points predicted by rate equation given in the text, for the actual concentrations at each point.

CATALYTIC UPGRADING OF H-COAL SYNCRUDES. Dennis J. O'Rear, Richard F. Sullivan, and Bruce E. Stangeland, Chevron Research Company, P.O. Box 1627, Richmond, California 94802.

The net liquid product from the H-Coal liquefaction process was refined to liquid fuels by commercial catalysts in pilot plants which simulate advanced state-of-the-art petroleum hydroprocessing technology. Liquids derived from two different coals were studied: Illinois No. 6 coal (Burning Star Mine) and Wyodak coal. One hydrotreating stage, operated at several severities, upgraded the whole product to either jet, diesel, or heating fuels. In addition, a naphtha was produced which can be used for hydrogen production or as feed to a catalytic reformer. The kerosene jet fuel meets all critical specifications, including smoke point and stability. The maximum yield of jet derived from Illinois coal is almost 90%. The diesel and heating fuels meet most specifications when additives are used. For maximum gasoline production, the hydrotreated H-coal product was converted to naphtha in a single-stage extinction-recycle hydrocracker.

HYDROTREATMENT AND BIOLOGICAL TEST OF SRC-II COAL LIQUID

Dexter Sutterfield, W. C. Lanning

U.S. Department of Energy, Bartlesville Energy
Technology Center, P. O. Box 1398, Bartlesville, OK 74003

and R. E. Royer

Inhalation Toxicology Research Institute,
Lovelace Biomedical and Environmental Research Institute,
P. O. Box 5890, Albuquerque, New Mexico 87115

Introduction

Distillate coal liquid from the SRC-II process has been hydrotreated at several levels of severity in a bench-scale continuous flow unit at the Bartlesville Energy Technology Center. The purpose was twofold with the immediate goal to survey process conditions with a commercially available catalyst to provide samples upgraded to varied degrees for detailed characterization analyses and investigation for biological activity. Long-range goals are to contribute to a data base to evaluate raw material sources, liquefaction or other production processes, characterization of feedstocks for further refining to transportation and other end-use fuels, selection of refining processes, and estimation of type and quality of end products expected from combinations of these steps.

The liquid feed and products have been screened for biological activity by the Ames test at Lovelace Biomedical and Environmental Research Institute, Albuquerque, New Mexico.

Experimental Materials and Procedures

The SRC-II liquid was obtained from the Pittsburg and Midway Coal Mining Co. The liquid was produced from Material Balance Run No. 77 SR-12 on coal from the Pittsburg seam from Consol's Blacksville No. 2 Mine in West Virginia. The middle (177-288° C) and heavy (288-454°C) distillates were blended to the same ratio as produced by the material balance run, e.g., 75.5 percent middle distillate and 24.5 percent heavy distillate. The feed contained 0.23 wt-pct sulfur, 1.06 wt-pct nitrogen and 3.29 wt-pct oxygen and boiled between 185 and 380° C (5-95 percent) by simulated distillation.

The bench-scale hydrogenation unit was designed for operation at up to 3,000 psig and 450° C, with once-through flow of hydrogen, down-flow of gas and liquid over a fixed-bed catalyst. Reactor temperature, pressure, and hydrogen flow and liquid level in the high-pressure product separator were controlled automatically. Liquid product was withdrawn periodically from a low-pressure separator, and the combined high- and low-pressure effluent gas was sampled for analysis.

The catalyst was 100 ml of American Cyanamid HDS-3A, a 1/16-inch diameter extrudate of nickel-molybdenum-alumina. It was diluted with inert, granular alpha-alumina to provide a bed depth of 18 inches in the middle section of a 0.96-inch ID vertical reactor with a 5/16-inch OD internal thermocouple well. The catalyst was progressively more dilute toward the top of the bed to minimize exothermic temperature effects, and end sections were packed with alpha-alumina to provide for preheat and cooling zones.

The catalyst was presulfided and operated for about 100 hours on a petroleum gas oil (200-500° C boiling range, 0.8 wt-pct sulfur) to check controls and provide some catalyst aging before exposure to the coal liquid.

Operating conditions selected as likely to maintain catalyst activity and provide the range of upgrading desired were 2,000 psig pressure, 325 to 400° C, and 0.5 to 1.0 LHSV (volume liquid feed/volume bulk catalyst/hour). Hydrogen flow was held constant at a rate corresponding to 10,000 SCF/bbl to 0.5 LHSV or 5,000 SCF/bbl at 1.0 LHSV. Variation in hydrogen flow rate in once-through operation has little effect at more than 5,000 SCF/bbl. Operation at each condition was for approximately 24 hours to allow 8-12 hours for equilibration plus time to accumulate about 750 ml of liquid product. Table 1 shows the sequence of reactor conditions and essential process results.

TABLE 1. Process conditions and results

Sample Period	Liquid Product					Approx. H ₂ Cons., SCF/bbl	Catalyst tempera- ture, °C	Liquid feed rate, LHSV
	Sp. gr., 60°/60°F	Hydrogen, wt-pct	Nitrogen, wt-pct	Sulfur wt-pct	Oxygen wt-pct			
(Feed)	1.003	8.42	1.057	.25	3.29	-	-	-
1	0.921	10.81	0.352	.01	.59	1,930	325	0.50
2	.948	10.06	.631	.02	1.65	1,270	325	1.0
3	.902	11.54	.033	.01	.17	2,670	350	0.50
4	.953	9.80	.700	.02	1.58	970	310	0.50
5	.887	12.24	.001	.01	.09	2,880	375	0.50
6	.877	12.39	.001	.01	.03	3,250	400	0.50
7	.868	12.82	.001	.01	.06	5,010	400	0.35
8	.962	9.68	.742	.01	2.00	980	325	1.0

Period 4 was a test of a very mild condition after a weekend shutdown. Period 7 was a test of the liquid feed pump at a low rate. Period 8 was a brief test for decline in activity from period 2, although the entire operation was too short for significant life testing. Periods in the order of 2,1,3,5, and 6 were intended to cover the desired range of increasing upgrading.

The liquid feed and products were screened for chemical mutagens by use of the Ames assay (1,2).

Results and Discussion

The results in table 1 show the expected trends as hydrotreating severity was increased with reaction temperatures in the range of 310 to 400° C. Specific gravity of the product liquid at 375°C decreased from 1.00 for the feed to 0.89 while nitrogen decreased from 1.06 wt-pct to less than .001 wt-pct and oxygen decreased from 3.29 wt-pct to 0.09 wt-pct. Hydrogen content increased from 8.42 wt-pct in the liquid feed to 12.24 wt-pct over this same range of nitrogen removal. Calculated

hydrogen consumptions for this range of conditions varied from 970 to 2,880 SCF/bbl which is within the ranges reported by others (2,3). Precise hydrogen content of the liquid product, used in calculation of hydrogen consumption, was determined by NMR through the courtesy of Phillips Petroleum Company. Analysis of the effluent gas did not include hydrocarbons heavier than ethane. Contributions of the heavier hydrocarbons to hydrogen consumption are small for hydrotreating at conditions which cause very little cracking of hydrocarbons since most of the consumed hydrogen goes into the liquid product.

The distillation range of the liquid products was shifted downward as hydro-treating severity was increased (table 2). The magnitude of the shift of the simulated distillation is shown in the last column which indicates 8 to 22 percent of the feed is converted to material boiling below the five percent point of the feed.

TABLE 2. - Simulated distillation of liquid feed and products

Sample Period	Temp., °C., at wt-percent distilled			wt-percent converted to below 185° C
	<u>5</u>	<u>50</u>	<u>95</u>	
(Feed)	185	255	379	-
4	112	239	361	15
2	131	247	369	9
3	101	235	344	18
4	133	248	375	8
5	96	229	331	21
6	98	225	329	22
7	94	221	326	21
8	156	252	379	7

The increase in product material boiling below 185° C results largely from saturation of aromatic rings and olefins and from removal of heteroatoms. Some hydrocarbons boiling lower than the feed would be formed by cleaving of heteroatom linkages, with very little cracking of hydrocarbons expected. For example, all product liquids had initial boiling points close to that of benzene/cyclohexane.

The results of the Salmonella/Typhimurium Mutagenicity (Ames) assay for the feed and liquid products are given in table 3. The assay was run essentially as described by Ames(1). The assay employs specially constructed strains of Salmonella Typhimurium which are reverted by a wide variety of mutagens from requiring histidine in their growth media back to bacteria capable of synthesizing histidine.

TABLE 3. - Results of the Ames assay

Sample	Concentration, ug/plate	Number of Revertants	
		Without/With Metabolic Activation TA 98	TA 100
Feed	250	30/ <u>1822</u>	144/ <u>322</u>
Feed	100	34/ <u>1122</u>	163/ <u>348</u>
Feed	50	27/ <u>547</u>	150/ <u>306</u>
Feed	25	21/ <u>316</u>	150/204
Feed	5	31/113	134/178
Background	0	21/60	144/142
8	100	15/ <u>131</u>	134/257
4	100	19/111	176/232
2	100	23/ <u>178</u>	151/226
1	100	16/64	158/218
3	100	10/40	161/194
5	100	22/64	162/194
6	100	19/70	128/186
7	100	17/65	153/218
Background	0	25/66	169/220

Some chemicals require metabolic activation (addition of microsomal enzymes) prior to showing mutagenic activity; thus, data are given as number of revertants without/with metabolic activation. The Ames test has thus far demonstrated a strong correlation between positive carcinogenesis in animal tests and mutagenicity in the Ames test (1,4). However, positive results from the Ames test do not conclusively show human risk.

The untreated SRC-II was tested at five concentrations with Salmonella strains TA 98 and TA 100, generally considered the most sensitive strains. In the results indicated in Table 3, an increase in the number of revertants greater than two times the background (no SRC-II feed or product) is sometimes considered to indicate a definite positive (mutagenic) response. The plates which showed a positive response by this criteria are underlined.

Activity decreased with decreasing concentration for the untreated feed but was still nearly double the activity of the background at a concentration of 5 ug per plate. A product dose of one hundred micrograms was selected as a satisfactory screening test since a strong response was observed for the untreated SRC-II at this concentration and since no appreciable cytotoxicity was noted. The hydrogenation periods are listed in order of increasing severity of processing. Activity was decreased essentially to the background level when nitrogen content was decreased to

0.35 wt-pct, oxygen content was decreased to 0.59 wt-pct and hydrogen content was increased from 8.4 to 10.8 wt-pct. This occurred at process conditions of 325° C and 0.5 LHSV feed rate, which had been planned as the lowest reaction temperature expected to give substantial upgrading.

A more complete investigation will require testing of fractions of the coal liquid to identify more active components. Nitrogen and oxygen compounds and aromatic ring structures are important in this respect, with mutagenically active components likely to be in higher-boiling fractions. Tests on mammalian systems are also needed before making assessments concerning potential human risk.

Summary

Distillate coal liquid from the SRC-II process was hydrotreated in a bench-scale process unit to provide a range of mildly upgraded products for compositional characterization and screening for mutagenicity. Hydrogen content of the liquid was increased from 8.4 to 12.24 wt-pct over the range of process conditions which removed essentially 100 percent of the nitrogen and 95 percent of the oxygen. Results of the Ames assay indicated mutagenic activity of the liquid product decreased by an order of magnitude for 35 percent removal of nitrogen and 52 percent removal of oxygen. Liquid product with 67 percent nitrogen removal and 82 percent oxygen removal showed no mutagenic activity distinguishable from that of the background samples. The full range of effect in decreasing mutagenic activity by the Ames assay was covered by relatively mild hydrotreatment, but assessment of potential human risk must be confirmed using additional mammalian tests.

References

1. Ames, Bruce N., Joyce McCann, and Edith Yamosaki. Methods for Detecting Carcinogens and Mutagens with Salmonella/Mammalian-Microsome Mutagenicity Test. *Mutation Research*, v. 31, 1975, pp. 347-363.
2. Frumkin, Harry A., Richard F. Sullivan, and Bruce E. Strangeland. Converting SRC-II Process Product to Transportation Fuels. Presented at the 87th National Meeting of AIChE, Boston, MA, August 20, 1979.
3. Lanning, W. C. The Refining of Synthetic Crude Oils. BETC/IC-76/2. July 1976, 11 pp.
4. McCann, Joyce, Edmund Choi, Edith Yamosaki, and Bruce N. Ames. Detection of Carcinogens as Mutagens in the Salmonella/Microsome Test: Assay of 300 Chemicals. *Proc. Nat. Acad. Sci. USA*, v. 72, No. 12, 1975, p. 5135.

SYMPOSIUM ON COAL LIQUIDS UPGRADING

PRESENTED BEFORE
THE DIVISION OF FUEL CHEMISTRY, INC.
AMERICAN CHEMICAL SOCIETY
HOUSTON MEETING
MARCH 25-28, 1980

CATALYST DEACTIVATION IN HYDROTREATING
COAL-DERIVED LIQUIDS

R. Sivasubramanian,¹ J. H. Olson and J. R. Katzer*
Center for Catalytic Science and Technology
Department of Chemical Engineering
University of Delaware
Newark, Delaware 19711

¹Air Products and Chemicals, Inc.; P.O. Box 538, Allentown,
Pennsylvania 18105

*To whom correspondence should be addressed. (302) 738-8056

CATALYST DEACTIVATION IN HYDROTREATING COAL-DERIVED LIQUIDS

Introduction

Coal liquefaction processes are likely to be commercialized within the next decade. Coal-derived liquids contain larger fractions of heteroatoms (sulfur, nitrogen, oxygen) than petroleum liquids. Hydroprocessing of these liquids will become necessary to improve the quality of the products. Considerable work has been done in determining catalyst deactivation rates in petroleum hydroprocessing. However, coal-derived liquids differ considerably from petroleum liquids in their aromaticity, metals content and C/H ratio. Coal-derived liquids are much harder to hydroprocess, cause more rapid catalyst deactivation, and represent a step upward in terms of difficulty of hydrotreating.

Characterization studies on aged catalysts can provide an understanding of the causes for catalyst deactivation and may lead to optimum design of reactors and improved catalysts. Characterization of three different coal-liquefaction catalysts that have been in direct contact with coal have been performed earlier in this laboratory (1,2,3). However, in the present study a catalyst that had been used to hydrotreat a coal-derived liquid is characterized.

Experimental

Ni-Mo/Al₂O₃ catalyst samples were obtained from a laboratory-size trickle-bed reactor that was used to hydrotreat an equal

volume mixture of raw anthracene oil and synthoil liquid. The properties of this particular feedstock is given in Table I. The feed oil had a sulfur content of 0.54 wt %, a nitrogen content of 1.21 wt % and 1.05 wt % ash. Table II presents the operating conditions in the trickle-bed reactor for the particular run from which the catalyst samples were obtained. At the end of the run, the reactor was shut down and the reactor was cut into three different sections and catalyst samples were obtained from the top, middle and bottom sections of the reactor. The spent catalyst pellets from the three different sections were analyzed with a scanning electron microscope (SEM) equipped with an energy dispersive x-ray analyzer (EDAX) and with an electron microprobe. In addition spent catalysts were regenerated (coke burnt off) and the hydrodesulfurization (HDS) and hydrodenitrogenation (HDN) activities of the fresh, spent and regenerated catalysts were compared.

Microscopy Studies

Most of the catalyst samples used in the microscopy studies were prepared by sectioning the catalyst; mounting the catalyst in potting material on a SEM sample holder, and then grinding the exposed surface flat with various grits down to 0.25 μ diamond dust. The lapped samples then were carbon shadowed. These samples then were inspected in light microscopy, SEM and the electron microprobe.

The SEM with EDAX was used in two modes, first conventional inspection of the surface coupled with spot analyses of distinctive

features. The second mode was to scan the surface for specific elements. The microprobe was used in three modes, inspection of the surface elemental scans (these scans are superior to the EDAX elemental scans), and finally to find the elemental response along a 100 x 0.5 micron line parallel to a tangent to the catalyst surface. The line scan was mechanically driven to sweep an area near the catalyst exterior surface.

Samples also were then prepared by cleaving the catalyst, mounting on an SEM post and then removing surface "coke" by plasma etching. This preparation method reveals the distribution of mineral matter on the catalyst surface.

Activity Studies

In order to determine the activity decay of the spent catalysts, the spent catalysts were regenerated and the activities of the spent catalysts were compared with that of the fresh and regenerated catalysts for hydrodesulfurization and hydrodenitrogenation using a mixture of dibenzothiophene and quinoline dissolved in hexadecane as a feedstock in a batch autoclave reactor. Earlier experiments by Chiou and Olson (2,3) were done by crushing the spent pellets to 140 mesh. For this work, in order to find out the effect of crushing the spent catalysts, it was decided to conduct experiments using crushed particles as well as using the spent catalysts as received (8/10 mesh).

A mixture of spent catalysts from all three sections of the reactor was obtained and this mixture was divided into two halves.

One half of this mixture was ground to a size of 140 mesh. Both halves were regenerated by controlled combustion of the coke deposited on the catalyst. The regeneration process was done by passing a 2% oxygen in helium over the spent catalysts at a temperature of 450°C at a flow rate of 100 cc/min. The burning process was continued until the weight of residual catalyst became constant.

All the experiments were conducted in a 300 cc standard autoclave reactor (Autoclave Engineers, Erie, PA) equipped with a variable speed magnadrive; the autoclave was operated in batch mode. A special injection system was used to inject a slurry of catalyst, reactants and carbon disulfide in a small amount of carrier oil into the reactor after it had been stabilized at reaction temperature. This technique allowed the precise definition of zero time and eliminated complications including reaction and possible catalyst activity changes arising from long heat-up times. The system has been described elsewhere (4). However, the above technique could not be utilized in runs involving catalyst pellets. For these runs a special basket was designed that held the catalyst in place inside the autoclave reactor. For the pellet runs, the reactants and carbon disulfide in carrier oil were injected after the reactor had reached the operation temperature. Two blank runs not containing catalyst were made to determine the effect of reactor walls and the catalyst basket.

Table III presents the operating conditions for the batch autoclave reactor for all the runs used in this study. N-hexadecane

was used as a carrier oil. All catalysts were presulfided, and in order to maintain the catalyst in the sulfided form during the reaction, an amount of CS_2 equivalent to 0.05 wt % of the carrier oil was added to the injection tubing together with catalyst and reactants. Under the operating conditions carbon disulfide was rapidly converted to hydrogen sulfide and methane. The amount of CS_2 created 1.4% higher concentration of H_2S than that required to keep the catalyst in the sulfided form. Liquid samples were analyzed using a gas chromatograph equipped with a glass capillary column (OV101, 75 m).

Results of Microscopic Investigations

The prior part of this section presents a fairly detailed narrative of the SEM results for the sample taken from the top (nearest the entrance) of the reactor and then less complete descriptions for the data gathered for the middle and bottom samples. This is followed by a presentation of the results from the microprobe investigations and plasma etching. The various experimental methods yield a reasonably consistent description for the deposition of mineral matter and coke at the catalyst surface.

SEM - Top Sample

Figures 1A and B are conventional photo micrographs of the polished cross section of the catalyst pellet. These two figures show the deposition of an irregular crust about 75 microns thick around the entire exterior surface of the catalyst. In addition there is a thin region about 10 microns thick which

appears on about one-third of the catalyst. The catalyst also has many circular regions about 40 microns in diameter which appear distinct from the polished section of the catalyst. Finally the zone near the surface contains many cracks with a thickness of 1-5 microns. The roughness of the catalyst exterior surface suggests that a small portion of the catalyst may have spalled away. The smaller boxed area in Figure 1B corresponds to a zone which was examined with scanning electron microscopy. The larger rectangle corresponds to a zone evaluated with the electron microprobe analyzer.

Figure 2A shows the surface of the catalyst pellet as seen with a scanning electron microscope. In contrast to the light microscope, the outer crust is seen to contain many large (~1 micron) cracks. In addition the outer crust contains about 20 percent of small particles (~0.5 micron) embedded in an indistinct matrix. The inner crust also is seen to contain many voids and cracks; this zone appears to be made by aggregation of small crystals. The catalyst support contains a number of extended large cracks near the external surface. In addition there are a number of shallow depressions, 40 microns in the largest dimension which will be described more completely later. In summary the surface has two distinct crusts and a zone containing large fissures near the exterior surface.

Figure 2B is an aluminum area scan made by recording the aluminum signal from the EDAX. Figures 2B and 2A correspond.

There are three distinct zones for the aluminum signal, the upper zone for potting material, the middle zone for the crust, and the bottom zone of the catalyst support. Closer inspection reveals that the cracks seen clearly in the backscatter electron scan also appear, although less distinctly, in the aluminum scan. The aluminum scan shows that the inner and outer crust regions contain aluminum and that the catalyst exterior surface has been roughened in the process.

Figure 3A is a SEM-EDAX area scan for silicon. This scan shows that the exterior crust contains a high concentration of silicon; the gray (intermediate) zone on Figure 2B corresponds exactly with the bright zone of Figure 3A. In addition there is some penetration of silicon into the interior of the catalyst near the exterior surface. Careful examination of the crust region identifies a few zones (~15 microns across) of very high silicon concentration.

Figure 3B is a SEM-EDAX area scan for calcium. The calcium signal in the catalyst is only slightly greater than background, and therefore the zones are far less distinct. However the high-silicon region of Figure 3A has a corresponding but less distinct zone on the calcium scan. In addition, the major cracks appear faintly. Some zones of high silicon concentration in the crust region of Figure 3A appear as voids in the calcium scan on Figure 3B. Finally there is a small calcium signal in the catalyst support; however the calcium signal in the catalyst is barely above background.

Figure 4A, the SEM-EDAX Area Scan for Sulfur, and Figure 4B, the SEM-EDAX Area Scan for Iron, will be discussed together. The demarcation between the catalyst and the crust can be seen on both figures but is far clearer on the iron scan. The catalyst is sulfided, and therefore there should be a distinct sulfur signal in the interior of the catalyst. The cracks seen clearly on Figure 2A appear faintly on the sulfur area scan. The crust region gives a near-perfect correlation between the two signals. Further, the high section zones are seen as voids in the two figures. There is a fairly distinct zone of higher sulfur concentration in the crust located in the center of the figure which also appears, although less clearly, in the iron scan. Thus the exterior and the interior crusts contain an iron-sulfur compound. There is some penetration of iron into the catalyst, and sulfur appears throughout the catalyst interior.

Figure 5A is a titanium SEM-EDAX scan of the area. The interior crust region of Figure 2A is seen to contain a high concentration of titanium. In addition there is a significant concentration of titanium in the exterior crust. Finally there is some penetration of titanium into the near surface of the catalyst.

Figure 5B shows a molybdenum SEM-EDAX scan of the catalyst. Molybdenum is the major active element in the catalyst. The molybdenum signal correlates with the intense aluminum signal of Figure 2B. The cracks in the catalyst can be seen as voids in the molybdenum signal.

The area scanned in Figures 2A-5B were also examined for nickel and zinc. These scans gave no signal above background even though EDAX spot and line analyses showed that these elements are present. Indeed, the catalyst contains nickel as a hydrogenation promoter.

Figure 6A is an electron backscatter readout taken in the microprobe analyzer prior to making the line scans. This area appears as the large rectangle on Figure 1B. Consistent with Figure 2B, the figure shows an outer and inner crust, major cracks in the catalyst near the surface, and several flat depressions about 40 microns in diameter. The line in the crust region corresponds to the orientation of the 60 micron line scan used to find the average composition of the crust.

Figure 6B is the titanium microprobe area scan which corresponds to Figure 6A. The microprobe area scan for titanium is much more sensitive than the SEM-EDAX area scan, and therefore more details emerge: the inner crust is seen to produce a very high titanium signal. The dense exterior crust contains an intermediate concentration of titanium; however the crust in the upper left portion of the figure appears to be nearly free of titanium. The shallow craters and the cracks in the catalyst interior are decorated with titanium. Thus the titanium is distributed in a complex way throughout the crust region of the catalyst.

SEM - Middle Sample

Figures 7A and 7B are conventional micrographs of the polished section of a catalyst pellet taken from the middle of the reactor. Consistent with the top sample, there is an irregular crust about 75 microns thick which completely covers the catalyst. Likewise there is a thin inner crust which covers about one-quarter of the surface. Again the surface region of the catalyst has many fissures, and the spent catalyst has many ponds which have been decorated with process material. The rectangular region on Figure 7B locates the region examined more closely with the SEM-EDAX and the microprobe. The region was chosen because the thin crust is unusually flat there.

Figures 8A and 8B are the SEM inspections of the sectioned catalyst. Owing to the greater depth of field of the SEM than for the light microscope, the cracks and the round depressions of the surface can be seen more clearly. Figure 8B, taken at 800X corresponds to the region examined by SEM-EDAX area scans. The latter data are recorded in Figures 9A-11B.

In harmony with the top sample the exterior crust has a high silicon concentration (Figure 9A) and contains grains of extremely high silicon concentration. The silicon density in the third of the crust nearest to the surface is greater than for the outer two-thirds; this density variation also can be seen in the SEM micrographs. The calcium concentration (Figure 9B) is fairly

uniform in both the crust and the catalyst interior. There is more calcium in the crust than in the catalyst.

The sulfur (Figure 10A) and iron (Figure 10B) area scans show a very high correlation for these two elements in the crust, a very low concentration of iron in the catalyst, and an intermediate concentration of sulfur in the catalyst. These results are similar to the top sample.

The titanium scan (Figure 11A) shows a very high concentration of this element in the inner crust, a high concentration in the outer crust, and decoration of the two shallow depressions on Figure 8B with titanium. In addition the small piece of material sitting on the surface of the catalyst at the extreme left is high in titanium. This speck appears to be a piece of inner crust which may have been displaced during sample preparation.

Bottom Sample

Figures 12A and 12B are conventional photo micrographs of the sectioned and polished catalyst sample taken from the bottom of the reactor. The small square shown on Figure 12A is examined at higher magnification with SEM; the micrographs are given in Figures 14A and 14B. The large rectangle area in Figure 12B was given SEM-EDAX scans; the data are given on Figures 15A-17B.

The bottom sample is distinctly different from the top and middle samples. First, the cemented exterior crust does not cover the entire surface, but instead appears to have filled in

regions where the surface of the catalyst has spalled away. Second, there is no titanium-rich inner crust on the catalyst in all of the samples investigated.

Figures 13A and 13B show two magnifications of the catalyst area in a zone where crust has formed. The enhanced depth of the field shows very large cracks and several round, shallow pits in the catalyst support. These features of the bottom sample are identical to the other two samples.

Figures 14A and 14B are two pictures at 1000x of the small square identified on Figure 12A. These pictures show that the flat crater is filled with polycrystalline material smaller than 0.5 microns which is similar to the inner crust material. A spot EDAX analysis shows that this zone contains significant quantities of titanium.

The SEM-EDAX area scans for the bottom sample are shown in Figures 15A-17B. The results for the six elements Si, Ca, S, Fe, Ti and Mo are identical effectively to the middle sample with the following exceptions:

- a) there are no particles very high in sulfur in the crust,
- b) there is less difference between the sulfur concentration in the crust and in the catalyst,
- c) the titanium concentration in the outer crust is very distinct, and there is significant but lower concentration of titanium in the catalyst close to the surface,
- d) the molybdenum is clearly conferred to the catalyst.

Microprobe Results

The electron microprobe results are displayed on Figures 18A, B, and C; this figure is arranged to permit an easy comparison of the three samples for the several elements considered. Figure 18A is the top sample, 18B the middle sample and 18C the bottom sample. These elements were examined in each scan and the data are referenced to the aluminum signal. The amplitude of the signal is proportional to the line averaged concentration of the element.

Molybdenum and nickel are the active elements in the catalyst. The molybdenum signal in the crust is only slightly greater than background, and therefore there does not appear to be migration of this element. The nickel signal was amplified far more than molybdenum and therefore the signal has far more noise. Nickel is above background in the crust in 18A, B, and C and the broadened transition of the profile between the interior and the crust suggest that nickel has migrated slightly.

Iron and sulfur are found in the exterior crust of 18A and 18B and in the crust of 18C. Previous work has established that this crust is nonstoichiometric ferrous sulfide. This material appears in surprisingly large quantities in this investigation; obviously the coal-derived liquid carries all of the mineral found in coal. On the other hand in the interior the iron signal decays to background level within 125 microns of the surface while the sulfur stabilizes on the value appropriate to the sulfided catalyst.

Whenever there is a void in the catalyst (18B has a clear example) the aluminum and sulfur signal will decrease together.

Titanium, calcium and silicon are elements found in the mineral matter of coal. The titanium signal in 18A and 18B shows clearly the inner crust; the concentration of titanium in the inner crust is about twice as high as in the exterior crust of 18A and 18B or the outer crust of 18C. Thus the laydown of the inner crust appears to occur by a different mechanism than the outer crust. There is a surprisingly large penetration of titanium into the interior of the catalyst. The decoration of cracks and voids with titanium is seen as an irregular but diminishing penetration of titanium into the catalyst interior.

Silicon is a major component in the outer crust of 18A and B and in the crust of 18C. Further there is a substantial penetration of this element into the catalyst interior. Since silicon is found in the cracks near the surface, it is apparent that the catalyst is spalling away by interactions of the mineral matter. Calcium, on the other hand, has only a very weak signal in the interior of the catalyst. Further calcium and silicon apparently exclude each other in the surface crust and interior deposition.

The zinc signal shows the deposition of very low quantities of this material near the catalyst surface, particularly in the top sample. Thus the catalyst appears more active for deposition in the early part of the run; this activity is lost down the reactor.

These microprobe results are consistent with the SEM and electron microprobe area scans. The inner crust is a real phenomena, and the refractory components of the clay mineral matter are small enough to penetrate a significant way into the catalyst. FeS_x remains in the feed slurry and becomes firmly attached to the catalyst exterior. These deposits diminish the extent to which the catalyst can be regenerated.

Plasma Etched Samples

Figures 19A and 19B are two magnifications of a catalyst sample which has been plasma etched to remove oxidizable material "coke" and then reveal the firmly attached exterior crust. Figure 18A shows two cleavage planes through the catalyst and the irregular surface at the left of the picture. The exterior surface is covered with waves of deposited material. Figure 18B shows the marked rectangle on 18A at higher magnification. The surface contains aggregates of crystalline material with an 0.5 to 2.0 micron crystal size. (The largest crystal in the figure was used as a marker. This crystal appears to be a chip held to the surface electrostatically.)

Figure 20B is a view along the transverse axis of a pellet cleaved on the radial plane. The sample was taken from the bottom of the reactor where the external crust is irregular. After plasma etching no residual crust was found. However the radial plane is dotted with round pits and plateaus which have been observed in all of the polished sections. The pits near the

surface occasionally are partially filled with deposited mineral matter. Further the exterior surface of the catalyst has eroded to become quite rough. This micrograph shows that the round pits seen in all of the micrographs are not an artifact of sample preparation.

Catalyst Activity Results

A total of eight experimental runs were conducted. Table IV presents the catalysts used in each run. Two of the runs were blank runs to determine the background activity of the reactor. The fresh, spent and regenerated catalysts were used in two different sizes comprising of the other six runs. All experiments were conducted at the same operating conditions presented in Table III. However the duration of the runs varied.

Figures 21 and 22 show the total nitrogen removal and the total sulfur removal for crushed catalyst run in the fresh, spent and regenerated states. These figures show that these reactions follow pseudo first-order kinetics over limited ranges of element removal. Equivalent plots are obtained for runs made with the three states of pelleted catalysts.

Table V presents the first-order rate parameters corrected for background activity. This table shows that the pelleted catalysts have either equal or larger activities than the corresponding crushed catalyst; these results are contrary to the usual effect of isothermal transport limitations in catalysts. These results will be described more fully below.

Figure 23 shows the network for the hydrogenolysis of quinoline developed by Shih *et al.* (4). The individual rate constants for this network are obtained as pseudo first-order rate parameters using the techniques developed by Himmelblau *et al.* (5). The experimental data were analyzed using three different weighting schemes and the best weighting scheme was chosen based on the overall fit of the data and the reduction of the sum square error. Figures 24 and 25 show a comparison of the data with the parametric representation. These figures show reasonable agreement between the model and the data; the pseudo first-order form provides a simple and adequate representation of the network.

The individual rate parameters for this network analysis, corrected for background reactivity, are presented in Table VI. The rate parameters for pellets are lower than those for crushed catalyst in the three states, fresh, spent and regenerated for all parameters except k_6 . The parameter k_6 governs the conversion of 1,2,3,4-tetrahydroquinoline to orthopropylaniline; the rate parameter for subsequent step for nitrogen removal cannot be obtained reliably from the data, and thus this step represents an apparent dead end for nitrogen removal. Hence it is useful to calculate the concentration of all intermediate nitrogen compounds using the parameters of the reaction network.

Figure 26 compares the data for total nitrogen concentration with the values predicted by the model for fresh crushed catalyst; the model represents the data adequately. Similar comparisons

were made with the other five cases, and the experimental data are represented with equivalent acceptability. Thus the network representation is consistent with the overall rate of nitrogen removal for all cases.

There is direct evidence that some of the reaction rates in pellets are inhibited by transport considerations. Figure 27 shows the 1,2,3,4-tetrahydroquinoline (1THQ) and quinoline concentrations as a function of time for fresh crushed and pellet catalysts runs under otherwise identical conditions. Consistent with the lower forward apparent rate parameter for the reversible reaction, the pellet data show a higher concentration of quinoline, a lower concentration of 1THQ, than for crushed catalyst. In addition the maximum in the 1THQ concentration occurs earlier for the crushed catalyst than for the pelleted run. Therefore the pellets exhibit direct evidence for transport limitations in the catalyst.

The utility of this assumption can be tested by calculating the effectiveness factor for the pellet catalyst based upon the crushed catalyst parameters. This calculation assumes that the crushed catalyst is small enough to give intrinsic rates for all rates; this assumption can be examined later. Table VII outlines the results of the calculation.

The parameter values for the pellet catalyst agree reasonably well with the calculated values; the exceptions are k_6 and k_8 .

A similar calculation for the regenerated (Table VIII) catalyst shows that again with the exception of k_6 the calculated values for the pellet catalyst are too high in comparison to the data.

The low values found for the pellets show that there is a significant loss in the effective diffusivity for the pellets. This loss is the result of deposition of mineral matter on the exterior of the pellets; this transport resistance is removed (or avoided) when the regenerated catalyst is crushed.

Table IX gives the percentage activity remaining in the five catalyst forms relative to fresh crushed catalyst. The values observed stem from several causes: 1) intrinsic loss in kinetic activity, thus the spent catalyst has about 3-4 percent of the fresh catalyst activity and the regenerated catalyst has circa 60 percent of the original activity; 2) internal diffusional transport losses; 3) contributions from the external and near surface mineral material on the pellets, and 4) an abnormal enhancement of the k_6 and k_8 rate parameters in pellets. With reference to the latter, Bhide (6) has shown that the hydrogenolysis rate has the approximate form $\text{rate} = kKC/(1+KC)^2$, where C is the reactant concentration and K is the adsorption term. This rate expression is negative order for KC greater than one, and thus a decreasing concentration profile to the center of the pellet will increase the effective reaction rate. Thus the enhanced overall rate for HDN in pellets is in part the result of coupling transport limitations with the very strong adsorption equilibrium of nitrogen hetrocycles.

The reaction network shown in Figure 28 for dibenzothiophene hydrodesulfurization has been determined earlier by Houalla *et al.* (7). However, their reaction network was determined using only dibenzothiophene as a reactant. In this study, dibenzothiophene and biphenyl were observed for the crushed particles, and runs using pellets contained traces of cyclohexyl benzene in addition to the above two products. Concentration profiles suggested that cyclohexyl benzene is a secondary product. Bhide (6) found that quinoline inhibits the hydrogenation steps in the dibenzothiophene network strongly, and in our experiments the concentration of quinoline was very high.

Based on all the above information the dibenzothiophene HDS data were analyzed using the following network:

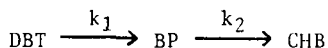


Table VIII presents the individual rate constants. The table shows that spent catalyst had a very low activity. However, unlike nitrogen removal, the spent catalyst is not totally non-reactive. For fresh catalyst the pellets are significantly more active than crushed pellets. Further cyclohexyl benzene, a hydrogenated product from biphenyl, was found only in the pellet runs. Broderick (8) and Sapre (9) have studied biphenyl hydrogenation and have shown that biphenyl hydrogenation is extremely slow and is severely inhibited by the presence of quinoline. This observation can be explained in terms of transport limitations in pellet runs in two

different ways. Since transport limitations exist in the case of pellets, the biphenyl concentration will probably be higher in the interior of the catalyst particles than for crushed catalyst. The higher concentration of biphenyl and the significantly longer residence time in the catalyst couple to increase the probability of formation of cyclohexylbenzene. The concentration profile for nitrogen hetrocycles in the catalyst interior also contributes to the observed difference between pellets and crushed catalysts. The catalyst pellets have a lower interior concentration of quinoline and THQ as opposed to the crushed particles, and hence the inhibiting effects of quinoline on dibenzothiophene is lower in the case of pellets. Thus the interior reactivity is higher for pellets, but the overall rate is lower than would be observed if quinoline were absent.

Discussion

The photomicrograph data provides detailed information on the deactivation of catalyst and an opportunity to compare the hydroprocessing of a coal-derived liquid with the hydroprocessing of coal. These data supplement the results from the activity studies.

The one percent suspended minerals in the feed is very significant in the deactivation of the catalyst. These suspended material are very finely divided and therefore can penetrate rather easily into the interior of the catalyst. Hence silicon, which is a major constituent of the clays in coal, is found in the interior 100 microns of the catalyst in all three samples.

This observation is consistent with the behavior of coal hydro-processing experiments.

The catalyst is deactivated by the laydown of coke. The plasma etching experiments show that the exterior crust is largely coke, and regeneration by burning decreases the sample weight by twenty percent. Thus a significant fraction of the activity can be regained by burning away the coke deposits as evidenced by the results from activity studies, however the deposited mineral matter remains.

The exterior crust also contains FeS_x ; previous studies have shown that these deposits are $\text{FeS}_{1.1}$. The crystal size of FeS_x is smaller in this system than for the synthoil catalyst. There is no evidence that the FeS_x was formed in the trickle-bed reactor; the weak penetration of iron into the catalyst correlates with the penetration of silicon, and it therefore appears that FeS_x is cemented on the catalyst with coke.

The nickel profiles indicate a small migration of this element away from the catalyst support into the crust on the surface. The migration of this promoter may affect catalyst function; in particular the effect of nickel upon the rate of coking may change.

The most unique feature of these studies is the formation of the titanium-rich inner crust on the top and middle catalyst samples.

Spent catalyst was found to be essentially non-reactive for both sulfur and nitrogen removal. Network analysis for quinoline HDN and dibenzothiophene HDS indicate that the laydown of coke seems to affect both hydrogenation and bond-breaking steps in the same way. The results from the experiments using the regenerated catalysts show that half of the activity was recovered by the regeneration process. A comparison of the runs using catalyst pellets and crushed particles shows that the catalyst interior is filled with coke and inactive. These results also raise some interesting questions on the interplay between diffusion limitations and the interactions between nitrogen and sulfur-containing compounds upon the intrinsic kinetics.

The results presented here are similar to the ones observed from characterization studies performed on catalysts that have been in direct contact with coal, except for a few minor differences.

Since 50 to 60 percent of the catalyst activity can be recovered by burning the coke, the mineral matter is secondary in the direct deactivation of the catalyst. However, the deposited mineral matter is a potential catalyst for coke formation; thus the effective lifetime for the regenerated catalyst may be less than that for a fresh catalyst.

Acknowledgements

This work was supported by a grant from the Department of Energy.

Literature Cited

1. Stanulonis, J. J., Gates, B. C., and Olson, J. H., AICHE J., 22, 576 (1976).
2. Chiou, M. J. and Olson, J. H., Am. Chem. Soc., Div. Pet. Chem., Prepr., 23 (4), 1421 (1978)
3. Chiou, M. J. and Olson, J. H., 'Catalyst Deactivation in Coal Liquefaction Processes,' submitted to AICHE J.
4. Shih, S. S., Katzer, J. R., Kwart, H., and Stiles, A. B., Am. Chem. Soc.; Div. Pet. Chem. Prepr., 22(3), 919 (1977).
5. Himmelblau, P. M., Jones, C. R., and Bischoff, K. B., Ind. Eng. Chem. Fundam. 6, 539 (1967).
6. Bhide, M., Ph.D. Thesis, University of Delaware, 1979.
7. Houalla, M., Nag, N. K., Sapre, A. V., Broderick, D. H., and Gates, B. C., AICHE J. 24, 1015 (1978).
8. Broderick, D. H., Ph.D. Thesis, University of Delaware, 1979.
9. Sapre, A. V., Ph.D. Thesis, University of Delaware, in preparation.

TABLE I

Feed Oil PropertiesEqual Volume Mixture of Raw Anthracene Oil and
Synthoil Liquid

Carbon, wt %	84.92
Hydrogen, wt %	6.57
Sulfur, wt %	0.54
Nitrogen, wt %	1.21
Ash, wt %	1.05

TABLE II

Operating Conditions in the Trickle-Flow Reactor

Temperature -	371°C
Pressure -	.1500 psig
Liquid Volume Hourly Space Time -	1.25 hrs
H ₂ /Oil Ratio -	7500 scf/bbl
Run Duration -	674 hours

TABLE III

Operating Conditions in Batch Autoclave Reactor

Temperature -	350°C
Pressure -	36 atm
Catalyst Concentration -	0.5 wt %
CS ₂ Concentration -	0.05 wt %
Carrier Oil -	Hexadecane
Quinoline Concentration -	2 wt %
Dibenzothiophene Concentration -	1 wt %

TABLE IV

Catalysts Used in Batch Experimental Runs

<u>Run No.</u>	<u>Catalyst Used</u>	<u>Catalyst Size</u>	<u>Duration, minutes</u>
1	Fresh	140 mesh	600
2	Spent	140 mesh	1280
3	Regenerated	140 mesh	1260
4	Fresh	8/10 mesh	1200
5	Spent	8/10 mesh	1800
6	Regenerated	8/10 mesh	1250
7	Blank run without boat		600
8	Blank run with boat		2500

TABLE V

Total Nitrogen and Sulfur Removal
Pseudo First Order Rate Constants, $\frac{\text{g of oil}}{\text{g of cat. minutes}}$

	<u>Fresh</u>		<u>Spent</u>		<u>Regenerated</u>	
	C	P	C	P	C	P
Nitrogen	0.195	0.214	0	0	0.116	0.165
Sulfur	0.333	0.491	0.333	0.222	0.168	0.165

TABLE VI

Individual Reaction Rate Constants
for the Quinoline Network, $\frac{\text{g of oil}}{\text{g of cat. minutes}}$

	<u>Fresh</u>		<u>Spent</u>		<u>Regenerated</u>	
	C	P	C	P	C	P
k ₁	81.19	9.045	0.908	0	46.07	3.566
k ₂	12.92	1.835	0.135	0	10.96	0.620
k ₃	1.120	0.676	---	0.042	0.627	0.216
k ₄	0.167	0.114	0.0042	0	0.153	0.121
k ₅	0.727	0.422	---	0	0.182	0.025
k ₆	0.101	0.218	0.0042	0	0.064	0.107
k ₇	---	---	---	0	---	---
k ₈	1.752	1.66	0	0	1.372	0.170

TABLE VII

Theoretical Calculation of Rate Parameters for Fresh Pellets

	<u>Crushed Rate</u> <u>g oil/g cat min)</u>	<u>Thiele Modulus</u>	<u>η</u>	<u>P_{cal.}</u>	<u>P_{found}</u>
k ₁	81.19	13.51	0.074	9.27	9.045
k ₂	12.92	5.39	0.185	2.39	1.83
k ₃	1.12	1.59	0.58	0.65	0.68
k ₄	0.167	0.61	0.89	0.15	0.11
k ₅	0.727	1.28	0.67	0.49	0.422
k ₆	0.101	0.48	0.93	0.093	0.218
k ₈	1.752	1.98	0.49	0.85	1.66

TABLE VIII

Theoretical Calculation of Rate Parameters
for Regenerated Pellets

	<u>Crushed Rate</u> <u>(g oil/g cat·min)</u>	<u>Thiele</u>	<u>n</u>	<u>P_{calc}</u>	<u>P_{found}</u>
k ₁	46.1	10.18	0.098	4.53	3.57
k ₂	11.0	4.97	0.20	2.21	0.62
k ₃	0.63	1.19	0.70	0.44	0.22
k ₄	0.15	0.587	0.90	0.134	0.121
k ₅	0.18	0.637	0.88	0.16	0.025
k ₆	0.064	0.40	0.95	0.058	0.107
k ₈	1.372	1.76	0.53	0.74	0.170

TABLE IX

Rate Constants in the Quinoline NetworkRelative to Fresh Catalyst, %

	k_1	k_2	k_3	k_4	k_5	k_6	k_7	k_8
Spent pellets	0	0	6	0	0	0	--	0
Spent particles	1	1	0	3	0	4	--	0
Regenerated Pellets	39	33	32	100	6	49	--	10
Regenerated particles	57	85	56	92	25	63	--	78

TABLE X

Individual Rate Constants for
 Dibenzothiophene Hydrodesulfurization, $\frac{\text{g of oil}}{\text{g of cat} \cdot \text{minutes}}$

	Fresh		Spent		Regenerated	
	C	P	C	P	C	P
k_1	0.333	0.491	0.033	0.022	0.168	0.165
k_2	---	0.008	---	---	---	0.007



LIST OF FIGURES

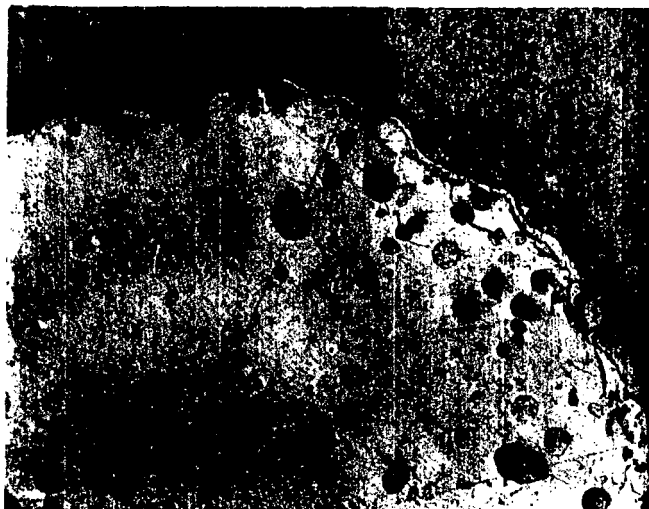
Figure

- 1 Light microscopy of top sample A. 100x; B. 200x.
- 2 SEM top sample A. backscatter electron; B. aluminum EDAX.
- 3 SEM-EDAX of top sample A. silicon; B. calcium.
- 4 SEM-EDAX of top sample A. sulfur; B. iron.
- 5 SEM-EDAX of top sample A. titanium; B. molybdenum.
- 6 Microprobe area scans A. backscatter electron;
B. titanium.
- 7 Light microscopy of middle sample A. 100x; B. 200x.
- 8 SEM of middle sample A. 400x; B. 800x.
- 9 SEM-EDAX of middle sample A. silicon; B. calcium.
- 10 SEM-EDAX of middle sample A. sulfur; B. iron.
- 11 SEM-EDAX of middle sample A. titanium; B. molybdenum.
- 12 Light microscopy of bottom sample A. 100x; B. 200x.
- 13 SEM of bottom sample A. 200x; B. 400x.
- 14 SEM of interior spot A. backscatter electron;
B. ground current.
- 15 SEM-EDAX of bottom sample A. silicon; B. calcium.
- 16 SEM-EDAX of bottom sample A. sulfur; B. iron.
- 17 SEM-EDAX of bottom sample A. titanium; B. molybdenum.
- 18 Electron microprobe results for the three samples
A. top; B. middle; C. bottom.
- 19 SEM of plasma etched surface of top sample A. 200x;
B. 2000x.
- 20 SEM of plasma etched surfaces A. 200x middle sample;
B. 100x bottom sample.
- 21 Comparison of total nitrogen removal for fresh, spent
and regenerated catalysts.

Figure

- 22 Comparison of total sulfur removal for fresh, spent and regenerated catalysts.
- 23 Network for quinoline hydrodenitrogenation.
- 24 Comparison of experimental data and predicted values for quinoline and 1,2,3,4-tetrahydroquinoline concentrations.
- 25 Comparison of experimental data and predicted values for orthopropylaniline, 5,6,7,8-tetrahydroquinoline and decahydroquinoline concentrations.
- 26 Comparison of experimental data and predicted values for total nitrogen removal for fresh catalysts.
- 27 Effect of catalyst particle size on quinoline and 1,2,3,4-tetrahydroquinoline concentration.
- 28 Network for dibenzothiophene desulfurization.

Light Microscopy—top sample



100x



200x

Scanning Electron Microscopy - top sample



400x
Backscatter
Electron

SEM-EDAX Area Scan - top sample

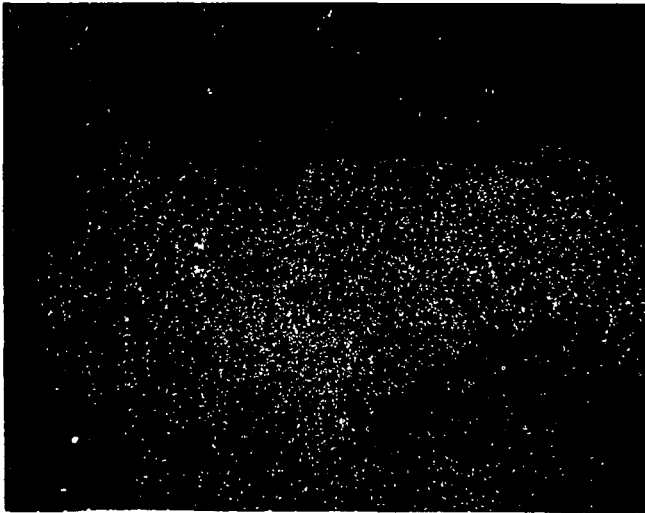


400x
Aluminum
EDAX

SEM-EDAX Area Scans - top sample

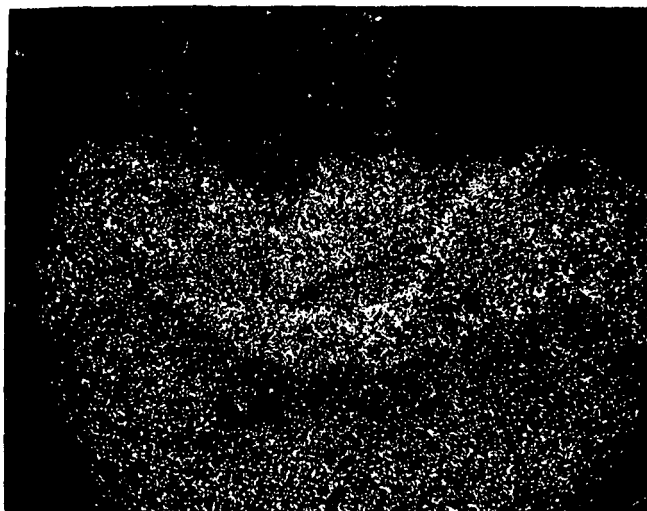


400x
Silicon

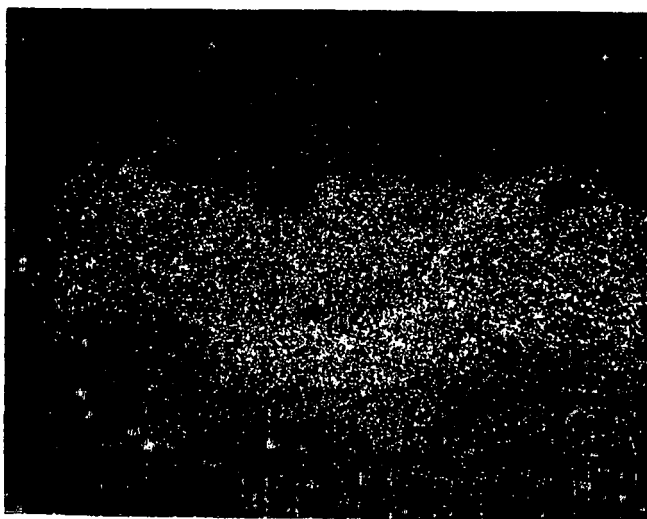


400x
Calcium

SEM-EDAX Area Scans - top sample



400x
Sulfur



400x
Iron

SEM-EDAX Area Scans - top sample



400x
Titanium

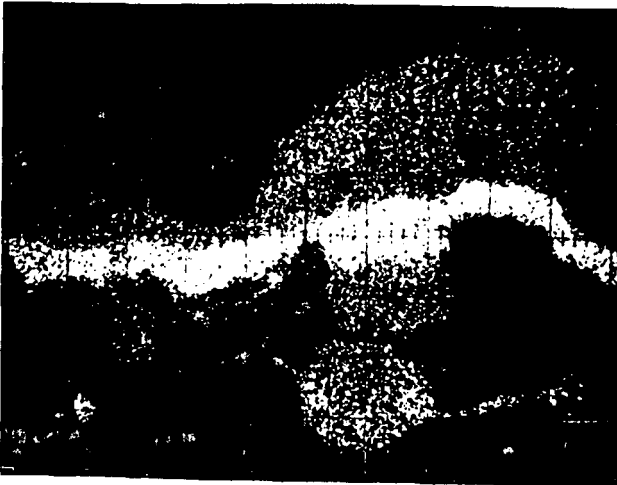


400x
Molybdenum

Microprobe Scans - top sample



500x
Backscatter
Electron



500x
Titanium

Light Microscopy – middle sample



100x



200x

Scanning, Electron Microscopy – middle sample

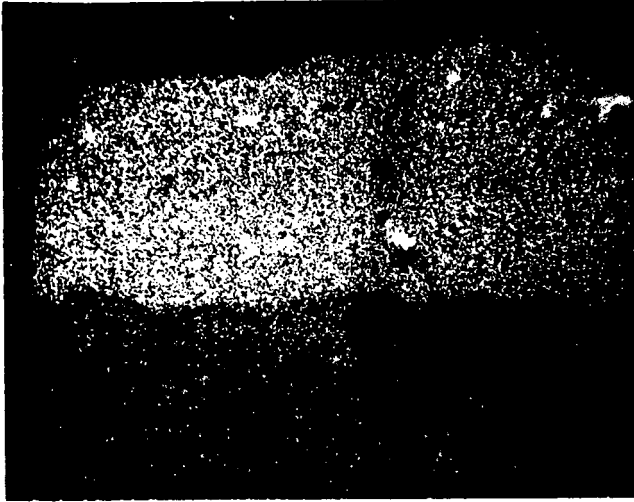


400x

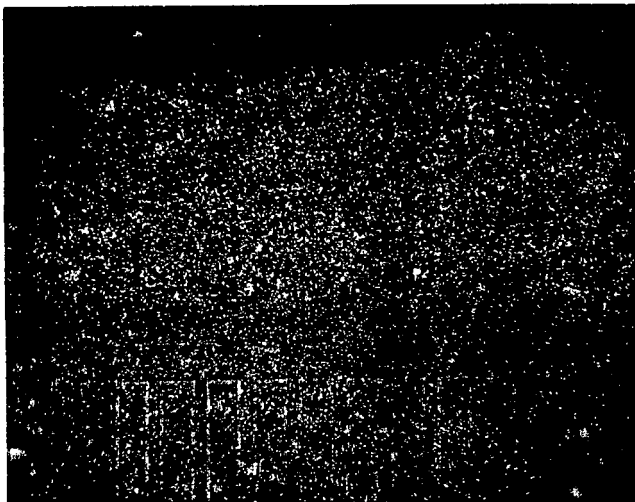


800x

SEM-EDAX - Area Scans - middle sample

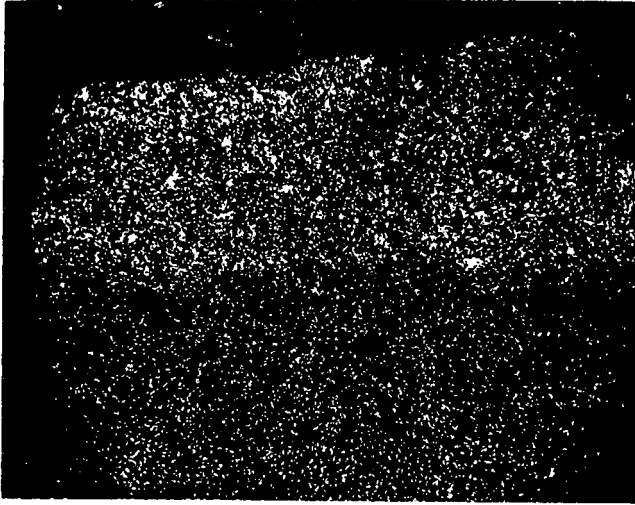


800x
Silicon

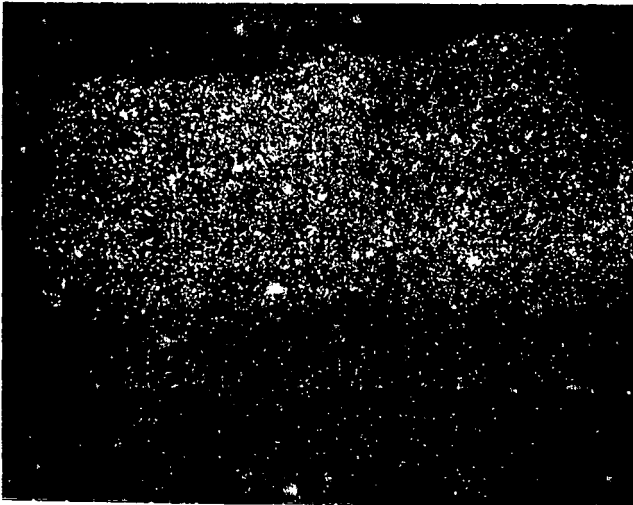


800x
Calcium

SEM-EDAX Area Scans - middle sample



800x
Sulfur

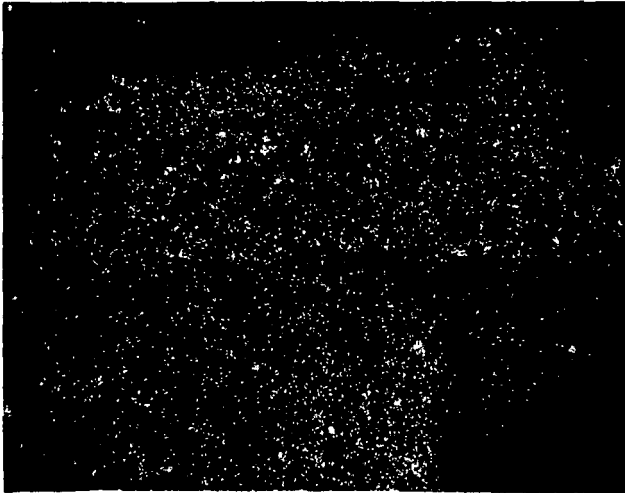


800x
Iron

SEM-EDAX Area Scans - middle sample

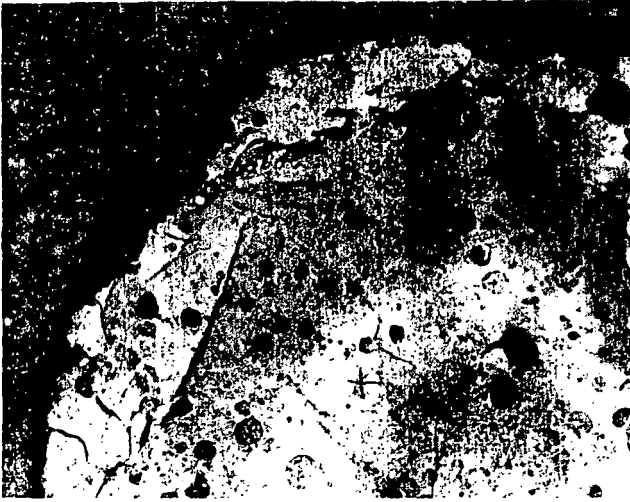


800x
Titanium

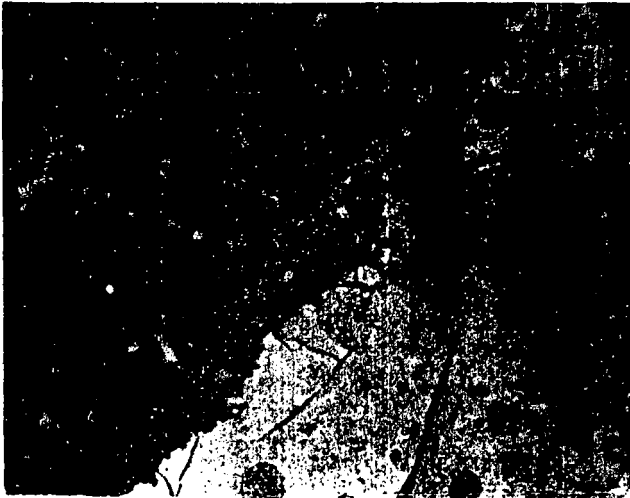


800x
Molybdenum

Light Microscopy - bottom sample

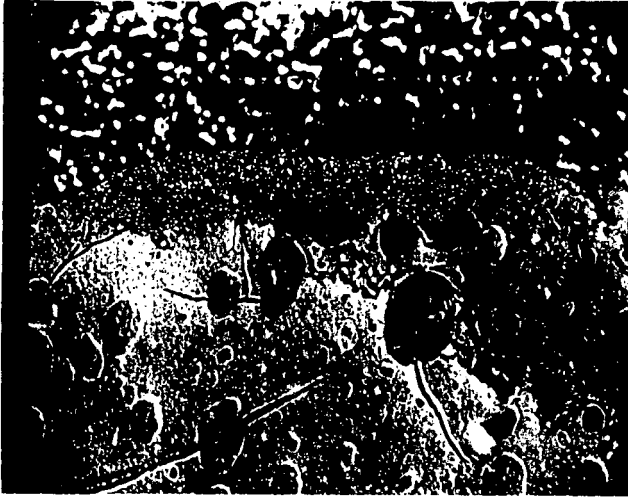


100x



200x

Scanning Electron Microscopy - bottom sample

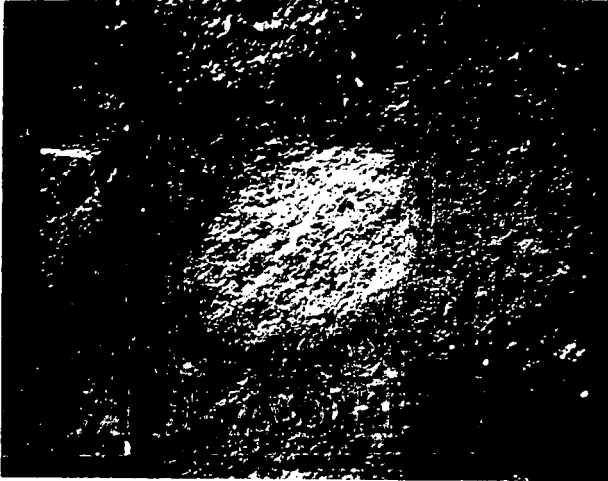


200x

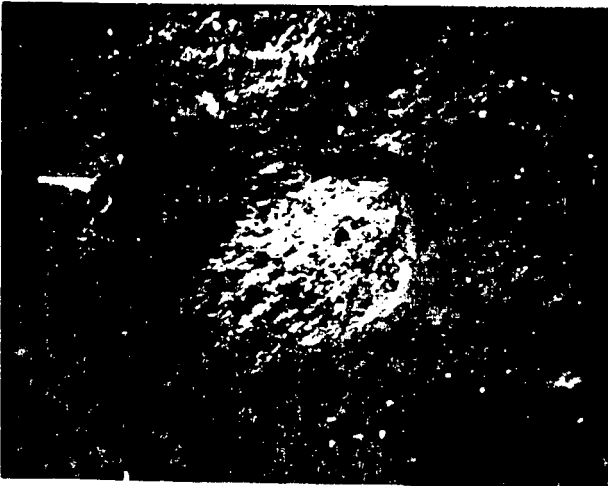


400x

Scanning Electron Microscopy
Interior Spot - 1000x, 45° tilt

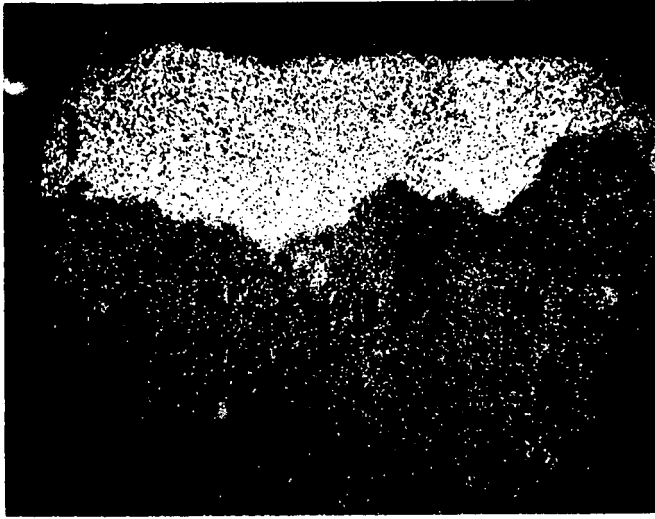


Backscatter
Electron

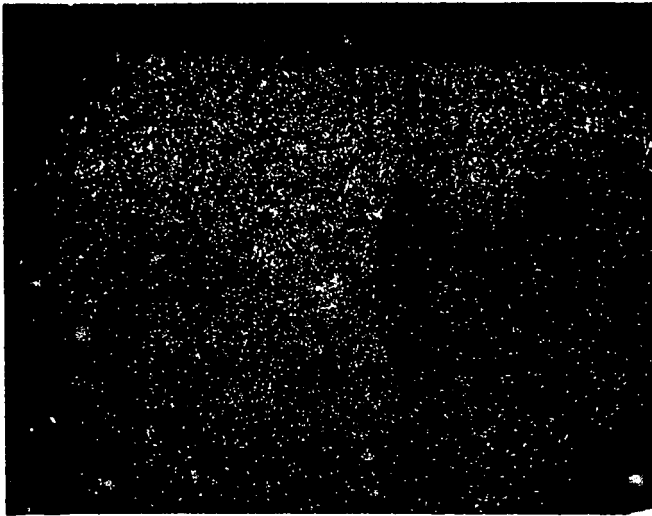


Ground
Current

SEM-EDAX Area Scans - bottom sample



400x
Silicon

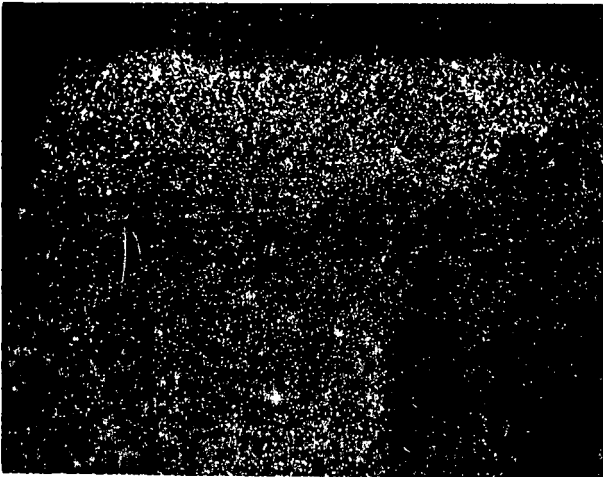


400x
Calcium

SEM-EDAX Area Scans - bottom sample

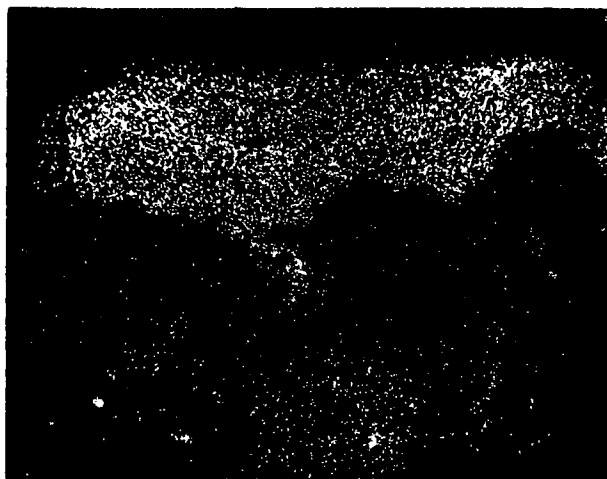


400x
Sulfur

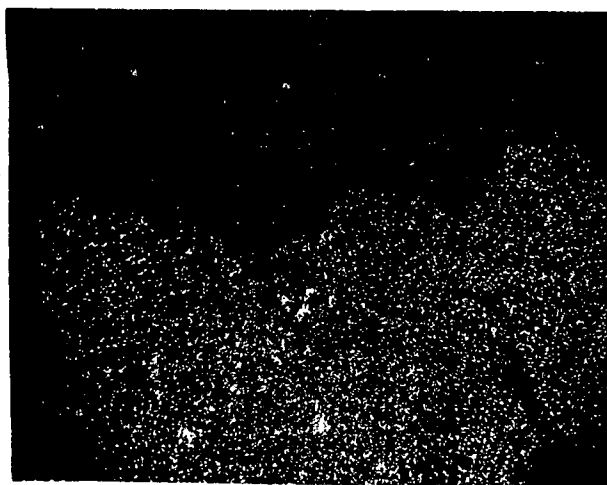


400 x
Iron

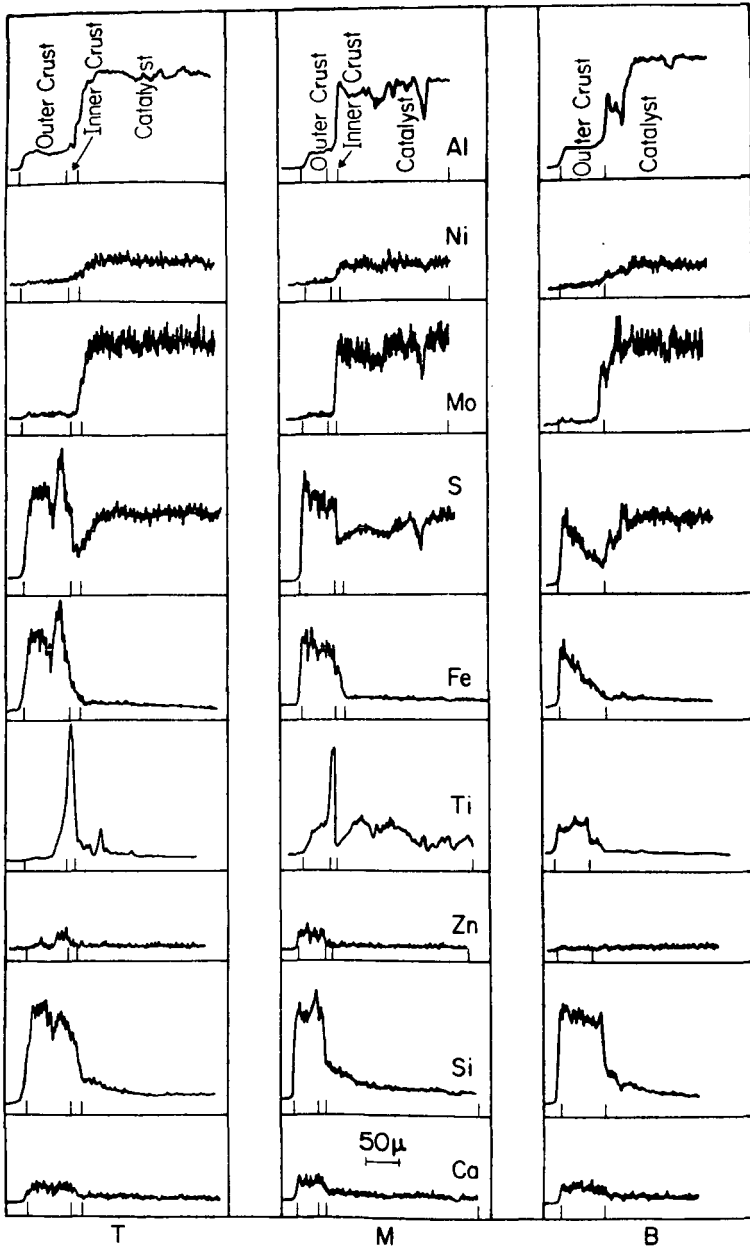
SEM-EDAX Area Scans - bottom sample



400x
Titanium

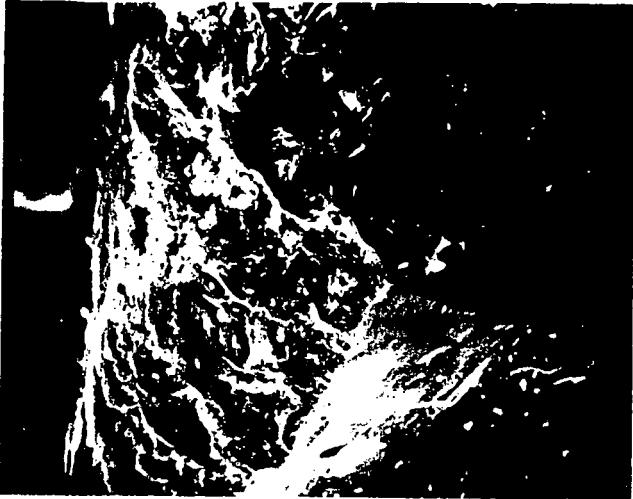


400x
Molybdenum

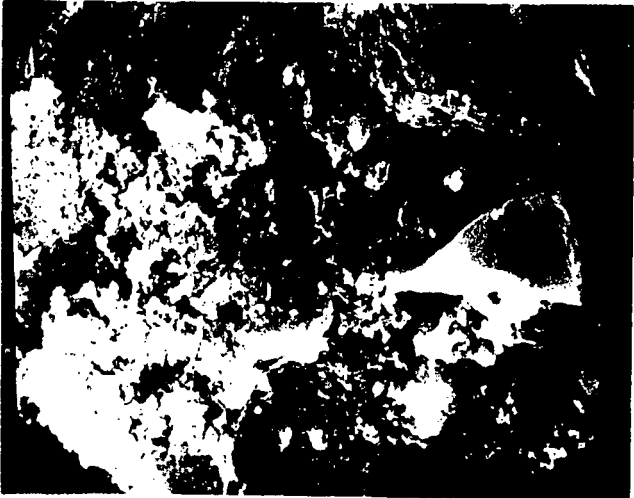


RELATIVE CONC PROFILES

SEM Plasma Etched Surface - top sample

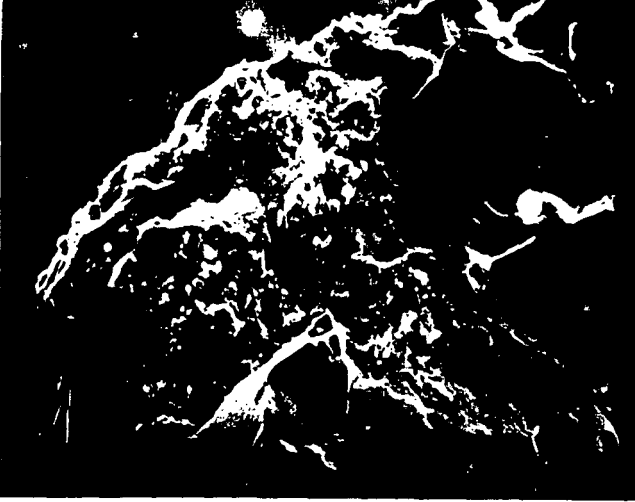


200 x



2000 x

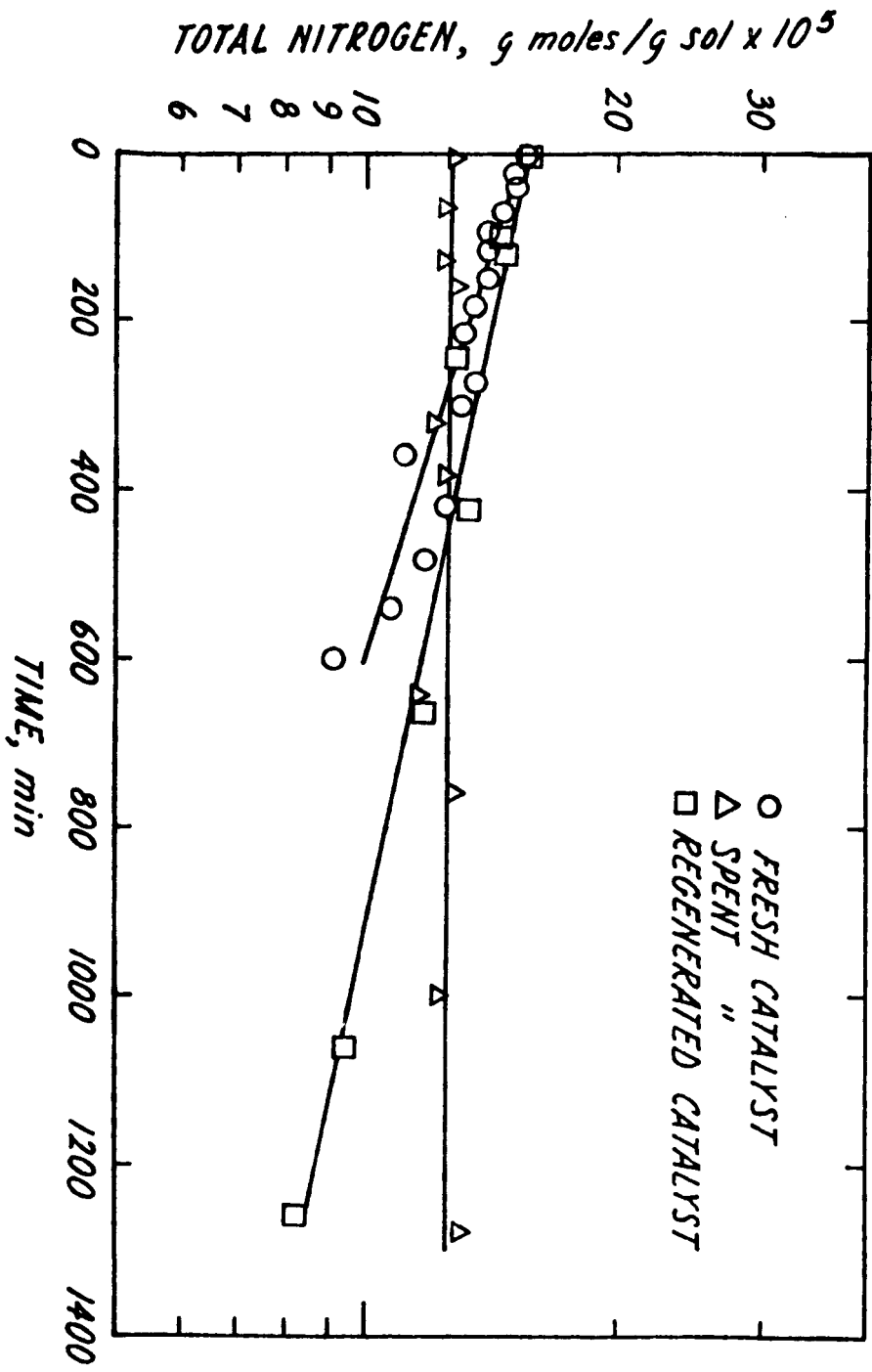
SEM Plasma Etched Surfaces



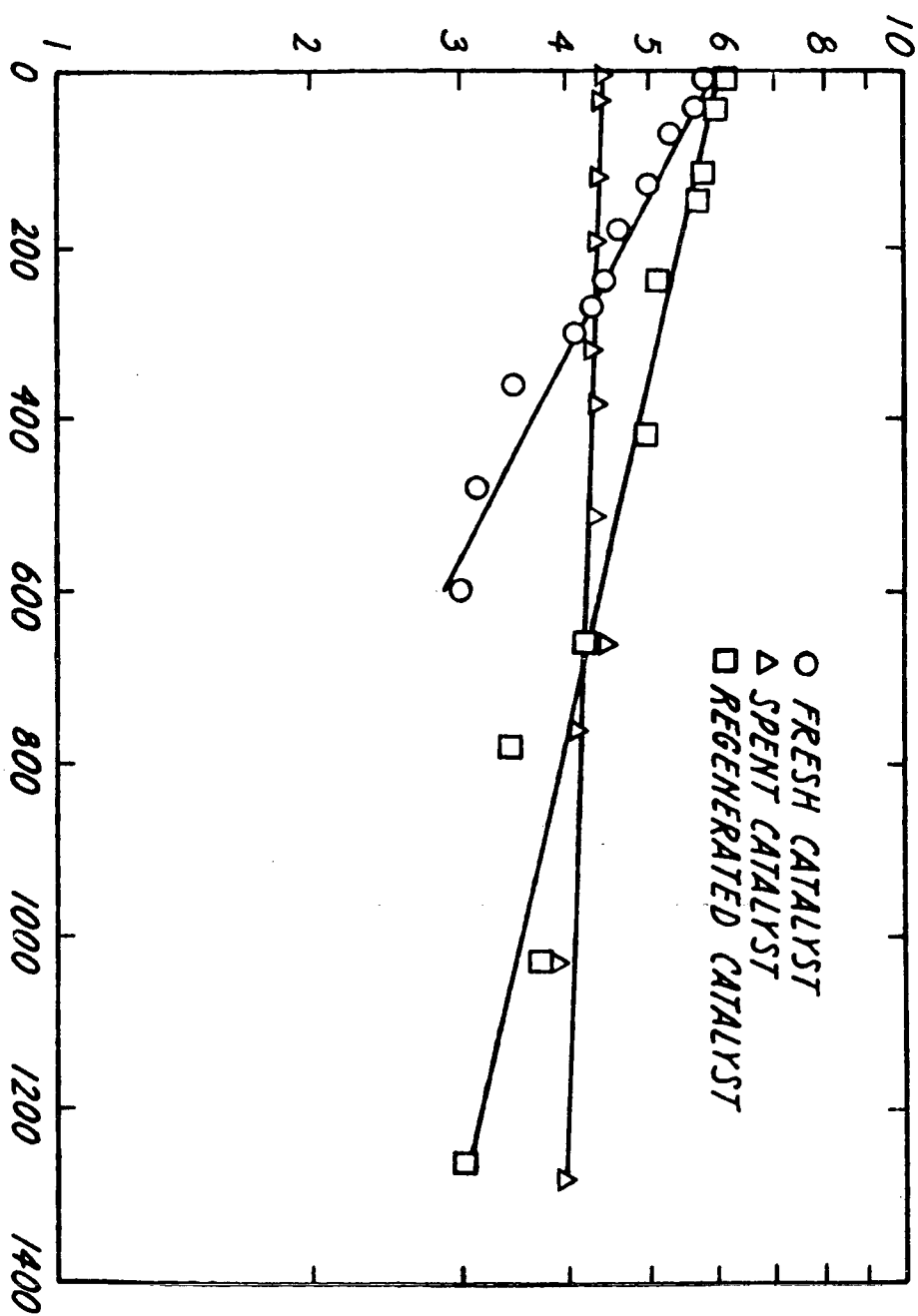
200x
Middle
Sample

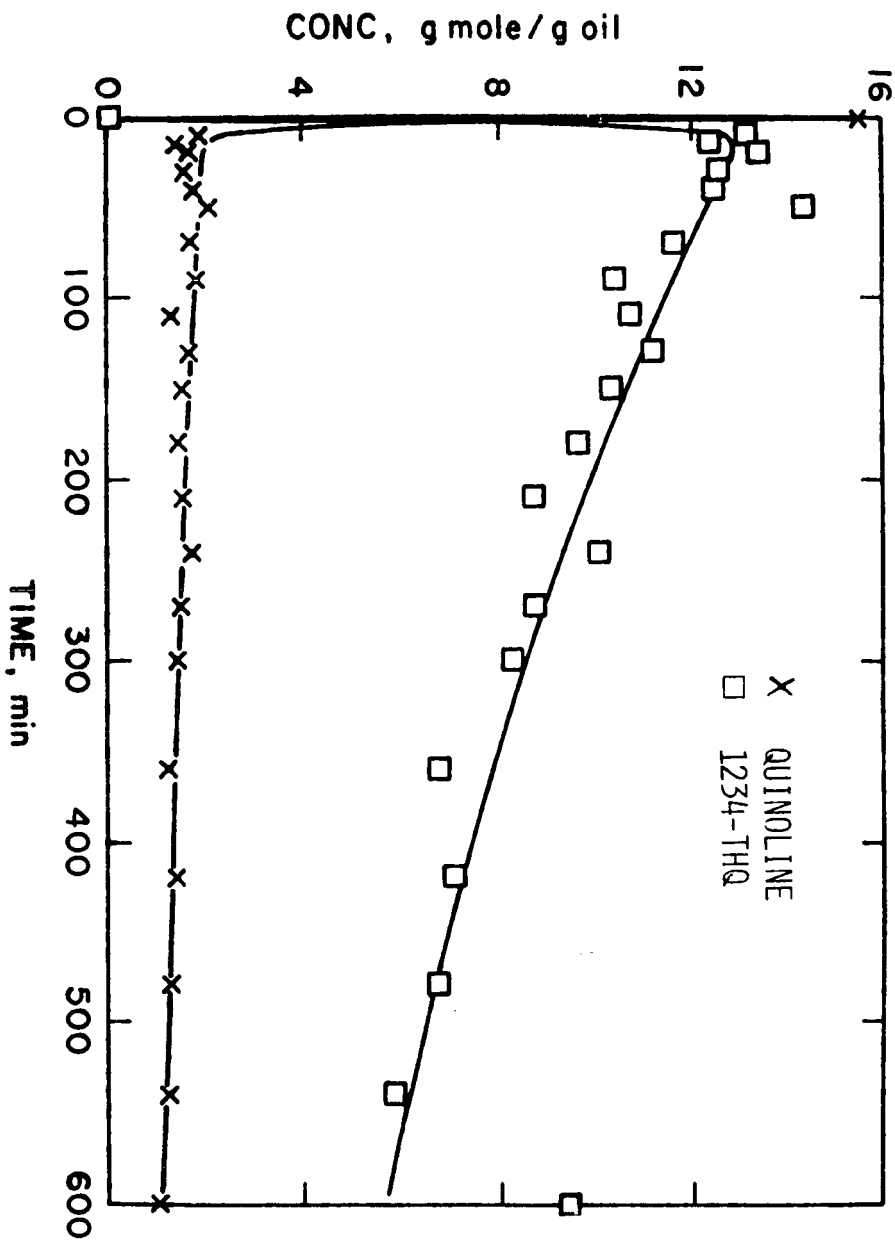


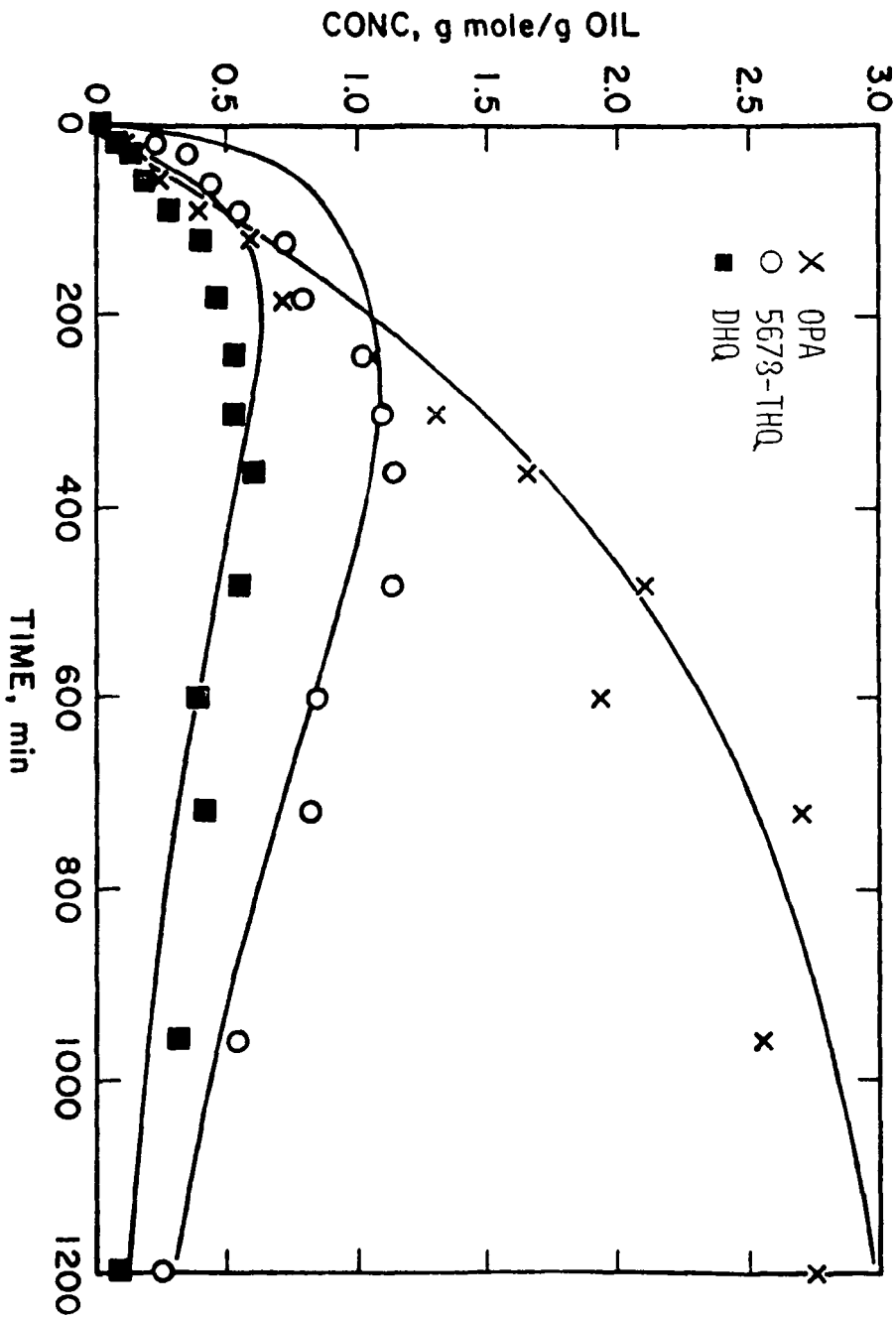
100x
Bottom
Sample

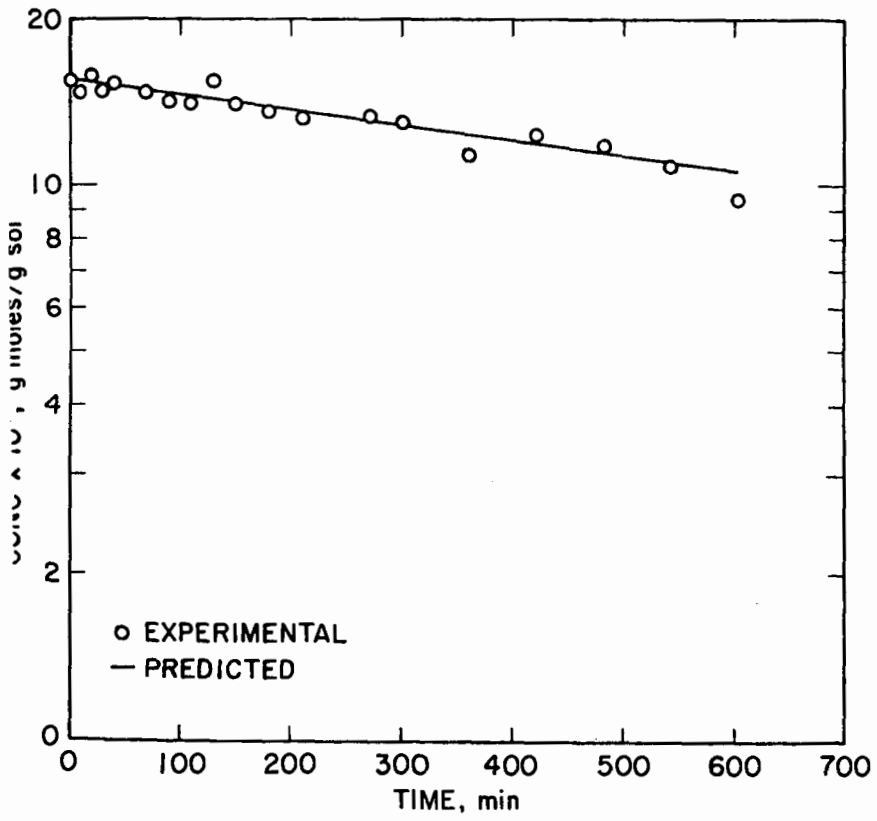


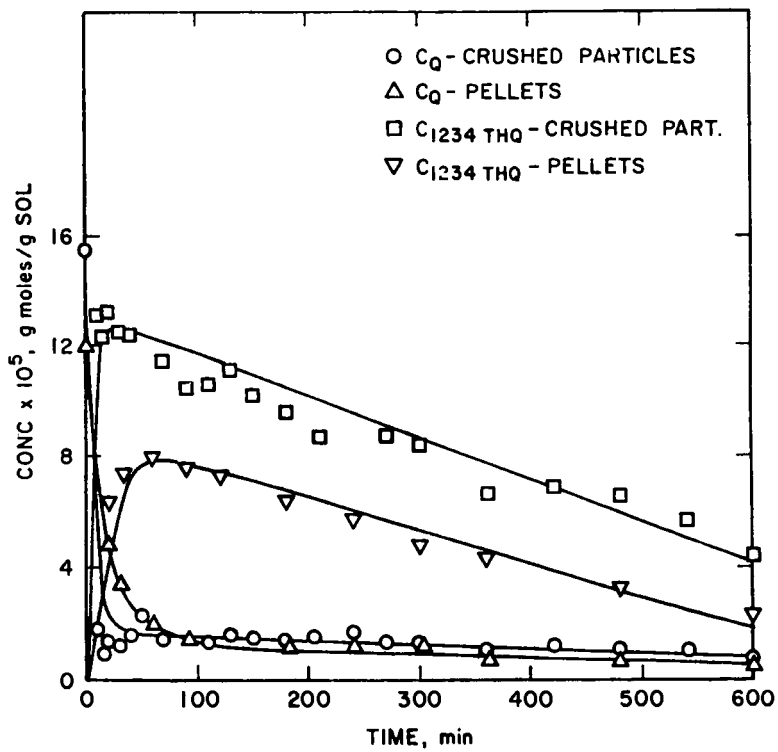
TOTAL SULFUR, g moles/g oil $\times 10^5$

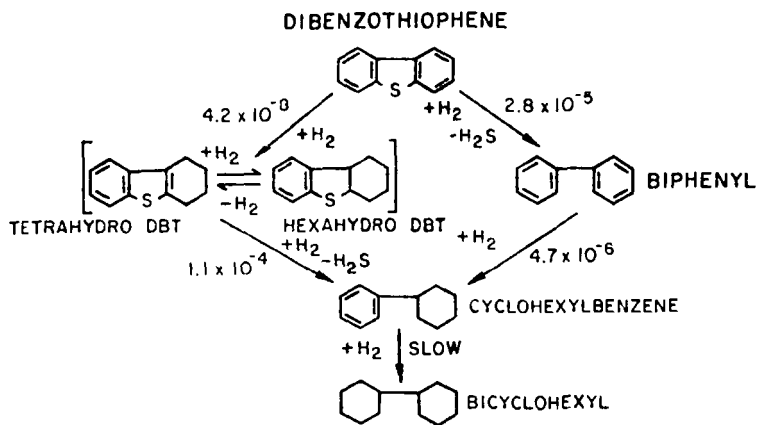












CATALYST DEACTIVATION IN HYDROTREATING COAL-DERIVED LIQUIDS by R. Sivasubramanian, J.H. Olson and J.R. Katzer. Center for Catalytic Science and Technology, Department of Chemical Engineering, University of Delaware, Newark, Delaware 19711.

Ni-Mo/Al₂O₃ catalysts aged in hydrotreating coal-derived liquids were characterized by scanning electron microscopy, electron microprobe, and catalytic activity. Aged catalyst from three different sections of the trickle-bed reactor used for the hydroprocessing were plasma etched to remove the carbon coating and were then examined. An inner crust and an outer crust were observed on the exterior of the catalyst particles; the inner crust was not present on catalyst near the reactor exit. The inner crust was composed principally of titania; whereas the outer crust contained ferrous sulfide, silica, and traces of other metals. Titania was also deposited within the interior of the catalyst. The activities of fresh, aged, and regenerated (coke burnt off) catalysts were compared for hydrodesulfurization (HDS) and hydrodenitrogenation (HDN) using a mixture of dibenzothiophene and quinoline in n-hexadecane in a batch autoclave reactor. The aged catalyst was inactive for HDN and had very low activity for HDS. Burning the carbon off the catalyst resulted in approximately 60% recovery of the HDN activity and 50% recovery of the HDS activity compared to that of the fresh catalyst. Pseudo first-order rate constants were determined for each of the reactions in the quinoline and dibenzothiophene reaction networks.

Refining of Coal and Shale Derived Syncrudes

R. H. Fischer and R. E. Hildebrand

The Department of Energy is funding a program in refining of syncrudes with the objective of assessing the ability of existing technology to process syncrude, developing new more efficient technology designed especially for syncrude and determining the relationship between refining severity and product end use performance and toxicity. Also the Air Force sponsors a program that is developing new methods of refining shale oil. The achievements of these programs in 1979 will be reviewed and the Department's plans for 1980 and 1981 will be discussed.

APPLICATION OF LC-FINING TECHNOLOGY FOR UPGRADING SRC IN TWO-STAGE LIQUEFACTION
CONCEPT. J. D. Potts, K. E. Hastings, and R. S. Chillingworth, Cities Service
Co., Box 300, Tulsa, OK 74102; H. Unger, C-E Lummus Co., 755 Jersey Ave.,
New Brunswick, NJ 08902; E. M. Phillips, Air Products and Chemicals, Inc.,
Box 538, Allentown, PA 18105

The concept of Two-Stage Liquefaction (TSL) hinges on recognition of the fact that the deashed solid Solvent Refined Coal (SRC), obtained from a first stage coal dissolution, is a high boiling residual type hydrocarbon stream. This material can be efficiently upgraded to liquid fuels by a second stage application of conventional hydrocracking or hydroprocessing technology extensively developed and demonstrated in the petroleum industry over the last twenty years (LC-Fining). That is, by judicious hydrocracking of the SRC product from the first stage, in the presence of a selective catalyst and under optimum conditions of temperature, space velocity, and reactor pressure, the production of middle distillate liquid fuels can be enhanced, the formation of light hydrocarbon gases can be minimized, and the overall utilization of hydrogen is optimized. In addition, the operation of a separate stage of LC-Fining provides wide operating latitude to tailor the overall product slate distribution (i.e., ratio of liquids to solids) and the product quality to both current and future market product requirements.

This study will also present the results of additional PDU runs which will delineate the effects of total reactor pressure and space velocity on the hydrotreating of coal extracts.

CATALYST ASSESSMENT FOR UPGRADING SHORT CONTACT TIME
SRC TO LOW SULFUR BOILER FUELS

S. S. Shih, P. J. Angevine, R. H. Heck and S. Sawruk

Mobil Research and Development Corporation
Paulsboro, New Jersey 08066

Introduction

Solvent refined coal (SRC) can be upgraded via catalytic hydroprocessing into low sulfur fuels (1,2). Reduced process cost can be effected by several factors, including the following: higher catalyst activity, improved utilization of hydrogen, and optimized SRC concentration in the feedstock. To this end, a series of commercial and proprietary catalysts was evaluated for the hydroprocessing of 50 wt % W. Kentucky short contact time SRC (SCT SRC). The commercial catalysts tested were alumina-based and were known to have good hydrotreating activity for heavy petroleum or coal-derived liquids. The rates of hydrogenation and pore size distribution will be discussed. A developmental catalyst with relatively high desulfurization and efficient hydrogen utilization was tested in a constant temperature aging run to establish process conditions needed to produce 0.4 wt % sulfur boiler fuels.

Experimental

The experiments were conducted in a continuous down-flow fixed bed pilot unit. The feedstock, 50 wt % W. Kentucky/SRC recycle solvent blend, was prepared in a charge reservoir and transferred to a weigh cell by gravity flow. Both the charge reservoir and weigh cell were kept at 350°F. After the reactor, hydrogen and light gases were separated from hydrotreated oil through high (300°F) and low (75°F) temperature separators in series. To maintain fluidity of the high SCT SRC concentration blend, all lines and valves from the charge reservoir to the high temperature separator were heat-traced to 340-420°F. The detailed description of the pilot unit is available elsewhere (1). The selection of SCT SRC as the feed was based on a recent finding that the hydrogen utilization efficiency for production of hydrogen-rich coal liquids can be improved by coupling mild short resident time hydroliquefaction (to produce SCT SRC) with catalytic hydroprocessing (3).

The catalysts were presulfided with a 10% H₂S/H₂ mixture and tested at a reactor pressure of 2000 psig and a hydrogen circulation of 5000 scf/B. Each catalyst was subjected to a standard sequence of temperatures and liquid hourly space velocities, ranging from 720-800°F and 0.5-2.0 hour⁻¹, respectively.

Results and Discussions

Fresh Catalyst Properties - Three Mobil catalysts were tested and have been identified as HCL-1, -2, and -3. Because of the proprietary nature of these catalysts, properties have been excluded. The major properties of the four commercial and two developmental catalysts are shown in Table 1. The four commercial catalysts evaluated were NiMo/Al₂O₃: Harshaw's 618X and HT-500, and American Cyanamid's HDN-1197 and HDS-1443. The NiMo catalysts were

tested in a greater number than the CoMo catalysts because it had been thought that improved hydrogenation activity was needed to treat the highly refractory SRC. Also, nickel-promoted hydroprocessing catalysts form less coke than cobalt-promoted catalysts, possibly resulting in better stability. The 618X, HT-500, and HDS-1443 catalysts all have similar metals loading; their major difference is found in surface area, going from relatively low to medium to high, respectively. The shift in surface area can also be seen in the different pore size distributions. Harshaw 618X has a well-defined distribution with 77% of its pore volume in the 100-200Å diameter region. HT-500 has a broader distribution and smaller median size, having half of its pore volume in the 80-100Å region. HDS-1443 has a bimodal distribution: it has most of its pores in 30-80Å, but it also has some 200Å⁺ pores. HDN-1197 has a higher metals loading than the other NiMo catalysts and also has most of its pores in the 30-80Å region.

Two developmental catalysts were evaluated in this study. These include Amocat 1A and 1B, recently developed by Amoco for testing in the H-Coal[®] Process (4). Both catalysts were made of the same support and had primarily 100-200Å pores with some macropores (>1000Å). Amocat 1B is an unpromoted Mo/Al₂O₃ while 1A is CoMo/Al₂O₃.

Fresh Activity Comparisons - The nine catalysts have been divided into two groups in order to simplify the activity comparisons. Group A is made up of the more active desulfurization catalysts and includes Mobil HCL-2, Mobil HCL-3, American Cyanamid HDS-1443, and Amocat 1A. Group B includes Mobil HCL-1, Harshaw 618X, American Cyanamid HDN-1197, and Amocat 1B. For the activity comparisons, the heteroatom removals (and CCR reduction) are plotted versus reactor temperature at a liquid hourly space velocity of 1.0. Consequently, catalyst activity can be compared on the basis of temperature requirements for achieving specific liquid product heteroatom (or CCR) contents.

The comparisons of desulfurization activities are shown in Figure 1 and Figure 2 for Group A and Group B catalysts, respectively. At the 80% desulfurization level, Mobil HCL-2 is 10-15°F more active than HDS-1443, followed by HCL-3, Harshaw 618X, and Amocat 1A (Figure 1). Surface area and pore size distribution seem to be important parameters for the fresh catalyst activity. The relatively high fresh activity of HDS-1443 may be partially explained by its high surface area and presence of macropores (Table 1). The presence of macropores may be responsible for the improvement of the relative positions of HDS-1441 and Amocat 1A at more severe conditions (0.5 LHSV).

The importance of pore size distribution also explains the low activity of HT-500, which has 75% of its pore volume in the 100Å region. Cyanamid HDN-1197 seems to have a high desulfurization activity (Figure 2). However, it yields an inhomogeneous product, probably due to its high hydrogenation activity coupled with its small pore size. Inhomogeneous products have also been observed in the upgrading of regular SRC by small pore catalysts (1). The SCT SRC, with its high polar asphaltenes content, is particularly susceptible to "front end, back end" incompatibility.

The ranking of deoxygenation activity was very similar to that of the desulfurization activity (Figure 3). The results may suggest that, like desulfurization, the deoxygenation reaction could occur without pre-hydrogenation. The comparison of denitrogenation activities is shown in Figure 4. Mobil HCL-3 was the most active catalyst followed by Mobil HCL-2 and Harshaw 618X.

The CCR reduction activity for the nine catalysts is similarly plotted as a function of temperature in Figure 5 and Figure 6. Mobil HCL-2, HCL-3, and Amocat 1B are the most active catalysts. Generally, heteroatom removal can be achieved with only minor changes in chemical structure. However CCR reduction in SCT SRC occurs with significant alteration of GEC classes, primarily toward the formation of less polar compounds. The classes of W. Kentucky SCT SRC, separated by GEC (gradient elution chromatography), are given in Table 2 and show that 75% of the SRC is polar and non-eluted polar asphaltenes.

Table 2: GEC Analyses of W. Kentucky SCT SRC

Saturates	0.3 wt %
Aromatic Oils	0.4 wt %
Resins/Asphaltenes	24.8 wt %
Polar Asphaltenes	45.1 wt %
Non-Eluted Asphaltenes	29.4 wt %
	<u>100.0</u>

The conversion of polar asphaltenes (lumped with non-eluted asphaltenes) as a function of process severity, expressed by hydrogen content in the liquid product, is shown in Figure 7. Amocat 1B and HDS-1443 show a significantly high conversion of polar asphaltenes at a given process severity. It is worth noting that Amocat 1B and HDS-1442, the Co-Mo version of HDS-1443, have been found to be active catalysts for coal hydroliquefaction (4).

Hydrogen consumption is a major economic factor in any coal liquid hydroprocessing operation. In Figure 8, the total hydrogen consumption is plotted vs. total liquid product (TLP) sulfur content. Three selectivity curves have been drawn from Figure 8: the solid curve represents Harshaw 618X, and the dashed curves are for Amocat 1A and 1B. To a rough approximation HCL-2, HDS-1443, and Amocat 1A are "low" hydrogen consumption catalysts; Harshaw 618X and Mobil HCL-3 are relatively "high" hydrogen consumption catalysts. At the same level of desulfurization Harshaw 618X uses approximately 500 scf/B more than Amocat 1A. However, Amocat 1B, a low desulfurization activity catalyst, shows a very high hydrogen consumption.

Analyses of Used Catalysts - The analyses of five used catalysts tested with 50% W. Kentucky SCT SRC are given in Table 3. The coke and iron depositions appear to be strongly dependent upon catalysts; Harshaw 618X and HDS-1443 are high, but Amocat 1A and 1B are low in coke deposition. Since surface area measurements can include contribution by contaminants (particularly coke), these values have no clearcut meaning. Besides the coke deposition, metal deposition on the catalysts contributes to the catalyst deactivation.

Table 3: Used Catalyst Properties as Received

	Harshaw 618X	Harshaw HT-500	Cyanamid HDS-1443	Amocat 1B	Amocat 1A
Surface Area, M ² /g	132	147	201	137	125
Pore Volume, cc/g	0.349	0.253	0.568	0.510	0.487
Pore Diameter, Å	106	69	113	149	156
Iron, Wt Pct	0.61	0.30	0.35	0.77	0.61
Coke, Wt Pct	20.6	23.0	18.0	12.8	13.0

The deposition of metal contaminants on a used Harshaw 618X catalyst was analyzed with a scanning electron microscope (SEM). The SEM x-ray emission spectra for fresh and used catalysts at different locations in the catalyst particle are shown in Figure 9. The used catalyst, tested after our standard procedure, showed a large buildup of iron and titanium in a narrow band (<2 microns) of the catalyst exterior. Other contaminants (e.g., K, Ca, Si) were detected at lower concentrations. As shown in Figure 9(b), strong intensities of deposited metals were clearly shown in the x-ray emission spectrum taken near the extrudate external surface. The intensities were substantially reduced in analyses made away from the exterior edge, as shown in Figures 9(c) and 9(d). These results indicate that the hydroprocessing of coal liquids is well suited to ebullated bed reactors; the motion of the fluidized catalysts may provide a continuous, partial regeneration by mildly abrading the metals-rich pellet exterior.

Aging Run - Based on the fresh activity evaluation, Amocat 1A was tested in an aging run for the hydroprocessing of 50% W. Kentucky SCT SRC. The run was made at constant conditions (2000 psig, 775°F, 0.5 LHSV) and was smoothly operated for 15 days. The run was then terminated due to incipient plugging in the reactor. The results are shown in Figure 10, where sulfur content in the liquid products has been plotted vs. days-on-stream. During this first four days the temperature was varied to obtain an activation energy estimation, and these data have been omitted.

A simple deactivation equation was used for a fixed bed reactor:

$$\frac{1}{C_A} - \frac{1}{C_{A0}} = \frac{k_0 e^{-E/RT} e^{-t/\tau}}{\text{LHSV}}$$

where C_{A0} and C_A are the initial and final concentrations of reactant (i.e., heteroatom or CCR). Here, k_0 is the fresh pre-exponential factor, LHSV is liquid hourly space velocity, E is activation energy, T is reaction temperature, t is time on-stream and τ is catalyst deactivation time constant. The estimated values for τ , k_0 , and E are as follows:

	$\frac{k_0}{1}$ Wt %-hr	$\frac{E}{\text{Btu}}$ lb mole	$\frac{\tau}{\text{Days}}$
Sulfur	1.992×10^{13}	69,900	18.3
Nitrogen	3.368×10^5	34,600	36.1
Oxygen	6.895×10^9	57,800	8.9
CCR	2.553×10^7	50,400	21.9

The temperature rise necessary to maintain a constant product sulfur concentration is about 2-3°F/day. The measured and model-predicted values for sulfur and CCR are shown in Figure 10.

The simulated operating conditions for the fixed bed reactor to produce a 900°F⁺ fuel with a sulfur content of 0.4 wt % are shown in Figure 11, using a charge of 50% W. Kentucky SCT SRC. Figure 11 shows the reactor temperature required to achieve these sulfur levels as a function of days-on-stream and LHSV. The temperature rise is 2.5-3.0°F/day. The cycle length, a function of both LHSV and the limit of reactor temperature, can be determined from Figure 11. For example, at 0.3 LHSV and a maximum reactor temperature of 850°F, the cycle length is 60 days.

Conclusions

Short contact time SRC can be upgraded via catalytic hydroprocessing into low sulfur boiler fuels. However, the solid SCT SRC feedstock requires solvent dilution to reduce its viscosity. Furthermore, even for a 50 wt % W. Kentucky SCT SRC blend, all pilot unit lines and valves have to be heat-traced above 350°F in order to achieve smooth mechanical operations.

Catalytically, the SCT SRC is more susceptible to form an inhomogeneous product than the regular SRC, particularly where small pore catalysts are used. The upgrading costs can be significantly reduced through increased activity as well as efficient hydrogen utilization. A proprietary catalyst, Mobil HCL-2, and a developmental catalyst, Amocat 1A, were observed to have these two important properties. For hydroprocessing of the 50 wt % W. Kentucky SCT SRC blend, the aging rate was moderate with a 2-3°F/day of temperature rise required to keep constant desulfurization activity. The catalysts are believed to be deactivated by coke and metal depositions on the surface. A large buildup of iron and titanium was found in a narrow band of the catalyst exterior of a spent catalyst. Improved catalyst aging is likely to occur by the use of an ebullated bed reactor, primarily by decreased interparticle coke formation as well as by mild abrasion of metal contaminants.

Acknowledgement

This work was performed under EPRI/Mobil research project RP 361-2. Dr. W. C. Rovesti is the EPRI project manager.

Reference

- (1) Stein, T. R., et al, Annual Report, EPRI Contract No. AF-873 (RP 361-2). Mobil Research and Development Corporation, December 1978.
- (2) Givens, E. N., Collura, M. A., Skinner, R. W., and Greskovich, E. J., Hydrocarbon Processing, 195, November 1978.
- (3) Mitchell, T. O., and Heck, R. H., Presented at AIChE 71st Annual Meeting, Miami Beach, Florida, November 13, 1978.
- (4) Bertolacini, R. J., Gutberlet, L. C., Kim, D. K., and Robinson, K. K., Final Report, EPRI Contract No. AF-1084 (Project 408-1), Amoco Oil Company, June 1979.

Table 1

FRESH CATALYST PROPERTIES

<u>Compositions, Wt %</u>	<u>Harshaw</u>	<u>Harshaw</u>	<u>Cyanamid</u>	<u>Cyanamid</u>	<u>Amoco*</u>	<u>Amoco</u>
	HT-500	HDN-1197	HDS-1443	1B	1A	
Ni	2.7	2.4	3.7	2.9	0	2.9
CoO						19.7
MoO ₃	14.8	14.0	21.7	15.5	14.9	
<u>Physical Properties</u>						
Surface Area, m ² /g	140	193	130	306	167	154
Pore Volume, cc/g	0.60	0.511	0.379	0.764	0.67	0.662
Pore Diameter, Å	172	104	117	100	160	172
<u>Pore Size Dist., cc/g</u>						
0-30 Å	0.025	0.005	0.059	0.165	>	0.065
30-80 Å	0.037	0.125	0.123	0.355	0.027	0.046
80-100 Å	0.036	0.252	0.112	0.020	0.063	0.063
100-200 Å	0.464	0.123	0.035	0.033	0.419	0.385
200 Å +	0.038	0.007	0.050	0.192	0.153	0.103

* Amoco's Analyses

Figure 1

COMPARISON OF DESULFURIZATION ACTIVITIES: GROUP A CATALYSTS

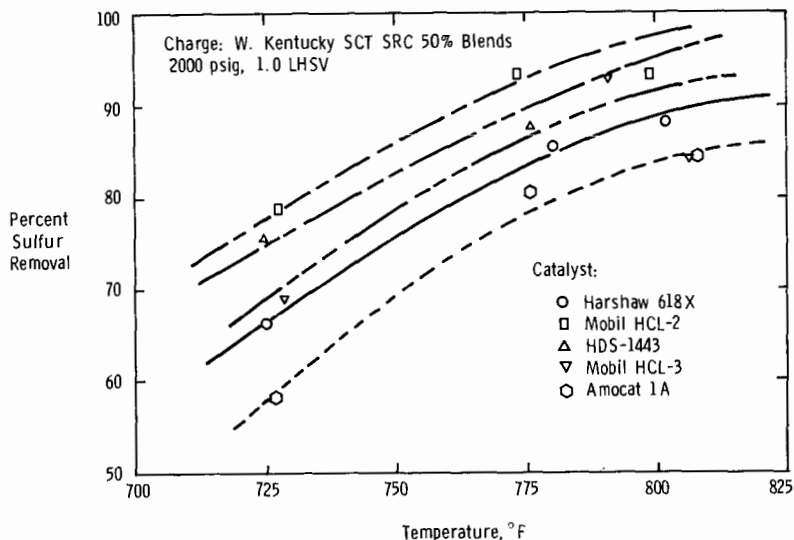


Figure 2

COMPARISON OF DESULFURIZATION ACTIVITIES: GROUP B CATALYST

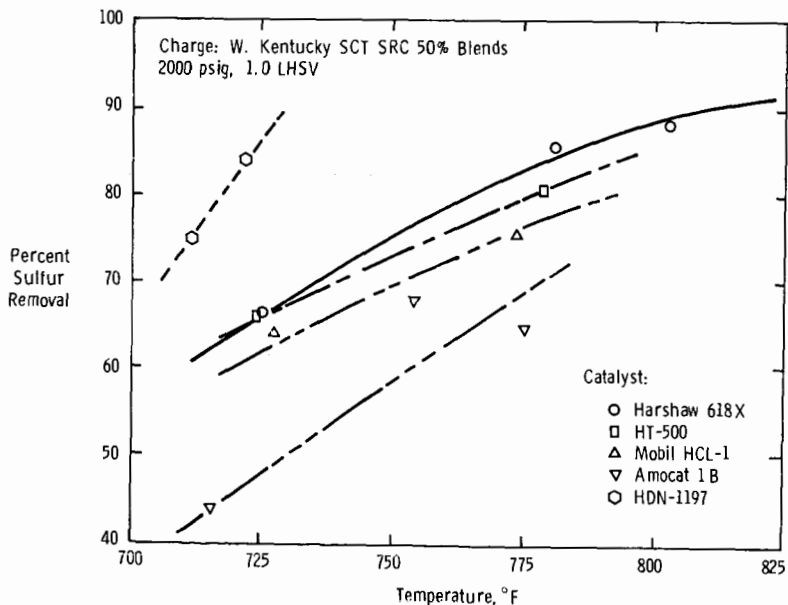


Figure 3

COMPARISON OF DEOXYGENATION ACTIVITIES: GROUP A CATALYSTS

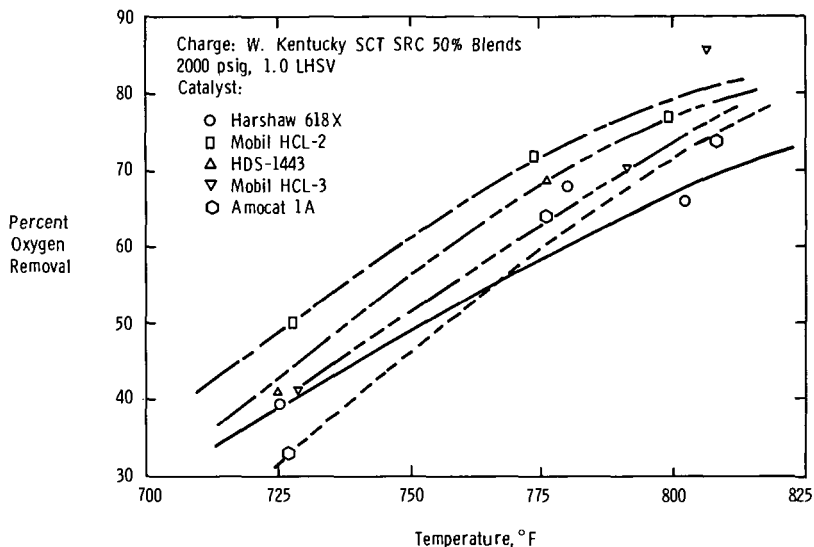


Figure 4

COMPARISON OF DENITROGENATION ACTIVITIES: GROUP A CATALYSTS

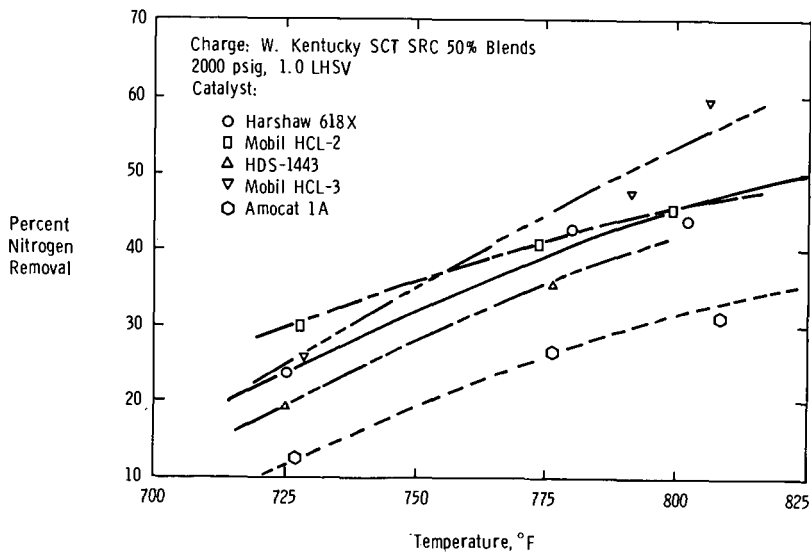


Figure 5

COMPARISON OF CCR REDUCTION ACTIVITIES: GROUP A CATALYSTS

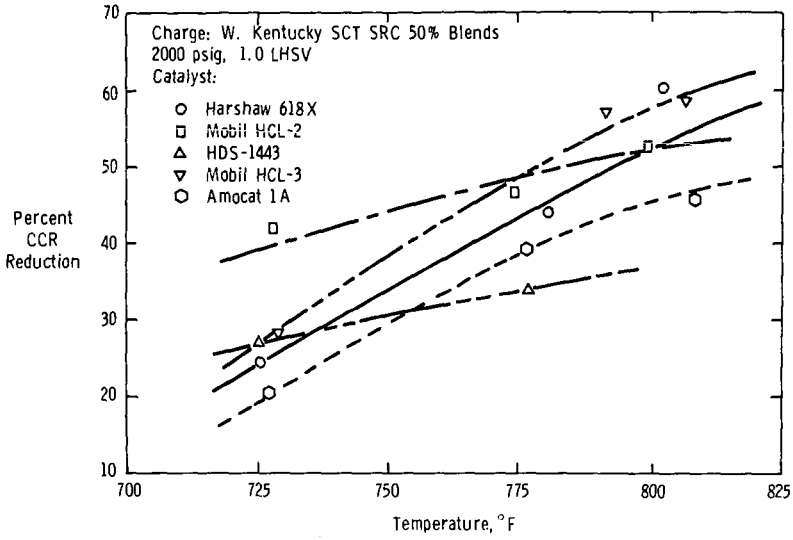


Figure 6

COMPARISON OF CCR REDUCTION ACTIVITIES: GROUP B CATALYSTS

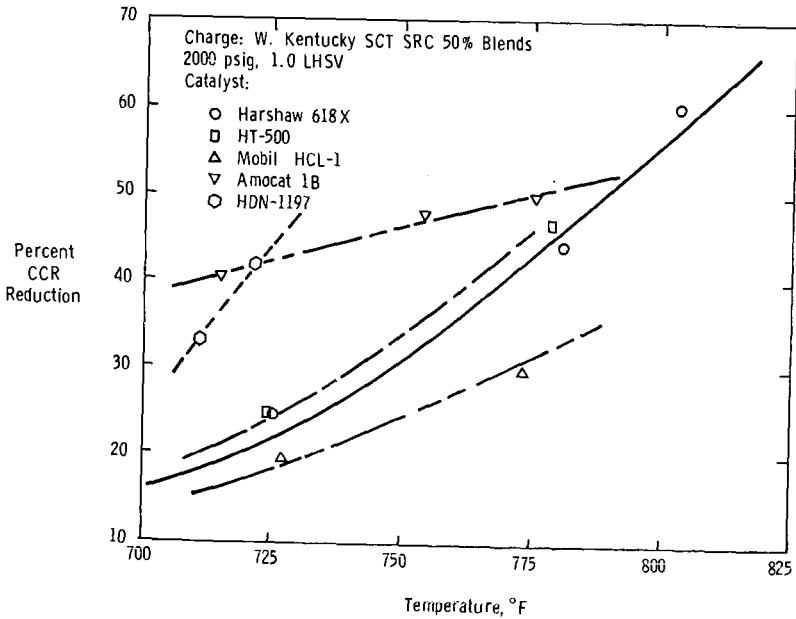


Figure 7

POLAR ASPHALTENES CONVERSION AS A FUNCTION OF HYDROPROCESSING SEVERITY

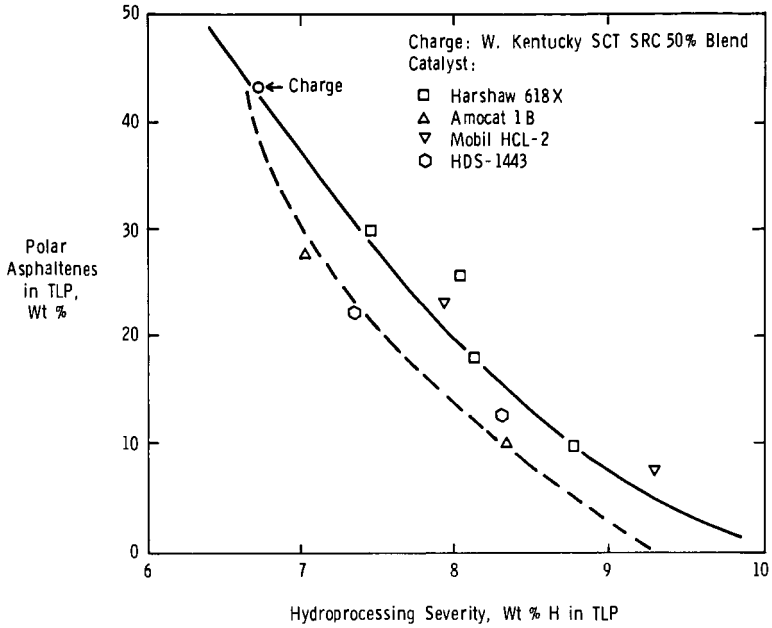
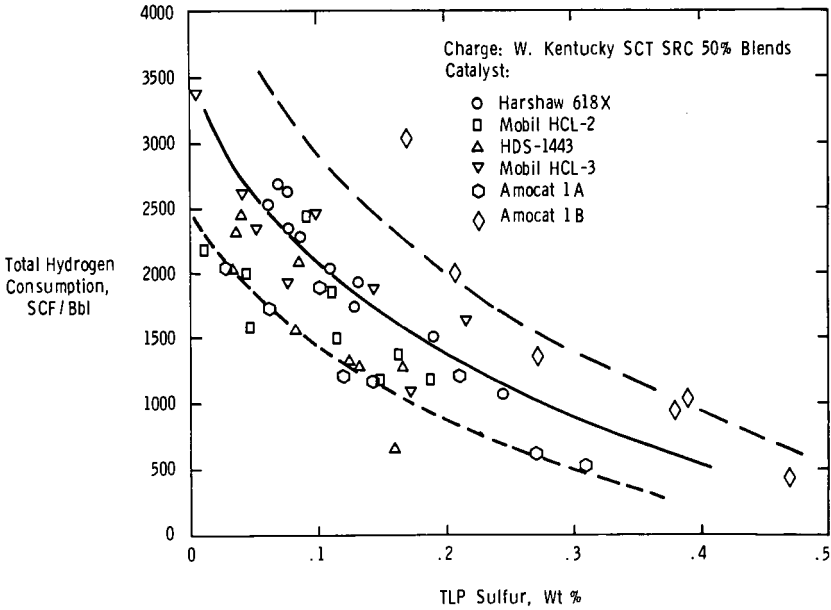
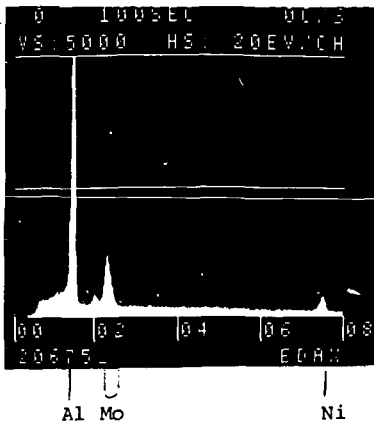


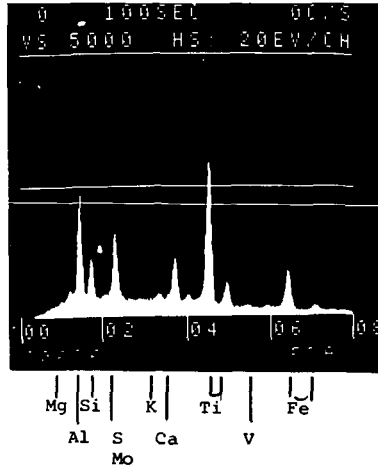
Figure 8

TOTAL HYDROGEN CONSUMPTION AS A FUNCTION OF SULFUR IN LIQUID PRODUCT

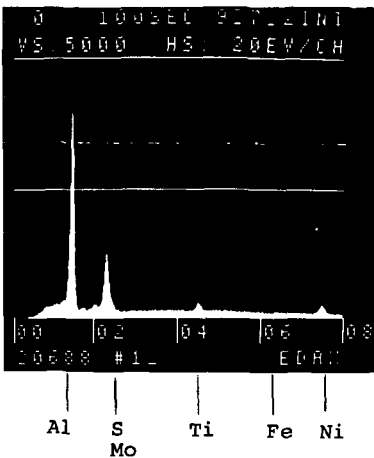




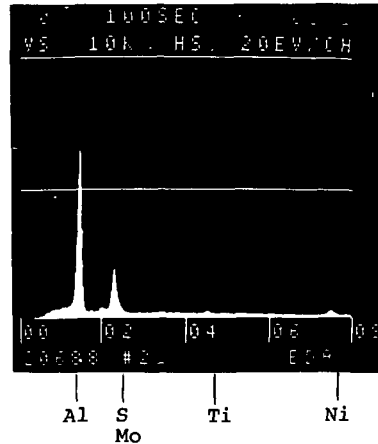
(a)



(b)



(c)



(d)

FIGURE 9: SEM Examination of Fresh and Used Harshaw 618X

- (a) X-ray emission spectrum taken of external surface of fresh catalyst showing presence of Al, Mo and Ni.
- (b) X-ray emission spectrum taken of external surface of used catalyst showing presence of Mg, Al, Mo, K, Ca, Ti, V and Fe.
- (c) X-ray emission spectrum taken at 0-20 μ from the edge of the cross section of used catalyst showing presence of Al, Mo, Ti, Fe and Ni.
- (d) X-ray emission spectrum taken at 60-80 μ from the edge of the cross section of used catalyst showing presence of Al, Mo, Ti and Ni.

Figure 10

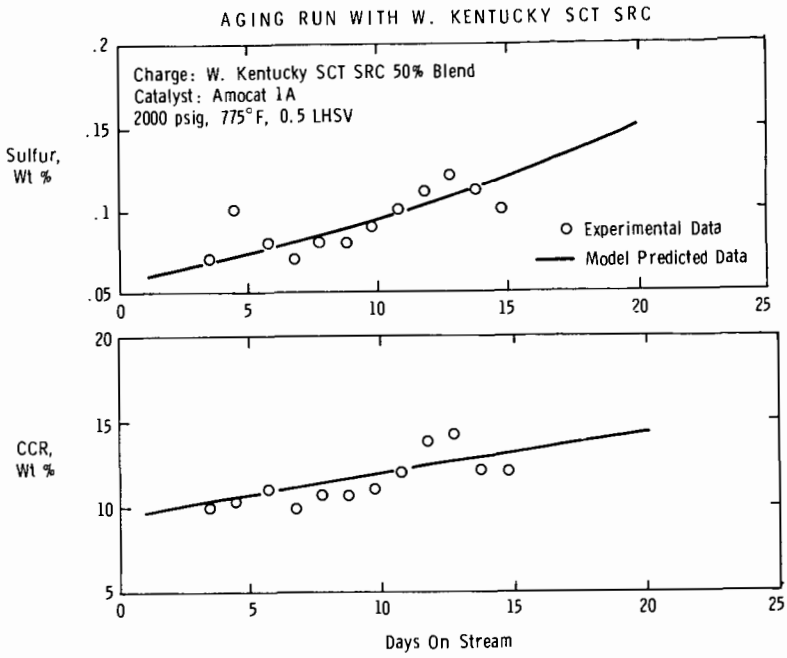
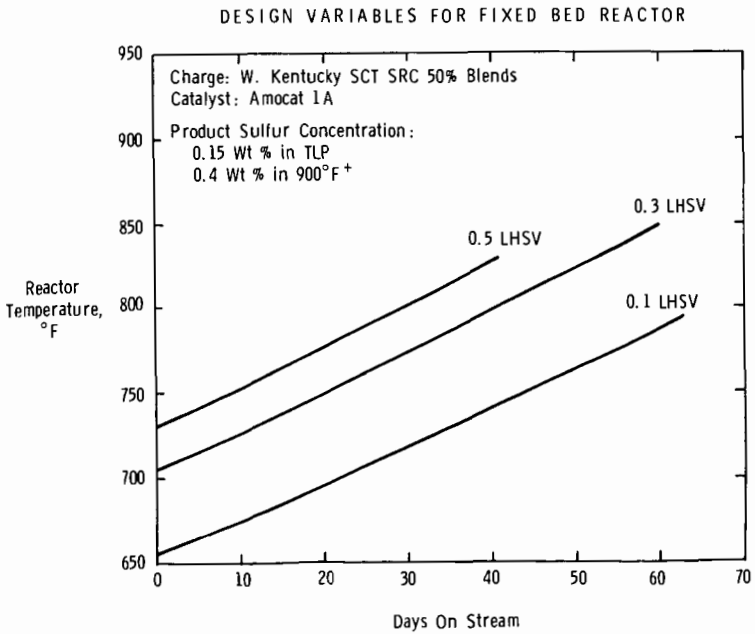


Figure 11



HYDROTREATING OF SRC I PRODUCT - OPTIMIZATION
OF PROCESS VARIABLE SPACE

D. Garg, A. R. Tarrer,
J. A. Guin, and J. M. Lee

Chemical Engineering Department
Auburn University
Auburn, Alabama 36830

INTRODUCTION

In the Solvent Refined Coal Process, coal is dissolved in a coal-derived solvent to produce a filterable liquid. This is accomplished by means of a mild liquid phase hydrogenation of the coal. The liquid is separated from the insoluble minerals and unreacted organic matter by filtration. The solvent is recovered for recycle by vacuum distillation, and the SRC is obtained as a black shiny solid at room temperature. Some of the sulfur present in the coal is removed in the form of hydrogen sulfide gas.

The present sulfur standards (0.97 percent sulfur in SRC) are being met by conventional SRC processing. New Source Performance Standards (NSPS) recently proposed by the Environmental Protection Agency (EPA) would require a sulfur content of 0.5 to 0.6 percent in SRC for most coals. The proposed NSPS could be met using the conventional SRC process with the application of severe operating conditions (e.g., a reaction temperature of 450°C, a H₂ pressure of 2,000 psig or 13.9 MPa and a long reaction time of 30 to 60 minutes. This would result in an unreasonably high hydrogen consumption and operating cost. Therefore, a modification of the conventional SRC process is necessary to meet the proposed NSPS with minimum hydrogen requirements.

For the coal studied here, a bituminous Western Kentucky #9/14 coal, dissolution of the coal has been shown to occur very rapidly, requiring less than 30 minutes to liquefy most of the coal (~90 percent). However, a relatively long reaction time (120 min.) is required to reduce its sulfur level low enough to meet even the current standards (1). A new short residence time two-stage SRC type process has been suggested by Auburn University (2) for solvent refining this coal. This process has been shown to have the potential of producing a low-sulfur solid SRC product that meets the proposed NSPS. It involves the dissolution of the coal (first stage) in the presence of an inexpensive mineral additive, and then subsequent hydrotreating of the filtered liquid from the first stage in the presence of a presulfided Co-Mo-Al catalyst.

The objective of the present work is to evaluate the effect of a wide range of process or reaction variables--reaction temperature, hydrogen partial pressure, catalyst loading, and reaction time--on hydrodesulfurization and hydrogenation of filtered liquid product (coal-derived liquid) obtained from the coal dissolution stage in the presence of a commercial presulfided Co-Mo-Al catalyst. The selectivity for desulfurization over hydrogenation (Se) is used to rate the effectiveness of the above mentioned process variables. Se is defined as the fraction of sulfur removal per unit (g) of hydrogen consumed, that is,

$$Se = \frac{S_f - S_o}{\frac{S_o}{H_2 \text{ Used, g}}}$$

where Se: Selectivity,
 S_o: Original sulfur content of the coal liquids, and
 S_f: Sulfur content of the hydrotreated coal liquids.

The purpose of this study is to identify a set of operating conditions for hydrotreating reactions at which maximum selectivity is attained for a specified sulfur content of the solid SRC product.

There are many different types of search routines used to locate optimum operating conditions. One approach is to make a large number of runs at different combinations of temperature, reaction time, hydrogen partial pressure, and catalyst amount, and then run a multivariable computer search routine (like the Hooke-Jeeves method or Powell method). A second approach is to formulate a mathematical model from the experimental results and then use an analytical search method to locate the optimum. The formulation of a mathematical model is not an easy task, and in many cases, this is the most critical step. Sometimes it is impossible to formulate a mathematical model for the system, as in the case of the system studied here, and an experimental search must be performed.

The experimental strategy used here is to perform a series of small experiments instead of a single comprehensive experiment. A univariate search was made in which only one variable was changed at a time. The information obtained in the earlier experiments performed during the univariate search was used to plan subsequent experiments. By doing so, the results were available quickly, and the experimental error was checked and minimized during the course of experimentation.

In the first step of the univariate search a series of experiments were performed in which base values were used for the initial hydrogen partial pressure, reaction time and reaction temperature, and only the amount of catalyst used was varied. The amount of catalyst which yielded the best performance (i.e. maximum selectivity) and best satisfied practical constraints was selected. In the next step a series of experiments was performed in which the selected amount of catalyst was used, base values were used for temperature and time, and only the initial hydrogen partial pressure was varied. An initial hydrogen partial pressure was selected as was done for the amount of catalyst in the first step.

The dependence of selectivity (Se) on the reaction time and temperature was modeled using empirical expressions for desulfurization and hydrogen consumption kinetics. The same values selected for initial hydrogen partial pressure and amount of catalyst in the first two steps of the univariate search were used in determining these kinetic expressions. The final step of the search procedure was to perform a series of experiments mapping the region close to the above determine optimum conditions for verification.

EXPERIMENTAL

Reagents and Materials

Light recycle oil (LRO) and Western Kentucky #9/14 coal were obtained from the Wilsonville SRC Pilot Plant, operated by Southern Company Services, Inc. The

LRO contains 0.26% sulfur, and the Western Kentucky #9/14 coal is analyzed to be 67% C, 4.9% H, 3.10% S, and 12 % mineral matter. The coal was dried overnight at 100°C and 25 inches Hg vacuum before use.

The coal liquid is obtained by reacting Ky #9/14 coal-LRO slurry for 60 minutes at 410°C in an autoclave reactor under 2000 psig (13.9 MPa) hydrogen pressure. The product from the autoclave is collected and filtered using Watman #51 filter paper to remove the mineral matter and undissolved coal. The liquid product is saved and used for further hydrotreating studies. The analysis of the filtered product from the coal dissolution step is given in Table I.

Co-Mo-Al is a commercial catalyst from Laporte Industries, Inc. (Comox 451). The catalyst was ground and screened to -325 mesh before use. Presulfided Co-Mo-Al was prepared by collecting the solid residue after reaction of creosote oil (S = 0.64 percent) with Co-Mo-Al in the autoclave reactor. The sulfur content of the presulfided Co-Mo-Al was 2.76%.

Hydrogen gas cylinders (6000 psi grade) were supplied by Linde.

Equipment

A commercial 300 ml magnedrive autoclave (Autoclave Engineers) reactor was used for all reaction studies and has been previously described (3-6). Varian gas chromatographs (Model 920 and 1800) were used for analysis of gas samples and products from the hydrotreating reactions. A LECO sulfur determinator (Model 532) was used for analysis of sulfur in the products.

Procedure

One hundred grams of coal liquid was combined with a predetermined amount of presulfided Co-Mo-Al catalyst and charged to the autoclave. Reaction temperature for the runs varied from 360 to 435°C, depending on the run. A stirring setting of 1000 rpm was used, and the initial total pressure was varied from 1500 (10.4 MPa) to 2500 (17.3 MPa) psig. The heat-up rate was about 12 to 20°C/min, thus requiring a total heat-up time of about 20-25 min. After a specified reaction time, a gas sample was taken; the autoclave was cooled to below 100°C, and the reaction products were collected. The filtered liquid product was vacuum distilled under <1.0 mm Hg pressure to recover the process solvent added prior to the reaction. The 270°C + fraction obtained by vacuum distillation was defined as the solvent refined coal (SRC). A sulfur analysis was performed on each fraction.

The conversion of SRC to oil and gases is defined as

$$\text{SRC Conversion, \%} = \frac{(\text{Amount of SRC})_{\text{original liquid}} - (\text{Amount of SRC})_{\text{hydrotreated liquid}}}{(\text{Amount of SRC})_{\text{original liquid}}}$$

and is used as a constraint.

RESULTS AND DISCUSSION

Effect of Catalyst Loading

The effect of the amount of Co-Mo-Al catalyst present in the hydrotreating reaction is tabulated in Table II. It was observed that increasing the amount of Co-Mo-Al from 1 g to 15 g increases the sulfur removal by 52 percent, increases hydrogen consumption by 87 percent, and increases SRC conversion from 16 to 24 percent. Figure 1 shows the variation of selectivity versus the amount of catalyst used while keeping the other reaction variables constant. It can be seen that the maximum selectivity resulted when

10 g of Co-Mo-Al was used. However, the variation in selectivity for the different amounts of catalyst used was insignificant, that is, within the range of experimental error (standard deviation is only 3 percent). The change in SRC conversion to oil and gases, as shown in Table II, was also within the range of experimental error (standard deviation is less than 8 percent). The use of 1 g of Co-Mo-Al gave the lowest amount of SRC conversion (~ 16 percent). From the shape of the selectivity versus amount of Co-Mo-Al catalyst used curve (Figure 1), it appears that hydrodesulfurization is favored over hydrogenation in the range in which 1 g to 10 g of catalyst were used. However, increasing the Co-Mo-Al amount beyond 10 g tends to favor hydrogenation and a decrease in selectivity was observed. Thus 10 g of Co-Mo-Al was used throughout the remainder of the study. A search in the vicinity close to where maximum selectivity occurs (10 g of Co-Mo-Al) was not done because the insensitivity of selectivity and SRC conversion to the amount of catalyst used.

Effect of Pressure

Table III shows the effect of the initial hydrogen partial pressure on selectivity, sulfur removal, hydrogen consumption, and SRC conversion. It was observed that increasing the initial hydrogen partial pressure by 1500 psig (10.4 MPa) decreased the selectivity by 72 percent, increased hydrogen consumption by a factor of 2.6, enhanced sulfur removal by a factor of 1.9, and did not affect SRC conversion appreciably. For initial hydrogen pressures of 1500, 2000, and 2500 psig, the variation of selectivity was within the range of experimental error. Use of a 1000 psig hydrogen pressure gave the maximum selectivity. However, at 1000 psig the sulfur requirements set by the proposed NSPS (0.5 to 0.6 percent SRC sulfur) were not met (SRC sulfur content at 1000 psig is 0.66%). The use of a 2000 psig hydrogen partial pressure gave a slightly higher selectivity than was obtained with either 1500 or 2500 psig, and a sufficient amount of sulfur was removed. Therefore, a hydrogen pressure of 2000 psig was chosen for further studies.

Effect of Reaction Time and Temperature

The amount of catalyst (10 g of Co-Mo-Al in 100 g of coal liquids) and the initial hydrogen partial pressure (2000 psig) determined above were used to study the effect of reaction time and temperature. Hydrodesulfurization and hydrogen consumption kinetics were determined, as outlined in the following paragraphs.

In order to determine the rate equation for hydrodesulfurization, a semi-logarithmic plot of the total sulfur content with time was made (Figure 2). The plot indicated two independent first-order reactions with greatly different rate constants. This is in agreement with the findings of Gates et al. (7) and Pitts (3). A procedure similar to that of Pitts (3) was used to describe the hydrodesulfurization kinetics. The rate expression is given below

$$S_{\text{Total}} = S_{10} \text{ EXP } [-K_{10} \text{ EXP } (-\Delta E_1/RT) t] + S_{20} \text{ EXP } [-K_{20} \text{ EXP } (-\Delta E_2/RT) t]$$

The empirical parameters S_{10} , S_{20} , K_{10} , K_{20} , ΔE_1 , and ΔE_2 were determined by a numerical search routine. Figure 3 compares the theoretical curves with the experimental data and represents a satisfactory curve fit.

The amount of hydrogen gas present in the reactor was plotted against reaction time on a semi-logarithmic scale (Figure 4). This plot gave a straight line indicating a first-order rate expression. Pitts (3) also suggested a first-order rate expression

for hydrogen consumption. A procedure similar to that of Pitts (3) was used. The hydrogen consumption rate expression is given by

$$\frac{H_g}{H_{g0}} = \text{EXP} [-K_0 \text{EXP} (-\Delta E/RT)t]$$

A numerical search routine was applied to determine the value of K_0 and ΔE . Figure 4 compares the theoretical curve with the experimental data and represents a satisfactory curve fit. The total sulfur content and SRC sulfur content for hydro-treated product were plotted (Figure 5), and a linear relationship was shown to exist between them.

The rate expression for hydrodesulfurization and hydrogenation described above were used to compute selectivity. The optimum process conditions for different SRC sulfur contents (specifically, 0.6, 0.5, and 0.4 percent) were determined. The optimization procedure used is illustrated below for a specified SRC content of 0.5% or a total sulfur content of 0.23% (see Figure 5).

The variation of the calculated total sulfur values versus reaction time and reaction temperature was plotted (Figure 6). A dashed line was drawn at a total sulfur level of 0.23 percent; the region above this line was labelled as being infeasible because, for a total sulfur content higher than 0.23 percent, the SRC content was more than 0.5 percent. So, the feasible region of search was that below the dashed line. The computed values of selectivity versus reaction time and temperature was plotted (Figure 7).

The maximum selectivity for each temperature was found to be located on the dashed curve shown in Figure 7, that is, at the boundary. The maximum selectivity values for each temperature were compared (Table IV). The highest temperature and the shortest reaction time used gave the maximum selectivity. The conversion of SRC to oil with reaction time and temperature were plotted also for comparison purposes (Figure 8). As shown in Table IV, the highest temperature and the shortest reaction time resulted in the lowest amount of conversion of SRC to oil. Similar analyses were performed for different SRC sulfur contents, and for each case, the highest temperature and the shortest reaction time gave the maximum selectivity and the lowest SRC conversion. A summary of the optimum reaction conditions obtained for different sulfur levels is given in Table V.

The optimization study discussed above suggests the use of a high temperature and a short-reaction time. Because of the heat-up and cool-down time limitations of the autoclaves used, this study was limited to reaction temperatures $\leq 435^\circ\text{C}$. Verification studies at higher temperatures ($>435^\circ\text{C}$) are ongoing using micro-reactors. The present study should be supported by complementary catalyst aging studies to determine the maximum temperature limit below which serve deactivation and aging does not occur.

CONCLUSIONS

The proposed NSPS can be met by hydrotreating the coal liquids obtained by filtering the product from the coal dissolution stage. The desulfurization kinetics can be presented by two parallel first-order rate expression, and hydrogen consumption kinetics can be presented by a first-order rate expression. A linear relationship exists between total sulfur content and SRC sulfur content of the hydrotreated product. For

the Western Kentucky bituminous #9/14 coal studied here, the maximum selectivity and lowest SRC conversion to oil for a fixed SRC sulfur content are obtained using the highest reaction temperature (435°C) and the shortest reaction time (≈ 7 min.).

ACKNOWLEDGEMENTS

This work was supported by the Department of Energy. The authors wish to acknowledge the technical assistance of Don Colgrove and David Watson of the Auburn University Chemical Engineering Department.

REFERENCES

1. Garg, D., Ph.D. Dissertation, Auburn University, Auburn, Alabama (1979).
2. Garg, D., Tarrer, A. R., Guin, J. A., Lee, J. M., and Curtis, C., Fuel Processing Technology, 2, 189-208 (1979).
3. Pitts, W. S., M.S. Thesis, Auburn University, Auburn, Alabama (1976).
4. Guin, J. A., Tarrer, A. R., Prather, J. W., Johnson, J. R., and Lee, J. M., Ind. Eng. Chem. Process Des. Dev. 17(2), 118 (1978).
5. Lee, J. M., Van Brackle, H. F., Lo, Y. L., and Tarrer, A. R., Am. Chem. Soc. Div. Fuel Chem., prepr., 22(6), 120 (1977).
6. Lee, J. M., Van Brackle, H. F., Lo, Y. L., Tarrer, A. R., and Guin, J. A., Symposium of the 84th National ALChE Meeting, Atlanta, GA, Feb. 26 - March 1, 1978 (516).
7. Gates, B. C., J. R. Katzer, J. H. Olson, H. Kwart, and A. B. Stiles, Quarterly Progress Report, Prepared for U.S. Dept. of Energy, No. EX-76-C-01-2028, (December 2, 1976 - March 20, 1977).

Table I. Analysis of the Liquid Product Used in Hydrotreating Stage

Distillation Product Distribution, %	
Distillate (Oil)	61.6
SRC	38.4
Sulfur Distribution, %	
Distillate (Oil)	0.21
SRC	0.97
TOTAL LIQUID	0.54
TetraIn/Naphthalene Ratio	
Distillate is performed under <1 mm Hg pressure	0.24
Distillate: 270°C - fraction of vacuum distillation	
SRC: 270°C + fraction of vacuum distillation	

Table II. Effect of Catalyst Amount on Hydrotreating of Kentucky #9/14 Coal Liquid
Coal Liquid = 100 g, Time = 30 min., T = 410°C, P = 2000 psi (13.9 MPa)H₂, 1000 RPM, Reactor - Autoclave

Amount of Catalyst	1.0	5.0	10.0	15.0
H ₂ Used, g	0.11	0.17	0.18	0.21
Total Sulfur S _f , %	0.36	0.22	0.20	0.17
$S_e = \frac{S_o - S_f}{S_o}$	2.8	3.3	3.4	3.2
H ₂ Used, g				
SRC Conversion, %	16	21	22	24
S _o = 0.54%				

Table III. Effect of Hydrogen Partial Pressure on Hydrotreating of Kentucky #9/14 Coal Liquid
Coal Liquid = 100 g, Co-Mo-Al = 10 g, T = 410°C, 1000 RPM, Reaction Time = 30 min., Reactor - Autoclave

Pressure, Psig H ₂	1000	1500	2000	2500
H ₂ Used, g	0.08	0.13	0.18	0.22
Total Sulfur S _f , %	0.35	0.30	0.20	0.19
SRC Sulfur, %	0.66	0.57	0.49	0.45
$S_e = \frac{S_o - S_f}{S_o}$	4.1	3.3	3.4	2.9
H ₂ Used, g				
SRC Conversion, %	22	19	22	21

Table IV. Maximum Selectivity at Different Reaction Conditions Meeting 0.5% SRC Sulfur Content

Temp., °C	Time, Min.	Se	Standard Deviation in Se, %	SCR Conversion, % (Estimated from Fig. 8)
370	114	2.50	6.3	>20.0
385	62	2.80	7.5	>20.0
400	38	3.20	7.2	---
410	27	3.5	7.2	20.5
420	20	3.70	7.0	--
435	13	3.85	7.3	19.5

Table V. Summary of Operating Conditions for Various Maximum SRC Sulfur Contents

SRC Sulfur, %	Total Sulfur, %	Temperature, °C	Time, Min.	Se
0.6	0.29	435	7	5.40
0.5	0.23	435	13	3.85
0.4	0.17	435	21	2.80

Figure 1. Effect of Amount of Catalyst (Co-Mo-Al) on Selectivity

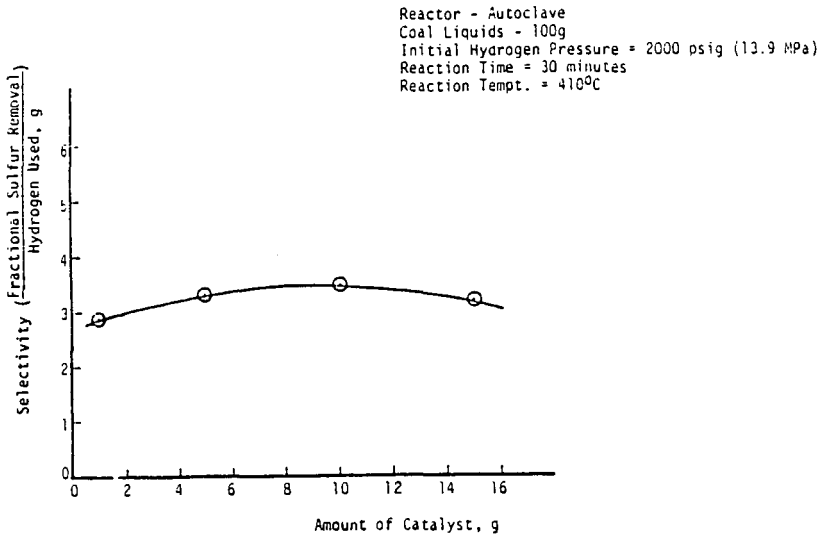


Figure 2. Semi-Log Plot of Total Sulfur (%) vs. Time for Hydrotreating Reaction in The Presence of Co-Mo-Al

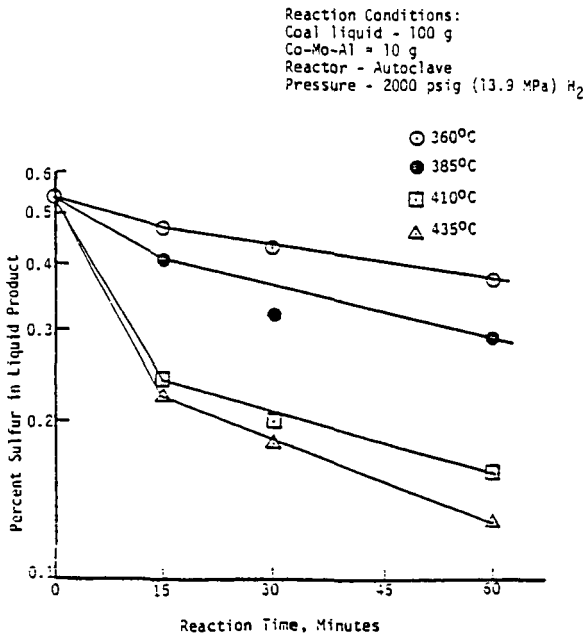


Figure 3. Effect of Hydrotreating Reaction Time on Total Sulfur Content

Reaction Conditions: See Figure 2

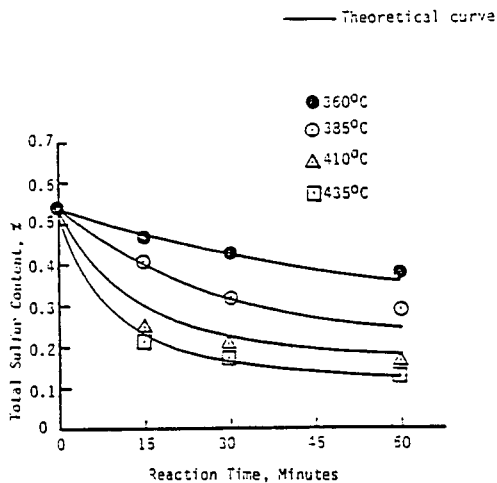


Figure 4. Semi-Log Plot of H_g/H_{g0} vs. Time for Hydrotreating Reaction in the Presence of Co-Mo-Al

Reaction Conditions: See Figure 2
 H_g = amount of hydrogen (g) in the reactor at any time
 H_{g0} = amount of hydrogen (g) initially charged to the reactor

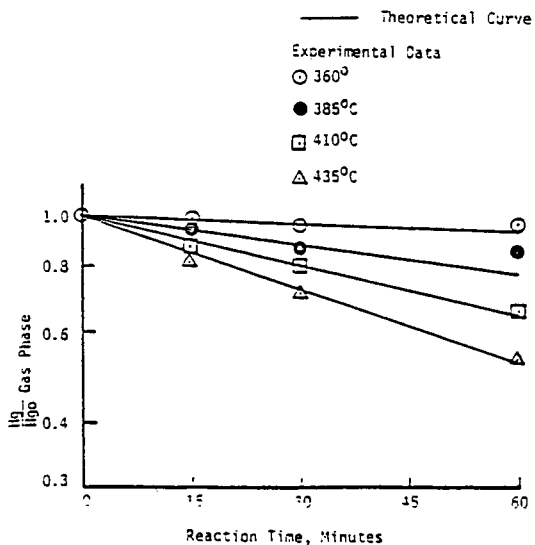


Figure 5. Relationship Between Hydrotreated Total Sulfur Content (%) and SRC Content (%)

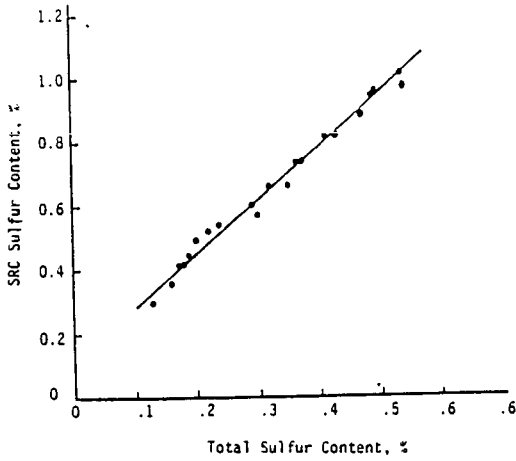


Figure 6. Variation of Total Sulfur Content with Reaction Time and Temperature for Hydrotreating Reaction

SRC Sulfur = 0.50%
 Total Liquid Sulfur = 0.23%

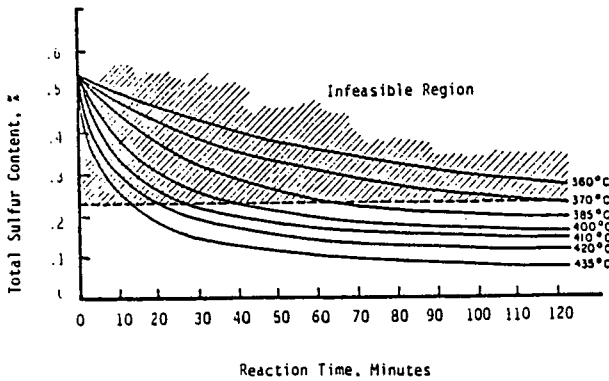


Figure 7. Variation of Selectivity with Reaction Time and Temperature for Hydrotreating Reaction

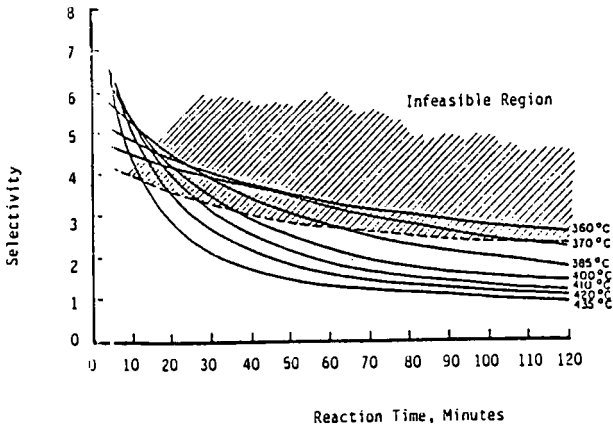
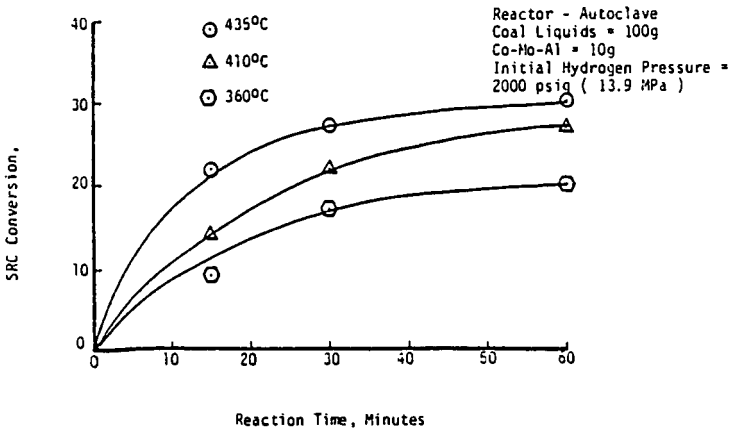


Figure 8. Conversion of SRC with Hydrotreating Reaction Time and Temperature



A COMPARISON OF THE HYDRODESULFURIZATION AND HYDRODENITROGENATION ACTIVITIES
OF MONOLITH ALUMINA IMPREGNATED WITH Co AND Mo AND NALCOMO 474 CATALYSTS

Dalip S. Soni
International Research and Technology Corporation
7655 Old Springhouse Road
McLean, Virginia 22102

Billy L. Crynes
Oklahoma State University
Stillwater, Oklahoma 74074

INTRODUCTION

In the wake of precarious supplies of petroleum, the need to turn to the abundant reserves of coal as an energy base can hardly be overemphasized. However, to accomplish the objective of using coal extensively, much research effort in the field of converting coal to environmentally clean and convenient fuel is required. The work presented here is so directed and is a part of the research program, at Oklahoma State University, which has the goal of tailoring catalysts for upgrading of liquids derived from coal.

In this study, a novel Monolith alumina structure was of interest as a base (or a carrier) material for Co-Mo-Alumina catalysts. The specific interest centered around assessing the suitability of the catalyst prepared by impregnating the novel alumina support with Co and Mo for hydrodesulfurization (HDS) and hydrodenitrogenation (HDN) of a relatively high boiling stock. The Monolith catalyst was also tested on a low boiling coal-derived liquid.

OBJECTIVE

The objective of this work was to study the activity of the Monolith catalyst for removing sulfur and nitrogen from a Synthoil process liquid (heavy stock) and Raw Anthracene Oil (light feedstock), and to make a preliminary assessment of the advantages and/or disadvantages of the Monolith catalyst over a commercial catalyst used in the petroleum industry.

MATERIALS

Feedstocks:

As mentioned before, two coal-derived liquids were used. One was Raw Anthracene Oil obtained from Reilly Tar and Chemical Corporation. The other was a Synthoil liquid obtained from Pittsburgh Energy Research Center. The properties of these two liquids are given in Tables I and II. As is clear from the boiling point ranges of the two liquids, Synthoil is very high boiling as compared to the Raw Anthracene Oil.

Catalysts:

The properties of the two catalysts used in this study are given in Tables III and IV. The Monolith catalyst was prepared in the laboratory at OSU by impregnating Co and Mo on the Monolith alumina support received from the Corning Glass Company. The Nalco 474 catalyst was received from the Nalco Chemical Company. It is a commercial preparation and was used as a reference catalyst in this study.

Figure 1 shows the pore size distribution of the two catalysts as determined from the mercury porosimeter data. The most frequent pore radius of the Monolith catalyst is 80 \AA as compared to 33 \AA of the Nalco 474 catalyst. On the other hand, the surface area of the Monolith catalyst is 92.0 m²/gm. as compared to 240 m²/gm. of the Nalco 474 catalyst. The chemical compositions of the two catalysts also differ widely as shown in Tables III and IV.

TABLE I
PROPERTIES OF THE RAW ANTHRACENE OIL

Boiling Range		
Volume Distilled, <u>Percent</u>	Vapor Temperature, C(F), <u>at 50 mm Hg.</u>	Vapor Temperature, C(F), <u>at 760 mm Hg.</u>
10	138.9 (282)	229.4 (445)
20	169.4 (337)	263.9 (507)
30	186 (367)	283.3 (542)
40	202.7 (397)	302.2 (576)
50	215 (419)	315.5 (600)
60	227.2 (441)	331.1 (628)
70	240.5 (465)	345 (653)
80	256 (493)	362.7 (685)
90	278.9 (534)	387.8 (730)

Wt. %	
Carbon	90.3
Hydrogen	5.57
Sulfur	0.47
Nitrogen	1.035
Oxygen	2.625
Ash	Nil
API Gravity	-7

TABLE II
PROPERTIES OF THE SYNTHOIL LIQUID

Boiling Range		
Volume Percent <u>Distilled</u>	Vapor Temperature, C(F), <u>at 50 mm Hg.</u>	Weight <u>Percent S.</u>
10	170.5 (339)	0.2
20	211.6 (413)	0.242
30	260 (500)	0.332
33	276.6 (530)	0.366
Bottoms		1.7

Wt. %	
Carbon	80.5
Hydrogen	7.72
Sulfur	1.02
Nitrogen	1.19
Ash	3.4
Specific Gravity	1.12

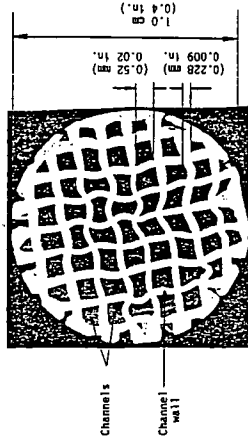
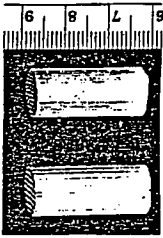
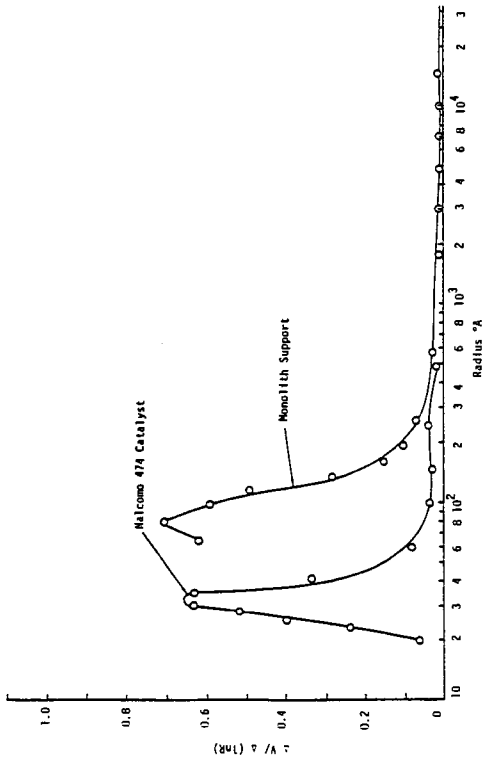


Figure 2: Monolith Alumina Structure

Figure 1: Pore Size Distribution of the Catalysts

TABLE III
PROPERTIES OF THE MONOLITH CATALYST

	Wt. %
CoO	3.37
MoO ₃	7.25
Support	Alumina
Surface Area, m ² /gm.	92.0
Pore Volume, cm ³ /gm.	0.55
Most Frequent Pore Radius, \AA	80.0

TABLE IV
PROPERTIES OF THE NALCOMO 474 CATALYST

	Wt. %
Alumina	82.39
MoO ₃	12.5
CoO	3.5
Na ₂ O	0.08
Fe	0.03
SiO ₂	1.5
Surface Area, m ² /gm.	240.0
Pore Volume, cm ³ /gm.	0.46
Most Frequent Pore Radius, \AA	33.0

Figure 2 shows the shape and size of the Monolith alumina supports. These are in the form of cylindrical segments of about 2.54 cm. (1 in.) in length and about 1.0 cm. (0.4 in.) in diameter. These have longitudinal and parallel channels along their length. The size, shape and thickness of the walls of the channels are also shown in Figure 2.

The Monolith structure has about 60 to 80 percent of its cross-sectional area open. Therefore, a bed of regularly stacked Monoliths would offer significantly less pressure drop than that encountered in conventional packed beds. This has been observed by Satterfield and Ozel (1) for water-air systems. Some of the other important advantages listed by them are:

- (1) Where intraparticle diffusion appreciably affects the rate of the reaction, reduction in catalyst particle size would be necessary to increase the effectiveness factor and hence conversion. But this may not be possible due to the pressure drop limitations in conventional packed beds. In such situations, the use of Monoliths would provide the advantage of higher effectiveness factor.
- (2) When processing coal derived liquids which contain fine solid particles, the possibility of bed plugging may be minimized.
- (3) The flow of the liquid through regular channels would provide better gas-liquid contact, liquid distribution and wetting of the catalyst.

- (4) The compressive strength of Monoliths would be much higher than the catalyst particles generally used in packed beds. Therefore, the use of Monoliths would enable deep beds to be constructed without using intermediate supports and gas-liquid distributors.

All of the above advantages stem from the special geometry of the Monoliths as compared to that of the usual catalyst particles.

EXPERIMENTAL SETUP AND PROCEDURE

Reactor System:

A trickle bed reactor system was employed in this study. A schematic diagram of the experimental system is shown in Figure 3. The reactor was a 12.7 mm (0.5 in.) O.D. stainless steel tube packed with the catalyst. The catalyst bed height was 35.5 cms. (14 in.). When using Monolith catalyst, redistributors were put at intervals of 10.15 cms. (4 in.) each to ensure that the liquid passes through the channels. Figure 4 shows cross-section of the reactor packed with the Monolith and Nalcomo 474 catalysts. The latter catalyst was used in the form of 8-10 mesh (2 mm.) size particles.

The reactor was heated with the help of massive aluminum blocks placed around the reactor. The reactor temperature was measured at every inch of the catalyst height by traversing a thermocouple in a thermowell placed along the reactor bed. The reactor was operated at nearly isothermal conditions.

Method of Operation:

After loading the reactor with the catalyst and installing it in the experimental setup, the catalyst was activated. This was done by first calcining the catalyst at 232.2 C (450 F) and then sulfiding it with a mixture of 5.14 volume percent H₂S in H₂. The reactor was then brought to the operating conditions and the flow of hydrogen and oil started. After about 32 hours of reactor-in-oil operation, representative product oil samples were taken at specified reactor conditions. The line out time of 32 hours was allowed to stabilize the activity of the catalyst. The product oil samples were analyzed for their sulfur and nitrogen contents with the help of a Leco Model 634-700 automatic sulfur analyzer and Perkin Elmes Model 240 elemental analyzer, respectively.

RESULTS

Figure 5 and 6 show the results of this study along with the results of Sooter (2) and Satchell (3) who conducted similar studies using the same experimental setup but with Nalcomo 474 catalyst and Raw Anthracene Oil. The graphs presented here are either weight percent sulfur or nitrogen in the product oil from the reactor vs. the volume hourly space time. Low sulfur or nitrogen in the product oil would correspond to higher activity of the catalyst under consideration.

The results with each feedstock and catalyst were obtained over a single reactor run lasting 105-132 hours. In each reactor experimental run, the start up reactor conditions were repeated at the end to check for loss, if any, of the catalyst activity. No significant decrease in catalyst activity was observed over the conditions studied.

The overall reproducibility of each reactor experimental run was checked by comparing the mode of response of desulfurization and denitrogenation to changes in space time as observed from the two reactor runs on the same feedstock. Figures 5 and 6 show that reactor runs were reproducible.

An estimate of the precision of sulfur and nitrogen analyses was made by analyzing Raw Anthracene Oil and Synthoil liquid a number of times. The results of sulfur

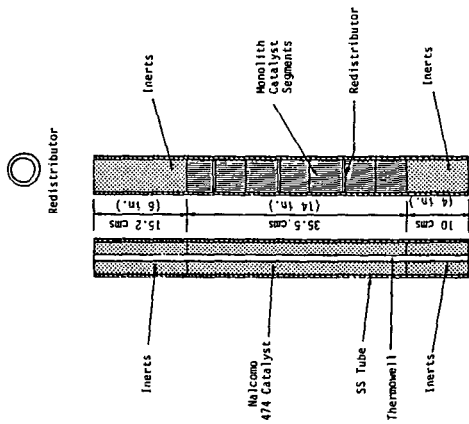


Figure 4: Cross Sections of the Reactors Packed with Malcombo 474 and Monolith Catalysts

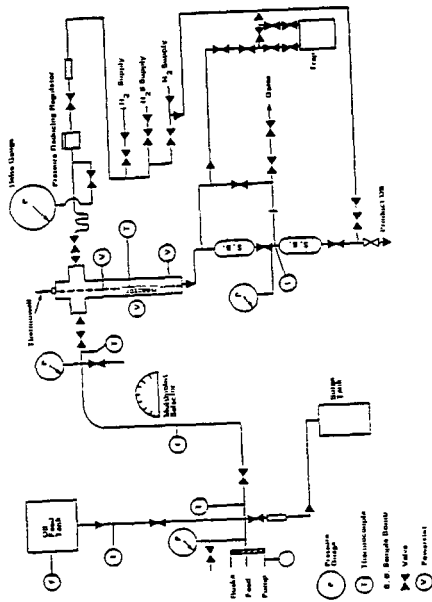


Figure 3: Reactor System

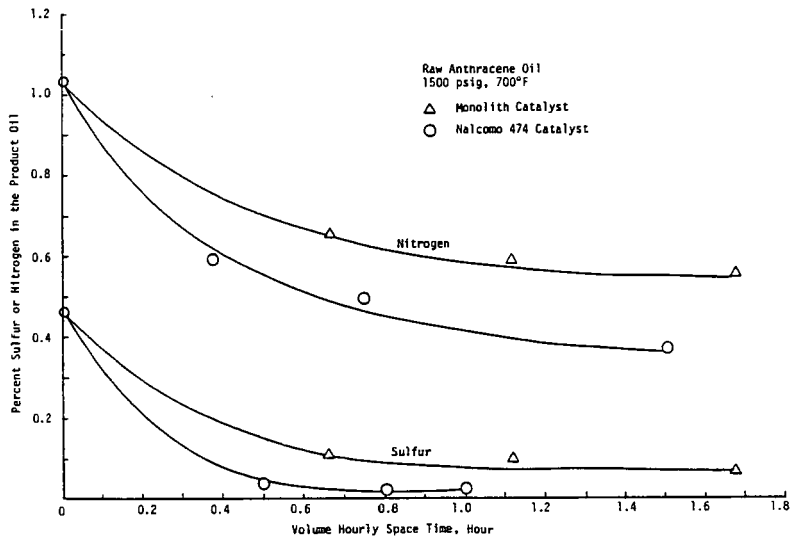


Figure 5. HDS and HDN Responses to the Changes in the Volume Hourly Space Time

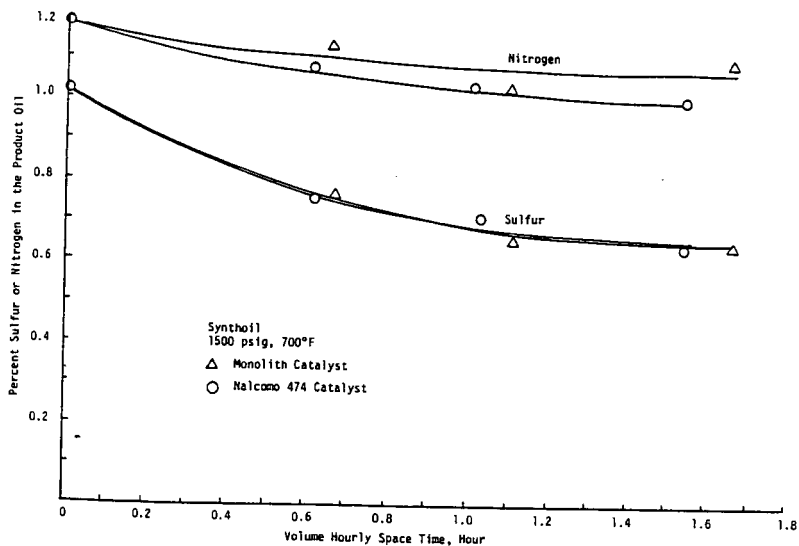


Figure 6: HDS and HDN Responses to the Change in the Volume Hourly Space Time

analysis of Raw Anthracene Oil were found to be precise within 0.25%. But precision of other results was within 5.0%.

DISCUSSION

Figure 5 indicates that on volume basis, the activity of the Monolith catalyst is less than the activity of Nalcomco 474 catalyst when Raw Anthracene Oil was the feedstock. Similar behavior was observed when comparison was made on weight basis. Figure 6 shows that when tested on Synthoil, the HDS activity of the two catalysts were almost the same on volume basis. However, when comparison was made on the weight basis, Monolith catalyst was observed to remove more sulfur per unit weight of the catalyst.

Since the surface areas of the two catalysts differed widely, comparison of activities of the two catalysts on unit surface area basis was studied. Figures 7 and 8 represent such a comparison. The abscissa of these graphs is S/Q , where S is the total surface area of the catalyst in the reactor and Q is the volumetric flow rate of oil. S/Q or S/W are quite akin to volume hourly or weight hourly space times. Figure 7 shows that for removing sulfur from the Raw Anthracene Oil, essentially same amount of surface areas of the two catalysts would be required. However, with regard to removing nitrogen, surface areas required of two catalysts would be different. This indicates that as far as the desulfurization of lighter stock such as Raw Anthracene Oil is concerned, the unit surface activity of the two catalysts is the same. But the surface activity towards denitrogenation is higher for the Monolith catalyst than for the Nalcomco 474 catalyst.

Figure 8 shows the comparison of the surface activities of the two catalysts on the heavier feedstock, i.e., Synthoil. In this case, the activity of the Monolith catalyst is far greater than that of the Nalcomco 474 catalyst. This behavior is different from that observed on the Raw Anthracene Oil, and as further discussion will show, this difference in the superiorities of the Monolith catalyst on the two feedstocks throws light on some interesting and important observations and conclusions of this study.

To have a quantitative idea of the higher unit surface area activity of the Monolith catalyst, rate constants based on surface area were considered essential to know. To accomplish this, the global reaction kinetics of desulfurization and denitrogenation were determined. For the desulfurization, the following three kinetic models, as suggested in literature, were tested to see as to which one best represented the data of this study.

(1) Second order; $\frac{1}{C_A} = kt + \frac{1}{C_{AO}}$

(2) Combination of two first order reactions; one for the lighter and the other for the heavier fractions of the stock;

$$\frac{C_A}{C_{AO}} = \alpha e^{-k_1 t} + (1 - \alpha)e^{-k_2 t}$$

where α is the fraction of light or heavy component in the feed.

(3) First order; $\frac{C_A}{C_{AO}} = e^{-kt}$

The second model was discarded because the value of the rate constant k_2 found by the non-linear regression of data was approximately zero which was not considered reasonable on a physical basis. Of the other two models, the first model, i.e., the

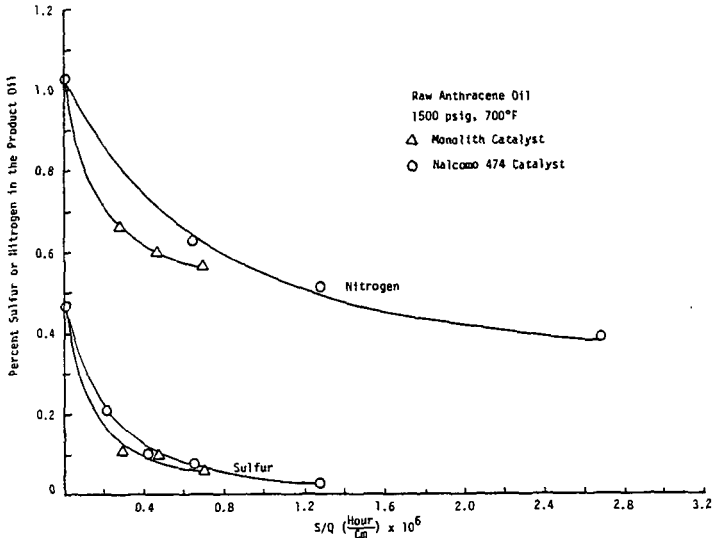


Figure 7: HDS and HDN Responses to the Change in Surface Area/Volumetric Flow Rate of Oil

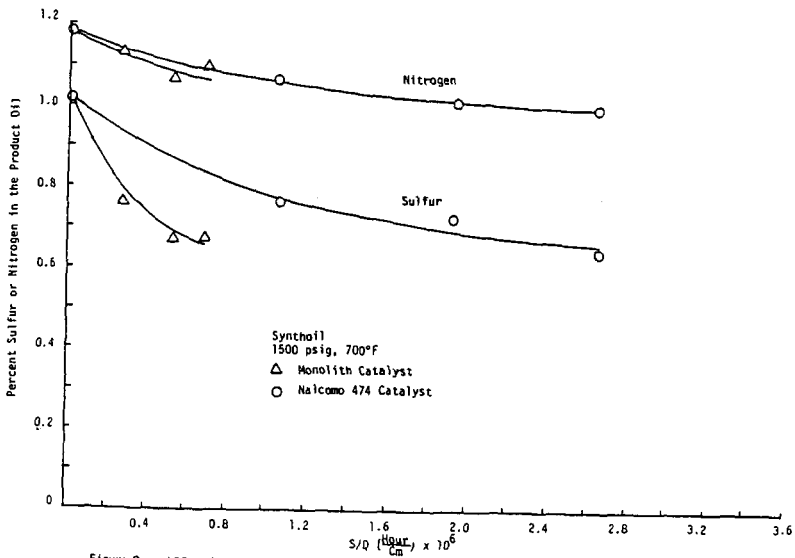


Figure 8: HDS and HDN Responses to the Change in Surface Area/Volumetric Flow Rate of Oil

TABLE V
SECOND ORDER RATE CONSTANTS (VOLUMETRIC)

$$k, \frac{\text{cm}^3}{(\text{gm.})(\text{hour})}$$

	Raw Anthracene Oil		Synthoil	
	Monolith Catalyst	Nalcomo 474 Catalyst	Monolith Catalyst	Nalcomo 474 Catalyst
Desulfurization	8.68	48.8 ^a	0.427	0.431
Denitrogenation	0.724	1.4 ^b	0.084	0.134

TABLE VI
SURFACE AREA RATE CONSTANTS

$$k, \frac{\text{cm}^4}{(\text{gm.})(\text{hour})}$$

	Raw Anthracene Oil		Synthoil	
	Monolith Catalyst	Nalcomo 474 Catalyst	Monolith Catalyst	Nalcomo 474 Catalyst
Desulfurization	2282	2400 ^a	108	25
Denitrogenation	190	81 ^b	24	8.5

^aCorresponds to the volumetric rate constant obtained using Sooter's data (2)

^bCorresponds to the volumetric rate constant obtained using Stachell's data (3)

second order rate expression was found to fit the data better. For denitrogenation, only the first and second order models were examined, and in this case also the latter model was found to represent the data better.

Table V gives the values of the second order rate constants for the HDS and HDN for both liquids and catalysts studied. The values of the rate constants for HDS and HDN of Raw Anthracene Oil using Nalcomo 474 catalyst were obtained by applying the same non-linear regression analysis technique to the data of Sooter (2) and Satchell (3). The comparison of the rate constants lead one to the same conclusion as shown by Figures 5 and 6.

The rate constant based on surface area, k_s , was calculated from the volumetric rate constants by using the following equation:

$$k_s = k \frac{V_r}{S}$$

where k = volumetric rate constant, $\frac{\text{cm}^3}{(\text{hour})(\text{gm.})}$

V_r = volume of the reactor, cm^3

S = total surface area of the catalyst, cm^2

The values of k_s calculated for the various values of k are given in Table VI. In the case of Synthoil, the observed surface area rate constants for desulfurization as well as denitrogenation are about 3 to 4 times higher for the Monolith catalyst than those for the Nalcomco 474 catalyst. This further confirms that the observed surface activity of the Monolith catalyst for treating heavier liquids is much higher than the commercial Nalcomco 474 catalyst. However, in the case of Raw Anthracene Oil, the observed surface area rate constants for desulfurization are about the same for both catalysts and hence they have the same observed surface activity for this lighter feedstock. But the denitrogenation rate constant even on this liquid is higher for the Monolith catalyst than for the Nalcomco 474 catalyst.

Thus, the Monolith catalyst seems to have potential superiority over the commercial catalysts used in this study, especially for treating high boiling stocks.

Reasons for the Higher Observed Unit Surface Area Activity of the Monolith Catalysts:

There can be three main reasons:

- (1) Intrinsic activity of the Monolith catalyst was higher than that of the Nalcomco 474 catalyst.
- (2) Fluid dynamic effects in the reactor when Nalcomco 474 catalyst was used did not provide efficient solid-liquid contacting.
- (3) There were severe diffusional limitations in the case of Nalcomco 474 catalyst, which had a pore radius of 33 μ , due to which its surface area utilization was very low as compared to surface area utilization in the case of Monolith catalyst which had pore radius of 80 μ .

If one considers that the Monolith catalyst was intrinsically more active than the Nalcomco 474 catalyst then the observed superiority of the Monolith catalyst should be almost the same, or at least have the same order of magnitude, when tested on two different feeds. But as explained earlier, the observed surface activities of the two catalysts for HDS are almost equal in the case of Raw Anthracene Oil, while on Synthoil the observed surface activity of the Monolith is about 4 times that of the Nalcomco 474 catalyst. Therefore, there is sufficient ground to believe that the Monolith catalyst used in this study was not intrinsically more active than the Nalcomco 474 catalyst as far as the HDS was concerned.

In previous studies, Sooter (2) and Satchell (3) observed that reducing the particle size of the Nalcomco 474 catalyst from 8-10 mesh to 40-48 mesh did not have any significant effect on the desulfurization and denitrogenation of Raw Anthracene Oil under similar experimental conditions as employed in this study. This suggests that the fluid distribution and hence the fluid dynamic effects were not important in the trickle bed reactors as operated for this work. If these effects were important,

then the reduction in particle size should increase conversion, or the HDS and HDN, by improving fluid distribution and reducing the intraparticle diffusion resistances.

Under the likelihood that the first two reasons do not explain the results of this study or are not important in the present context, intraparticle diffusion limitations appear to be responsible for differentiating the activities of the two catalysts. Tables I and II show that the Synthoil is a high boiling liquid as compared to Raw Anthracene Oil. This means that the molecules that constitute Synthoil are larger on the average than the molecules that constitute the Raw Anthracene Oil. Therefore, the smaller pore size, 330A, of the Nalco 474 catalyst and its longer diffusion path, which is the radius of the catalyst particle, about 1 mm, would offer much higher intraparticle diffusion resistance to Synthoil molecules than to the Raw Anthracene Oil molecules. This would severely limit surface area utilization of Nalco 474 on Synthoil liquid but not as much on Raw Anthracene Oil. Therefore, observed unit surface area activity of Nalco 474 catalyst on Synthoil would be lowered appreciably as compared to the lowering of the activity of the same catalyst on Raw Anthracene Oil. On the other hand, pores of the Monolith catalyst are approximately two and a half times larger than the pores of the Nalco 474 catalyst. The diffusion path is only 0.114 mm, i.e., half the thickness of the channel wall. This is 1/9 times the diffusion path length of the Nalco 474 catalyst. Due to this, the Monolith catalyst would offer much less diffusion resistance to Synthoil molecules than that offered by Nalco 474 catalyst. Therefore, the percent surface area utilization of the Monolith catalyst would be much higher than the percent surface area utilization of the Nalco 474 catalyst. But the larger pore size and smaller diffusion length of the Monolith catalyst could not have any advantage when a lighter feedstock like Raw Anthracene Oil is processed because, as determined by Sooter (2) and Satchell (3), this feedstock does not have significant diffusion problems with the Nalco 474 catalyst.

To have a quantitative idea of the problem of intraparticle diffusion, "Effectiveness Factors" for the two catalysts were calculated from the observed reaction rates using the relationship between ϕ and η (5) and the "triangle method" suggested by Satterfield (4). The Effectiveness Factors for the Monolith and Nalco 474 catalyst were found to be 0.94 and 0.216, respectively.

SUMMARY

The results of this study indicated that at the reactor operating conditions of 371 C and 1500 psig, the observed HDS activity based on unit surface area, was much higher for the Monolith catalyst as compared to the Nalco 474 catalyst when processing the heavier feedstock, i.e., Synthoil. But it was about the same when processing a lighter feedstock like Raw Anthracene Oil. Since the average pore radius and the intraparticle diffusion length of the Monolith catalyst were 87.6 μ A and 0.114 mm against 31 μ A and 1 mm of the Nalco 474 catalyst, the intraparticle diffusion was considered to be responsible for the lower observed activity of the Nalco 474 catalyst on the heavier feedstock. From the observed rates of reaction, the Effectiveness Factors for the Monolith and Nalco 474 catalysts were found to be 0.94 and 0.216, respectively, for the HDS of Synthoil.

REFERENCES

1. Satterfield, C.N. and F. Ozel, Paper presented at the American Institute of Chemical Engineers Meeting at Chicago, 17 C, (1976).
2. Sooter, M.C., Ph.D. Thesis, Oklahoma State University, Stillwater, OK. (1974).
3. Satchell, D.P., Ph.D. Thesis, Oklahoma State University, Stillwater, OK. (1974).
4. Satterfield, C.N., Mass Transfer in Heterogeneous Catalysis, M.I.T., Press, Cambridge, Mass. (1970).
5. Thiele, E.W., Industrial and Engineering Chemistry, 31, 7 (1939).

THE THERMAL CRACKING OF COAL-DERIVED MATERIALS

R.S. Bernhardt, W.R. Ladner, J.O.H. Newman and P.W. Sage

National Coal Board, Coal Research Establishment, Stoke Orchard
Cheltenham, Glos. GL52 4RZ, England

SUMMARY

Up to 27% benzene, toluene and xylenes and 24% ethylene were obtained by cracking a highly hydrogenated coal extract, compared to less than 4% of each from unhydrogenated coal, coal extract and anthracene oil. The importance of naphthenes as BTX and ethylene precursors was confirmed.

INTRODUCTION

Many of the feedstocks for the chemical industry, especially aromatic hydrocarbons, were originally obtained as byproducts from the carbonisation of coal (1,2). However, nowadays most of these chemical feedstocks are derived from petroleum. Nevertheless, it is probable that, within the next few decades, the shortage of world reserves of petroleum will mean that BTX will once again have to be produced from coal, as will ethylene. It is, therefore, appropriate to examine ways in which these materials can be produced from coal; the present investigation was designed to study the formation of BTX and ethylene by the thermal cracking of coal-derived materials from the NCB coal liquefaction/hydrogenation processes (3).

EXPERIMENTAL

Feedstocks

The vapours from the carbonisation of a bituminous, low-rank coal, an anthracene oil and a coal extract in anthracene oil were diluted with nitrogen and cracked; their product yields were compared with those from the cracking of a partially hydrogenated anthracene oil and coal extracts hydrogenated to various extents. The coal was Linby (National Coal Board, Coal Rank Code 802) and the extract was prepared by digestion at 673 K and 8 bar in anthracene oil, filtration to remove mineral matter and dissolved coal, followed by distillation under reduced pressure until the extract contained about 70% coal. The two coal extract hydrogenates were prepared by catalytically reducing a dilute extract from Annesley (NCB, CRC 702) coal in a trickle bed reactor and fractionating the product. The fractions were further reduced in a vapour phase reactor to give two highly hydrogenated liquids.

Four model compounds, n-undecane, tetralin, cis/trans decalin and mesitylene, and a natural gas condensate from the North Sea were also cracked. Analyses and the reference code key of the coal-based feedstocks and the gas condensate are given in Table 1. Paraffin, naphthene and aromatic type analyses were calculated from gas chromatographic analyses of the partially hydrogenated anthracene oil and gas condensate, whereas mass spectrometric analysis was performed on the two coal extract hydrogenates and their further hydrogenated products.

Apparatus and Procedure

The experiments with the solid feedstocks and the initial experiments on liquid samples were carried out in the apparatus shown in Figure 1a. The vapours from a stainless steel, stirred-bed carboniser/vaporiser at 873 K were cracked at atmospheric pressure in a tube reactor heated in a platinum-wound furnace.

The reactor was 30 mm ID and had a 100 mm long hot zone within 20 K of the maximum reactor temperature. Solid feedstocks were introduced at about 1 g min^{-1} from a vibratory table through a water-cooled port. Liquids were injected at the same point from a mechanically driven syringe at 0.1 to 0.8 ml min^{-1} . The amount fed was determined by weighing the feeders.

Liquid products were collected in two glass traps at 258 K and in a glass wool filter. The gas was measured in a dry gas meter and sampled over mercury into glass bottles. The reactor and collection train were weighed and the liquids removed with a known amount of chloroform. The effects of vapour residence time and cracking temperature on the product yields from each feedstock were investigated. The effects of variables such as reactor surface, type and area, feedstock vapour concentration and the addition of steam was also tested over a limited range of conditions with a hydrogenated coal extract. Gaseous and liquid products were analysed by chromatography.

Later experiments with the hydrogenated feedstocks, which were completely vaporisable, were performed by injecting the liquids into the top of the smaller reactor (9 mm ID) shown in Figure 1b: the liquid feed rate was only a tenth of that required for the larger apparatus; the furnace and collection systems were similar. Comparative tests with cis/trans decalin and hydrogenated anthracene oil showed that the smaller reactor gave marginally higher BTX and ethylene yields than the larger reactor.

RESULTS

The Effect of Surface, Reactant Concentration and Diluent

Results from the cracking of a hydrogenated coal extract similar to (D) in the larger reactor with and without copper or stainless steel packing, which increased the surface area about threefold whilst decreasing the reactor volume by only 10%, showed that neither copper nor stainless steel significantly affected the yields of BTX and ethylene. An eightfold reduction in the concentration of the feedstock vapour (at constant vapour residence time) also had no significant effect. Replacement of part of the diluent nitrogen to give a 70% steam + 30% nitrogen mixture had a negligible effect on the yields of BTX and ethylene although xylenes were favoured at the expense of benzene.

Unhydrogenated Coal-derived Materials

Preliminary experiments on cracking the vapour from coal extract (B) at 1133 K for 0.7 to 8 s showed that the BTX yield peaked at 2 s whereas ethylene was favoured by shorter residence times. Figure 2 shows the effect of cracking temperature at 2 s vapour residence time on the yields of BTX, benzene and ethylene from Linby coal (A), coal extract (B) and anthracene oil (C). Yields of BTX and benzene peaked at about 1273 K whereas the maximum ethylene yields were obtained at about 1100 K. The mass balances and yields of the gaseous and liquid products at one condition, 1273 K for 2 s, are given in Table 2.

The yields of BTX and ethylene are low, less than 3.5% BTX and 1.5% ethylene: the highest yields were from Linby coal. Although the BTX yields are greater than the 1% from conventional, high temperature coal carbonisation (2), they are only a fraction of those obtainable from petroleum feedstocks (4).

Hydrogenated Coal-derived Materials

The yields from the partially hydrogenated anthracene oil (C1), two coal extract hydrogenates (D and E) and their further hydrogenated products (D1 and E1) when cracked at 1133 K, which favoured ethylene formation, are listed in Table 2 together with the yields from the gas condensate at 1158 K. The BTX,

benzene and ethylene yields from the two further hydrogenated materials (D1 and E1) are plotted against cracking temperature in Figure 3.

Table 2 shows that the parent hydrogenates (D and E) gave relatively low yields of BTX and ethylene (<10%) whereas considerable yields of polynuclear aromatics such as naphthalene, methyl naphthalenes, acenaphthylene, fluorene, anthracene and phenanthrene were obtained. In contrast, the further hydrogenated materials (D1 and E1) gave higher yields of BTX and ethylene (>20%) and relatively low yields of polynuclear aromatics. The highest yields of BTX, 27% at 1083 K for 1 s and at 1108 K for 0.4 s, and of ethylene, 24% at 1158 K for 0.4 s, were both obtained from D1. The curves in Figure 3 for a vapour residence time of 0.4 s show broad maxima in BTX and ethylene yields; similar maxima were obtained at 1 and 2 s but at slightly lower cracking temperatures.

The yields from the partially hydrogenated anthracene oil (C1), also given in Table 2, are relatively low, little more than 10% BTX and ethylene being obtained.

Natural Gas Condensate

To compare the yields from coal-derived materials with those from a petroleum material, a full range, North Sea gas condensate (F) was cracked at 1158 K for 0.4 s. Its analysis is given in Table 1 and the yields obtained are listed in Table 2. More ethylene (30%) but less BTX (16%) were produced than from the highly hydrogenated coal materials.

Model Compounds

Four model compounds (mesitylene for aromatics, tetralin for hydroaromatics, decalin for naphthenes and n-undecane for paraffins) were cracked singly and as mixtures at 1133 K for 1 s. The yields of BTX, ethylene, butadiene and methane are shown as a bar chart in Figure 4. Decalin gave the highest BTX yield, 25%, compared with less than 7% from n-undecane. Mesitylene gave only 8% BTX. Tetralin produced the least BTX, 3%, its major products being polynuclear aromatics. n-Undecane gave 37% ethylene compared to 20% from decalin, 3% from tetralin and 0.2% from mesitylene. Six binary, four ternary and the quaternary mixtures of the four compounds were cracked and the observed product yields were within $\pm 2\%$ of the values calculated from the constituents' yields.

DISCUSSION

The low yields of BTX and ethylene from the unhydrogenated feedstocks reflect the stability of the condensed aromatic structures which constitute much of their volatiles and confirm the findings of a literature review (5). It is interesting that the coal extract (B), which contained 70% coal, yielded even less BTX and ethylene than the coal itself; this is probably due to elimination of reactive constituents and cross-linking during digestion/extraction of the coal.

Yields of BTX and ethylene increased with increasing extent of hydrogenation of coal extract, as indicated by the H/C ratios listed in Table 1. This was reflected in their naphthene contents, which were in the order D1 > E1 > D > E, and confirms the finding (6) that polynuclear aromatic hydrocarbons need to be fully hydrogenated to the naphthenic structure to maximise their conversion to BTX and ethylene. Concomitantly, the yields of tar and polynuclear aromatics decreased with decrease in the (hydroaromatic + aromatic) content of the feedstock, suggesting that the higher aromatics result from the dehydrogenation of hydroaromatics to the parent aromatics and from the survival of those aromatic hydrocarbons already present. 34% of C₂-C₄

gaseous hydrocarbons (C_2H_6 , C_2H_4 , C_3-C_4 unsaturates and saturates) were obtained from E1 at 1133 K for 0.4 s (up to 17% C_3-C_4 unsaturates were obtained at a lower cracking temperature of 1083 K). The sum of BTX + valuable gaseous hydrocarbons amounted to 55% at 1133 K, 60% at lower temperatures.

Some acetylene and polyacetylenes, which are undesirable, explosive byproducts, were also formed. The amount increased with the severity of cracking but was only 2.5% of the maximum ethylene yield; this value is about that found in the industrial cracking of petroleum naphtha to ethylene (7,8).

Cracking temperature and vapour residence time were the most important parameters controlling the cracking reactions. Within the range of conditions tested, other variables such as type and area of cracking surface, the vapour concentration of the feedstock and presence of steam made little difference to the yields of BTX and ethylene. Steam is used as a diluent and carrier in industrial ethylene crackers, where it reduces carbon laydown in the reactors (9).

The aromatic and hydroaromatic components of coal-derived feedstocks are potential sources of carbon laydown and steam would be needed to reduce reactor fouling.

The high ethylene and moderate BTX yields from the gas condensate are commensurate with its 56% paraffin and 12% naphthene content (see Table 1). This was confirmed by the 37% ethylene and 7% BTX obtained from the model paraffin, n-undecane (see Figure 4).

The model compound studies confirmed that the molecular structure of the hydrogenated coal extract is of paramount importance in determining the product pattern: hydroaromatics dehydrogenate to aromatics, which either survive or polymerise to tars and, eventually, to carbon; naphthenes crack principally to BTX and ethylene; aliphatics mainly give small unsaturates such as ethylene and butadiene. The abnormally low yield of BTX from mesitylene is attributed to its high symmetry and thermal stability.

CONCLUSIONS

The results from the thermal cracking of unhydrogenated and hydrogenated coal-derived materials, a gas condensate and model compounds led to the conclusions that:

- (i) only low (< 3.5%) BTX and ethylene yields were obtained by cracking the vapours from a bituminous coal, an anthracene oil and the anthracene oil extract of the coal;
- (ii) the BTX and ethylene yields increased with increasing extent of hydrogenation of the extract (which increased the naphthene content); tar was mainly derived from the aromatic and hydro-aromatic components;
- (iii) about 27% BTX and 24% ethylene were obtained from the highly hydrogenated coal extract; in comparison, a paraffinic North Sea gas condensate gave 16% BTX and 30% ethylene;
- (iv) the product yields from mixtures of model compounds were predicted to within $\pm 2\%$ from those of the constituents.

ACKNOWLEDGEMENTS

We thank the National Coal Board for permission to publish this paper and the European Coal and Steel Community for financial support. The views expressed are those of the authors and not necessarily those of the National Coal Board.

REFERENCES

1. Lowry, H.H., The Chemistry of Coal Utilisation, Supplementary Volume, John Wiley and Sons Inc., New York, 1963.
2. Dryden, I.G.C., Carbonisation and Hydrogenation of Coal, United Nations, 1973.
3. Thurlow, G.G., The Chemical Engineer, 733, October 1978.
4. Wett, T., The Oil and Gas Journal, 71, 73 November 26, 1973.
5. Ladner, W.R., Newman, J.O.H. and Sage, P.W., to be published in J. Inst. Energy.
6. Korosi, A., Woebecke, H.N. and Virk, P.S., Am. Chem. Soc., Div. Fuel Chem. Preprints, 21 (6), 190 (1976).
7. Krönig, W., Hydrocarbon Processing, 49 (3), 121 (1970).
8. Prescott, J.H., Chem. Eng., 82 (14), 52 (1975).
9. Miller, S.A., Ethylene and Its Industrial Derivatives, Ernest Benn Ltd., London, 1969.

Table 1 Analysis of Feedstocks

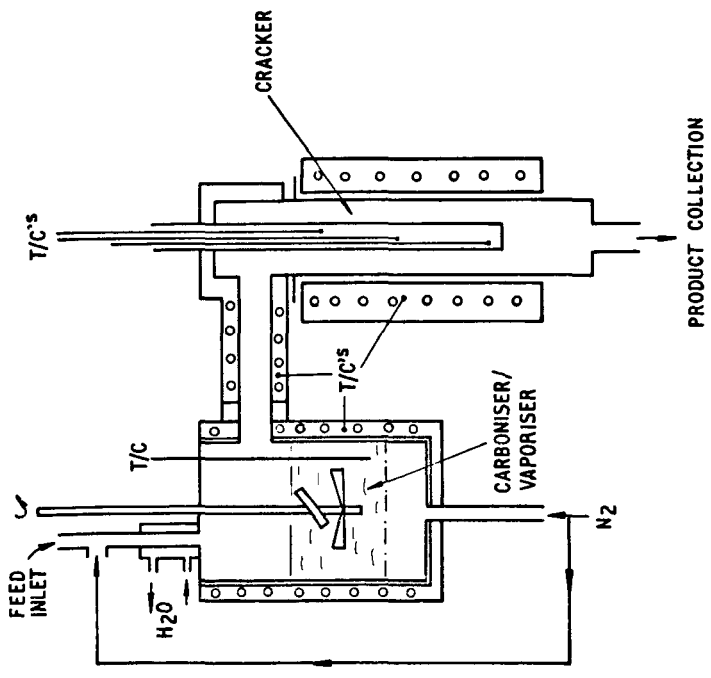
Solid Feedstock	Key	Size, μ m	Proximate Analysis, % w/w			Ultimate Analysis, % w/w d.a.f.						H/C atomic ratio
			Moisture, a.d.	Ash, a.d.	Y.M. d.a.f.	C	H	O	N	S		
Lumpy coal	A	210 to 350	8.3	6.0	39.1	82.4	5.3	9.0	1.95	1.00	0.77	
	B	210 to 350	0.3	0.3	50.5	86.7	4.8	3.8	1.90	0.55	0.65	
Anthracene oil extracted of lumpy coal												
Liquid Feedstocks:												
Anthracene oil												
Partially hydrogenated anthracene oil												
High-sulfated coal extracts												
Further hydrogenated coal extracts												
Natural gas condensate												

N.D. = Not Determined

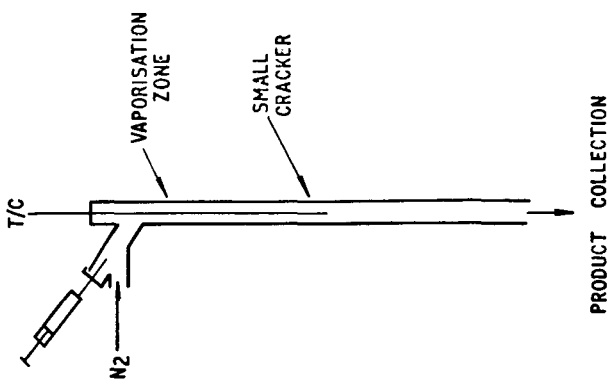
Table 2 Yields from Cracking Coal-derived Feedstocks and a Natural Gas Condensate

Cracking Temperature, °F Vapour Residence Time, s	* wt%									
	1273			1133			1156			
	2.0			1.0			0.4			
Feedstock	Light coal A	Anthracene oil Liny coal* B	Anthracene oil C	Partially hydrogenated anthracene oil Cl	Hydrogenated coal extract D	Hydrogenated coal extract E	Further hydrogenated coal extract D1	Further hydrogenated coal extract E1	Further hydrogenated coal extract F	Natural gas condensate Y
<u>Product</u>										
Benzene	3.1	1.8	2.1	6.6	3.5	2.5	17.1	13.5	11.9	
Toluene	0.1	0	0	2.7	1.9	1.3	5.3	5.1	2.4	
Xylene	0	0	0	1.3	1.7	1.1	3.0	2.8	1.7	
Total BTX	3.2	1.8	2.1	10.6	7.1	4.8	25.4	21.4	16.1	
Cl ₄	4.3	2.6	2.7	8.2	6.4	5.5	17.0	10.8	13.4	
C ₂ H ₆	0.2	0	0	0.8	1.0	0.8	1.5	1.7	1.7	
C ₂ H ₄	0.3	0.1	0.09	10.8	9.1	7.5	23.1	21.5	30.3	
C ₂ H ₂	N.D.	N.D.	N.D.	0.3	0.1	0.1	0.4	0.1	0.2	
C ₃ -C ₄ nats.	0.4	0.1	0	0	0.05	0.05	0.1	0.1	0.2	
C ₅ -C ₄ unnat.	0	0	0	1.8	3.4	2.7	7.9	10.6	11.2	
H ₂	1.3	1.0	1.3	1.2	1.1	0.9	1.3	1.2	1.0	
CO	7.8	1.7	1.6	0	0	0	0	0	0	
CO ₂	3.8	0.4	0.4	0	0	0	0	0	0	
Indene	< 0.01	< 0.01	< 0.01	1.3	3.4	2.2	1.9	1.8	0.8	
Naphthalene	0.3	0.2	1.4	19.5	23.5	15.6	4.6	5.3	2.9	
Methyl naphthalene	< 0.01	< 0.01	< 0.01	3.1	7.9	6.6	1.3	2.5	0.6	
Dibenzyl	0.03	0.01	< 0.01	1.1	3.3	4.1	0.4	0.3	0.3	
Acenaphthylene	0.09	0.06	0.07	1.8	3.9	5.1	0.9	1.3	0.4	
Fluorene	0.01	0	0.07	0.5	0.5	2.2	0.3	0.3	0.2	
Anthracene and phenanthrene	0.7	0.2	1.7	1.4	0.4	6.0	0.9	0.2	0.2	
Fluoranthene	0.06	0.2	0.4	0	0.3	0.2	0	0.1	0	
Pyrene	0.06	0.2	0.4	0.5	0.3	0.3	0	0.4	0	
<u>Mass Balance</u>										
Gas	21	13	8	28	24	20	58	57	70	
Liquid/Lnr	17	15	56	46	69	82	29	31	11	
Solid	61	72	23	10	10	5	11	5	11	
Total	99	100	87	84	103	107	98	93	94	

* Combustion temperature: 873 K.
N.D., Not Determined



1a. CARBONISER/VAPORISER/CRACKER



1b. SMALL VAPORISER/CRACKER

FIGURE 1. CRACKING APPARATUS

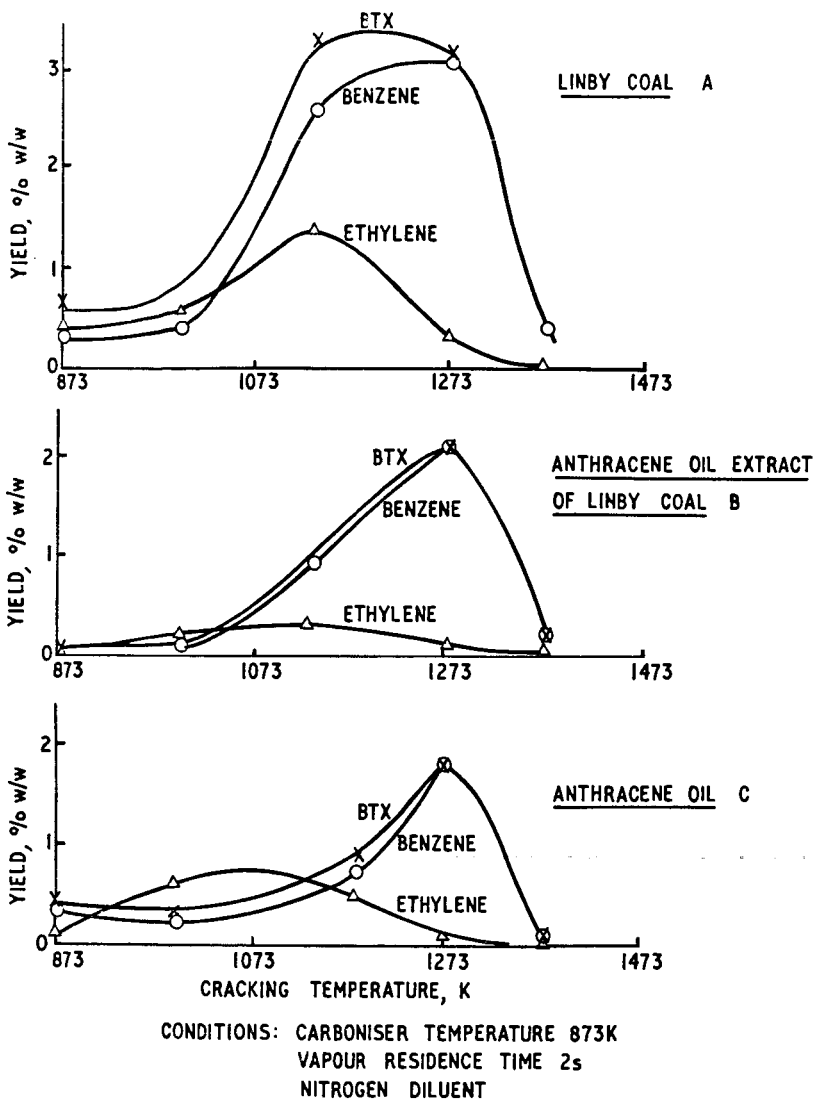


FIGURE 2. THE EFFECT OF CRACKING TEMPERATURE ON YIELDS OF BTX, BENZENE AND ETHYLENE FROM UNHYDROGENATED COAL MATERIALS.

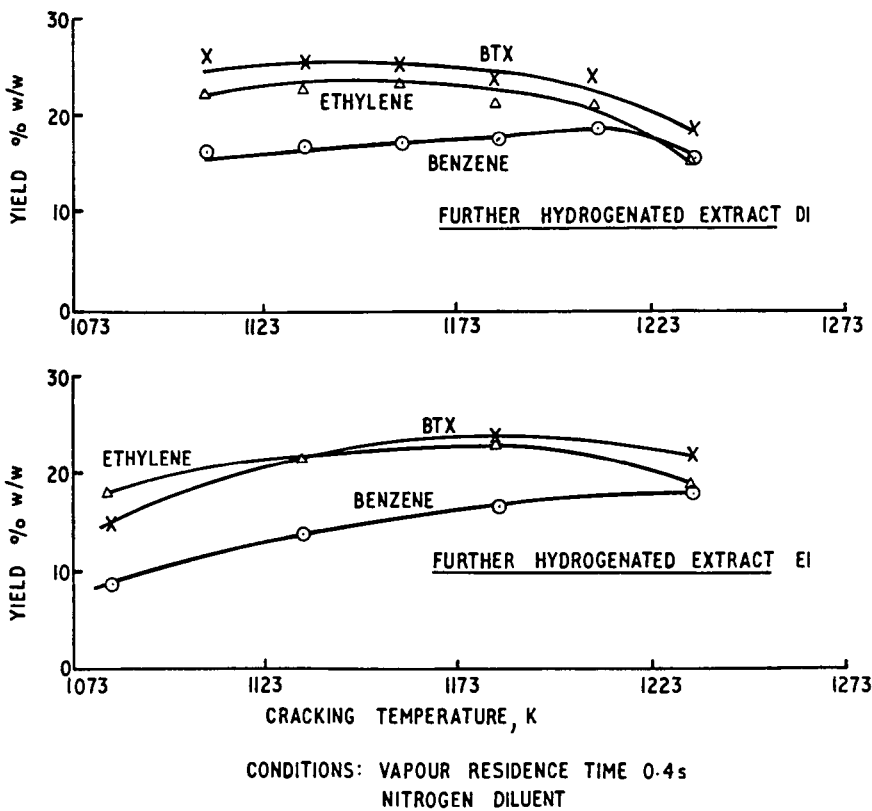
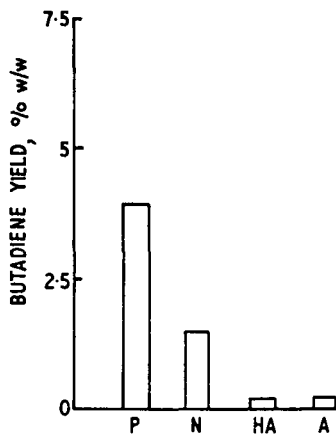
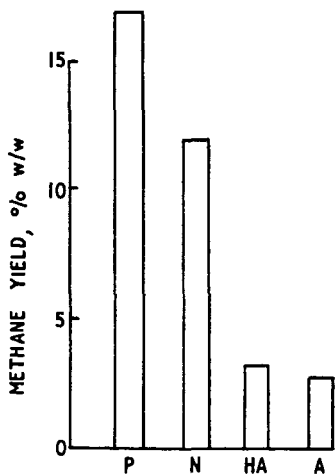
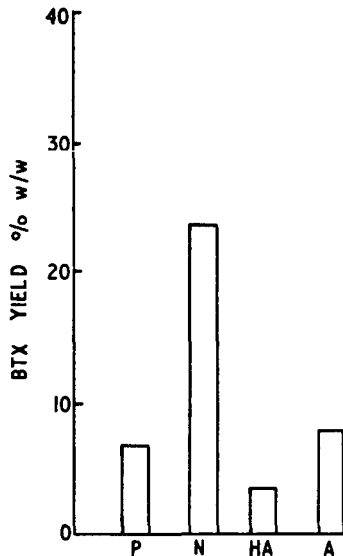
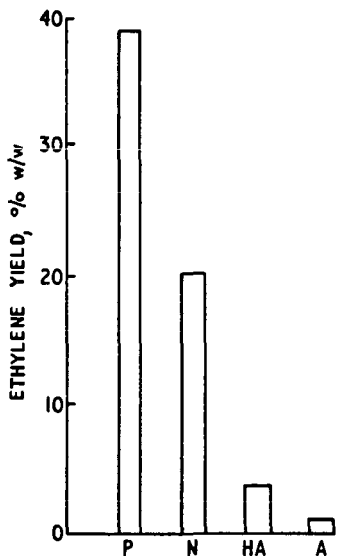


FIGURE 3. THE EFFECT OF CRACKING TEMPERATURE ON YIELDS OF
BTX, BENZENE AND ETHYLENE FROM FURTHER
HYDROGENATED EXTRACTS.



CRACKING TEMPERATURE 1133K
VAPOUR RESIDENCE TIME 1s

KEY: PARAFFIN P=n-UNDECANE; HYDROAROMATIC HA=TETRALIN;
NAPHTHENE N=CIS/TRANS DECALIN; AROMATIC A=MESITYLENE

FIGURE 4. THE VARIATION OF YIELDS WITH HYDROCARBON TYPE

Western Low-Rank Coal Development Analysis

G.H. Gronhovd and E.A. Sondreal

U.S. Department of Energy, Grand Forks Energy Technology Center
Box 8213, University Station
Grand Forks, North Dakota 58202

J.A. Kotowski and G.A. Wiltsee

Energy Resources Co. Inc., 1148 Alpine Road, Suite B
Walnut Creek, California 94596

Introduction

An analysis of the technical, environmental, and economic constraints to expanded development of the U.S. low-rank coal resource is in progress. The primary objective of the study is to propose a comprehensive national R&D program focusing on technology development for enhanced utilization of lignite and subbituminous coal. Utilization of these fuels has expanded rapidly in recent years and will continue to expand in line with national energy priorities. This will require technological improvements and developments to solve unique problems associated with the physical and chemical properties of low-rank coals. These properties include high moisture content, dispersed alkaline mineral matter content, high reactivity, and low sulfur content. The majority of coal R&D programs in this country are oriented towards bituminous coal, which exhibits significantly different behavior in most extraction, combustion, and conversion processes.

The study is being directed by the Grand Forks Energy Technology Center (GFETC), which has the lead mission within the Department of Energy for technology "applications for low-rank coals." To fulfill this assignment, GFETC must:

1. Identify the properties of low-rank coals that affect the applicability and economics of technologies;
2. Identify R&D needs unique to low-rank coals, and establish priorities based on potential impact on expanded development; and
3. Ensure that DOE's coal R&D programs address those needs.

Historically, GFETC has focused on lignite R&D, primarily on Northern Great Plains lignite. This has included programs in coal combustion, preparation, liquefaction, gasification, and environmental control technologies. The Center has also sponsored a biennial lignite Symposium, designed to encourage the transfer of low-rank coal technology data between government, industry, and academia (1,2). The present study was initiated as a means to identify other needed R&D areas associated with the whole spectrum of U.S. low-rank coals.

As a result, the scope of the study is broad, encompassing all of the major lignite and subbituminous coal deposits in this country, and including

some attention to peat as well. The technical analysis includes assessment of resources; technologies, from extraction through final utilization (including environmental control); and regulatory, environmental impact, and market factors. The R&D requirements definition will be based on these assessments plus a review of current R&D programs, costs, and impacts.

Study Approach

The study approach is summarized in Table 1, which shows the eight major tasks or areas of investigation. As a rough indicator of the relative emphasis being placed on these various tasks, the percentage of the total contract funding allocated to each task is indicated on the table.

The initial task, labelled "Development Scenarios," includes a literature review, definition of key issues and analytical methodologies, and establishment of the study's data base. In Task 2, the U.S. low-rank coal resources are being defined in terms of their occurrence, quantity, quality, characteristics, and physical/chemical properties. An effort is being made to classify the resources according to their behavior in various utilization processes, which influences their development potential. This effort is closely tied to Task 3, the technology evaluation. A comprehensive list of technologies applicable to low-rank coals is being evaluated to ensure that the resulting preliminary R&D "wish list" is as exhaustive as possible.

Table 1
Major Tasks in the Low-Rank Coal Study

- | | |
|---|---|
| <ul style="list-style-type: none"> 1. Low-Rank Coal Development Scenarios (6%) <ul style="list-style-type: none"> 1.1 Literature Review 1.2 Technology Definitions 1.3 Regulatory/Environmental/Market Definitions 1.4 Low-Rank Coal Data Base | <ul style="list-style-type: none"> 5. Environmental Impact Analysis (3%) <ul style="list-style-type: none"> 5.1 Land Use/Reclamation 5.2 Air Quality 5.3 Water Quality 5.4 Ecological Effects 5.5 Socio-Economic Effects |
| <ul style="list-style-type: none"> 2. Resource Characterization (8%) <ul style="list-style-type: none"> 2.1 Occurrence 2.2 Properties/Characteristics 2.3 Classification | <ul style="list-style-type: none"> 6. Market Analysis (6%) <ul style="list-style-type: none"> 6.1 Existing Markets and Penetration 6.2 Potential Markets |
| <ul style="list-style-type: none"> 3. Technology Evaluation (42%) <ul style="list-style-type: none"> 3.1 Extraction 3.2 Transportation Systems 3.3 Preparation and Storage 3.4 Processing and Utilization 3.5 Environmental Control Technology | <ul style="list-style-type: none"> 7. RD&D Program Evaluation (11%) <ul style="list-style-type: none"> 7.1 Definition and Priorities 7.2 Review of Current RD&D Programs 7.3 Cost and Impact Analysis |
| <ul style="list-style-type: none"> 4. Regulatory Requirements/Constraints (4%) <ul style="list-style-type: none"> 4.1 Definition 4.2 Roadmap 4.3 Effects on Development | <ul style="list-style-type: none"> 8. Task Force Utilization (20%) <ul style="list-style-type: none"> 8.1 Development Scenarios Evaluation 8.2 Technical Analysis Evaluation 8.3 RD&D Program Definition 8.4 RD&D Program Impacts and Recommendations |

In addition to these purely technical considerations, there are various social, economic, and environmental factors in the regions containing low-rank coals that will affect the development of these resources. These factors are the subject of Tasks 4, 5, and 6. Each of these analyses is being conducted on a regional basis, with detailed calculations being made for a few carefully selected examples, in contrast to the more comprehensive approach being utilized in Tasks 2 and 3.

In Task 7, we will define and establish priorities for the R&D activities necessary to stimulate the effective development and utilization of low-rank coals in this country. This will be done in light of the present related governmental and industrial research and development efforts, and will include a preliminary analysis of costs and impacts of the proposed program. The practical difficulties of evaluating and ranking R&D projects, even when the most rigorous decision/analytical techniques are used, are great but do not diminish the need for this type of exercise.

Because of the scope and difficulty of the effort, we have enlisted a task force of recognized experts on the technical and regional issues germane to the study to meet with the study team at four critical points. At the periodic formal review meetings, interim results are discussed and decisions are made regarding emphasis, priorities, and methodologies for the analysis. In particular, the task force will participate actively in the development of R&D recommendations. This task force utilization effort is listed on Table 1 as Task 8.

The schedule for the study is June 1979 through June 1980, and is such that preliminary R&D recommendations will be in the formulation stage at the time of the American Chemical Society meeting in late March. The authors expect to summarize some of the key conclusions and recommendations of the study at that time. It is not possible to do so in this preprint because the work is in progress. Therefore, the remainder of this paper provides some preliminary findings and background information on some of the study areas.

Occurrence and Properties of Low-Rank Coals

The locations of the major lignite and subbituminous coal deposits in the U.S. are shown in Figure 1, and the magnitude of the resources contained in the largest low-rank coal-bearing regions is indicated in Table 2. The two major lignite-bearing areas are the Fort Union Region and the Gulf Coast Lignite Region, with the predominant surface-minable reserves being in the states of North Dakota, Montana, and Texas. The largest subbituminous coal deposits are in the Powder River Region of Montana and Wyoming, the San Juan Basin of New Mexico, and in Northern Alaska. Whether one considers the total identified resources (over one trillion tons) or just the strippable reserve base (over 100 billion tons), the potential supply of energy from low-rank coals is enormous.

Figure 1
United States Low-Rank Coal Resources

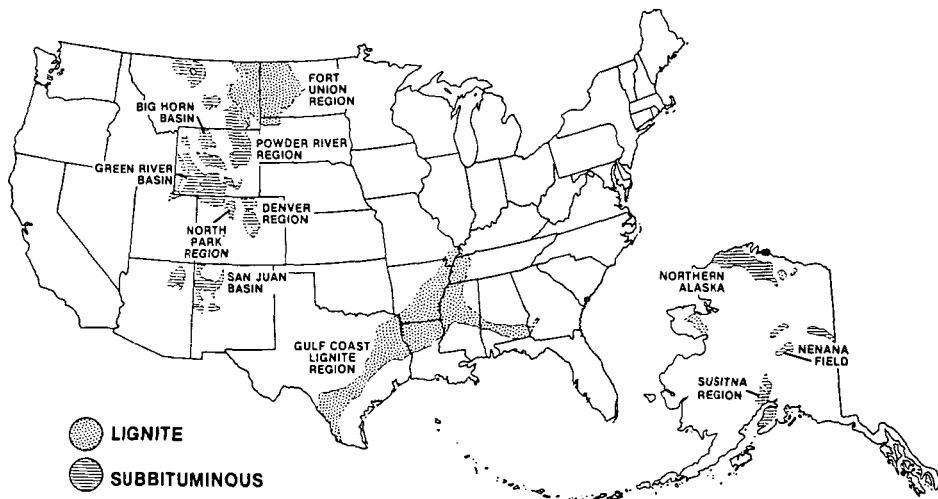


Figure 2
New Source Performance Standards for SO₂ Emissions from
Electric Utility Steam Generators

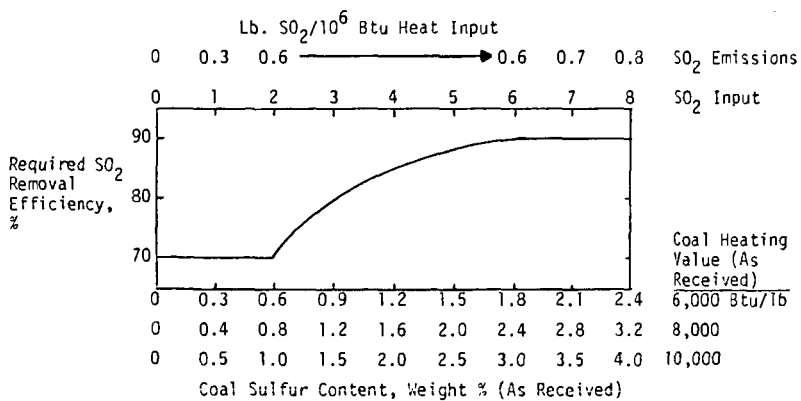


Table 2
Major United States Low-Rank Coal Regions

<u>Region</u>	<u>Predominant Coal Rank</u>	<u>Identified Resources, Billion Short Tons</u>	<u>Strippable Reserve Base, Billion Short Tons</u>
Fort Union Region	Lignite	465.3	31.9
Powder River Region	Subbituminous	238.1	57.5
San Juan Basin	Subbituminous	50.6	1.8
Northern Alaska	Subbituminous	100.9	5.0
Gulf Coast Lignite	Lignite	68.3	11.6
Others (see Fig. 1)	Subbituminous, some Lignite	<u>165.2</u>	<u>0.9</u>
		1,088.4	108.7

Sources: References 3-9

The distinguishing properties of low-rank coals are derived from their fundamental composition. Coals are complex aggregations of physically distinctive and chemically different organic materials (macerals) and inorganic materials (minerals). Strictly speaking, the rank of coal expresses only the degree to which geologic alteration processes (metamorphism) have affected the properties of the organic substances. In this sense, rank classification is independent of inorganic content; nevertheless, U.S. low-rank coals do exhibit characteristic differences from high-rank coals in their mineral matter content and therefore in their ash properties. This is apparently a coincidental or indirect relationship caused by the respective geologic ages and geographic locations of the U.S. low-rank coals and high-rank coals (10,11).

Some important properties of the organic and inorganic fractions of U.S. coals are summarized in Table 3. The data on organic content are based on samples of essentially pure vitrinite, which is the predominant maceral in U.S. coals (10). All of the properties listed have an impact on the coal's behavior in extraction, utilization, or conversion processes; the most noticeable properties are the high inherent moisture and oxygen contents of low-rank coal macerals, and their corresponding low heating values.

The data on mineral matter content are reported as ash, which is the residue left after complete incineration of the combustible constituents. The ash compounds are reported as oxides; however, they may actually occur as a mixture of silicates, oxides, and sulfates (11). Due to the wide variations in coal ash composition, the data are presented as ranges. A notable trend is the higher proportion of the alkali components CaO, MgO, and Na₂O in low-rank coals. The acidic components SiO₂ and Al₂O₃ are more prominent in the higher rank coals. The generally higher proportions of SO₂ in low-rank coal ash reflect the high retention of coal sulfur by the alkaline ash, which averages 78% for lignites, 26% for subbituminous coal, and 10% for the generally higher sulfur bituminous coals (11).

Table 3
Selected Analyses of U.S. Coals of Different Ranks

Organic Content (Vitrinite Samples)	Lignite	Subbituminous	Bituminous	Anthracite	
Moisture Capacity, Wt.%	40	25	10	< 5	
Carbon, Wt. % DMMF*	69	74.6	83	94	
Hydrogen, Wt. % DMMF	5.0	5.1	5.5	3.0	
Oxygen, Wt. % DMMF	24	18.5	10	2.5	
Vol. Mat., Wt. % DMMF	53	48	38	6	
Aromatic C/Total C	0.7	0.78	0.84	1.0	
Density (He, g/cc)	1.43	1.39	1.30	1.5	
Grindability (Hardgrove)	48	51	61	40	
Btu/lb, DMMF	11,600	12,700	14,700	15,200	
Inorganic Content (Weight % of Total ASTM Ash)					
Acidic Components	SiO_2	6-40	17-58	7-68	48-68
	Al_2O_3	4-26	4-35	4-39	25-44
	Fe_2O_3	1-34	3-19	2-44	2-10
	TiO_2	.0-.8	.6-2	.5-4	1-2
	P_2O_5	.0-1	.0-3	.0-3	.1-4
Alkali Components	CaO	12.4-52	2.2-52	.7-36	.2-4
	MgO	2.8-14	.5-8	.1-4	.2-1
	Na_2O	.2-28	-	.2-3	-
	K_2O	.1-1.3	-	.2-4	-
	SO_3	8.3-32	3.0-16	.1-32	0.1-1

*Dry, mineral-matter-free basis.

Sources: References 10 and 11

These mineral matter properties of U.S. low-rank coals have wide-ranging effects, such as: 1) high fouling rates on boiler tubes, primarily linked to high sodium content; 2) high fly ash resistivity, thus relatively poor ESP performance; 3) unique opportunities for sulfur removal, such as ash-alkali wet scrubbing, dry scrubbing, and ash recirculation in fluid bed combustors; and 4) catalytic effects on certain reactions such as coal hydrogenation (liquefaction).

One additional characteristic of U.S. low-rank coal is its typically low sulfur content, as shown in Table 4. When these percentages are converted from a dry to an as-mined basis, about 90 percent of the reserve base of U.S. low-rank coal is shown to have less than one percent sulfur (13).

Table 4
Distribution of U.S. Low-Rank Coal Reserve Base by Sulfur Content

<u>Sulfur Content, % (Dry Basis)</u>	<u>1.0 or Less</u>	<u>1.1-1.8</u>	<u>1.8-3.0</u>	<u>Over 3.0</u>	<u>Total</u>
Subbituminous	89.5	8.1	2.0	0.4	100.0
Lignite	40.7	33.4	23.4	2.5	100.0

Source: Reference 12

Utilization and Processes

Present use of low-rank coal is concentrated in electric utility steam generating units fed by surface-mined coal. This conventional application of the resource is experiencing rapid change. As the data in Table 5 indicate, existing small stoker and cyclone-fired units have given way to very large pulverized-coal-fired, dry bottom furnaces. All of the new plants will incorporate SO₂ removal systems as mandated by the recently issued New Source Performance Standards (see Figure 2). The same regulation also requires highly effective particulate removal systems, and combustion system modifications to meet NO_x emission limits, in all new or modified electric utility steam generating units larger than about 25 MWe (250 million Btu/hr. input).

The dominating near-term R&D issues for low-rank coals revolve around the environmental control technologies that are being developed to meet these requirements. In the area of SO₂ control, the variable percentage removal requirement shown in Figure 2 (which translates to a 70% removal requirement for the majority of low-rank coals) was instituted for the express purpose of encouraging the further development of dry scrubbing techniques for low- and medium-sulfur coals (14). The combined stack gas cleaning strategy of dry SO₂ scrubbing plus the use of baghouses for particulate removal has a number of apparent advantages over today's wet scrubber/ESP systems, and appears to be strongly encouraged by the NSPS. However, the lack of operational experience with such systems provides ample opportunity for well-directed R&D. Wet scrubbers (particularly ash-alkali systems for low-rank coals) and electrostatic precipitators (combined with novel conditioning or removal devices) will both continue to have applications for specific coals; however, many problems relating to enhanced removal efficiencies, sludge disposal, sulfate and sulfuric acid mist carryover, and trace element emissions, remain to be solved. Potential operating problems associated with combustion modifications for NO_x control also need R&D. Finally, the task of integrating the study of these interrelated problems and opportunities through a systems engineering approach is just beginning, for example in the EPRI Arapahoe program (15).

Ash fouling of boiler tubes continues to be a major problem encountered in burning lignites and subbituminous coals. Sodium content has been identified as the most important of a number of factors that contribute to the fouling problem. The possible control methods to decrease chances of fouling include: 1) boiler designs involving low volume heat release and low furnace exit temperature; 2) restrictions on the sodium level in the coal by selective mining, blending and upgrading, 3) the use of additives; and 4) possibly the use of overfire air with fuel-rich burners (16).

Table 5
U.S. Low-Rank Coal-Fired Electric Power Plants

Fuel Location Plants, Capacity	Lignite				Subbituminous Coal			
	Fort Union Reg.		Texas		West		Midwest	
	No.	MWe	No.	MWe	No.	MWe	No.	MWe
<u>Operating Plants (1979)</u>	19	3,357	11	5,660	20	7,389	79	10,627
Furnace: PC	8	1,614	11	5,660	20	7,389	58	6,705
Stoker	7	205	-	-	-	-	9	97
Cyclone	4	1,538	-	-	-	-	7	1,265
Unknown	-	-	-	-	-	-	5	2,560
Wet Scrubber:								
Limestone	5	1,720	5	3,575	12	3,783	10	3,477
Ash-Alkali	2	670	-	-	-	-	4	2,116
Spray Dryer	2	716	-	-	-	-	-	-
Particulate Removal:								
ESP	16	3,329	11	5,660	17	7,192	48	7,131
Baghouse	-	-	2	1,150	-	-	8	1,788
Mechanical	5	210	-	-	2	230	21	518
Unknown	7	72	-	-	-	-	5	1,929
<u>Plants Under Construction and Announced</u>	6	1,947	18	10,390	5	1,349	34	15,372
Furnace: PC	6	1,997	9	5,175	4	1,249	2	1,100
Stoker	-	-	-	-	-	-	6	107
Cyclone	-	-	-	-	1	100	1	200
Unknown	2	1,050	9	5,215	-	-	25	13,004
Wet Scrubber:								
Limestone	-	-	8	4,600	-	-	1	800
Ash-Alkali	-	1,100	-	-	-	-	5	3,100
Spray Dryer	2	880	-	-	1	330	-	-
Particulate Removal:								
ESP	-	-	9	5,175	2	450	-	-
Baghouse	-	-	-	-	1	350	-	-
Mechanical	-	-	-	-	-	-	3	18
Unknown, ECT	1	410	14	8,675	2	589	31	15,934

Numerous advanced technologies are being pursued in a wide range of government and industry R&D programs. Many of these technologies will contribute to enhanced utilization of low-rank coals in the future. Extraction of the abundant thick, deep coal seams in the western U.S. will eventually be pursued. A variety of techniques, including advanced longwall and in situ conversion systems (such as underground coal gasification), are currently being researched.

Coal cleaning and preparation techniques have historically not been applied to U.S. low-rank coals because of cost considerations and the relatively low ash content of the coals. The fact that most of the mineral matter in low-rank coals tends to be highly dispersed and/or organically bound means that typically only 15-30% of the mineral matter is separable in a carbon tetrachloride float-sink separation (17). Lignite is characterized by high moisture content which is also bound in the coal structure. Upon drying, the

structure of low-rank coal tends to change and to produce smaller, friable particles which may be either highly oxidized (when air-dried) or highly reactive (when inert-dried) (18). Nevertheless, wider geographic marketability and improved over-all process economics could potentially be achieved if energy-efficient techniques for selective removal of moisture or mineral matter were developed.

Fluidized-bed combustion (FBC) systems are receiving major emphasis as the potential next generation of industry, and possibly utility, boilers. Almost all major projects are utilizing bituminous coal. The technology has a good apparent fit with low-rank coals because of their inherent sulfur absorption capability. A particularly promising market appears to be developing in Texas, which has a high concentration of industry fuel users juxtaposed with large lignite deposits. Some of the FBC research needs specific to low-rank coals include selection of bed materials, use of ash recycle, control of ash agglomeration, and possible corrosion/erosion problems.

In the highly visible synfuels area, none of the major developing U.S. processes for liquefaction or gasification appears to be optimized or tailored to the unique properties of low-rank coals, with the possible exception of the CO₂ Acceptor gasification process. Low-rank coals are well suited for fixed-bed gasification because they do not agglomerate or cake when heated. The high inherent moisture content of low-rank coal has a variety of effects on gasification processes. Plant water requirements may be lower if coal moisture is recovered. High moisture, however, can cause heat balance problems and pre-drying of the coal can produce an excessive amount of fines which cannot be included in feed for fixed-bed reactors. Large volumes of gas liquor may be produced, affecting waste water treatment requirements. These factors, plus the reactive nature of low-rank coals and the presence of catalytically active mineral matter, justify the need for development of low-rank coal specific processes (19).

Coal liquefaction processes also need to be adapted to special problems posed by low-rank coals. The high content of functional groups (particularly oxygen) affects liquefaction chemistry. Low-rank coals react very rapidly with carbon monoxide providing the basis for development of processes using synthesis gas instead of more expensive hydrogen. High moisture content adds to reactor pressure. Drying can deactivate the coal because of surface oxidation and collapse of the pore structure (20). The special forms of low-rank coal mineral matter may catalyze liquefaction reactions; they can also lead to formation of calcium carbonate deposits in the reactors. Viscosity of the distillation bottoms is higher for low-rank coals, which affects process design and operability (21). All of these factors affect the optimization of recycle solvent composition and product separation techniques, which are important research areas for liquefaction processes in general.

REFERENCES

1. Proceedings of the Tenth Biennial Lignite Symposium, Sponsored by the U.S. DOE Grand Forks Energy Technology Center, and the University of North Dakota, Grand Forks, N.D., May 30-31, 1979.
2. Proceedings of the Ninth Biennial Lignite Symposium, Sponsored by the U.S. DOE Grand Forks Energy Technology Center, and the University of North Dakota, Grand Forks, N.D., May 18-19, 1977.
3. 1979 Keystone Coal Industry Manual, McGraw-Hill Mining Publ., New York, N.Y., 1979.
4. Demonstrated Coal Reserve Base of the U.S. on January 1, 1976, USBM Mineral Industry Survey.
5. Glass, G.B., Wyoming Coal Fields, 1978, Geological Survey of Wyoming, Public Info. Circular 9, 1978, 91 pp.
6. Clardy, B.F., Arkansas Lignite Investigations, Preliminary Report, Arkansas Geological Commission, 1979, 133 pp.
7. Roland, H.L., Jr., Lignite - Evaluation of Near-Surface Deposits in NW Louisiana, Louisiana Geological Survey Mineral Resources Bulletin No. 2, 1976.
8. Averitt, P., Coal Resources of the United States, January 1, 1974, USGS Bulletin 1412, 1975, 121 pp.
9. Combo, J.X. and others, Coal Resources of Montana, USGS Circular 53, 1949.
10. Neavel, R.C., Coal Structure and Coal Science: Overview and Recommendations, presented at the ACS Symposium on Coal Structure, Honolulu, Hawaii, April 2-6, 1978, ACS, Div. of Fuel Chem. Preprints, v. 24, No. 1, pp. 73-77
11. Sondreal, E.A., W.R. Kube, and J.L. Elder, Analysis of the Northern Great Plains Province Lignites and their Ash: A Study of Variability, USBM RI 7158, 1968, 94 pp.
12. Hamilton, P.A., D.H. White, Jr., and T.K. Matson, The Reserve Base of U.S. Coals by Sulfur Content; Part 2, The Western States, BuMines IC8693, 1975, 322 pp.
13. Selle, S.J., F.I. Honea, and E.A. Sondreal, Direct Use of Lignite for Power Generation, presented at IGT Symposium on New Fuels and Advances in Combustion Technology, Chicago, Illinois, March 26-30, 1979, 24 pp.
14. Environmental Protection Agency, New Stationary Sources Performance Standards; Electric Utility Steam Generating Units, Federal Register v. 44, No. 113, June 11, 1979, 45 pp.
15. Giovanni, D., Integrated Environmental Control, Fossil Fuels and Advanced Systems Division R&D Status Report, EPRI Journal, May 1979, v. 4, No. 4, pp. 41-46

16. Honea, F.I., S.J. Selle, and E.A. Sondreal, Factors Affecting Boiler Tube Fouling from Western and Gulf Coast Lignites and Sub-bituminous Coals, presented at NACE Corrosion/79 Symposium, Atlanta, Georgia, March 12-16, 1979, 30 pp.
17. Sondreal, E.A., P.H. Tufte, and Willis Beckering. Ash Fouling in the Combustion of Low-Rank Western U.S. Coals. Combustion Sci. and Tech., v. 16, 1977, pp. 95-110
18. Oppelt, W.H., W.R. Kube, and T.W. Kamps. Drying North Dakota Lignite to 1,500 Pounds Pressure by the Fleissner Process. BuMines R.I. 5527, 1959, 30 pp.
19. Eilman, R.C., L.E. Paulson, and D.R. Hajicek, Slagging Fixed-Bed Gasification Project Status at the Grand Forks Energy Technology Center, presented at the Tenth Biennial Lignite Symposium, Sponsored by the U.S. DOE Grand Forks Energy Technology Center and the University of North Dakota, Grand Forks, N.D., May 30-31, 1979.
20. Willson, W.G., C.L. Knudson, G.G. Baker, T.C. Owens, and D.E. Severson, Application of Liquefaction Processes to Low Rank Coals. Presented at the Tenth Biennial Lignite Symposium, Sponsored by the U.S. DOE Grand Forks Energy Technology Center and the University of North Dakota, Grand Forks, N.D., May 30-31, 1979.
21. Mitchell, W.N., K.L. Trachte, and S. Zaczepinski, Performance of Low-Rank Coals in the Exxon Donor Solvent Process, presented at the Tenth Biennial Lignite Symposium, Sponsored by the U.S. DOE Grand Forks Energy Technology Center and the University of North Dakota, Grand Forks, N.D., May 30-31, 1979.

CURRENT RESEARCH ON THE INORGANIC CONSTITUENTS
IN NORTH DAKOTA LIGNITES AND SOME
EFFECTS ON UTILIZATION

D. K. Rindt, F. R. Karner, W. Beckering, and H. H. Schobert

Grand Forks Energy Technology Center
U.S. Department of Energy
Box 8213 University Station
Grand Forks, ND 58202

Introduction

Although coal is often considered to be simply an organic rock, most coals contain appreciable quantities of inorganic materials. With the resurgence of interest in coal utilization and conversion processes in recent years has come an increased appreciation for the need to understand both the mineralogical characteristics and the chemical behavior of the inorganic constituents of coal. The recent coal literature contains numerous discussions of the importance of knowing the character, distribution, and behavior of the inorganic species; these discussions span the whole spectrum of coal technology-- preparation and storage, combustion, liquefaction, gasification, and environmental studies.

This paper discusses results of laboratory studies on the characterization of inorganic constituents in low-rank coals and on elucidation of the role of these constituents in combustion and conversion processes. The laboratory studies were undertaken in support of pilot plant activities at the Grand Forks Energy Technology Center (GFETC) of the U.S. Department of Energy. Engineering and process-related details of the various projects have appeared in previous publications, which are noted in the reference section.

Inorganic Constituents in Lignite

Samples from two major lignite mines in western North Dakota were obtained (4) and studied by polarized light microscopy, x-ray diffraction, scanning electron microscopy, and electron microprobe analysis. The initial results of the laboratory studies of these two samples show that the inorganic constituents occur as minerals or combined with organic substances; are closely related in origin to the overburden and underclay; and illustrate part of a complex series of events in the geochemical evolution of the lignites. While the systematic variations that are presented are believed to be significant, they are not claimed to be necessarily representative at this point in the study.

The abundant lignite in North Dakota is contained in the upper part of the Fort Union group within the Bullion Creek formation and the overlying Sentinel Butte formation. Recent summaries of the general geology of the lignite-bearing rocks in western North Dakota are available (1-3).

Lignite, lignite overburden, and underclay were collected from measured, vertical sections on the highwalls at the South Beulah mine, Beulah, and the Baukol-Noonan mine, Center (4). Both mines produce lignites from the Sentinel Butte Formation with major production from the 3.8 m Beulah-Zap bed at South Beulah and the 3.5 m Hagel bed at Baukol-Noonan. Inorganic constituents in the two lignites are similar and contain detrital and authigenic minerals, listed in Table 1 and illustrated in Figure 1, as well as organically bound materials. The bulk chemistry of overburden, lignite, and underclay has been obtained by a rapid microprobe method.

At the South Beulah mine, four samples of overburden above the Beulah-Zap bed consist largely of clayey silt grading downward to organic-rich clay. Illite, quartz, and montmorillonite are the major minerals and kaolinite, chlorite, plagioclase, and mica are present in lesser amounts. Calcite is present in the uppermost sample while dolomite occurs in the other three samples; both decrease in abundance downwards. The Beulah underclay contains major illite, kaolinite, and quartz and lesser montmorillonite and calcite.

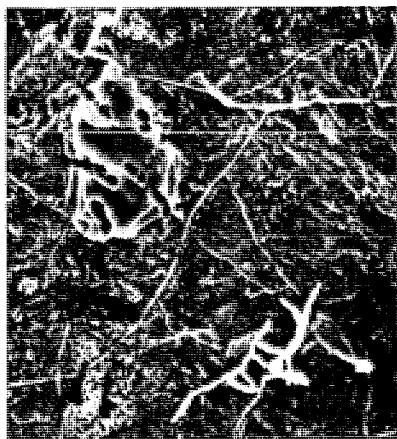
TABLE 1. - Minerals Identified in Two North Dakota Lignites

<u>Common (in approximate order of abundance)</u>	<u>Rare or uncertain</u>
Kaolinite	Montmorillonite?
Quartz	Dolomite?
Pyrite	Barite
Gypsum	Enstatite
Calcite	Corundum
Hematite	Ca, Mg Aluminosilicate?
Na Plagioclase	Ca, Na Aluminosilicate?
Alkali Feldspar?	
Chlorite?	
Hornblende	
Augite?	
Illite?	
Biotite?	

The twelve samples of overburden and the sample of underclay from the Baukol-Noonan mine are mineralogically similar to the Beulah samples. The lower part of the overburden is silty sand and the upper part, clays and silty clays. Overall montmorillonite is somewhat less abundant than at Beulah but is highly variable.

The mineralogical and chemical studies combined with the observation that lignites are aquifers suggest that hydrogeochemical processes have strongly affected the sodium and calcium distribution by removal of calcium by dissolution of carbonate minerals in the lower part of the overburden, concentration of sodium and calcium in the central parts of the lignite seams, and increase in the $\text{CaO}/\text{Na}_2\text{O}$ ratio in the upper parts of the lignite seams (5). Groundwater processes also appear to be a major factor in oxidation and reduction reactions as suggested by sulfide and sulfate distribution in fracture zones at the Baukol-Noonan mine (6). Pyrite development in fractures followed by growth of small gypsum crystals on the pyrite (Figure 1) indicates that groundwater carried and deposited iron and sulfur under reducing conditions, and carried and deposited calcium at a later stage under oxidizing conditions.

The original detrital minerals and organically bound inorganic constituents in lignite have been strongly affected by hydrogeochemical processes in the depositional and post-depositional history of lignite and the associated sediments. Current laboratory studies emphasize cataloging and characterization of inorganic constituents in lignite; establishment of mineralogical and chemical distribution patterns in overburden, lignite, and underclay; and evaluation of the geochemical history of the lignite-bearing sediments.



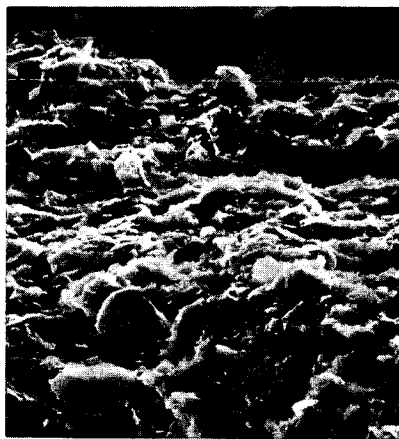
A



B



C



D

Figure 1. Scanning electron microscope photographs of inorganic constituents in lignite-bearing strata. Sentinel Butte Formation, North Dakota.

- A. Detrital quartz (?) in ion-etched Beulah lignite. 1540X.
- B. Secondary pyrite with gypsum crystals on surface from fracture zone in Baukol-Noonan lignite. 770X.
- C. Secondary barite in fracture zone in Baukol-Noonan lignite. 270X.
- D. Montmorillonite in overburden at Beulah mine. 1400X.

Gasification

The inorganic constituents of lignite can have several effects in gasification processes. Numerous articles have appeared in the recent literature describing the catalysis of gasification reactions by various inorganic species. Studies at GFETC have focused on the development of an understanding of the relationship between coal ash slag composition and viscosity. These studies have been done in support of the slagging fixed-bed gasification pilot plant at GFETC. Details of the pilot plant project have been given in a series of publications, most recently by Ellman and co-workers (7). Maintaining slag viscosity low enough to allow continuous discharge from the gasifier is crucial to successful operation.

Direct measurement of slag viscosity is a demanding operation, and few laboratories are equipped with suitable high-temperature viscometers. Therefore the development of predictive or correlative techniques for relating viscosity to composition is an important component of gasification research. A previous publication (8) has demonstrated that it is possible to develop empirical equations which give a good fit of experimental viscosity data provided that the equations are developed for, and their use restricted to, slags of a given petrographic classification.

The petrographic normative calculation (9) is a formation used to calculate a set of standard, or normative, mineral species, which then establishes the types of silicate structures to be expected in the slag. The degree of polymerization of silicate species has an important role in determining viscosity behavior (10).

The transformations involved in the formation of slag from the inorganic species in the coal have been partially elucidated in laboratory studies of char and slag samples obtained from the gasifier hearth after a test had been ended and the bed contents quenched. The data presented here were obtained from samples collected from a 1.4 MPa test with Indian Head lignite. Process data from this test, number RA-12, have been published (11).

Discreet slag particles were found in samples collected 0.9 m above the bottom of the bed. The composition at this point was 22% Na_2O , 24% Al_2O_3 , and 53% SiO_2 . This composition lies in the nepheline region of the $\text{Na}_2\text{O}-\text{Al}_2\text{O}_3-\text{SiO}_2$ ternary (12) and has a melting point of approximately 1200°C. This is consistent with typical temperatures of about 1260°C observed 1.2 m above the hearth bottom. Samples collected at 0.3 and 0.6 m were complex mixtures of silicates and sulfates. Total melting occurred in the bottom-most 0.3 m of the bed, where temperatures exceeding 1700°C have been observed. Some slag components are volatilized in this region, particularly sulfur (approximately 80% is lost), sodium and potassium (30-35%), and phosphorus (25%). Smaller amounts of magnesium, calcium, and silicon are also volatilized.

At 0.1 to 0.3 m above the hearth bottom some reduction of iron compounds to metallic iron occurs. Normally the iron metal drains with the slag and does not appear to interfere with slag flow. However, formation of iron metal removes a potential source of FeO , which is considered to be an excellent slag flux.

The viscosity behavior of the slag with temperature will be determined by its composition; specifically, by the relative amounts of polymer-forming constituents such as SiO_2 and Al_2O_3 and of polymer-breaking species such as Na_2O or CaO . The slag composition is in turn determined by two factors. The composition and nature of the inorganic constituents in the lignite feed broadly determines the relationships between polymer formers and polymer breakers. The thermal and chemical environment established by the gasification and combustion reactions in the gasifier hearth then "fine tune" the slag composition through such processes as volatilization of SO_3 and Na_2O and reduction of Fe_2O_3 to FeO or metal.

Liquefaction

The product distribution from coal liquefaction will vary between a heavy distillate, a light oil, and a gas depending on the extent and method of treatment of the intermediate products. The catalytic effect of naturally occurring inorganic species and minerals on the conversion and product yield is being investigated extensively with Eastern coals and also with low-rank Western subbituminous and lignitic coals. In general certain inorganic constituents of Eastern coals have shown a self-catalyzing effect on the liquefaction yield. High yields have been achieved by adding pyrite, magnetite plus pyrite, sulfur plus magnetite, and coal ash plus sulfur to coals which initially gave a low yield.

The lignites in the Northern Great Plains are distinguished from the higher rank coals by having high moisture, lower sulfur, and high inherent ash content. Most of the alkali and alkaline earth cations exist as humic acid or phenolic salts. These cations are ion exchangeable and are uniformly distributed throughout a coal particle. The majority of the extraneous ash exists as small particles of quartz, pyrite, hematite, and clay. In addition lignites have a large amount of oxygen-containing functional groups. These properties affect the liquefaction behavior of lignite in terms of reactivity, product quality, product yield, catalyst life, and solid residue.

The role of these unique properties of lignite in liquefaction is being investigated in a program at GFETC which seeks to develop a chemical and engineering data base for liquefaction of lignites and subbituminous coals. The programmatic background and process engineering results have been presented in a recent paper by Willson and co-workers (13).

Some of the parameters being studied with the batch autoclave and continuous process unit at GFETC are temperature, pressure, residence time, slurry coal concentrate recycle, solvents, and mineral effects. Extensive research on the effects of individual minerals on the product yield has not been performed thus far. However, a significant increase in the overall product yield was observed when the reaction solids were recycled in the continuous unit. In a recent run using a lignite from the Beulah mine in Mercer County, ND, a deposit formed in the feed slurry and was analyzed for possible minerals and inorganics using a polarizing light microscope and a scanning electron microscope (SEM). Calcium carbonate was initially suspected as a main ingredient in the deposit. However, quartz was the only mineral identified in the product. An elemental analysis of the bulk product using the SEM resulted in a composition not unlike that of the ash in the original coal. Analysis for calcium by atomic absorption also showed no preferential buildup of calcium. Thermogravimetric analysis indicated the presence of some carbonates but no particular cation could be associated with the carbonate. Other workers in liquefaction have reported calcium carbonate deposits when using lignites but thus far no major accumulations have been observed at GFETC. The implications of a low-level carbonate buildup using lignites should be fewer shut downs caused by carbonate plugging.

Combustion

Ash fouling-- the buildup of ash deposits on walls and heat exchange surfaces of boilers-- is a major problem associated with the use of lignite. The causative effects of sodium content in the fouling behavior of low-rank coals has been discussed in previous publications (14-15). Some of the current laboratory research at GFETC relating to ash fouling involves the chemical and physical characterization of ash deposits to develop a better understanding of the mechanisms involved in deposit formation and to predict fuel additives to control fouling.

A typical profile of an ash deposit formed in the 34 kg/hr, PC-fired pilot plant combustor at GFETC is shown in Figure 2 (16). The deposit was collected on an



FIGURE 3. - SEM photomicrograph (3000X) showing particles in the initial stages of attachment.

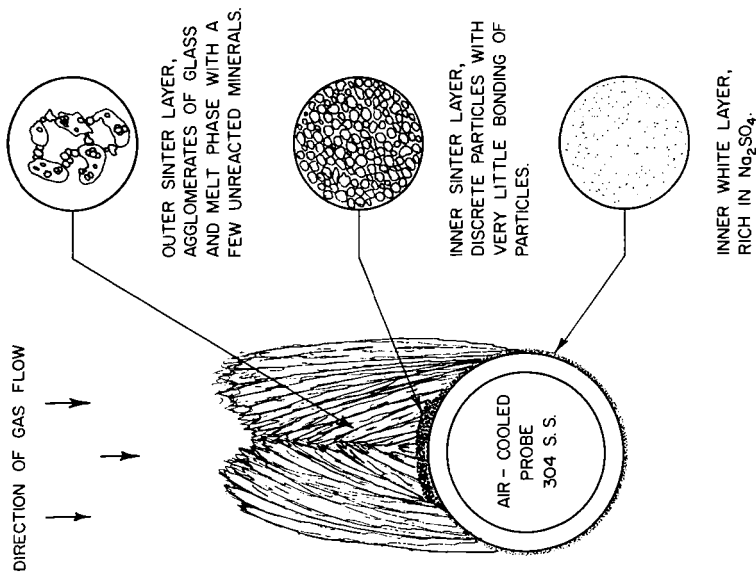


FIGURE 2. - Physical structure of a typical ash deposit formed in the GFEC combustor.

air-cooled probe maintained at 540°C. X-ray diffraction studies have shown that sulfates, mainly Na_2SO_4 and CaSO_4 , predominate near the probe and in the inner sinter layer. The sulfates are present on the surfaces of the ash particles and in the inner white layer immediately surrounding the probe. The melt and reaction of these surface sulfates to form an intermediate $\text{Na}_2\text{Ca}(\text{SO}_4)_2$ eutectic has been proposed (18,19). Figure 3 illustrates the particle-to-particle bonding which occurs upon the melt and reaction of the various sulfates (16).

A second mechanism involving sodium has been observed: the fluxing action of sodium with aluminosilicate (presumably kaolinitic clay) mineral assemblages. Volatilized sodium is believed to react with kaolin particles in the combustion zone to form low-melting (900-1100°C) sodium aluminum silicate compounds. These species react with the molten sulfates in the deposit to form complex melilites $(\text{Na,Ca,K})_2 [(\text{Mg,Fe}^{+2},\text{Fe}^{+3},\text{Al,Si})_3 \text{O}_7]$. X-ray diffraction studies of deposits from the GFETC combustor have shown that melilite formation increases as the distance from the probe increases (16).

The physical strength of the deposits has been observed to increase as a result of continued exposure to SO_2 and SO_3 at high temperatures. This phenomenon is referred to as the sulfating process. X-ray diffraction analysis of deposits obtained from the Hoot Lake Power Company, Fergus Falls, Minnesota, has shown that more anhydrite was present than melilites.

Fouling problems in fluidized bed combustors are not expected to be as severe due to the lower combustion temperatures in FBC's (700-950°C) compared with PC-fired or cyclone combustors (1650°C). Scanning electron microscope studies have been made of bed agglomerates from the GFETC pilot plant FBC from a test burning Beulah lignite with Al_2O_3 bed material, and from the pilot scale FBC of Fluidyne Engineering Corporation of Minneapolis, burning Indian Head lignite with an SiO_2 bed. The agglomerations from the GFETC FBC showed thin films of Na_2SO_4 , CaSO_4 , and $\text{Na}_2\text{Ca}(\text{SO}_4)_2$ surrounding a layer of complex silicates (a typical composition is 11% Na_2O , 9% MgO , 21% Al_2O_3 , 11% CaO , 45% SiO_2) with a core which is predominantly Al_2O_3 . No sulfates were observed in the agglomerations from the Fluidyne combustor (17). A calcium-rich coating surrounded a sodium-rich layer which in turn contained core material that was predominantly SiO_2 and Al_2O_3 .

This preliminary evidence suggests that agglomerates form around particles of bed material via reactions with the inorganic materials in the coal or ash, and may react further with SO_2 or SO_3 . Laboratory investigations of the mechanism of agglomerate formation are expected to provide continuing support to FBC research.

Summary

The results presented here exemplify the types of broad-ranging studies, which, it is hoped, will eventually provide an extensive data base on the origin, distribution, characteristics, and process behavior of the major inorganic species in lignites. For example, the hydrogeochemical history of a lignite deposit and the mineralogy of the overburden and underclay play an important role in determining the amount and distribution of sodium in the lignite. That sodium may then have a detrimental effect on the utilization of the lignite-- by contributing to ash fouling - or it may have a beneficial effect-- by reducing slag viscosity in a slagging gasifier. Continued research will allow coal scientists to follow the fate of the inorganic species from the Paleocene epoch to tomorrow's synfuels technology.

REFERENCES

1. Ting, F. T. C. (ed.) Depositional Environments of the Lignite-Bearing Strata in Western North Dakota. ND Geol. Survey Misc. Series 50, 1972.

2. Bluemle, J. P. Surface Geology of North Dakota. ND Geol. Survey Misc. Map 18, 1977.
3. Groenewold, E., L. Hemish, J. Cherry, B. Rehm, G. Meyer, L. Clayton, and L. Winczewski. Geology and Geohydrology of the Knife River Basin and adjacent areas of West-Central North Dakota. ND Geol. Survey Rept. Inv. 64, 1974, 402 pp.
4. Karner, F. R., S. F. White, D. W. Brekke, and H. H. Schobert. Geological Sampling of Lignite Mines in Mercer and Oliver Counties, North Dakota. Manuscript in preparation for publication as USDOE Fossil Energy Report.
5. Karner, F. R., G. Winbourn, S. F. White, and A. K. Gatheridge. Sodium and Calcium and Overburden, Lignite and Underclay at the Beulah and Baukol-Noonan Mines, Mercer and Oliver Counties, North Dakota (abs.): North Dakota Academy of Science Proceedings, vol. 33, pt. 1, 1979, p. 70.
6. Karner, F. R., and F. S. O'Toole. Secondary Pyrite, Barite and Gypsum on Fracture Surfaces in Lignite at the Baukol-Noonan Mine, North Dakota (abs.): North Dakota Academy of Science Proceedings, vol. 33, pt. 1, 1979, p. 71.
7. Ellman, R. C., L. E. Paulson, D. R. Hajicek, and T. G. Towers. Slagging Fixed-Bed Gasification Project Status at the Grand Forks Energy Technology Center. Pres. at the Tenth Biennial Lignite Symposium, sponsored by USDOE and the University of North Dakota, Grand Forks, ND, May 30-31, 1979.
8. Schobert, H. H. Petrochemistry of Coal Ash Slags. 2. Correlation of Viscosity with Composition and Petrographic Class. Division of Fuel Chemistry Preprints 22 (4) 143, 1977.
9. Barth, T. F. W. Theoretical Petrology. John Wiley and Sons, New York, 1962.
10. Vorres, K. S. Melting Behavior of Coal Ash Materials from Coal Ash Composition. Division of Fuel Chemistry Preprints 22 (4) 118, 1977.
11. Ellman, R. C., B. C. Johnson, H. H. Schobert, L. E. Paulson, and M. M. Fegley. Current Status of Studies in Slagging Fixed-Bed Gasification at the Grand Forks Energy Research Center. Technology and Use of Lignite, USDOE Report GFERC/IC-77/1, 1977.
12. Levin, E. M., C. R. Robbins, and H. F. McMurdie. Phase Diagrams for Ceramists. American Ceramic Society, Columbus, 1964.
13. Willson, W. G., C. L. Knudson, G. G. Baker, T. C. Owens, and D. E. Severson. Application of Liquefaction Processes to Low-Rank Coals. Pres. at the Tenth Biennial Lignite Symposium, sponsored by USDOE and the University of North Dakota, Grand Forks, ND, May 30-31, 1979.
14. Gronhovd, G. H., W. Beckering, and P. H. Tufte. Study of Factors Affecting Ash Deposition from Lignite and Other Coals. Pres. at the ASME Winter Annual Meeting, Los Angeles, CA, 1969.
15. Sondreal, E. A., P. H. Tufte, and W. Beckering. Ash Fouling in the Combustion of Low Rank Western U.S. Coals. Combustion Science and Technology, Vol 16, 1977.
16. Rindt, D. K., S. J. Selle, and W. Beckering. Investigations of Ash Fouling Mechanisms for Western Coals Using Microscopic and X-Ray Diffraction

Techniques. To be presented at the ASME Winter Annual Meeting, New York, NY, 1979.

17. Montgomery, G. G. Monthly Progress Report, Analytical Section, Grand Forks Energy Technology Center, U.S. Department of Energy, August 1979.
18. Brown, H. R., R. A. Durie and G. H. Taylor. Factors Influencing the Formation of Fireside Deposits During the Combustion of Morwell Brown Coal, in the Mechanism of Corrosion by Fuel impurities. Johnson and Littler, Butterworths Scientific Publications, London, 1963, p. 469.
19. Procter, N. A. A., and G. H. Taylor. Microscopical Study of Boiler Deposits Formed from Australian Brown Coals. J. Inst. Fuel, Vol. 39, 1966, p. 284.

ANALYSIS OF THE INORGANIC CONSTITUENTS IN AMERICAN LIGNITES

M. E. Morgan, R. G. Jenkins, and P. L. Walker, Jr.

Department of Materials Science and Engineering

The Pennsylvania State University, University Park, PA 16802

INTRODUCTION

The relatively untapped reserves of lignite coals in the western United States have generated a large amount of interest in the past few years. In general, lignites exist in relatively thick seams which are close to the surface. Thus they are amenable to extraction at a low cost. These coals tend to react quite differently in coal conversion processes than coals of higher rank. All of the reasons for this behavior are not well understood. One of the characteristics peculiar to low rank coals is the amount of ion-exchangeable inorganics. These inorganics are usually taken to be cations in association with carboxyl groups. These cations are believed to be responsible for catalysis of gasification, formation of calcite during liquefaction, and the behavior of lignite ash during combustion. However, characterization of this organic-inorganic system has not been satisfactorily accomplished for American lignites.

The research described here was concerned with the characterization of the ion-exchangeable cations and the carboxyl groups with which they are associated for three important deposits of American lignites. This has been accomplished by ion-exchange techniques, utilizing ammonium acetate and barium acetate, respectively. The cations analyzed for were Na, K, Mg, Ca, Sr, and Ba. Also the amounts of the major discrete mineral phases present in the lignites have been determined. This was accomplished by the use of semi-quantitative x-ray diffraction and infrared spectroscopy techniques.

EXPERIMENTAL

The carboxyl group analysis was modeled after that of Schaefer (1,2). Briefly, demineralized coal (3) which has been ground in N_2 to pass 200 mesh is mixed with 1N barium acetate solution at a pH equaling 8.25 to 8.30. The slurry is refluxed in a flask through which purified N_2 is passed to prevent oxidation of the coal and subsequent formation of barium carbonate. After 4 hr, the solution is cooled, the pH recorded, and enough 0.05 N barium hydroxide is added to restore the original pH of the solution. After three 4 hr periods, the slurry is filtered under N_2 and washed with 1N sodium acetate at a pH equaling 8.25 to 8.30. The hydrogen ions released from the exchange are quantified by the total amount of barium hydroxide added to the solution. The exchanged barium is then removed by boiling the coal in 0.2 N perchloric acid for 20 min. The barium released is quantified by emission spectrometry.

The cations were analyzed by extraction of the coal with 1N ammonium acetate as suggested by Miller (4). Using this procedure, the coal is stirred at room temperature in the ammonium acetate solution (pH equals 7.0 to 7.2) for 3 hr. The slurry is then filtered and the coal transferred back to the beaker with fresh ammonium acetate for another 3 hr extraction. This is followed by three more 3 hr extractions, followed by extraction overnight and a final 3 hr period in the morning. Each of the extracts is then analyzed for Na, K, Mg, Ca, Sr, and Ba by emission spectrometry. The use of fresh ammonium acetate is essential to achieve complete exchange since the existence of any cations in the slurry will result in an equilibrium value on the coal.

Characterization of discrete mineral phases present in the low temperature ash (LTA) of the lignites was accomplished by x-ray diffraction and infrared spectroscopy. The procedure for LTA follows that described by Miller (4). Calcite, quartz, and pyrite are analyzed by x-ray diffraction, while kaolinite and anhydrite are analyzed by infrared spectroscopy. Techniques for these analyses are described by Jenkins and Walker (5). It has been shown (4,5) that mineral phases can form in the LTA process when lignites are ashed. That is, cations present fix sulfur, carbon, and oxygen to form carbonates and sulfates. In order to study this phenomenon, mineralogical analyses of both the raw lignites and the ammonium acetate treated lignites were performed.

RESULTS AND DISCUSSION

Table 1 shows the results of the carboxyl group analysis. Each value, calculated from the titration results, represents the average of six to eight runs, with the value of one standard deviation also shown. In order to investigate the accessibility of the carboxyl groups to the reagent, both minus 80 and minus 200 mesh fractions of PSOC 623 were investigated. There was no effect of particle size on the results. Table 1 also shows carboxyl group values calculated using the barium release method for selected runs. Carboxyl group contents are calculated assuming that two carboxyl groups are exchanged with one barium ion. Close agreement of these results supports this assumption and confirms the accuracy of the technique. The choice of three 4 hr refluxes was based on the finding that, in all cases, less than 5% of the carboxyl groups were exchanged in the final 4 hr period. The oxygen contained in the carboxyl groups of these coals accounts for 46% (North Dakota), 37% (Texas), and 42% (Montana) of the oxygen by difference value calculated in the ultimate analysis.

TABLE 1. CARBOXYL CONTENTS OF LIGNITES

PSOC Coal	State	Seam	Carboxyl Content, Mequiv/g DMMF	
			Titration	Ba Released
246	N. Dakota	Hagel	3.13 ± 0.05	3.24
623	Texas	Darco	2.11 ± 0.08	2.22
833	Montana	Fort Union	3.00 ± 0.07	3.07

Table 2 lists concentrations of cations associated with carboxyl groups found on the lignites. The values shown represent the average of four runs and have a precision of ± 3% or better. Calcium and Mg are the predominant cations. However, there are significant variations in concentration of the cations among the coals studied. For these coals, it was estimated that 43% (North Dakota), 44% (Texas), and 60% (Montana) of the total carboxyl groups are associated with the cations listed in Table 2. The basis for the selection of a 27 hr total exchange time is displayed in Figure 1, where the cumulative percentage of the total exchange versus time is plotted for Mg and Ba. Magnesium is essentially totally exchanged in 12-15 hr, while Ba exchange proceeds more slowly to completion. These results confirm the evidence of other investigators (4,6) who show that Ba should be more strongly held than Mg. Among the divalent cations, the ions with smaller hydrated ion radii have been found to be held most strongly.

Since the cations are thought to be active catalytically in gasification and liquefaction processes, it is of interest to estimate the fraction of total surface area covered by the total cations present. Table 3 shows the CO₂ (total) surface

areas calculated from adsorption at 25°C, the surface areas occupied by the carboxyl groups calculated by assuming 7.7 Å² per site or carboxyl group, and the percentages of the CO₂ surface area occupied by the total carboxyl groups and cations associated with carboxyl groups. A significant portion of the CO₂ surface area is covered by the carboxyl groups and by those associated with cations.

TABLE 2. CATION CONTENTS OF LIGNITES ASSOCIATED WITH CARBOXYL GROUPS

PSOC Coal	Cation Concentrations, 10 ⁻⁴ g/g DMMF						
	Mg	Ca	Na	K	Ba	Sr	Total
246	34.4	171	27.8	1.89	6.51	3.30	244.9
623	22.6	129	8.69	3.42	3.36	2.38	169.5
833	59.8	212	10.0	5.30	10.9	3.34	301.3

TABLE 3. SURFACE AREAS OF AND GROUP COVERAGES ON LIGNITES

PSOC Coal	Surface Areas, m ² /g DMMF		Coverage of CO ₂ Surface Area, %	
	CO ₂	Carboxyl	Carboxyl	By Cations
246	200	130	65	28
623	180	78	43	19
833	210	128	61	37

Results of the mineral matter analysis are summarized in Table 4. Each value corresponds to triplicate determinations. In general, a reproducibility of ± 2-4% (absolute) is found. Infrared spectroscopy showed a greater degree of precision than x-ray diffraction, and the larger values are more relatively precise than the smaller ones. The effect of the presence of cations in the raw lignites on the mineral matter analysis is seen. The amount of LTA decreased by up to 50%, when the cations were removed from the lignites prior to ashing. The disappearance of calcite and anhydrite can also be seen. These results show clearly that the yield of LTA produced from raw lignites is enhanced by the formation of sulfates and carbonates. One would predict the existence of other carbonates and sulfates, but their concentrations would be too low to observe by the techniques used.

CONCLUSIONS

- 1) The ion exchange techniques described in this paper to define the carboxyl groups and exchanged cations are relatively precise, simple, and suitable for characterization of American lignites.
- 2) Calcium and Mg are the major cations in the coals studied, but considerable variations in absolute and relative concentrations exist among the cations analyzed.
- 3) The cations and carboxyl groups cover a significant fraction of the CO₂ surface areas of the lignites.
- 4) Up to 50% of the LTA of the raw lignites studied is an artifact of the ashing procedure, which is mainly due to cation fixation of CO₂ and SO₂ to form carbonates

and sulfates.

5) The real significance of this work lies in the ability to correctly characterize the inorganics in lignites. With the information gained by such analyses, effects of inorganics on coal conversion processes and combustion can be more fully understood.

TABLE 4. MINERAL MATTER IN LTA RESIDUES OF LIGNITES

LTA, wt %/g <u>Coal Dry</u>		<u>wt %/g LTA</u>					
		<u>Kaolinite</u>	<u>Quartz</u>	<u>Pyrite</u>	<u>Calcite</u>	<u>Anhydrite</u>	<u>Others</u>
PSOC 246							
Raw	11.5	5	9	nil*	11	21	54
NH ₄ Ac	5.9	8	15	nil	nil	1	76
PSOC 623							
Raw	20.5	41	12	nil	2	14	21
NH ₄ Ac	16.9	41	12	nil	nil	1	46
PSOC 833							
Raw	17.4	20	19	nil	16	10	35
NH ₄ Ac	8.7	41	26	nil	nil	4	29

*minerals detected but in quantities too small to quantify.

ACKNOWLEDGEMENTS

This work was supported by DOE on Contract EX-76-C-01-2030. Mr. Morgan also received support from an ERG Traineeship and an Office of Education Mining and Mineral Fellowship. Professor W. Spackman kindly supplied the coals studied.

REFERENCES

- 1) Schaefer, H. N. S., Fuel, 49, 197 (1970).
- 2) Schaefer, H. N. S., Fuel, 49, 271 (1970).
- 3) Bishop, M. and Ward, D., Fuel, 37, 191 (1958).
- 4) Miller, R., Ph.D. Thesis, The Pennsylvania State University (1978).
- 5) Jenkins, R. G., and Walker, P. L., Jr., in Analytical Methods for Coal and Coal Products, Vol. II (Clarence Karr, Jr., Editor), Academic Press, New York, 1978, pp. 265-292.
- 6) Amphlett, C. B., Inorganic Ion Exchangers, Elsevier Pub. Co., New York, 1964.

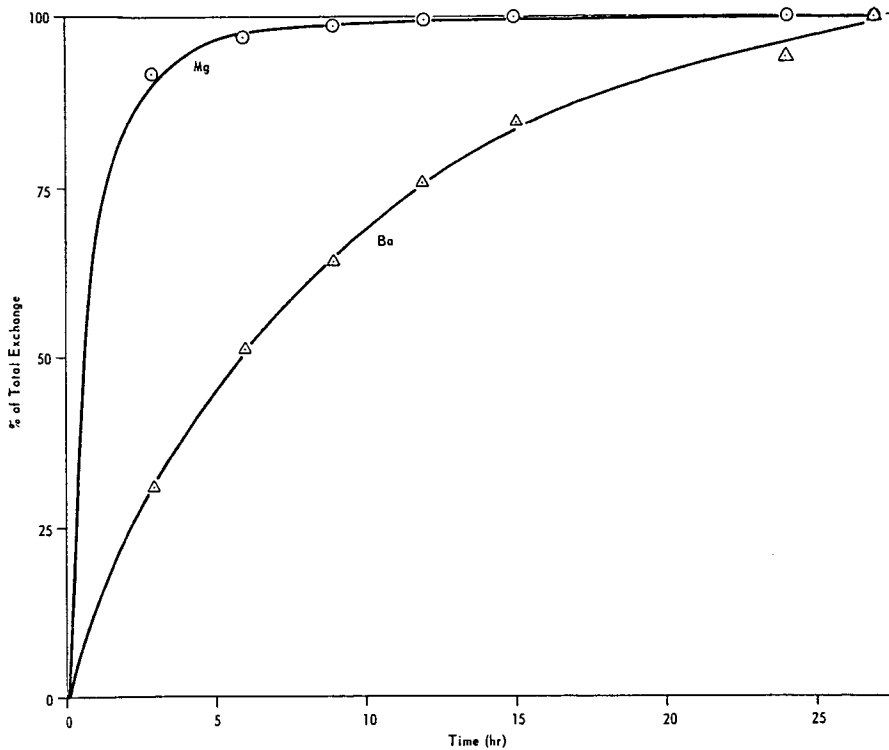


Figure 1. REMOVAL OF CATIONS FROM CARBOXYL GROUPS ON LIGNITE PSOC-246 IN AMMONIUM ACETATE SOLUTION

REMOVAL OF SODIUM FROM LIGNITE BY ION EXCHANGING WITH CALCIUM CHLORIDE SOLUTIONS

L. E. Paulson and J. R. Futch

Grand Forks Energy Technology Center, DOE
Box 8213 University Station
Grand Forks, ND 58202

Lignite resources in North Dakota are estimated at 350 billion tons, comprising 20 percent of the nation's total coal resources on a tonnage basis. Using present technology, 16 billion tons of this lignite is mineable (1). Analyses of over 400 samples of coal taken throughout the region show that the average sodium oxide content is 5.5 percent of the ash (2).

The major use of lignite is as fuel for electric power generation. These large power plants (up to 450 MW) cannot operate efficiently burning high sodium lignite because of fouling of heat transfer surfaces. Field tests and boiler experience have shown that when sodium oxide content in the ash becomes greater than 5 percent, excessive boiler fouling can be expected (3).

Sodium does not occur as in the discrete mineral particles in lignite but is evenly dispersed throughout the coal matrix (4,5). Sodium, along with calcium, magnesium, iron and aluminum cation, is attached to exchange sites on the lignite structure and can be replaced by ion exchange with other elements (6). Combustion tests using lignite in which sodium has been replaced by calcium in ion exchange have shown less fouling than untreated lignite.

This paper presents selected results based on laboratory batch tests in which calcium from calcium chloride solution is used to replace sodium in a high sodium lignite. Test parameters include coal moisture content, particle size, solution concentration, temperature, solid-to-liquid ratio and contact time.

EXPERIMENTAL PROCEDURE

Lignite selected for the tests was from the Beulah mine (North Dakota) and contained 8.7 percent sodium oxide in the ash. Ash analysis, as determined by x-ray fluorescence, is shown in Table 1. Ash content of the coal was 10.8 percent on a dry basis.

Table 1. - Ash Analysis of Test Coal
by X-ray Fluorescents:
(Beulah mine, North Dakota)

<u>Element</u>	<u>Percent</u>
SiO	19.7
Al ₂ O ₃	12.0
Fe ₂ O ₃	7.6
TiO ₂	0.5
P ₂ O ₅	0.3

CaO	19.3
MgO	5.2
Na ₂ O	8.7
K ₂ O	0.7
SO ₃	<u>25.0</u>
TOTAL	99.0

The test coal was crushed to desired size and stored in double plastic bags to minimize moisture loss. The test procedure consisted of combining the desired weight ratio of lignite with calcium chloride solution in a 400 ml beaker and stirring with a propeller-type mixer for the specified length of time. The lignite was separated from solution by filtering with a Buchner funnel using Whatman No. 41 filter paper. The filtrate was analyzed for pH and specific gravity, and the dissolved elements were measured by an inductively coupled argon plasma spectrometer (ICAP). The lignite was rinsed with 200 ml deionized water and filtered. This filtrate was also analyzed. The coal sample was dried and ashed, and the ash analyzed by x-ray fluorescence spectrometry.

RESULTS AND DISCUSSION

Each of the test parameters is discussed individually.

Coal Moisture

The relationship between the extent of sodium removal by ion exchange and lignite moisture content is shown in Figure 1. Moisture reduction was accomplished by air drying the lignite at 25°C. In this set of tests, coal sized to 80 x 0 mesh was contacted with .05 molar calcium chloride solution for 5 minutes. The coal-to-liquid weight ratio was 1 to 4. The moisture content of the coal varied from 34 to 15 percent. Results indicate that reducing the coal moisture to 28 percent had little effect on the rate of exchange. Below 28 percent moisture, the rate of exchange was reduced considerably.

Lignite has a porous structure and the inherent water is believed to be trapped in capillaries (7). Organically bound ions such as sodium may adhere to the surface of the capillaries. In the ion exchange process, calcium diffuses from the solution into the water-filled passages and replaces sodium. Reducing the lignite's moisture content collapses and seals off a portion of the capillary thus reducing ion exchange potential.

Particle Size

The effect of particle size on the rate of ion exchange is shown in Figure 2. In this set of tests, various sized coal was treated with .05 molar CaCl₂ for 5 minutes at solid to liquid weight ratio of 1 to 4. Coal moisture content was 34 percent.

Results show that treating 40 x 0 mesh lignite reduced the sodium content in the lignite by 80 percent, while treating 8 x 0 mesh, at the same test conditions, reduced the sodium by 63 percent. Treating ¼ x 0 inch sized lignite removed only 15 percent of the sodium originally in the coal. The lignite's particle size determines the distance that the exchanging ion must travel through the capillary network and, for that reason, effects the rate and extent of exchange.

Solution Concentration

The sodium content of the treated lignite (dry basis) as a function of starting calcium concentration in solution is shown in Figure 3. The calcium content of lignite resulting from the treatment is also shown. In this series of tests, calcium chloride solution in molar concentration varying from 0 to .2 molarity was mixed with 80 x 0 mesh lignite for 3 minutes. The solid-to-liquid weight ratio was 1 to 5.

Results indicate a direct relationship between solution concentration and sodium removal. The calcium content of the lignite increases proportionally to the decrease in sodium content.

Temperature

The relationship between the temperature of the calcium solution and sodium removal is shown in Figure 4. In this test series, 8 x 0 mesh lignite was treated with .05 molar CaCl_2 solution for 5 minutes. The solid-to-liquid ratio was 1 to 4. The solution temperature was varied from 70 to 145 degrees F. Results indicate that 63 percent of the sodium was removed from the lignite at 70 degrees F., while 72 percent was removed at 120 degrees F. Temperatures higher than 120 degrees F. did not increase the removal efficiency.

Figure 5 shows the moles of sodium removed from the lignite per mole of calcium added as a function of temperature. Under these test conditions, one mole of calcium will replace 1.15 to 1.25 moles of sodium. Under ideal conditions, this ratio should be two sodiums removed for every calcium added. In the present case, other metals in the lignite, such as magnesium or iron, which are also ion exchangeable, may have been replaced, thus reducing the molar ratio of calcium replacing sodium.

Solid-Liquid Weight Ratio

The solid-to-liquid ratio effects sodium removal efficiency as is shown in Figure 6. In this series of tests, lignite sized 8 x 0 mesh was contacted with .05 molar calcium chloride for 5 minutes. The solid-to-liquid weight ratios were 1 to 2, 3 to 8, and 1 to 4.

Results in Figure 6 show that increasing the quantity of liquid (thus increasing the quantity of calcium present) in proportion to solids will increase the sodium removed. The reason is that with higher ratios more calcium is in contact with the coal. Figure 7 shows the ratio of moles of sodium removed to moles of calcium added to the lignite for this set of tests. As shown, the molar quantity of sodium removed to calcium added to the coal varied from 1.25 to 1.35 and compared favorably to that previously shown in Figure 5.

Contact Time

The effect of solid-liquid contact time on sodium removal efficiency is shown in Figure 8. In this series of tests, .05 molar CaCl_2 solution was mixed with 8 x 0 mesh lignite in a weighed solid-to-liquid ratio of 1 to 4. Contact time was 5, 30 and 120 minutes.

Results show that the quantity of sodium removed for this size coal increased with contact time up to 30 minutes. After 30 minutes, there was no significant increase. This indicates that equilibrium under these test conditions with this size limit has been achieved in less than 30 minutes.

SUMMARY

The quantity of sodium removed from lignite by ion exchange with calcium is a function of the coal's moisture content, particle size, quantity of calcium present in solution, solution temperature and contact time. The greatest exchange occurred with lignite containing more than 28 percent moisture and smallest particle size (80 mesh x 0). The rate of exchange increases slightly with temperature to 120°F. The sodium removal is a direct function of solution calcium concentration. Solution concentration and solid-liquid ratio are interdependent variables which determine total quantity of calcium which contacts a unit quantity of lignite.

REFERENCES

1. Wiebner, J. D., "Lignite and North Dakota." *Mining Engineering*, Vol. 29, No. 8 (August, 1977).
2. Cooley, S. A. and R. C. Ellman, "Analysis of Coal and Ash from Lignite and Subbituminous Coals of North Dakota and Eastern Montana," unpublished.
3. Gronhovd, G. H., A. E. Harak, and P. H. Tufte, "Ash Fouling and Air Pollution Studies Using a Pilot Plant Test Furnace," Proceedings of the Symposium on Technology and Use of Lignite, Bureau of Mines - University of North Dakota, Grand Forks, ND, May 1-2, 1969, Comp. by J. L. Elder and W. R. Kube, Bureau of Mines IC 8471, 1970, pp 69-88.
4. Tufte, P. H. and W. Beckering, "A Proposed Mechanism for Ash Fouling Burning Northern Great Plains Lignite," presented at Winter Annual Meeting of American Society of Mechanical Engineers, New York, NY, November 17-22, 1974.
5. Paulson, L. E., W. Beckering, and W. W. Fowkes, "Separation and Identification of Minerals from Northern Great Plains Province Lignite," *Fuel*, Vol. 51, No. 3, July, 1972, pp 224.
6. Paulson, L. E. and W. W. Fowkes, "Changes in Ash Composition of North Dakota Lignite Treated by Ion Exchange," Bureau of Mines Report of Investigation 7176, September, 1968.
7. Lavine, I., Lignite Occurrence and Properties, Grand Forks, North Dakota, 1939.

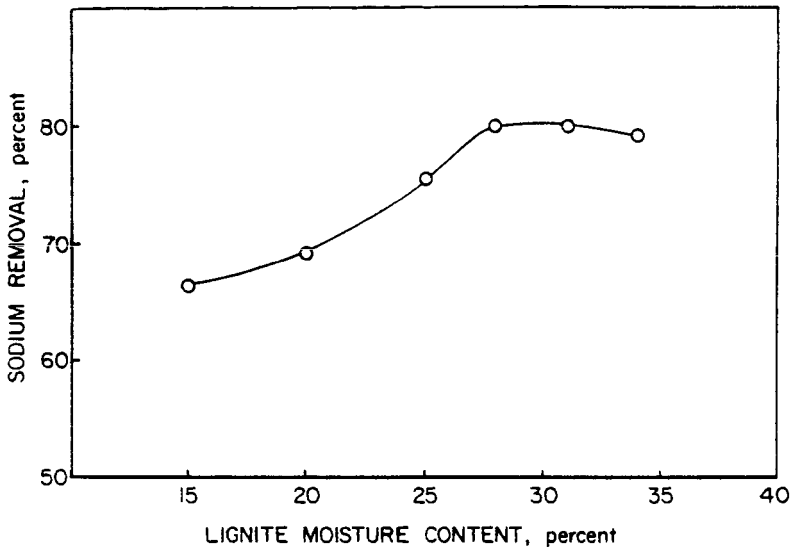


FIGURE 1. - Sodium removal as a function of lignite moisture content.

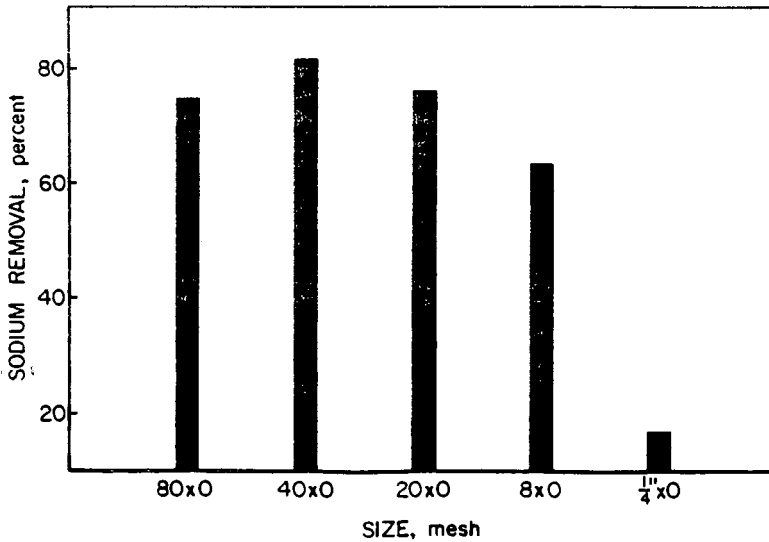


FIGURE 2. - Sodium removal as a function of lignite particle size.

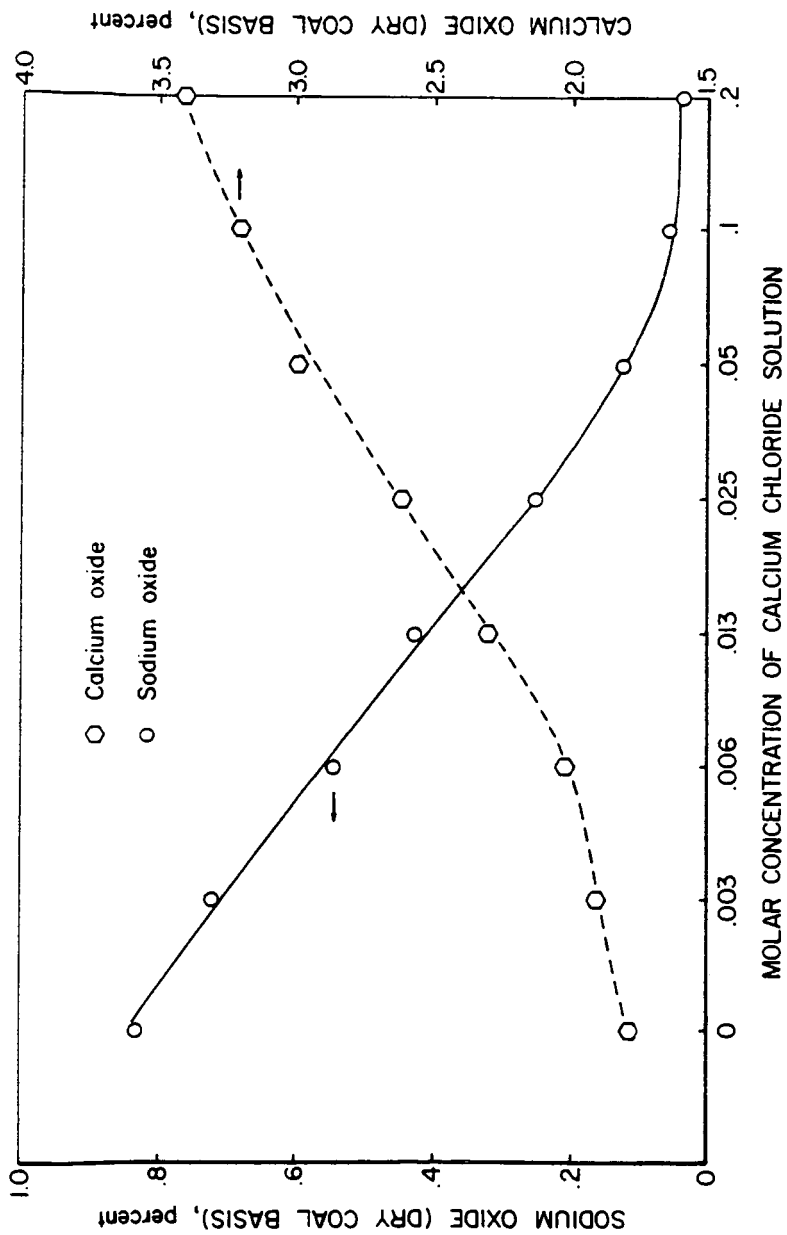


FIGURE 3. - Sodium removal and calcium addition to lignite as a function of calcium chloride solution concentration.

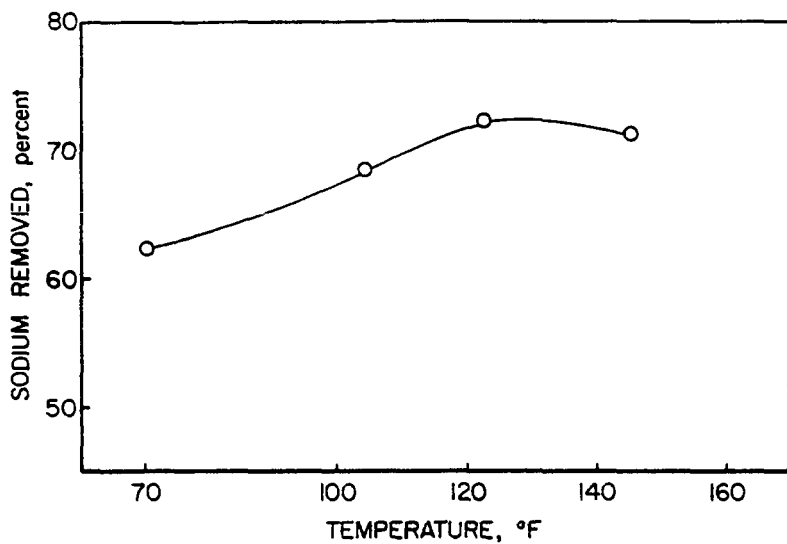


FIGURE 4. - Sodium removal from lignite as a function of temperature of treating solution.

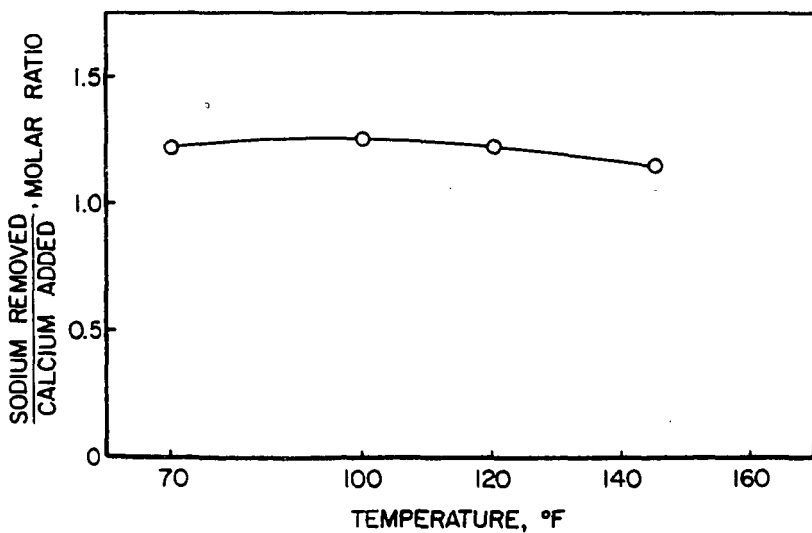


FIGURE 5. - Ratio of sodium removal from lignite to calcium added as a function of solution temperature.

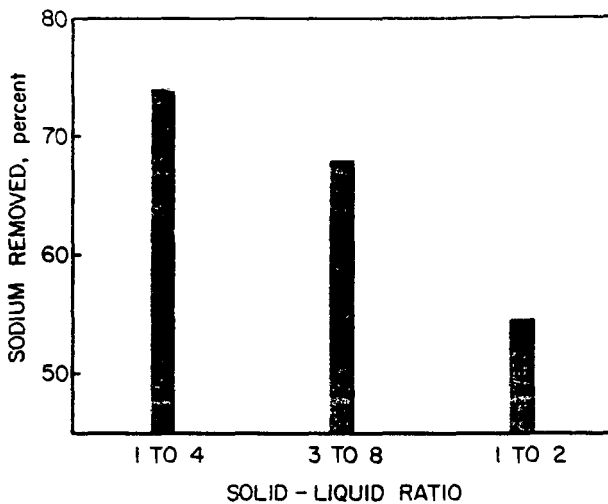


FIGURE 6. - Sodium removal from lignite as a function of solid to liquid ratio.

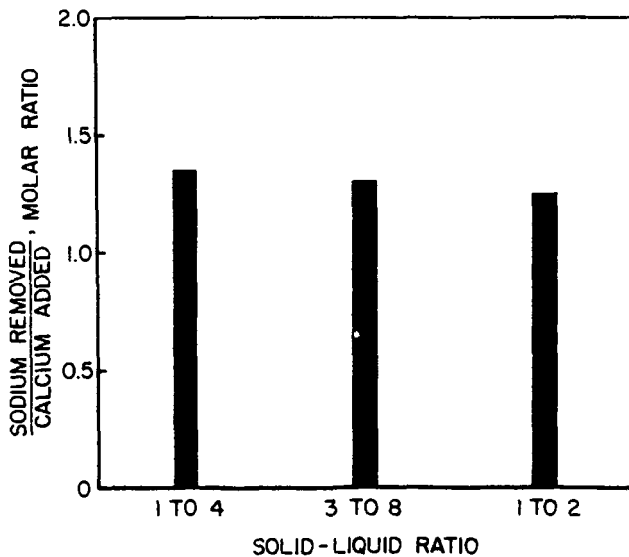


FIGURE 7. - Ratio of sodium removal from the lignite to calcium added as a function of solid to liquid ratio.

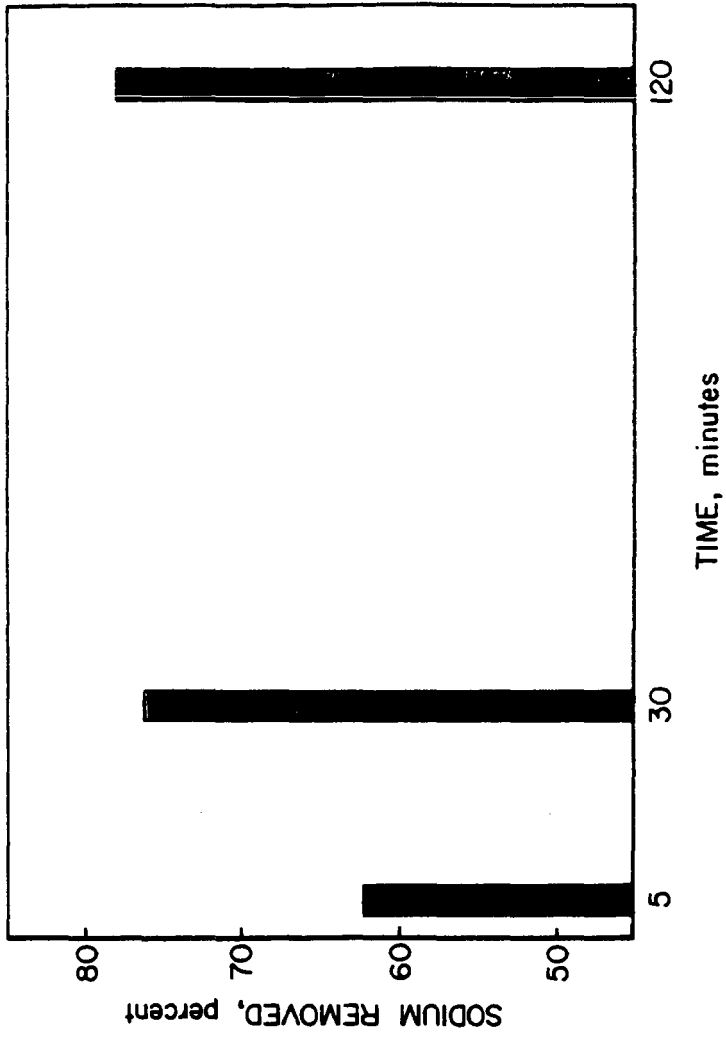


FIGURE 8. - Sodium removal from lignite as a function of solid-liquid contact time.

Laboratory Batch Liquefaction of Low Rank Coals

A.M. Souby, T.C. Owens, D.E. Severson

Department of Chemical Engineering, University of North Dakota

Grand Forks, ND 58202

INTRODUCTION

Laboratory autoclave studies of low rank coals, particularly lignitic coals, have been conducted in the Department of Chemical Engineering at the University of North Dakota over a period of nearly 15 years. Recent research work is focused on providing process support data for the "surviving" liquefaction technologies with particular emphasis on western low rank coals. Early work in the current program was directed to screening several liquefaction solvents. Two solvents were selected for subsequent work; one was a distilled anthracene oil (AOD1 and AOD2) and the second was hydrogenated distilled anthracene oil.

One of the objectives of the research program is to study the effect on liquefaction yields of the identity and quantity of mineral constituents of the coal.

Five North Dakota lignites (Beulah, Gascoyne, Zap, Larson, and Velva), three Montana or Wyoming subbituminous coals (Absaloka, Wyodak, and Decker), and a single Alaska subbituminous coal (Usibelli) were investigated. Analyses of the coals and of the coal ashes are given in Tables 1 and 2, respectively. The elements often considered to be important in liquefaction are iron, calcium, magnesium, sodium, potassium, and sulfur. There is a considerable body of opinion that the various forms of iron sulfides are the primary catalysts in liquefaction. Tables 1 and 2 show that the high ash lignite (BEU 3) and subbituminous (ABS 1) are also high in both iron and sulfur, while the calcium and magnesium contents are in the range of the other coals. The sodium level is relatively high for the Beulah (BEU 3) and Zap lignites, and for the Absaloka coal when it is compared with the other subbituminous coals.

PRODUCT AND SLURRY ANALYSES

Analyses of liquefaction solvent and of reaction products are largely physical in nature. Solvent and slurry are characterized by vacuum distillation (ASTM-D-1160) and by dissolution of the undistillable portion in tetrahydrofuran (THF). Slurry material not soluble in THF was considered to be unconverted lignite or ash, and the ash was determined independently.

Three distillate fractions were determined in the vacuum (5 torr) distillation. These were the initial boiling point (IBP) to 120°C - light oil; 120°C to 260°C - middle oil; and the fraction distilled above 260°C - heavy oil. The THF soluble, but nondistillable, portion of the product slurry was called soluble residuum. Condensable vapors that were discharged with the reactor gases were collected in cold traps and are also considered to be light oils. It will be noted that the solvents consist primarily of material in the middle oil range. For purposes of data reduction it was assumed the ash was unchanged during the reaction.

EXPERIMENTAL RESULTS

Cold Charge Autoclave

In cold charge autoclave experiments, solvent, lignite, and gas (nominally

an equimolar mixture of CO and H₂) were charged to the autoclave. The autoclave was heated to the desired reaction temperature at the rate of approximately 3°C/minute. When the maximum temperature was reached the power was immediately shut off. Reactor gases were discharged through cold traps when the reactor temperature dropped to 400 F.

Figures 1 and 2 show the effects of maximum reactor temperature on the product distribution when using Velva lignite in the cold charge autoclave. Distilled anthracene oil (AOD 1) was used as the solvent for the runs presented in Figure 1, while hydrogenated anthracene oil (HAD 29) was the solvent for the data shown in Figure 2. As the temperature exceeds 420°C, the yields of gas and light oil increase, while the heavier distillate yields decrease dramatically and the overall conversion is unchanged or slightly diminished. This indicates that heavier products (soluble residuum and heavier distillates) are converted to lighter products, but some of the solvent or products are polymerized, coked, or charred and thus rendered insoluble in THF. Figures 3 and 4 show the results obtained when using Absaloka subbituminous coal at the same temperatures and with the same solvents. The same general observations can be made although there are some differences apparent between the lignite and the subbituminous coal. The results for the various products of the two types of coal are shown in Figure 5 through Figure 10.

Figure 5 shows that the yield of soluble residuum is high at the lower temperatures, but decreases with increasing temperature for the Absaloka coal, while the soluble residuum yield reaches a maximum at about 420°C for Velva lignite. Additionally, the overall conversion of Absaloka coal is largely unaffected by reaction temperature, but the conversion increases from 69 percent to 89 percent when reaction temperature is raised from 380°C to 420°C for the lignite. Differences in the yields of THF soluble product and of distillate show a greater effect of reaction temperature for the lignite than for the subbituminous coal (Figure 6). The yields of the components of the distillate products follow similar trends although the yield of the middle and heavy oil fraction shows greater variation with temperature changes for the lignite coal (Figure 7).

Figures 8, 9, and 10 show the same general trends when hydrogenated anthracene oil (HAD 29) was the solvent and the same two coals were used.

The highest distillate yield obtained was with Zap lignite using the distilled anthracene oil solvent (AOD 1), while the Larson and Beulah lignites showed the lowest distillate yields. The overall conversion was also highest for Zap lignite. Changing to the hydrogenated solvent (HAD 29) caused a decrease in distillate yield for Beulah lignite, while the yield of gas increased. Overall conversion increased slightly, and the yield of soluble residuum was nearly constant. It appears that distillate (including solvent) was converted to lighter products while other products were unaffected. For the Larson and Velva lignites, the distillate and gas yields and the overall conversion increased, and the yield of soluble residuum decreased.

Comparing the conversion and product yields when using the anthracene oil solvent (AOD 1) for North Dakota lignites and for the subbituminous coals show that the conversion of lignite is generally higher. Correspondingly, the distillate yields are higher for lignite. Changing to the hydrogenated solvent (HAD 29) caused the conversion for the subbituminous coals to increase noticeably; the conversion of lignite increased, but to a lesser extent. Thus, it appears that the presence of a solvent containing greater amounts of hydrogen has a greater effect on the higher rank (subbituminous) coal.

Although the coal screening work has not been completed, results obtained so far do not seem to indicate a positive relation between ash content of the feed coal and overall conversion or production of distillate product. More work will be done

in looking at the effects of the various ash constituents on conversion and yields.

Hot Charge Autoclave

Gas (equimolar CO/H₂ mixture) and the solvent/coal slurry were charged to the hot one-gallon autoclave, and periodic samples of both reactor gas and slurry were taken during a run. The same lignites and subbituminous coals and the same solvents were studied. Nominal temperatures were 420°C and 460°C.

Recovery of products on the hot charge system ranged from 88.0 to 96.5 percent, with closure generally in the 92 to 95 percent range. Failures in the runs were generally caused by plugging in the slurry sampling system. In some of the runs, the time samples exhausted the product slurry, so that no end-of-run results were obtained. In other runs, the sampling system plugged so that all of the time samples were not obtained, but end-of-run results could be determined. It is interesting to note that with Decker subbituminous coal and hydrogenated solvent the sampling system plugged each time a run was attempted. However, some end-of-run results were obtained.

The end-of-run data for Beulah, Velve, Larson, and Gascoyne lignites and for Wyodak and Absaloka subbituminous coals are shown in Figures 11 and 12, where yields of distillable oil, soluble residuum, and unconverted coal are plotted against temperature over the range 420° to 460°C. The most obvious difference is the much higher conversion (lower yield of unconverted coal) and much higher yields of distillable oil realized with the hydrogenated solvent HAD 20 as compared with the unhydrogenated anthracene oil, AOD 1 or 2. When comparing results with the different coals, first with the hydrogenated and then with the unhydrogenated solvents, there appears to be little significant difference between any of them. However, the data from the slurry time samples show some differences between lignites and between the two subbituminous coals.

The results of the slurry time sample data were calculated on an MAF coal basis on the assumption that the ash content of the slurry sample is the same as the total ash in the coal charged (this is the so-called "ash-conversion"). This is not strictly accurate, but information on trends was obtained by cross-averaging the data for the three lignites and for the two subbituminous coals for each solvent at each of the two temperatures.

The averaged data are plotted in Figure 13 for the lignites and in Figure 14 for the subbituminous coals. At the lower temperature of 420°C with both solvents and both coals, total conversion (THF solubles and lighter) increases with time, whereas the conversion to distillates and lighter decreases slightly with time. There appears to be no significant difference, considering the scatter of the data, between the lignites and the subbituminous coals. At the higher temperature of 460°C, with the unhydrogenated solvent, total conversion is initially high with the lignites and then decreases, whereas with the subbituminous coals it increases to a maximum and then decreases with time. With the hydrogenated solvent, conversion of the lignites increases with time, whereas conversion of the subbituminous coals is initially high and remains high. The apparent decreasing conversion is the result of repolymerization or condensation reactions to produce THF insolubles occurring to a greater extent than the solubilization reactions.

Here again, future work will be concerned with the effects of the mineral matter constituents on conversion and yield distribution.

TABLE 1
ANALYSES OF COALS

Mine	S. Beulah	Peerless	Moontan	Velva	Indianhead	Woodak	Absaloka	Decker No. 1	Usibelli
Town	Beulah	Gascoyne	Larson	Velva	Zap	Gillette	Sarpy Creek	Decker	Usibelli
County	Mercer	Bowman	Burke	Ward	Mercer	Campbell	Big Horn	Big Horn	(Nenana Dist.)
State	N. Dak.	N. Dak.	N. Dak.	N. Dak.	N. Dak.	Wyoming	Montana	Montana	Alaska
Abbreviation I. D.	Beu 2	Gas 1	Lar 1	Vel 1	Zap 1	Wyo 1	Abs 1	Dec 1	Usi 1
Grand Forks No.	77-0712	78-4555	78-4867	78-4866	78-4868	78-4467	78-4557	78-4558	
Sample Date	2/77	10/78	11/78	11/78	11/78	7/78	10/78	10/78	
Bin No.	3518	3528	3499	3514	3519	3500	3527	3530	Drum
<u>Proximate Analysis</u>									
<u>As Received</u>									
Ash, Wt %	7.05	7.90	6.71	5.69	8.10	5.82	16.01	4.41	8.03
Moisture, Wt %	25.59	27.81	29.68	32.30	27.19	25.91	19.70	21.05	23.66
Volatile Matter, Wt %	39.47	32.96	31.37	32.94	37.75	38.63	28.94	34.45	
Fixed Carbon, Wt %	27.89	31.33	32.24	29.07	26.96	29.64	35.35	40.09	
Heating Value, Btu/lb	7515	7859	7833	7415	8154	8743	8314	9772	8006
<u>MF Basis</u>									
Ash, Wt %	9.47	10.94	9.54	8.40	11.12	7.86	19.94	5.59	10.52
Heating Value, Btu/lb	10100	10886	11139	10953	11199	11800	10354	12378	10492
<u>Ultimate Analysis</u>									
<u>MAF Basis</u>									
Carbon, Wt %	72.74	65.44	60.81	72.27	68.12		73.84		
Hydrogen, Wt %	5.78	5.14	5.65	4.29	4.29		4.45		
Nitrogen, Wt %	0.66	0.76	0.93	1.14	1.14		0.98		
Sulfur, Wt %	1.05	1.74	0.38	0.63	1.13		0.93		
Oxygen, Wt % (by difference)	20.97	26.92	32.73	21.47	25.32		19.80		
Heating Value, Btu/lb	11157	12223	12314	11957	12807		12933	13111	11726
H/C Ratio	0.96	0.94	1.11	0.76	0.76		0.72		

TABLE 2
ANALYSES OF COAL ASHES

Mine	S. Beulah	S. Beulah	Peerless	Noonan	Veiva	Indianhead	Wyotak	Abasioka	Decker No. 1	Usibelli
Town	Beulah	Beulah	Gascoyne	Larson	Veiva	Zap	Gillette	Sarpy Creek	Decker	Usibelli
County	Mercer	Mercer	Bowman	Burke	Ward	Mercer	Campbell	Big Horn	Big Horn	(Nenana Dist.)
State	N. Dak.	N. Dak.	N. Dak.	N. Dak.	N. Dak.	N. Dak.	Wyoming	Montana	Montana	Alaska
Abbreviation I.D.	Beu 2	Beu 3	Gas 1	Lar 1	Vel 1	Zap 1	Wyo 1	Abus 1	Dec 1	Usi 1
Grand Forks No.	77-0712	78-4356	78-4355	78-4867	78-4866	78-4868	78-4467	78-4357	78-4558	
Sample Date	2/77	10/78	10/78	11/78	11/78	11/78	7/78	10/78	10/78	10/78
Bin No.		3518	3528	3499	3514	3519	3500	3527	3530	Drum
Ash Content, Mt %	7.18	13.44	7.49	6.60	5.15	8.56	5.76	15.51	4.32	6.15
As Received	10.02	19.95	13.09	9.76	8.25	13.41	8.23	19.72	5.55	27.80
Dry Basis										
Ash Composition										
Oxides as Mt % of Ash										
SiO ₂	6.7	27.6	29.8	31.8	19.6	26.2	33.8	45.9	24.9	31.9
Al ₂ O ₃	40.9	14.0	19.4	18.5	12.7	10.7	16.7	21.9	19.5	17.5
Fe ₂ O ₃	18.4	14.2	2.0	5.0	5.8	14.0	5.1	11.3	11.9	7.7
TiO ₂	0.2	0.6	0.9	0.9	0.4	0.5	1.0	0.8	1.2	0.8
P ₂ O ₅	0.2	0.2	0.2	0.4	0.6	0.4	1.4	0.1	1.7	1.4
CaO	12.1	14.5	22.9	23.2	36.0	16.0	22.5	7.5	15.1	28.3
MgO	3.3	3.9	6.9	6.3	10.2	4.9	6.5	1.7	2.9	4.8
Na ₂ O	2.8	5.5	3.3	3.5	2.1	8.0	1.8	2.9	6.5	0
K ₂ O	0.1	0.4	0.2	0.4	0.3	0.9	0.3	0.9	0.4	1.0
SO ₃	15.3	19.1	14.4	10.0	12.3	18.4	10.9	7.0	15.9	6.6
Metals as Mt % of MF Coal										
Si	0.31	2.57	1.82	1.45	0.76	1.64	1.50	4.22	0.65	1.27
Al	2.17	1.47	1.34	0.96	0.55	0.76	0.73	2.29	0.57	0.79
Fe	1.29	1.96	0.18	0.34	0.33	1.32	0.29	1.56	0.46	0.46
Ti	0.01	0.07	0.07	0.05	0.02	0.04	0.05	0.09	0.04	0.04
P	0.01	0.02	0.01	0.02	0.02	0.02	0.05	0.01	0.04	0.05
Ca	0.86	2.06	2.14	1.62	2.12	1.53	1.32	1.06	0.60	1.72
Mg	0.20	0.47	0.54	0.37	0.50	0.39	0.32	0.20	0.10	0.25
Na	0.21	0.82	0.32	0.25	0.13	0.79	0.11	0.43	0.27	0
K	0.01	0.02	0.02	0.03	0.02	0.09	0.02	0.14	0.02	0.07
S	0.61	1.52	0.75	0.39	0.41	0.99	0.36	0.55	0.35	0.22

Figure 1
 Liquefaction of Valva Lignite with Distilled
 Crowley Chilled Anthracene Oil (ACD 1) 50/50
 H_2/CO 3200 - 4000 psig

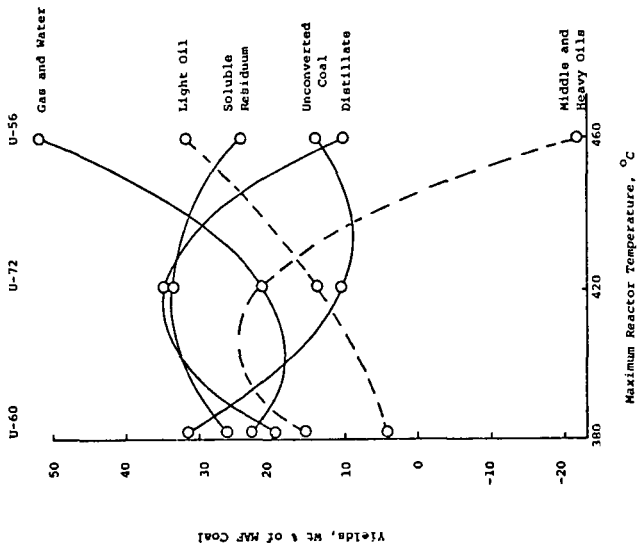


Figure 2
 Liquefaction of Valva Lignite with Hydrocracked
 Distilled Crowley Chilled Anthracene Oil (HACD 29)
 H_2/CO 4000 - 4200 psig

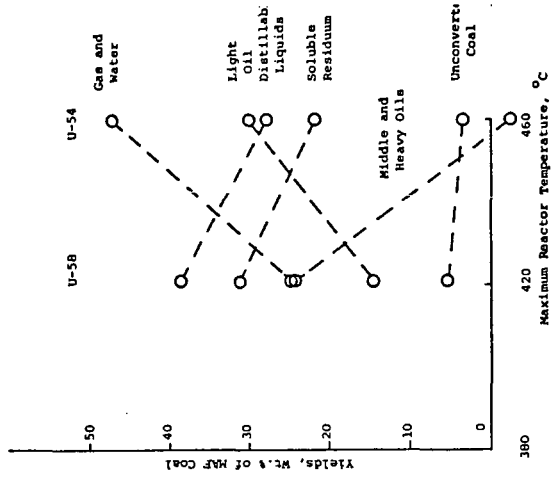


Figure 3

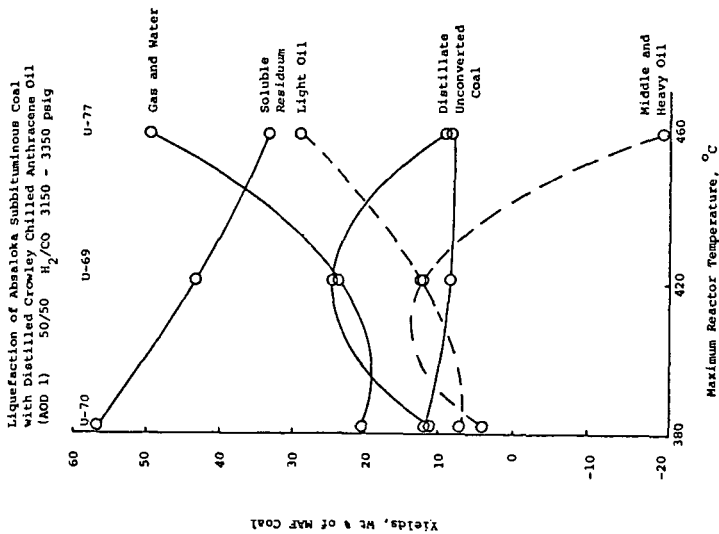


Figure 4

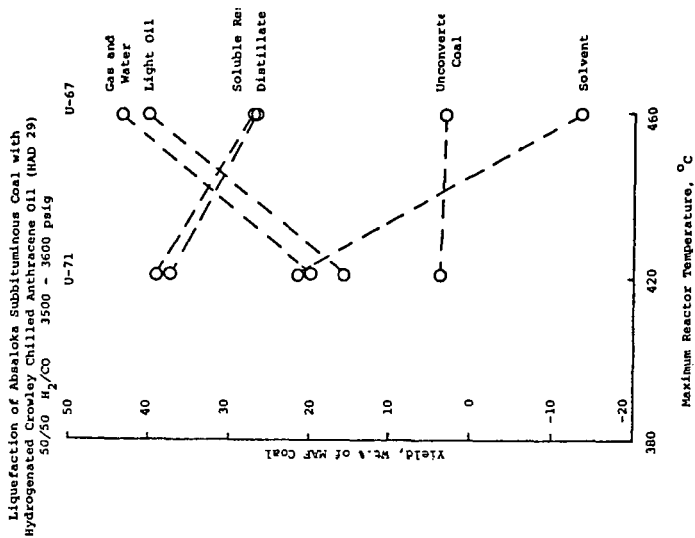


Figure 6

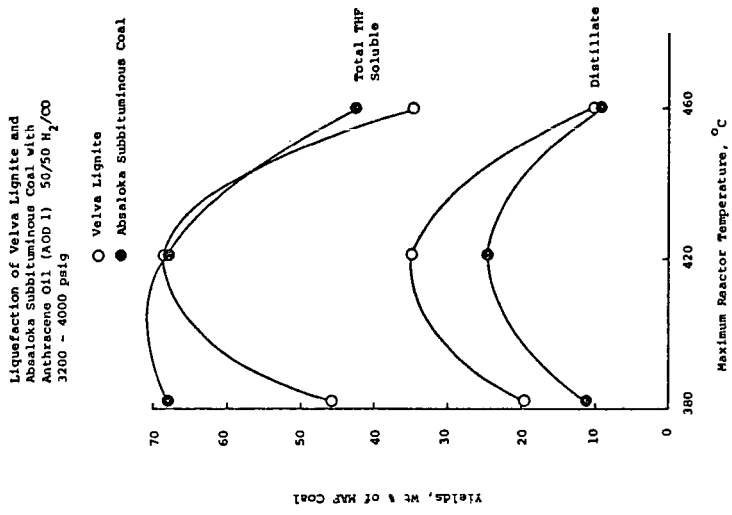


Figure 5

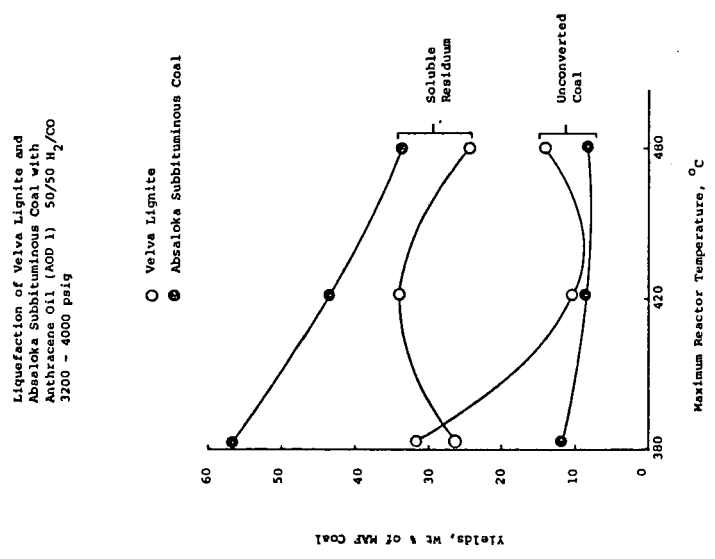


Figure 7
 Liquefaction of Velve Lignite and Absaloka
 Subbituminous Coal with Anthracene Oil (MOD 1)
 50/50 H₂/CO 3200 - 4000 psig

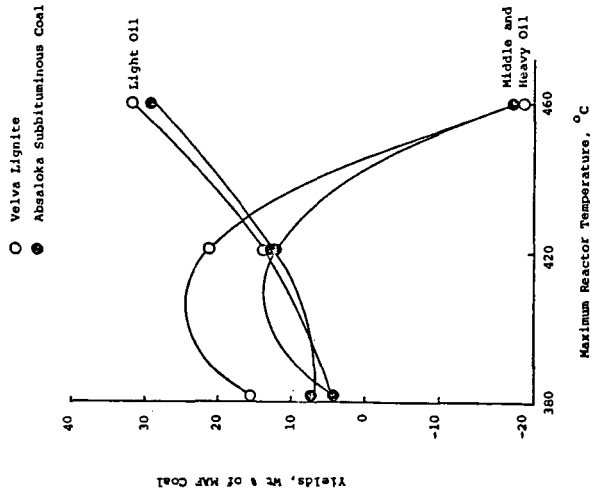


Figure 8
 Liquefaction of Velve Lignite and Absaloka
 Subbituminous Coal with Hydrogenated Anthracene Oil (MOD 29)
 50/50 H₂/CO 3500 - 4200 psig

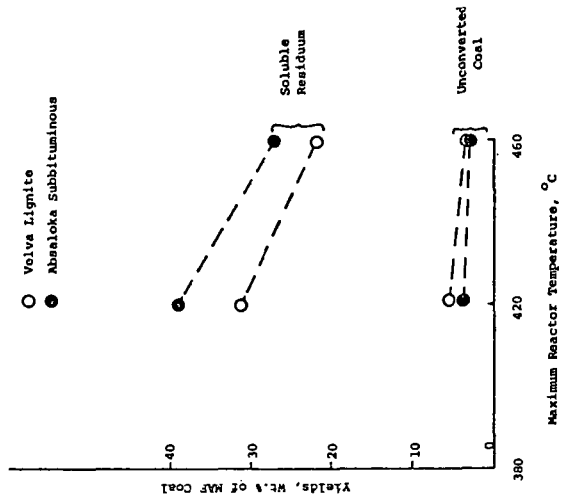


Figure 9

Liquefaction of Velva Lignite and Absaloka Subbituminous Coal with Hydrogenated Anthracene Oil (HAD 29)
 50/50 H_2/CO 3500 - 4200 psig

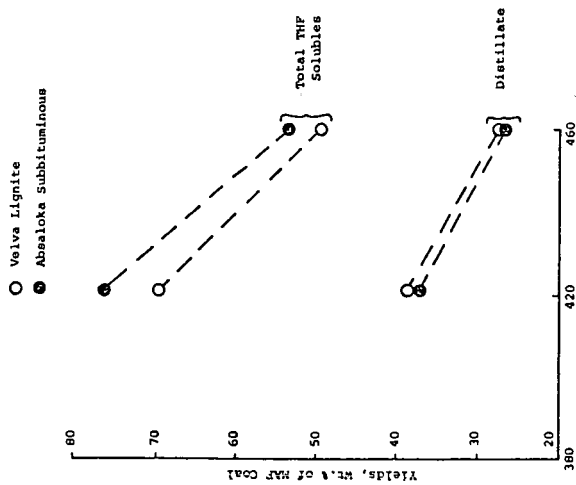


Figure 10

Liquefaction of Velva Lignite and Absaloka Subbituminous Coal with Hydrogenated Anthracene Oil (HAD 29)
 50/50 H_2/CO 3500 - 4200 psig

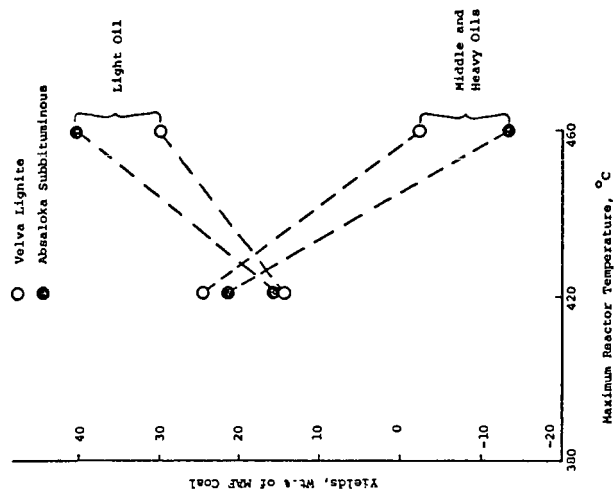


Figure 11

Liquefaction of Beulah, Velva, and Gascoyne Lignites in the Hot Charge Autoclave
End of Run Results

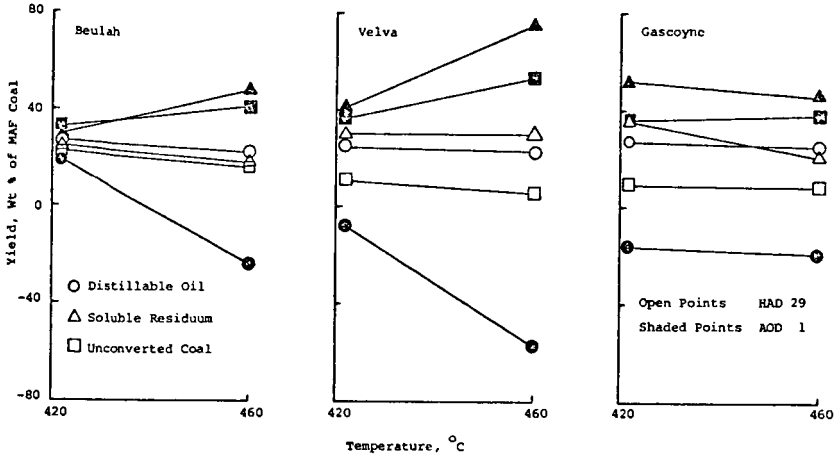


Figure 12

Liquefaction of Larson Lignite and Wyodak and Absaloka Subbituminous Coals in the Hot Charge Autoclave
End-of-Run Results

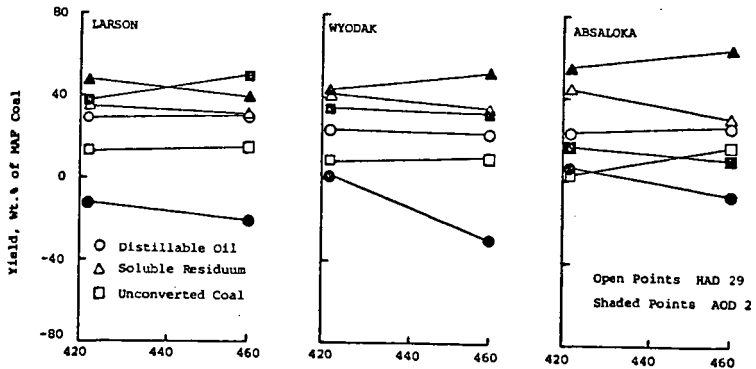


Figure 13

Hot Charge Autoclave Studies with Beulah, Gascoyne, and Valva Lignite, using AOD1 and HAD 29 Solvents at 420 and 460°C. Yields for all coals averaged with each solvent at each temperature.

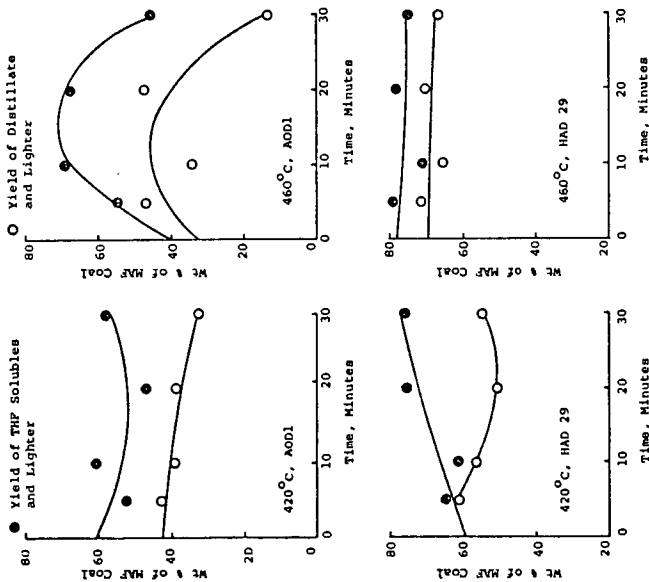
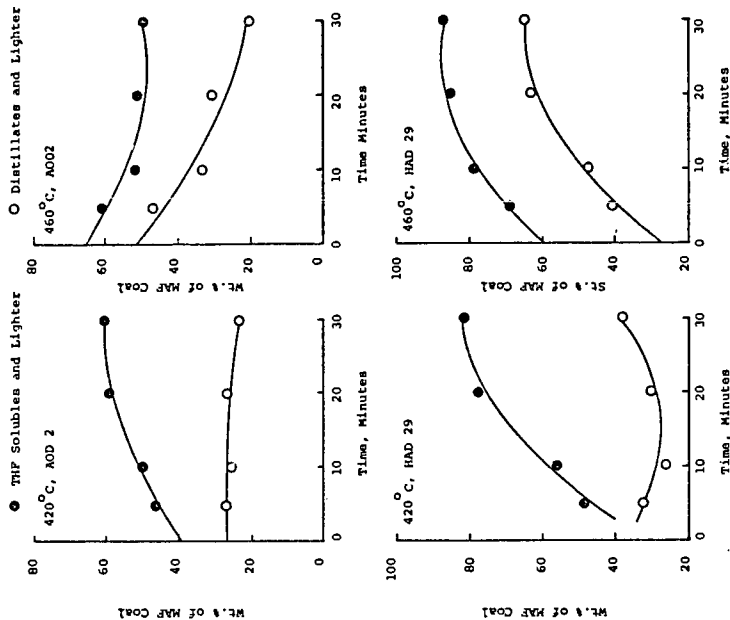


Figure 14

Hot Charge Autoclave Studies with Aberlona and Wyodak Subbituminous Coals using AOD 1 and HAD 29 Solvents at 420 and 460°C. Yields for Both Coals Averaged with Each Solvent at Each Temperature



CHARACTERIZATION OF LIGHT OILS FROM LIQUEFACTION OF LIGNITE

S. A. Farnum, E. S. Olson, B. W. Farnum, and W. G. Willson

Grand Forks Energy Technology Center
U.S. Department of Energy
Box 8213, University Station
Grand Forks, ND 58202

Introduction

Liquefaction of North Dakota Beulah seam lignite (Table 1) was carried out in a 2.3 kg coal/hr continuous processing unit at the Grand Forks Energy Technology Center. The design and engineering details of this unit have been described previously (1). Light oil (BP<300°C @ 27.5 MPa) which accounted for about 19% of the yield calculated on a MAF coal basis was withdrawn at the end of each pass and not added back to the recycle solvent. Slurry was prepared for each recycle pass by adding 30% by weight, pulverized (100% minus 60 mesh) as received (~30% moisture) lignite to the heavy product (BP>300°C @ 27.5 MPa) containing unreacted lignite and ash as well. Slurry feed rate to a 4.55 liter autoclave acting as a continuous stirred tank reactor (CSTR) at 2.3 kg/hr gave a nominal residence time of one hour. CO and H₂ gas (1:1) were added at 14.2 l/min. The pasting solvent for the first pass was redistilled anthracene oil (BP 296°C @ 1.3 Pa). The light oil sample studied was collected on the 24th recycle pass, and represents an essentially lined-out steady state product. A description of the detailed reactor conditions and of the composition of the other products was given by Farnum, Knudson and Koch (2).

Experimental

Separations

The light oil was condensed from the gases after depressurization via two let-down valves into a water cooled product receiver, separate from the heavy product let-down. The water vapor that condensed with the oil was separated in a separatory funnel.

The oil was further fractionated by extraction using the scheme suggested by Fruchter et al. (3) modified by the use of *n*-pentane rather than iso-octane. A flowsheet of the method with the percent recovery of each fraction is given in Figure 1. The number of components determined by capillary GC using a 50-meter OV-101 glass column (Table 2) indicates that the total detectable number of components is less than 277 since there is some overlap between fractions. There are less than 85 components above 1% in this lignite conversion product.

Separations of the four fractions using reverse phase HPLC with a MeOH-H₂O gradient (Altex Model 420) produced major component separations. The light oil was fractionated using the scheme of Dooley et al. (4), yielding fractions including weak acids, phenolics, basics, hydrocarbons and heteroaromatics. Gradient HPLC separation of the weak acids gave approximately 40 peaks; the phenolics, 45 peaks; and the basics, 36 peaks. The hydrocarbon fraction was resolved into 30 compounds. This separation was developed for use as an analytical scale separation technique with automatic fraction collection.

Analyses

Elemental and water analyses of the oil and the four fractions were carried out by combustion (C,H,N,S), Karl Fischer titration (H₂O), and neutron activation and

coulometry (O) (Table 3). The fractions were dried over anhydrous magnesium sulfate before analysis.

Spectroscopy

IR spectroscopic analyses were carried out on thin films of the oils between NaCl disks using a Perkin-Elmer 283* IR spectrometer.

UV studies were conducted using appropriate dilutions of the light oil and its fractions in CH_2Cl_2 . The Perkin-Elmer Hitachi model 340 with Data Handler was used either in the absorbance mode or programmed for the fourth derivative mode.

^1H NMR spectra were taken at 200 MHz with a Varian XL-200. The solutions were diluted 1:8 with CDCl_3 containing 1% of TMS. They were pulsed 25 times at flip angles of 45° or 90° . The integrated areas are shown in Table 4.

^{13}C NMR spectra were also acquired with the Varian XL-200, operating at 50 MHz using the broad band probe. The solutions were 30% oil in CDCl_3 with 1% TMS and 5×10^{-3} M $\text{Cr}(\text{AcAc})_3$. The pulse angle was 60° with 5000 to 15,000 pulses accumulated before integration. The results are presented in Table 5.

Trifluoroacetic Acid - Hydrogen Peroxide Oxidations

A trifluoroacetic acid - hydrogen peroxide oxidation (5) of the light oil was carried out. The resulting acids were derivatized to the *p*-bromophenacyl esters (6) to provide UV absorbance. They were then separated by solvent gradient ($\text{MeOH}-\text{H}_2\text{O}$) reverse phase HPLC and identified by comparison with the same sequence carried out with standards.

Results and Discussion

Basic Fraction

The basic fraction, 5% of the total, is dark in color, with heterocyclic character. The ^1H NMR has several resonance lines between 8.2 and 8.6 ppm as well as a large area between 6.5 and 7.8 ppm indicating pyridines. Some prominent lines between 2 and 3 ppm suggest methyl substituents. The IR contains all of the pyridine - quinoline stretching frequencies and also indicates ring substitution. As was expected, a very broad band appears in the NH , $\text{N}-\text{H}$ stretching region. The richly populated ^{13}C NMR spectrum of this fraction, however, shows a complex mixture of carbon types from 115 ppm to 160 ppm. Pyrroles, if present, are probably substituted since no ^{13}C peak is seen at 106-108 ppm. Indoles are possible.

Phenolic Fraction

The phenolic fraction, 25%, appears to be mainly phenols with cresols and other substituted phenols present in wide variety. Naphthols, if present, are a minor component.

The IR of this fraction, in addition to a broad OH stretching vibration, has a prominent C-H stretching vibration. The other characteristic bands of phenol are all present.

The UV (Figure 2) shows a maximum near 275 nm that is the absorption due to phenols. The fourth derivative UV (Figure 3) is well defined giving a characteristic pattern with a peak corresponding to the absorbance at 275 nm after wavelength correction.

Heteroaromatic Fraction

The ^1H NMR of the heteroaromatic fraction, 22%, (Figure 4b) is dominated by symmetrical multiplets at 7.8 and 7.5 ppm which are characteristic of naphthalene. The ^{13}C NMR (Figure 6a) shows two peaks of similar area at 127.8 and 125.7 ppm with a peak at 133.4, agreeing well with the assumption that unsubstituted naphthalene is present. The IR supports this assumption also in that the spectrum closely resembles that of naphthalene and the methylnaphthalenes with all of the frequencies represented. The weak N-H frequency in the IR along with the nitrogen present in the elemental analyses indicates that carbazoles may be present in this fraction. The ^1H and ^{13}C NMR, UV (Figures 2,3) and IR also suggest the presence of phenanthrenes.

All of the sulfur-containing compounds are present in this fraction (Table 3). Aromatic ethers are also indicated; however, no evidence of aliphatic ethers is seen.

Hydrocarbon Fractions

The hydrocarbon fraction is almost one-half of the light oil by weight. It is apparently a mixture of aliphatic molecules with some aromatic character, probably benzenoid substitution. The material is light in color, does not have an unpleasant odor, and is low boiling. The IR of the hydrocarbon fraction is very simple, dominated by the C-H aliphatic stretching frequencies and the CH_3 and CH_2 bending vibrations at $1465\text{-}1450\text{ cm}^{-1}$ and 1380 cm^{-1} . The major CH_2 rocking vibration appears at 745 cm^{-1} , $(\text{CH}_2)_2$. The aromatic C-C stretching is weakly represented at 1495 cm^{-1} .

The ^1H and ^{13}C NMR (Figure 6b) spectra are the simplest spectra seen for any of the four fractions. The aromatic protons are 15% of the total number of protons with the measured $C_{\text{ar}}/C_{\text{total}} = 0.33$ (Tables 4 and 5).

Unseparated Light Oil 28-14

The fourth derivative UV was used to compare the oil with its separated fractions. The two main UV-absorbing fractions, the phenolic and heteroaromatic fractions (Figure 2), show characteristic fourth derivative fingerprints (Figure 3). This characteristic fine structure of the fourth derivative UV is easily seen in the pattern for the complete light oil LO 28-14. The absorption near 275 nm is the main phenolic band which increases in concert with the increase in phenolic content as line-out is approached. Since the fourth derivative follows Beer's Law, the changes seen as the process proceeds may be quantitatively measured.

IR studies of the CH stretching region in the oil itself along with ^1H NMR are also very useful for monitoring the approach to line-out. The asymptotic approach of the IR ratio to a constant value as a function of recycle passes indicates that a lined-out product was obtained (2).

Trifluoroacetic acid - hydrogen peroxide oxidation of the light oil was carried out. Reverse phase solvent gradient HPLC was used to qualitatively separate the *p*-bromophenacyl esters of the acids formed during the oxidation. The following diacids were inferred from comparison with standards: 2C, 3C, 4C, 5C and 10C. Also seen were acetic, butanoic, pentanoic, cyclohexenecarboxylic and cyclohexylacetic acids.

Summary

The light oil 28-14 was separated into four fractions. The basic fraction was heterocyclic in nature containing most of the nitrogen compounds from the oil. The phenolic fraction was shown to be mostly phenols with naphthols only a minor consti-

tuent. The phenolic fraction is about 25% of the total weight of oil. The hetero-aromatic fraction, 22%, contains few components with more than three rings. It is largely composed of naphthalene and naphthalene derivatives, probably some aromatic ethers, neutral or slightly acidic nitrogen compounds and all of the sulfur compounds. The hydrocarbon fraction is the major fraction, 48%. It has no functionality as the elementary analysis shows no O, N or S. This fraction is aliphatic in nature with some benzenoid substituents.

In addition to the observed yield distribution approaching a constant value, which is one indication of line-out, by monitoring the aromatic to aliphatic proton ratio as a function of recycle pass number with IR or NMR spectrometry, the approach to constant composition can be determined.

Acknowledgement

We would like to express our appreciation to Dr. Warren Reynolds for the capillary GC separations.

* Reference to specific brand names and models is done to facilitate understanding and neither constitutes nor implies endorsement by the Department of Energy.

References

1. Willson, Warrack, G. G. Baker, C. L. Knudson, T. C. Owens, and D. E. Severson. "Applications of Liquefaction Processes to Low Rank Coals", Proceedings of the 1979 Symposium on Technology and Use of Lignite, Grand Forks Energy Technology Center, Grand Forks, ND 58202, May 1979.
2. Farnum, B. W., C. L. Knudson, and D. A. Koch. Am. Chem. Soc., Div. of Fuel Chem. Preprints, 24, (3), 195 1979.
3. Fruchter, J. S., J. C. Laul, M. R. Peterson, P. W. Ryan, and M. E. Turner. Analytical Chemistry of Liquid Fuel Sources, Adv. in Chem. Series 170, Amer. Chem. Soc., Washington, D.C., 1978.
4. Dooley, J. E., C. J. Thompson, and S. E. Scheppele. "Characterizing Syncrudes From Coal" in Analytical Methods for Coal and Coal Products, C. Karr, Jr. Editor, Academic Press, N.Y., 1978.
5. Deno, N.C., B. A. Greigger, and S. G. Stroud. Fuel, 57, 455, 1978.
6. Umeh, E. O.. J. Chromatography, 56, 29, 1971.

TABLE 1. - Analyses of Coal for Beulah 3, North Dakota, Lignite

Basis of reported analysis:	Coal Analysis (GF-79-2147)		
	As-received	Moisture-free	Moisture- and ash-free
Proximate analysis, pct.:			
Moisture	29.48	--	--
Volatile matter	30.21	42.84	50.53
Fixed carbon	29.58	41.94	49.47
Ash	10.73	15.22	--
TOTAL	100.00	100.00	100.00
Ultimate analysis, pct.:			
Hydrogen	6.20	4.15	4.89
Carbon	42.87	60.79	71.71
Nitrogen	0.48	0.68	0.80
Oxygen	37.91	16.59	19.57
Sulfur	1.81	2.57	3.03
Ash	10.73	15.22	--
TOTAL	100.00	100.00	100.00

* An "atypical" Beulah Lignite chosen specifically for its high ash content.

TABLE 2. - Capillary G.C. analysis of LO 28-14 fractions

Fraction	# Components			
	>1%	0.5-1.0%	0.25-0.5%	Total
Basic	12	7	21	48
Phenolic	26	23	10	84
Heteroaromatic	21	18	19	124
Hydrocarbon	26	14	20	121

TABLE 3. - Elemental analysis of light oil 28-14
and its fractions based on LO as 100%

	<u>% C</u>	<u>% H</u>	<u>% O</u>	<u>% N</u>	<u>% S</u>	<u>% H₂O</u>
28-LO-14	84.34	10.69	0.37	3.70	0.22	0.23
Basic	19.94	2.64	0.09	3.35	0.01	--
Phenolic	19.77	2.49	0.25	0.03	0.01	--
Heteroaromatic	22.38	2.21	0.035	0.32	0.20	--
Hydrocarbon	22.26	3.35	0.001	0.00	0.01	--

TABLE 4. - ¹H NMR areas for 28-LO-14
and fractions, CDCl₃, TMS

<u>Fraction</u>	<u>% Har</u> (8.8-5.7 ppm)	<u>% Hα</u> (4-1.9 ppm)	<u>% Ho</u> (1.9-0.3 ppm)	<u>% Hphe</u> (varies)
28-LO-14	23.1	23.0	53.3	--
Basic fraction	34.1	34.1	31.8	(part of Har)
Phenolic fraction	31.3	32.3	25.9	10.5
Heteroaromatic fraction	48.1	29.0	22.5	--
Hydrocarbon fraction	15.3	19.0	65.7	--

TABLE 5. - Integrated ¹³C areas for LO 28-14 and fractions

<u>Fraction</u>	<u>Car/Ctotal</u>	<u>Car/Caliph</u>
LO 28-14	0.45	0.83
Basic fraction	0.56	1.30
Phenolic fraction	0.66	1.93
Heteroaromatic fraction	0.81	4.24
Hydrocarbon	0.33	0.49

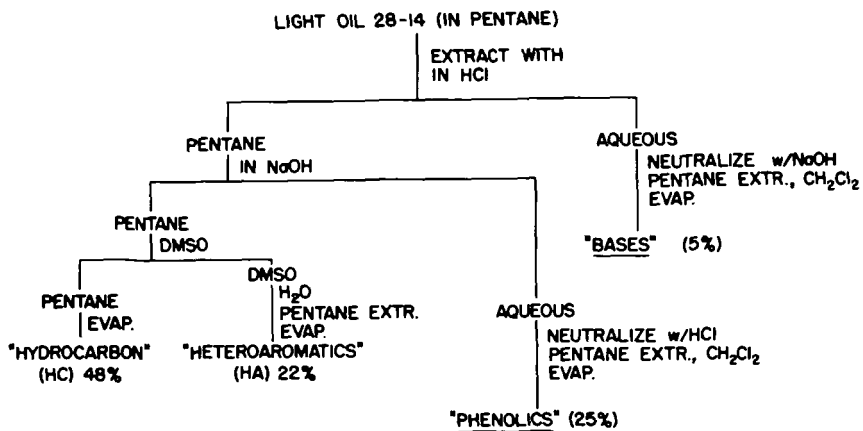


FIGURE 1. - Separation and recovery of the light oil fraction by extraction

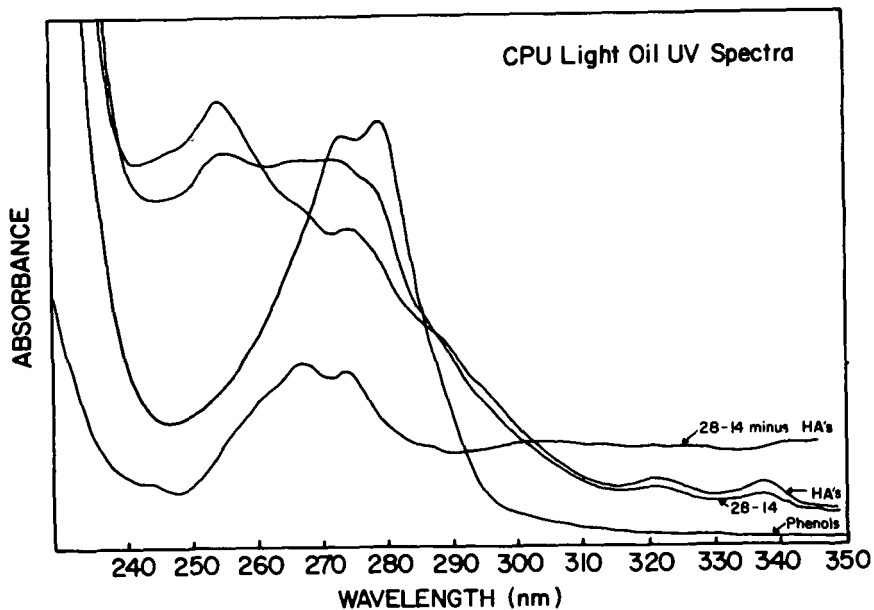


FIGURE 2. - UV spectra of LO 28-14 and fractions

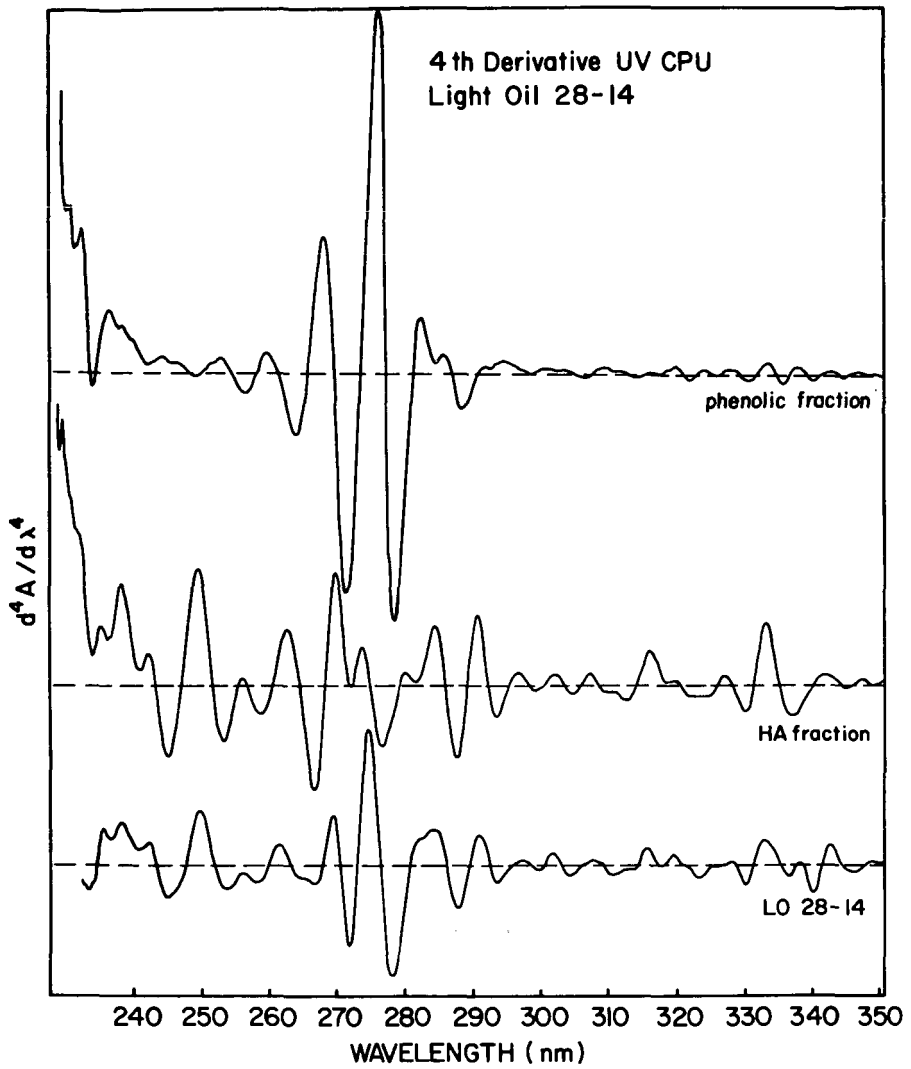


FIGURE 3. - Fourth derivative UV of light oil 28-14 and fractions

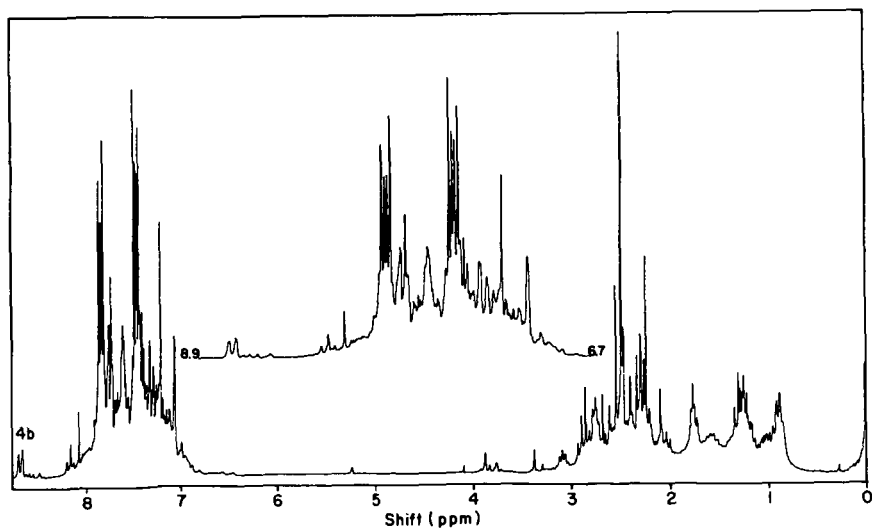
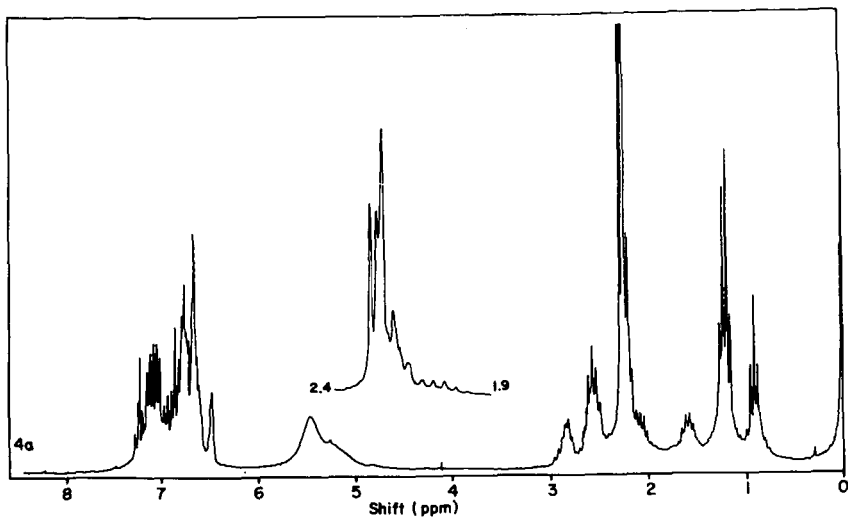


FIGURE 4. - 200 MHz ¹H NMR of light oil 28-14, a) phenolic fraction, b) heteroaromatic fraction

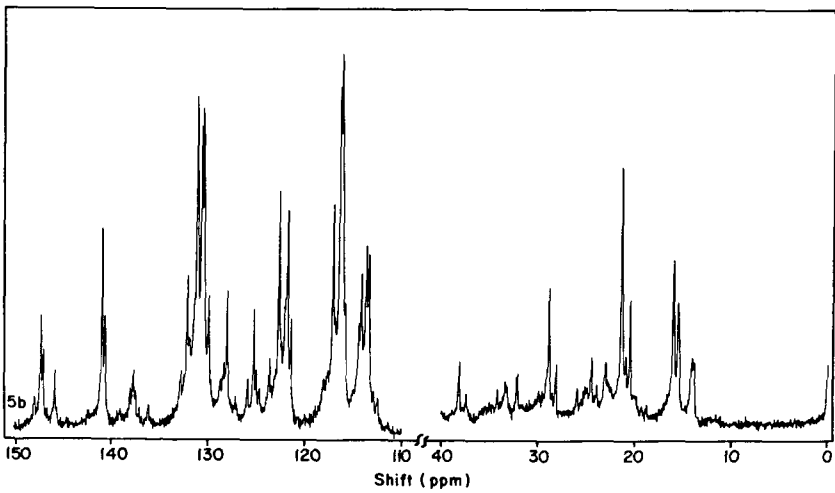
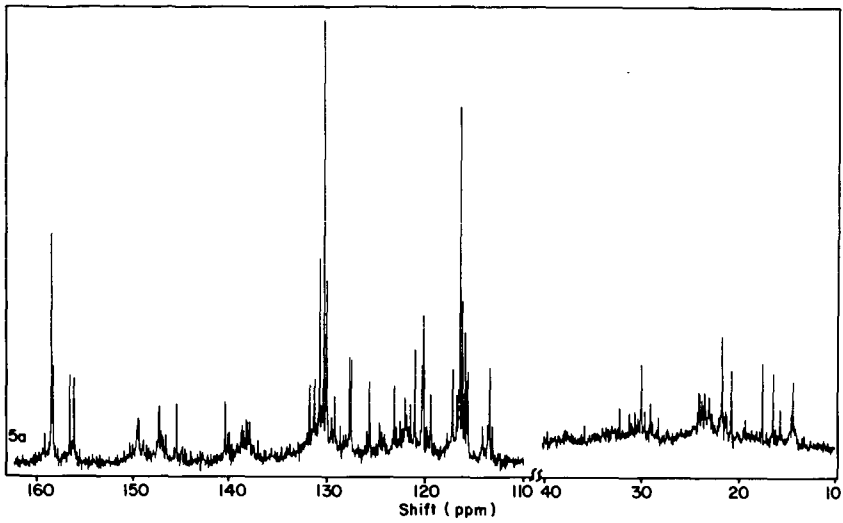


FIGURE 5. - 50 MHz ^{13}C NMR of the aliphatic and aromatic regions of light oil 28-14 (without NOE, $\text{Cr}(\text{AcAc})_3$, CDCl_3), a) basic fraction, b) phenolic fraction

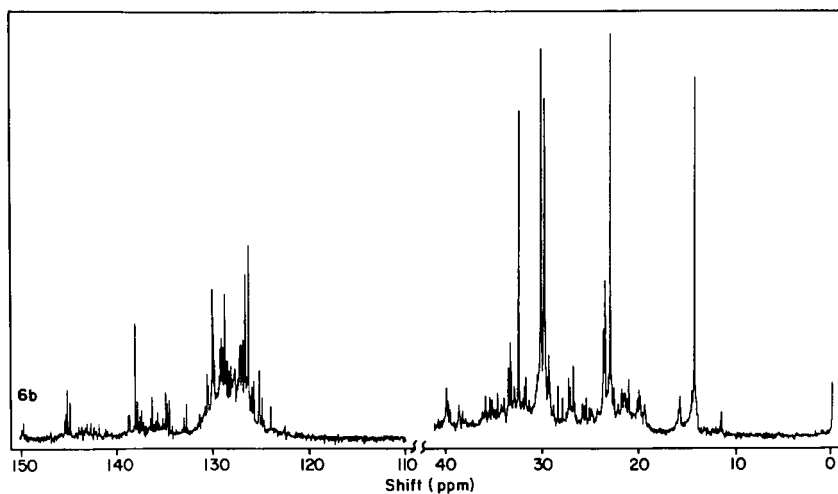
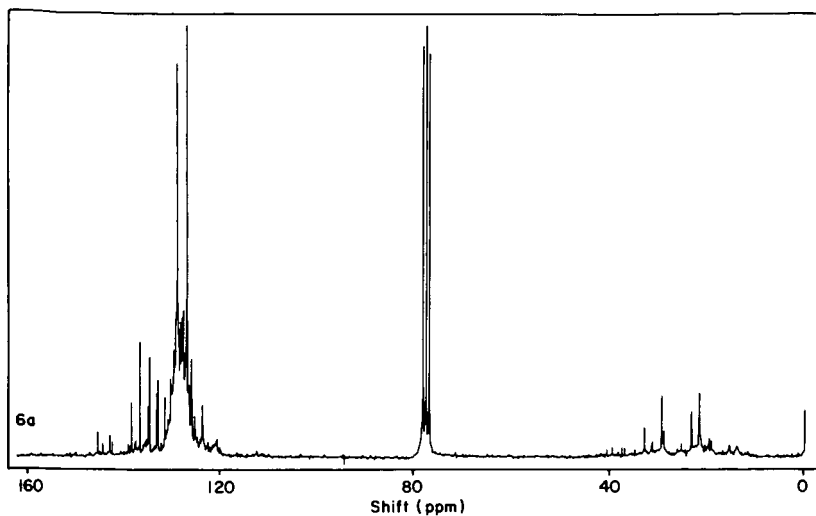


FIGURE 6. - 50 Mz ^{13}C NMR, a) of the heteroaromatic fraction, completely proton decoupled in CDCl_3 , b) aliphatic and aromatic regions of the hydrocarbon fraction (without NOE, $\text{Cr}(\text{AcAc})_3$, CDCl_3), of light oil 28-14

ORGANIC STRUCTURAL STUDIES OF LIGNITE COAL TARS

David J. Miller, Jacquelyn K. Olson, and Harold H. Schobert

Grand Forks Energy Technology Center
U.S. Department of Energy
Box 8213, University Station
Grand Forks, ND 58202

INTRODUCTION

The Grand Forks Energy Technology Center is operating a 900 kg/hr slagging fixed-bed gasification pilot plant. The pilot plant was installed in 1958 and was first operated until 1965 (1). The renewed interest in producing synthetic natural gas and the environmental concerns associated with commercial-scale gasification facilities led to resumption of operations of the Grand Forks gasification pilot plant in 1976. A major objective of the renewed gasification program was to utilize the gasifier to acquire environmental assessment data for a variety of low-rank coals (2). Of particular interest was the identification and characterization of effluents. It has been shown that tar composition can be correlated with the chemical properties of the lignite gasified (3). A detailed understanding of the chemical composition and structure of effluents, such as coal tar, is of two-fold importance. First, such understanding, when coupled with information about reaction conditions such as temperature and partial pressure of hydrogen, provides clues for deducing structural relationships in the lignites. Second, knowledge of the tar composition also provides guidance for designing down-stream effluent treatment or by-product recovery unit operations.

A previous publication (4) presents data on the low-voltage mass spectrometric analysis of nine tar samples, obtained from the gasification of four low-rank coals at a variety of gasification conditions. Extensive statistical analysis of the data, similar to that presented here, showed that the major factors affecting on tar composition are the partial pressure of hydrogen and the residence time of the coal in the gasifier. These results agree with conclusions developed in other laboratories (5). The success obtained in deriving these relationships from the mass spectrometric analyses and the agreement with known behavior of other systems led to the present study in which attention was focused on two tar samples obtained from the gasification of similar lignites under identical conditions. The results reported here are compared with data from other laboratories to suggest relationships between tar composition and possible structural features in the parent lignites.

EXPERIMENTAL

Sample Preparation

Samples of as-received gasifier tar were distilled at reduced pressure to remove water and volatile light oils. Saturate determinations were performed by column chromatographic elution with hexane from neutral alumina. Fractions for high resolution mass spectroscopic analysis were prepared by a method previously described (6).

Mass Spectrometry (HRMS and LVMS)

The instrument used was an AEI MS-30* single-beam high-resolution mass spectrometer interfaced with a DS-50 data system. Approximately 1 mg of gross sample or of column chromatography fractions was introduced into the mass spectrometer using an all-glass heated inlet system operating at 300°C. Source temperature was 300°C, the ion source pressure was $2.0\text{-}2.7 \times 10^{-4}$ Pa and the ionizing

voltage was 70 eV. A medium resolution spectrum (8000-9000 resolving power) was obtained for each fraction and for the gross sample for molecular formula assignment.

Quantitative data was obtained by lowering the ionization potential to 10 eV (7) and decreasing the resolution to 1500. A minimum of six scans are averaged and calibration with known hydrocarbons, oxygen compounds and nitrogen compounds was used to calculate concentrations from the low-voltage intensity data.

Gas Chromatography - Mass Spectrometry (GC-MS)

Materials were analyzed by GC-MS using a Varian 2740 gas chromatograph coupled with a DuPont 21-491B mass spectrometer. A 1.2 m x 2 mm i.d. glass column packed with 3% OV-17 on 80/100 Supelcoport was used for compound separation. The helium carrier gas flow rate was 30 ml/min and the column temperature was programmed from 70-300°C at 6°C/min. GC peak areas were determined using a Spectra Physics System I computing integrator and response factors were measured with appropriate pure standards. The ion source was at 250°C and ionizing voltage was 70 eV.

* Reference to specific brand names or models is done to facilitate understanding and neither constitutes nor implies endorsement by the Department of Energy.

RESULTS AND CONCLUSIONS

The mass spectrometric analysis of tars from the gasification of two North Dakota lignites, Indian Head (IH) and Baukol-Noonan (BN), provide the basis for this study. The as-received proximate analyses of these coals are nearly identical as shown in Table 1. The ultimate analyses, also shown in Table 1, indicate that Indian Head lignite has a much lower carbon/hydrogen atomic ratio than does Baukol-Noonan lignite, 1.2 and 2.3 respectively. However, the maf oxygen and nitrogen content of these coals are nearly identical. The operating conditions for gasification of the two lignites were nearly identical: 2.1 MPa operating pressure, 170 m³/hr oxygen feed rate, 1.0 oxygen/steam molar ratio, and 41 minutes average coal residence time. The two tests from which these samples were obtained are RA-52 (IH) and RA-66 (BN) in the current gasification program. Details of these tests have been published elsewhere (8).

Table 2 gives the low-voltage mass spectrometric carbon number data for the aromatic portion of Indian Head (35%) and Baukol-Noonan (37%) tars. Comparison of the tar analyses indicate several trends. Baukol-Noonan

TABLE 1. - Analyses of coals gasified

	<u>Indian Head</u> <u>lignite</u> Mercer Co Central, ND	<u>Baukol-Noonan</u> <u>lignite</u> Burke Co Northwest, ND
Proximate analyses, % as rec'd		
Moisture	29.1	32.6
Volatile matter	28.0	26.5
Fixed carbon	34.7	34.6
Ash	8.2	6.3

Ultimate analyses, % maf		
H	4.8	2.7
C	70.8	73.7
N	0.9	0.9
S	1.8	0.7
O (by difference)	21.7	22.1

1/ These values do not represent as-mined moisture because of partial drying during storage and handling.

tar contains generally larger amounts of compounds with no substitution and larger amounts of two-, three-, and four-ring compounds. Indian Head tar generally tends to have more one-ring compounds. Table 3 shows some of the comparisons.

Indian Head and Baukol-Noonan tar analyses were compared with data obtained by Hayatsu and co-workers (9). They reported the results of gas chromatographic analysis of the hydrocarbon-rich fraction of 3:1 benzene/methanol extraction of Decker lignite. Their chromatograms identified approximately 25 compounds isolated from the lignite extract. The mass spectrometric analysis of the gasifier tar contains 17 of the same compound types, based on Z number and molecular weight matches. The major difference between the lignite extract and the gasifier tar is that the latter lacks the highly substituted compounds, such as C₁₀ benzenes or C₅ tetralins. This difference is expected when conditions under which the samples were produced are taken into account since it is generally considered that aliphatic side chains are vulnerable to thermal cleavage during coal tar formation (10).

Ranking compounds in gasifier tar by quantity found provides a correlation with published data for the thermal stability of various polynuclear aromatic hydrocarbons. Sharkey and co-workers (11) determined the thermal stability of 20 compounds from the product ratio of the liquid-phase pyrolysis of polynuclear aromatic hydrocarbons. Table 4 shows the comparison between the published thermal stability ranking and quantities observed in Indian Head gasifier tar.

In general, only those compound types that could be identified unambiguously are included in the table. For example, compounds with a Z number of -16 may be fluorenes or acenaphthalenes; and therefore are not included in the table. An exception is 2,6-dimethylnaphthalene (Z= -12, MW=156); although an unambiguous assignment was not made, the 2,6-isomer is reported to be more stable than some other dimethylnaphthalenes (12) and is one of only two isomers reported in low temperature carbonization tar in an extensive compilation (13). The similarity of tar from the GFETC gasifier to that of other low-temperature carbonization processes has been shown previously (14).

Since unequivocal identifications were not made as a part of the study reported here, no attempt was made to correlate these compounds with other data. The Spearman rank correlation (15) found for this ranking was 0.725; a value of this magnitude could occur by chance with less than 0.01 probability.

The tar samples used in this study were chosen from tests at identical gasification conditions to eliminate the effects of operating conditions on tar composition which have been reported previously (16). The major difference between the two lignites, carbon/hydrogen ratio, indicates that Baukol-Noonan has a more aromatic nature than does Indian Head lignite. Thermal cracking of these coals during gasification results in distinctly different tars. Baukol-Noonan lignite produces a more aromatic tar, presumably as a result of the initial loss of smaller aliphatic units during carbonization. An indication of this reaction may be the greater amounts of methane produced during the gasification of Baukol-Noonan lignite as compared to Indian Head lignite (Table 5). It has been shown previously

TABLE 2. - Low Voltage Mass Spectrometric Analysis of the Aromatic Portion of Indian Head and Baukol-Noonan Tars

Probable Structural Type	Z#	Carbon Number																Total	
		6	7	8	9	10	11	12	13	14	15	16	17	18	19	20	21		
Benzenes	-6	0.04	0.17	0.22	0.40	0.00													0.83
		0.02	0.16	0.18	0.33	0.00													
Indanes/Tetralins	-8	0.07	0.71	1.27	1.05	0.69	0.40												4.19
		0.14	0.65	0.94	1.00	0.78	0.48												
Indenes	-10	0.00	0.32	0.00															0.32
		0.05	0.24	0.00															
Naphthalenes	-12	3.00	2.16	1.34	0.98	0.87	0.66	0.46	0.31	0.24									10.03
		0.58	1.23	1.18	1.10	1.17	0.98	0.65	0.45	0.31									
Acenaphthene/Biphenyl	-14	0.83	0.62	0.48	0.37	0.24	0.16	0.11											2.81
		0.92	0.74	0.67	0.49	0.32	0.23	0.15											
Fluorene/Acenaphthalenes	-16	2.01	2.86	0.69	0.43	0.39	0.25	0.21	0.18										7.02
		1.76	3.03	0.92	0.61	0.51	0.36	0.26	0.22										
Phenanthrene/Anthracenes	-18																		4.78
Pyrenes/Fluoranthenes	-22																		2.88
Chrysenes	-24																		0.96
Benzopyrenes	-28																		1.19

Indian Head
Baukol-Noonan

TABLE 3. - Comparison of Indian Head and Baukol-Noonan tars

	<u>Z#</u>	<u>Mass</u>	<u>IH (%)</u>	<u>BN (%)</u>
1 Ring	-6	92	0.2	0.2
		106	0.2	0.2
		120	0.4	0.3
	-8	132	0.7	0.6
		146	1.3	0.9
		160	1.1	1.0
	-10	130	0.3	0.2
2 Ring	-12	128	3.0	0.6
		142	2.2	1.2
		156	1.3	1.2
	-14	154	0.8	0.9
		168	0.6	0.7
		182	0.5	0.6
	-16	152	2.0	1.7
		166	2.8	3.0
		180	0.7	0.9
	3 Ring	-18	178	2.3
192			0.9	1.2
206			0.6	0.9
4 Ring		-22	202	1.8
	216		0.6	0.8
	-24	228	0.6	0.7
		242	0.2	0.3

TABLE 4. - Comparison of thermal stability with
observed quantity in Indian Head tar

<u>Compound</u>	<u>Thermal stability ranking</u>	<u>Quantity observed in Indian Head tar</u>	<u>Rank</u>
Naphthalene	1	3.00	1
Pyrene	2	1.81	3
Chrysene	3	0.59	8
2 - Methylphenanthrene	4	0.91	5
Acenaphthene	5	0.83	6
1 - Phenyl-naphthalene	6	0.47	10
2,6 - Dimethylnaphthalene	7	1.34	4
α - Methyl-naphthalene	8	2.16	2
1,2 - Diphenylethane	9	0.48	9
Dihydroanthracene	10	0.69	7
1 - (o-tolyl) - Naphthalene	11	0.31	11
Indene	12	0.00	13
Indane	13	0.07	12

TABLE 5. - Analyses of hydrocarbons in product gas

<u>Component (%)</u>	<u>IH</u>	<u>BN</u>
CH ₄	5.1	6.0
C ₂ H ₄	0.2	0.2
C ₂ H ₆	0.3	0.3
C ₃ H ₆	0.1	0.1
C ₃ H ₈	0.0	0.0
C ₄ H ₁₀	0.0	0.0
Total HC's	5.7	6.6

(17) by two-sided comparison of the means that the difference is statistically significant at the 95% confidence level. Conversely, Indian Head lignite, a more aliphatic coal, produces a tar consisting of primarily small and highly substituted aromatic compounds. This is possibly due to cleavage of hydro aromatic units in the coal at methylene bridges and reactions with available hydrogen.

The good correlation between the quantities of compounds in Indian Head tar and the thermal stabilities of those compounds indicates that the organic units found in the tar are the survivors of thermal degradation processes in the gasifier. At the same time, however, the relationships between the compound types in the tar and those obtained from mild solvent extraction conditions suggest that the molecular structures in the tar are determined not only by thermal processes but also by structural relationships in the parent lignite.

Since tar structures very likely reflect coal structures, differences in the tar analyses can be related to structural differences in the coals. The development of an understanding of the effect of the molecular frameworks in coal and the likely mechanisms of tar formation will assist in assessing and predicting the chemical nature of such effluents.

REFERENCES

1. Gronhovd, G. H., A. E. Harak, M. M. Fegley, and D. E. Severson. Slagging Fixed-Bed Gasification of North Dakota Lignite at Pressures to 400 psig. U.S. Bureau of Mines RI 7408, 1970.
2. Eilman, R. C., et al. Current Status of Studies in Slagging Fixed-Bed Gasification at the Grand Forks Energy Research Center. Technology and Use of Lignite. U.S. Department of Energy. GFERC/IC-77-1, 1977.
3. Miller, D. J., J. K. Olson, and H. H. Schobert. Mass Spectroscopic Characterization of Tars from the Gasification of Low Rank Coals. Pres. at Annual ACS Meetings, Washington, D.C., 1979. In preparation for publication.
4. Work cited in reference 3.
5. Duncan, D. A., J. L. Beeson, and R. D. Oberle. Research and Development of Rapid Hydrogenation for Coal Conversion to Synthetic Motor Fuels. DOE Report FE-2307-46, 1979.
6. Schiller, J. E., and D. M. Mathiason. Separation Method for Coal-Derived Solids and Heavy Liquids. *Analytical Chemistry* 49 1225, 1977.
7. Johnson, B. H., and T. Aczel. Analysis of Complex Mixtures of Aromatic Compounds by High-Resolution Mass Spectrometry at Low Ionizing Voltages. *Analytical Chemistry* 39 682, 1967.
8. Eilman, R. C., L. E. Paulson, and D. R. Hajicek, Slagging Fixed-Bed Gasification Project Status at the Grand Forks Energy Technology Center. Pres. at the Tenth Biennial Lignite Symposium, Sponsored by U.S. DOE and the University of North Dakota, Grand Forks, ND, May 30-31, 1979.
9. Hayatsu, R. et al. Trapped Organic Compounds and Aromatic Units in Coals. *Fuel* 57 541, 1978.
10. *Chemistry of Coal Utilization*, Suppl. Vol., H. H. Lowry Ed., John Wiley and Sons, Inc., New York, 1963.

11. Sharkey, A. G., Jr., J. L. Schultz, and R. A. Friedel. Mass Spectra of Pyrolyzates of Several Aromatic Structures Identified in Coal Extracts. *Carbon* **4** 365-374, 1966.
12. Fieser, L. F. and M. Fieser. *Advanced Organic Chemistry*. Reinhold Publishing Corp., New York, 1961.
13. Lowry, H. H. *Chemistry of Coal Utilization*. John Wiley and Sons, Inc., New York, 1945.
14. Schobert, H. H., B. C. Johnson, and M. M. Fegley. Carbonization Reactions in the Grand Forks Fixed-Bed Slagging Gasifier. *Division of Fuel Chemistry Preprints* **23** (3) 136, 1978.
15. Volk, W. *Applied Statistics for Engineers*. McGraw-Hill Book Co., New York, 1969.
16. Work cited in reference 3.
17. Olson, J. K., and H. H. Schobert. Production of C₁-C₄ Hydrocarbons in the Gasification of Some North Dakota Lignites. Pres. at the Annual Meeting, North Dakota Academy of Science, Grand Forks, ND 1978. DOE Report (In preparation, 1979).

THE DISSOLUTION OF LIGNITE IN ANHYDROUS LIQUID AMMONIA

R. L. Harris, L. H. Simons and J. J. Lagowski

Department of Chemistry, The University of Texas, Austin, TX 78712

INTRODUCTION

The rapid depletion of gaseous and liquid fossil fuels has focused attention on the problems associated with using the existent vast quantities of coal-substances for equivalent purposes, e.g. the production of energy and as a source of useful carbon compounds. Although our primary interest here is in the latter area, the ideas presented may have useful implications in certain aspects of the former.

The general strategy involves using the unusual solvent properties of liquid ammonia as a means to solubilize relatively large fractions of coal-substances at low temperatures and thereby providing (1) a method of obtaining potentially useful carbon-containing compounds directly and (2) information on the chemical nature of the original coal-substance.

The Chemical Nature of Coal-Substances

It is generally conceded that coal-substances originated primarily from plants through a series of evolutionary changes. The plant matter is transformed sequentially into humic acid, peat, lignite, subbituminous coal, bituminous coal, and anthracite. During this series of transformations, the carbon content increases while the oxygen content decreases. The precise chemical composition of coal-substances is unknown (indeed it may be unknowable in the chemical sense) because it may be derived from a variety of sources by numerous combinations of physical and/or chemical processes which lead to a nearly continuous variation of mixtures of carbon-containing (1) compounds. Nonetheless, a combination of techniques has led to the identification of broad classes of compounds present in coal-substances; viz., waxes, resins, terpenes, cellulose, protein, flavonoids, tannins, lignins, alkaloids and sterols as deduced from solvent extraction studies, (2) precursors of the heterocycle nitrogen bases, obtained by vacuum distillation of coal tar, (3) and humic acids (4). A large portion of carbon present in coal occurs in the form of saturated 6-membered condensed ring systems (naphthenes) linked together by oxygen bridges (4). Chemical analysis involving a variety of standard methods (5) has shown that coal-substances contain -OH groups (predominantly as phenolic units), carboxylic (as metal salts), ether, and carbonyl groups in varying proportions depending upon the rank of the sample; nitrogen (6) is believed to exist almost completely in cyclic structures whereas sulfur (6d, 7) appears as thioethers (-S-) or bis thioethers (-S-S-) groups. A model structure (8) for the coal-substance which summarizes the relationship among the known functional groups, consists of 6-7 aromatic ring clusters held together by saturated carbon chains (1-4 atoms long), ethers, sulfides, disulfides and biphenyl groups; the model suggests a predominantly 2-dimensional structure in the vicinity of the 6-7 aromatic rings, but the individual aromatic sections are not necessarily co-planar.

The Solvent Properties of Liquid Ammonia

Solubility in a two-component system involves a consideration of the attractive forces which exist between solute and solvent, solvent and solvent, and solute and solute; the attractive forces in the first instance favor the solubility of one substance in another, whereas the last two types of interactions oppose solubility. Because of its moderate dielectric constant, high dipole moment, ability to hydrogen bond, and relatively high basicity, liquid ammonia is a remarkably versatile solvent (9). The potential of ammonia to react with certain functional groups to produce soluble products also provides an additional advantage in the solubilization processes.

A consideration (9) of the polarity of the ammonia molecule as well as the dispersion forces generated by it suggest that ammonia should be a good solvent for covalently bound polar groups. In addition, arguments (9) based on internal pressure considerations (10) indicate that aromatic hydrocarbons and molecules containing polarizable atoms should exhibit a reasonable degree of solubility in liquid ammonia. Molecules which contain highly polar functional groups such as the carbonyl moiety (aldehydes, ketones, acid amides, and esters) that can interact strongly with the solvent dipole might be expected to interact strongly with ammonia. In addition, an enhancement of solubility would be expected in the presence of groups which can form hydrogen bonds to ammonia ($X-H \cdot \cdot NH_3$, e.g. alcohols, primary, and secondary amines) or be hydrogen-bonded by ammonia ($X \cdot \cdot \cdot HNH_2$, e.g., ethers, tertiary amines, oxygen functions, and nitrogen heterocycles). Lastly, molecules possessing acidic hydrogen atoms such as carboxylic acids or phenolic groups react with liquid ammonia to form ammonium salts which should be soluble in liquid ammonia.

The solubility principles developed here are illustrated by the data summarized in Table 1; these data are selected examples of a more extensive series available (9).

It is from this point of view that we decided to investigate the possibility of dissolving substantial fractions of coal substances in liquid ammonia under mild conditions using Rockdale (Texas) lignite for our preliminary experiments.

EXPERIMENTAL

The apparatus used for extraction of Rockdale (Texas) lignite with pure liquid ammonia is shown in Figure 1. The lignite ground to 100 mesh is placed in a Whatman extraction thimble which is then sealed by a staple. Sealing the extraction thimble prevents accidental mixing of the solid, unextracted lignite with ammonia. The thimble is placed in a conventional Soxhlet extractor; a condensing Dewar placed on top of the Soxhlet extractor and an empty flask placed below. The entire apparatus is purged with anhydrous gaseous ammonia; then a dry ice slush is added to the Dewar condenser on top, allowing the ammonia to condense and drip from the Dewar condenser onto the sample in the thimble. As extraction continues, an insulating layer of ice condenses on the outside of the apparatus. After six to ten hours the extraction is complete (25% by weight) for ca. 100 mesh samples. Extraction was conducted on samples weighing up to 50 grams.

After extraction of the lignite was complete, the precipitated tar from the ammonia solution, and the brown-black ammonia solution were let stand in air until only solid residue remained. The lignite remaining in the extraction thimble (75%) we term "treated lignite", whereas that which dissolved in the ammonia we term the ammonia extract.

Proton magnetic resonance spectra on d_6 -DMSO solutions of the ammonia extract were obtained using an NT200 spectrometer.

Infrared spectra of the samples prepared as KBr pellets were obtained with both Beckman IR5A and Beckman IR9 spectrometers.

Elemental analysis was conducted at Schwarzkopf Microanalytical Laboratory, Inc.

OBSERVATION AND RESULTS

The addition of ammonia gas to the system described in Figure 1 led to warming of the lignite sample. Later, when the first drops of liquid ammonia fell on the lignite, the outside of the Soxhlet extractor became quite hot. It was at this time that spattering of the lignite sample took place in open extraction thimbles which led us to the current method of sealing the thimbles. After about 10-20 minutes, the Soxhlet extractor was cooled by the liquid ammonia to below room temperature.

An extraction was attempted at room temperature using a pressure bomb. After several days, the mixture was filtered at room temperature, yielding 26% extract and 74% solid residue (treated lignite). Whereas the solid extract obtained from extraction at -33°C was a brown powder; the solid obtained at room temperature was black and lustrous. However, when the -33°C ammonia extract was dissolved in DMSO, which was then allowed to slowly evaporate, the appearance of the resulting product was identical to the room temperature reaction.

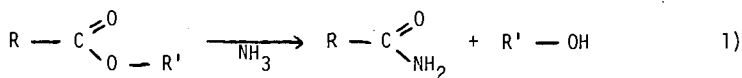
Preliminary GC-mass spectroscopic data indicated that the DMSO soluble extract contains well over 100 compounds, none of which could be resolved sufficiently for identification. Proton magnetic resonance spectroscopy revealed absorptions at 7.5, 1.2 and 0.9 τ (downfield from TMS). The ratio of the area of the 7.5 τ absorbance to the sum of the areas of the 1.2 τ and 0.9 τ absorbances, which is usually assigned as the ratio of aliphatic to aromatic protons, was ~1.3 for the ammonia-soluble fraction.

Elemental analysis (Table 2) suggests that at least some components in the lignite react with liquid ammonia, since both the extract and the treated lignite exhibit increased nitrogen content as well as increased atomic H/C ratios. The increased content of sulphur in the extract suggests preferential extraction of those portions of the lignite with a high hetero-atom content.

The solubility behavior of the treated lignite and the ammonia extract shows gross differences from the solubility behavior of the untreated lignite. The untreated lignite and treated lignite are not totally soluble in any solvent attempted, but they are both partly soluble in pyridine. The treated lignite has enhanced solubility in DMSO and dimethylformamide, which are considered good solvents for high molecular weight substances. The ammonia extract is at least partly soluble at room temperature in all solvents tested except water.

DISCUSSION

As mentioned in the introduction, one important consideration in these experiments is the solubility characteristics of functional groups in ammonia. We might expect that the lower rank coal-substances like lignite, which have a higher oxygen content, presumably in the form of functional groups that enhance solubility, would have a moderate solubility in ammonia. Another consideration is the ability of ammonia to react with certain functional groups, breaking a large unit into two smaller moieties. For example, ammonia reacts with esters (12) to create alcohols and amides (scheme 1) both of which should exhibit high ammonia solubility. If esters, or



similar compounds, are constituents of coal, ammonia will react, breaking the coal into smaller fragments. A recent study (11) on Texas lignite showed that hydrogenation of this coal-substance provides phenols, thus supporting the possibility that some of the linking groups in Rockdale (Texas) lignite are esters or ethers. Further support can be inferred from the observation that a saturated DMSO solution of the ammonia extract is more highly colored than a saturated solution of untreated lignite in DMSO. This observation implies that upon extracting with ammonia reactions took place, changing the nature of the remaining lignite as well as the ammonia extract, and creating more soluble moieties.

Yasukatsu Tamai and co-workers (12,14) treated bituminous coal with liquid ammonia; no more than 4% of the coal was actually extracted into the ammonia at 100-120°C. It is interesting to note that the coals they used had atomic hydrogen to carbon ratios of from 0.55 to 0.98. The ammonia extract always had a significantly higher atomic H/C ratio, whereas the treated coal maintained approximately the same

H/C ratio as the untreated coal. The same general trends are found for our lignite experiments (Table 3), although lignite has a much higher H/C ratio, thus perhaps explaining the greater amount extracted by ammonia. It should be noted that our method provided continuous extraction of 100 mesh particles whereas Matida, et.al. (13) extracted larger particles by 5 successive contacts of pure ammonia for one hour each. A priori, our method would be expected to extract more than this even at the lower temperature involved, but not as great a deviation as is observed. The difference must be accounted for in the chemical difference between lignite and bituminous coal.

There are similarities to our lignite-ammonia extract and the coal-ammonia extracts of Tamai and co-workers; infra-red bands at 3300, 1720 and 1660 cm^{-1} are characteristic of the ammonia extract obtained from coal. In our experiment the methanol soluble portion of the extract has broad bands at 1640 cm^{-1} with a shoulder at 1700 cm^{-1} , and 3400 cm^{-1} with a shoulder at 3200 cm^{-1} ; the C-H stretches are all below 3000 cm^{-1} . The ammonia extract itself had a strong band at 1380 cm^{-1} , a small broad band at 1460 cm^{-1} , large broad bands at 1620 cm^{-1} and 1700 cm^{-1} , large bands at 2950-2980 cm^{-1} and a large broad band at 3400 cm^{-1} .

The primary difference in the infrared spectra of the untreated lignite and of the ammonia extract was the growth of the band at 1380 cm^{-1} and a decrease in the ratio of heights of the bands at 3400 cm^{-1} to those at 2950 cm^{-1} , indicating an increase of alkyl group hydrogens to hetero-atom hydrogens in the ammonia soluble portion compared to the treated lignite portion. Of course, the treated lignite portion showed an increase in height of the band at 3400 cm^{-1} relative to the bands at 2950 cm^{-1} .

Even though the infrared results seem to indicate an increase in the aliphatic content of the ammonia extract relative to the OH and NH content, the NMR results indicate more aromatic protons than aliphatic.

CONCLUSION

It is clear that the original lignite structure can be modified and lignite separated into its component moieties by treatment with liquid ammonia. The usefulness of liquid ammonia to better identify lignite components has been demonstrated. The solubility of different coals should be further tested; the identity of the species dissolved in the ammonia should be more explicitly identified. We are currently engaged in both types of experiments.

ACKNOWLEDGEMENTS

We acknowledge the generous support of the Center for Energy Studies at The University of Texas and The University Coal Laboratory.

Table 1
Solubilities of Selected
Compounds in Liquid Ammonia

<u>Substance</u>	<u>Solubility</u>	<u>Reference</u>	<u>Atomic H/C</u>
C_6H_6	Moderately Soluble	a	1.00
$C_6H_5CH_3$	Slightly Soluble	a	1.14
$C_6H_5CH=CH_2$	Soluble	a	1.00
$C_6H_5CONH_2$	Soluble, 35%	b	1.00
$C_6H_5CH_2CO_2CH_3$	Miscible	b	1.11
$C_6H_5OCH_3$	Miscible	a	1.14
$(C_2H_5)_2O$	Miscible	a, c	2.50
$(C_4H_9)_2O$	Soluble	d	2.25
$C_6H_5NH_2$	Miscible	a	1.17
C_6H_5OH	Very soluble	a	1.00

a) E. C. Franklin and C. A. Kraus, *Am. Chem. J.*, 20, 820 (1898).

b) F. de Carli, *Gazz. Chim. Ital.*, 57, 347 (1927).

c) G. Gore, *Proc. Roy. Soc. (London)*, 20, 441 (1872).

d) F. A. White, A. B. Morrison, and E. g. E. Anderson, *J. Am. Chem. Soc.*, 46, 961 (1924).

Table 2
Solubilities of Lignite¹

<u>Solvent</u>	<u>Untreated Lignite</u>	<u>Treated Lignite</u>	<u>Ammonia Extract</u>
methyl sulphoxide	I ²	P	S
pyridine	P	P	S
acetone	I	I	P
methanol	I	I	P
water	I	I	I
chloroform	I	I	P
propylene carbonate	I	I	P
dioxane	I	I	P
acetonitrile	I	I	P
ethylenediamine	P ³	I	S
nitrobenzene	I	P	P
dimethylformamide	I	P	S

¹All solubilities except where noted at room temperature. S = totally soluble, ca. 1 mg. in ca. 1 ml; P = solvent becomes colored, but not all of the lignite dissolves; I = no discoloring of the solvent is observed.

²If the lignite is maintained in contact with DMSO at 100°C., the DMSO becomes colored. Concentrated solutions of the soluble lignite in DMSO are much less colored than concentrated solutions of the ammonia extract in DMSO.

³Lignite appears to react with ethylenediamine.

Table 3
Elemental Analysis

<u>Samples</u>	<u>C</u>	<u>H</u>	<u>N</u>	<u>S</u>	<u>Ash</u>	<u>Atomic H/C</u>
Rockdale lignite ¹						
Untreated lignite ²	51.70	4.85	1.03	1.27	12.0	1.12
Treated Lignite ²	53.37	5.18	2.71	1.72	11.8	1.16
Ammonia Extract ²	46.46	5.36	4.45	2.74	9.0	1.37
Mazachi coal ³						
Untreated coal	83.9	6.9	1.5	-	-	0.98
Treated coal ⁴	83.0	6.0	1.9	-	-	0.86
Ammonia Extract ⁵	87.2	10.1	1.4	-	-	1.38

¹Rockdale (Texas) lignite has been reported to contain up to 30% oxygen.

²Analysis by Schwarzkopf Microanalytical Laboratory.

³M. Matida, Y. Nishiyama and Y. Tamai, Fuel 1977, 56, 177.

⁴One hour in liquid ammonia at 120⁰ C.

⁵One hour contact with untreated coal.

EXTRACTION APPARATUS

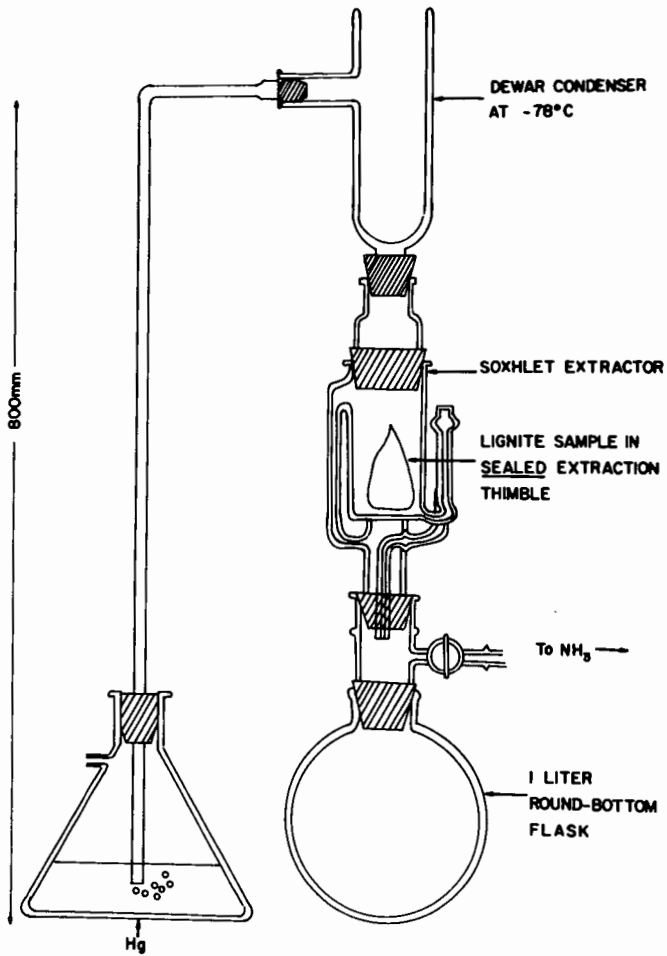


FIGURE 1. The apparatus used for extraction of Rockdale (Texas) lignite.

REFERENCES

1. For a review see D. D. Whitehurst, "Organic Chemistry of Coal," John W. Larsen, Ed., Chapter 1, American Chemical Society, 1978.
2. M. S. Kiebler in "The Chemistry of Coal Utilization," H. H. Lowrey, Ed., Vol. I, p. 677, Wiley & Sons, New York, 1945.
3. a) A. Pictet, O. Kaiser, and A. Labourchere, *Compt. Rend.*, 165, 113 (1917).
b) C. H. Fisher, *U.S. Bur. Mines Bull.*, 412, 31 (1938).
4. C. F. Brown and A. R. Collett, *Fuel*, 17, 359 (1938).
5. a) W. Fuchs and W. Strengel, *Brennstoff-Chem.*, 10, 303 (1929).
b) M. Ihnatowicz, *Prace Glow ego Inst. Gornective (Katowice)*, *Komm.*, 1952, 125.
c) L. Blom, L. Edelhausen, and D. W. van Krevelen, *Fuel*, 1957, 36.
6. a) W. Francis and R. V. Wheeler, *J. Chem. Soc.*, 127, 2236 (1925).
b) C. W. Shacklock and R. J. Drakeley, *J. Soc. Chem. Ind. (London)*, 46, 478T (1927).
c) A. E. Beet, *Fuel*, 19, 108 (1940).
d) L. Horton and R. B. Randall, *Fuel*, 26, 127 (1947).
7. a) A. Lessner and A. Nemes, *Brennstoff-Chem.*, 16, 101 (1935).
b) S. J. Gusey, *J. Appl. Chem. (USSR)*, 17, 362 (1944).
c) L. Wnekowska, 3rd. Intern Conf. on Coal Science, Valkenberg, 1959.
8. a) D. W. Krevelen, "Solvent Extraction of Coals" in *Coal-Topology, Chemistry, Physics, and Construction*, Chapter 10, Elsevier, New York, 1967.
b) G. R. Hill and L. B. Lyon, *Ind. Eng. Chem.*, 54, 36 (1962).
c) "Liquefaction and Chemical Refining of Coal," A Battelle Energy Program Report, July, 1974.
9. J. J. Lagowski, *Pure and Appl. Chem.*, 25, 429 (1971).
10. J. H. Hildebrand, *J. Chem. Ed.*, 25, 74 (1948).
11. C. V. Philip and R. G. Anthony, *Am. Chem. Soc., Div. Fuel Chem.* 1977, 22(5), 31.
12. A. Tomita, T. Tano, Y. Oikawa and Y. Tamai, *Fuel* 1979, 58, 609.
13. J. March, *Advanced Organic Chemistry: Reactions, Mechanisms, and Structure*, p. 338, McGraw-Hill, New York, 1968.
14. M. Matida, Y. Nishizama and Y. Tamai, *Fuel* 1977, 56, 177.

PEAT BENEFICIATION AND ITS EFFECTS ON DEWATERING AND GASIFICATION CHARACTERISTICS.
M.J. Kopstein: U.S. Department of Energy, Washington, D.C. 20545; M.C. Mensinger,
S.A. Weil, and D.V. Punwani: Institute of Gas Technology, Chicago, Illinois 60616.

In its natural state peat contains up to 90 weight percent water. Traditional methods of dewatering such as filtration and drying are unacceptable for large-scale peat utilization on an economic and technical basis. Wet-carbonization, a chemical pretreatment method using peat-water slurry, facilitates dewatering of peat in the effluent slurry by conventional pressure filtration. Decarboxylation and dehydratization reactions during wet-carbonization yield a beneficiated product which has higher energy value than the raw peat.

A wet-carbonization study, being performed at the Institute of Gas Technology with financial support from the Minnesota Gas Company and the U.S. Department of Energy, will determine the effects of wet-carbonization parameters (temperature, pressure, and reaction time) on the dewatering and gasification properties of the beneficiated peat. Peat from Minnesota, Maine, and North Carolina will be tested. The study will investigate the effects of reaction conditions upon the 1) energy value, 2) gasification characteristics, and 3) mechanical dewatering characteristics of wet-carbonized peat. One of the goals of the study is to identify wet-carbonization reaction conditions which permit mechanical weight. More severe conditions further enhance the energy value and dewatering characteristics of beneficiated peat, but would adversely affect the thermal efficiency of integrated peat gasification, liquefaction, and direct combustion facilities.

KINETICS AND CORRELATIONS FOR PEAT HYDROLYSIS. S.A. Weil, D.V. Punwani: Inst. of Gas Technology, Chicago 60616; M.J. Kopstein: U.S. Dept. of Energy, Washington, D.C. 20545; and A.M. Rader: Minnesota Gas Company, Minneapolis 55426.

The kinetics and correlations for rate and extent of conversion of peat to carbon oxides and light hydrocarbons during hydrolysis have been extended to cover North Carolina and Maine peats. The primary variations due to feedstock characteristics can be accounted for in terms of the ultimate yield of each product species. These limiting values can be approximately estimated from the ultimate and proximate analyses of the feedstocks.

The liquid products of hydrolysis of Minnesota peat have been analyzed. They are essentially aromatic. Higher temperatures and hydrogen pressures favor the formation of the lighter fractions (i.e., BTX) both relatively and absolutely. The heavier compounds as well as phenols and pyridines are reduced with the greater severity.

EXPERIMENTAL INVESTIGATION OF PEAT HYDROGASIFICATION. W.S. Hines, L.P. Combs, and F.D. Ranieri. Rockwell International, 8900 DeSoto Avenue, Canoga Park, California 91304.

This paper describes a series of experiments sponsored by the Department of Energy in which dried, pulverized Minnesota peat was hydrogasified in an engineering-scale (3/4 TPH) hydrogasifier system designed for pulverized coal feed. Pulverized carbonaceous solids are fed in dense phase (i.e., minimum transport gas) to the Rockwell 3/4 TPH entrained-flow hydrogasifier where they are very rapidly and thoroughly mixed with a high temperature hydrogen stream. The hot hydrogen heats and pyrolyzes the individual solid particles. Reactor operating pressure and temperature, together with reactant feed rates and residence time, are varied to achieve a desired performance, viz., overall carbon conversion and relative distribution of converted carbon among gaseous and liquid products.

Very interesting and promising hydrogasifier performance has been experienced with peat. Overall carbon conversion levels, substantially higher than previously observed with coals under comparable conditions, ranging to as high as 84.2%, were previously reported. This paper is an update of the continuing peat hydrogasification test program being conducted by Rockwell International. Overall conversion is measured with respect to reactor temperature, residence time, and pressure. Reactor conditions will be optimized to permit the most economical conversion of peat to substitute natural gas.

Detailed results of the peat hydrogasification experiments are presented and discussed. Included are comparisons with other investigators' findings.

DEVELOPMENTS IN PEAT BIOGASIFICATION. M.G. Buivid, D.L. Wise, Dynatech R/D Co., Cambridge, MA 02139, A.M. Rader, Minnesota Gas Co., Minneapolis, MN 55426, M.J. Kopstein, U.S. Dept. of Energy, Washington, DC 20545.

A four-phase development program is underway to confirm that biogasification is a technical and economical process for the conversion of peat into pipeline quality methane (SNG). The biogasification of peat is based on a two-stage process. In the first processing stage (assumed to follow hydro-mining) an oxidative pretreatment of peat breaks down the ligno-cellulosic structure to soluble, low molecular weight acids, wood sugars, and other soluble organic fragments. Unreacted peat solids are separated while the recovered liquid, containing the soluble organic material is converted to methane and carbon dioxide by conventional anaerobic fermentation in the second stage of the process. Phase I was a preliminary experimental investigation which indicated that a substantial percentage of the energy value in the solubilized peat from the first stage was fermented to methane in the second stage. Phase II was a preliminary process design and economic analysis that showed a 75 billion BTU/day peat biogasification plant to be cost competitive with other sources of natural gas. Presented are the details of the 8-month Phase I and II study. Phase III, which started October 1979, co-funded by Minnesota Gas and the U.S. Dept. of Energy, will optimize a continuous multistage bench scale biogasification process (18-month program). The objective is to provide scale-up data necessary for a process development unit (PDU) of approximately 1 ton/day (Phase IV). A significant advantage of the biogasification process appears to be that technical difficulties of dewatering necessary for peat utilization in conventional gasification or direct combustion, are eliminated.

ENHANCED REACTIVITY OF METAL-IMPREGNATED PEAT CHAR AND SEMICOKE DURING GAS PHASE HYDROGENOLYSIS

H.T. Tarki, A. Kiennemann and E. Chornet

Département de génie chimique
Faculté des Sciences appliquées
Université de Sherbrooke
Sherbrooke, Qué., Canada, J1K 2R1

INTRODUCTION

Chars and semicokes of different origins show a definite although moderate reactivity in hydrogenolysis and hydrogenation reactions. Early studies have substantiated this fact (1 - 3). This situation is in contrast with the low reactivity of ordered structures (graphite) as it has been documented by Walker et al. (4). Our attention has focused on the reactivity of peat char and semicoke and more precisely we have tried to improve the hydrogenolysis and hydrogenation of these materials by addition of metals in rather massive amounts (about 15% by weight using the ion exchange properties of humic materials). This follows our previous work on the preparation of finely dispersed metals on peat char and semicoke (5). It was felt that by a proper combination of metal characteristics, dispersion and operating conditions increased amounts of methane could be produced from our preparations even at pressures near atmospheric.

Former work on metal catalyzed hydrogen-char reactions has shown the importance of pretreatment conditions (6). Accordingly our study starts with some considerations on the peat char pretreatment followed by a study on the hydrogen-char reaction with and without addition of metals. Iron, nickel and cobalt have been considered as would-be catalysts for this reaction. The overall reactivity study was carried out using thermogravimetric methods.

EXPERIMENTAL

The impregnation and the carbonization conditions used were developed in our former study (5). By ammoniation of the peat prior to impregnation the amount of metal which can be incorporated in the peat structure is quite significant. In the present work preparations having 16.1% Ni, 14.9% Co and 17.9% Fe (weight percentage of anhydrous peat) have been achieved. After carbonization of the peat-metal preparations at 540°C specific surface areas of 365, 224 and 364 m²/g have respectively resulted. The surface area of the carbonized peat (without any metal added) is only 69 m²/g. Yields upon carbonization are of about 40%. The non-impregnated peat char contains 0.02% Fe either as pyrite or oxide.

The devolatilization and H₂ reactivity studies have been carried out in a Mettler thermobalance. 200 to 300 mg of sample were used for each run. Temperature programming was conducted between 2°C/min and 10°C/min with most runs at 4°C/min. H₂ and He flow rates were of 60 mL/min. Both gases were purified by passage through a molecular sieve and a Deoxo unit prior to introduction in the thermogravimetric cell. Atmospheric pressure was used in all the hydrogenolysis experiments. On-stream chromatography allowed intermittent sampling of the gases entering or produced during the reactions.

A typical run consisted of:

- a) Introduction of the sample in the thermobalance cell. Heating at 105°C under vacuum and in the presence of helium to eliminate all traces of moisture.

- b) Heating under helium up to the desired devolatilization temperature.
- c) Return to 20°C under helium, introduction of H₂ and programmed heating up to the desired temperature.

Our criteria for a valid experiment required less than 10% error in the overall material balances.

RESULTS

1. Heating rate effects

Weight losses during hydrogenolysis are strongly influenced by the heating rate. Thus on non-impregnated chars weight losses of 33%, 31.5%, 30.5% and 25.5% accompany heating rates of 2, 4, 6 and 15°C/min respectively for identical devolatilization conditions. On a Ni-doped char the weight losses are of 48% and 33% for 4 and 10°C/min respectively. Two levels of influence seem clear at this point: moderately low heating rates do result in higher overall reacted material as shown in Figure 1 and the presence of the metal enhances considerably the reactivity of the char.

2. Devolatilization studies prior to hydrogenolysis

Pretreatment (devolatilization) of the metal-char preparations has an important influence on further hydrogenolysis: when devolatilization under He is conducted at 750°C, 500°C, 250°C and 150°C, weight losses on further hydrogenolysis with programmed temperature up to 1200°C are 8%, 24.5%, 33.5% and 35% respectively.

During devolatilization under He of the peat chars initially prepared at 540°C only CO₂ and CO appear to be produced. Similar observations had previously been made on graphite where CO requires temperatures of 300°C to be produced (7, 8). With peat chars at temperatures as low as 105°C the presence of CO is easily detected, suggesting weak chemisorption of oxygen and low stability of surface oxides. The higher the temperature of devolatilization, the higher the amount of CO given off and thus the lower the concentration of oxygenated species on the surface. This seems to have a crucial effect on the rate of CH₄ formation upon subsequent hydrogenolysis. Figure 2 illustrates this point. Devolatilization at the lowest temperatures results in higher CH₄ yields. Moreover, the temperature of maximum CH₄ formation is also function of the devolatilization temperature which could be explained by a higher concentration of oxygenated surface species on the samples devolatilized at the lower temperatures.

3. Hydrogen reactivity of non-impregnated peat chars

Even on the samples devolatilized at high temperatures (500°C and 700°C) three major species are detected upon subsequent hydrogen-char reactions. CO₂ appears initially at temperatures around 185°C; it reaches a maximum rate of formation at about 390°C and slowly vanishes at about 500°C. Between 400°C and 500°C, CH₄ and CO begin to appear in such a way that the rise in the rate of formation of CH₄ also corresponds to a rise in the rate of formation of CO. Both species follow similar trends although quantitatively CH₄ is present in larger amounts (a factor of 3 to 4 times larger). This trend suggests that the formation of CH₄ from the reaction between peat char and hydrogen (with no O species externally added as O₂ or H₂O) proceeds via the methanation reaction between CO and H₂ using the O species still present at the surface rather than by direct reaction between the carbon atoms and hydrogen.

4. Hydrogen reactivity of peat chars impregnated with Fe, Ni and Co

The catalytic influence of transition metals has been studied following devolatilization at 150°C. Weight losses upon subsequent hydrogenolysis of the samples by temperature programming (4°C/min) up to 1200°C are as follows: uncatalyzed peat

char, 34%; Fe-peat char, 42%; Ni-peat char, 46.5%; Co-peat char, 84%. The case of cobalt is remarkable since it can be concluded that the hydrogenolysis of the organic matter in the char is nearly complete when taking into account the initial ash content of the char (8.5%).

Figure 3 shows the profiles of CH_4 formation during the hydrogenolysis. The reactivity is defined as $R_s = \text{mg}_{\text{CH}_4} \text{ formed} \times \text{g}_{\text{char}}^{-1} \times \text{min}^{-1}$ in which the g_{char} is taken at any time t during the experiment (and not at initial $t = 0$). For each of the three chars studied, the CH_4 profile shows two maxima: a low temperature peak (625°C for Co and 650°C for Ni and Fe) and a high temperature peak (1010°C for Co, 1020°C for Ni and 1050°C for Fe). In all three cases there is a marked decrease in the temperature of maximum CH_4 formation relative to the non impregnated char (750°C in this case). Furthermore the second peak is absent in the latter samples.

It is important to notice that both maxima are higher for cobalt impregnated chars than for iron or nickel preparations. Also, the effect of iron is more marked at the higher temperatures. Comparatively to observed literature results the impregnated peat chars do present some unique features as shown in Table 1.

Table 1: Temperatures of maximum rate of methane formation			
Metal	Low Temperature Peak (°C)	High Temperature Peak (°C)	Ref.
None	700*		
Fe	650*	1050*, 1020	(9)
Co	625*, 693	1010*, 950	(6), (9)
Ni	650*, 550, 535, 540, 685	1070*, 950, 683	(7), (9) (10), (11)
* - this work			

It is interesting to note that the raw peat char and the Fe preparation show a low temperature peak which has not been previously observed on graphite (9). Also the low temperature peak occurs at lower temperatures on the Co than on the Ni chars, contrary to previous observations on graphite. Metal dispersions might be responsible for this behaviour.

To emphasize the distinct behaviour of peat chars, Table 2 shows the percentage of reacted char (% conversion) as a function of selected temperatures. Appropriate literature references have also been included (9, 11).

Table 2: Percentage of reacted peat chars during hydrogenolysis at a programmed temperature of 4°C/min and 1 atm.

Metal	650°C		750°C		950°C		1050°C	
	(11)	this work	(9)	this work	(11)	this work	(9)	this work
None	0	21	0	26	2	29	8	31
Fe	0	22	0	27	3	33	9	37
CO	0	68	0.1	74	5	76	25	79
Ni	2	20	36	29	7	37	62	41

Differences between literature values used for comparison reflect distinct carbon structures (9, 11). It is important to realize that in all cases, except for Ni, peat chars, impregnated or not, show higher conversion figures at a given temperature. Although differences between the heating schedules might be partly responsible for the observed results, we favor nevertheless an explanation based on the concentration of oxygenated species in the chars. Thus, peat chars contain >10% oxygen. Whereas the carbons used as comparison range from 6.2% (9) to 1.4% (11). Moreover, a unique metal effect is observed in the sense that CO catalyzes the hydrogenolysis reaction in a very efficient way. Such catalytic action could be explained by the state of the metal on the carbon support. In fact X ray studies on the sample have shown that CO is present as a highly dispersed metal not having achieved a definite crystal structure. Ni is present as a crystalline metal whereas Fe is present both as a metal and as a mixture of oxides. Thus it is quite probable that the highly dispersed "amorphous" cobalt acts as a nucleus both for H₂ chemisorption and its subsequent dissociation and also its reaction with surface carbonyls or formed CO to produce methane.

Since the maximum rate of CH₄ formation takes place in between 625°C and 700°C a series of runs was carried out by programming the temperature (4°C/min) up to 700°C and letting the chars react at this temperature until no methane was evolved. Maximum reactivity values were very similar to those shown in Figure 3. Total conversions were: 77.5%, 31.0%, 25.0% and 24.5% for CO, Ni, Fe and raw char respectively. The significance of CO in hydrogenolysis of peat chars is thus again emphasized.

Modelling of the conversion vs time profile was attempted using the generalized model put forward by Chornet et al. (12). The parameter $\tau = t/t_{0.5}$ as defined by Mahajan et al. (13) could only be applied to the CO-char preparation since it was the only sample which resulted in $f > 0.5$. The generalized kinetic expression is: $df/dt = kf^a(1-f)^b$, where f is the conversion; t , the hydrogenolysis reaction time and k , a and b are constant characteristics of a particular reaction. For the CO-peat char sample and using the experimental run in which the temperature is held constant at 700°C a computer simulation yields the following values: $k = 1.65 \text{ min}^{-1}$, $a = 0.5$ and $b = 0.4$, with a correlation coefficient of 0.95 between the experimental values and those derived from the model. Evidence of the excellent fit for CO is presented in Figure 4. Similar profiles were also obtained for the other samples. No attempt has been done so far to interpret these profiles which

suggest some sort of autocatalytic reaction sequences.

DISCUSSION

Proposed mechanisms of direct CH_4 formation from carbon and hydrogen are numerous (1, 14, 16). The existence of two distinct reaction paths as evidenced from the two peaks observed in the present work on peat chars has also been documented on other carbon supports (1, 8, 9, 17). Its explanation is still a challenging problem. Several authors have suggested that the heterogeneity of the carbon surfaces may be responsible for the presence of two or several peaks during the hydrogenolysis: first the reaction focusses on the amorphous fractions, later on the crystalline sections (7, 9, 17, 8, 18, 11). Dissociation of hydrogen on the surface and further reaction with surface carbon atoms has been mainly proposed as the dominant mechanism (9, 19, 20). Direct reaction between weakened surface carbon atoms and gaseous hydrogen has also been considered (21).

In this study the role of oxygenated species present in the char is of paramount importance. The indications derived from our experiments can be summarized as follows: a) influence of the heating rate on CH_4 formation: a higher rate of CH_4 formation at the low heating rates is a consequence on increased surface reaction times which result in more CO reacted; b) the negative role of higher devolatilization temperatures on the rate of CH_4 formation is a result of a lower concentration of oxygenated surface species; c) the decrease in the formation of CO_2 is accompanied by an increase in CO; and d) the simultaneous presence of CH_4 and CO in the first reaction stage, tends to indicate that CH_4 formation is closely linked to the presence of CO.

A tentative reaction sequence consistent with the observed results can then be suggested as follows:

- 1- Decomposition of basic surface oxides (carbonyl or ether types) with formation of CO_2 starting at about 150°C , as suggested by Boehm and co-workers (22, 23).
- 2- Reaction between the CO_2 formed and the char to yield CO as proposed by Shaw (24). Some CO is probably also present as surface carbonyl.
- 3- Reaction between the surface CO and hydrogen as a true methanation step (25, 26). The in-situ production of steam during this reaction will allow regeneration of the oxygenated surface species via its subsequent interaction with the surface carbon atoms and eventually produce either CO_2 (27) or CO (24, 28). It is during this step that the impregnated metal plays a major role since Fe, Ni and Co are excellent catalysts for the methanation reaction when present in a peat-derived carbon matrix (28).
- 4- At high temperatures ($>>700^\circ\text{C}$) direct reaction between hydrogen and the char takes place, the metal probably facilitating the dissociation of the incoming hydrogen and its migration toward adjacent carbon atoms for further methane formation.

CONCLUSIONS

In the present study, the gas phase hydrogenolysis of peat chars prepared at about 540°C and previously impregnated with Fe, Ni and Co has been investigated. The following points summarize the main findings of this work:

devolatilization of the char is an important factor for its subsequent reactivity toward hydrogen. The lower the devolatilization temperature prior to hydrogenolysis, the higher the rate of methane formation during hydrogenolysis.

- the catalytic effect of the metals is important at two levels: higher conversions to methane and lower temperatures of maximum rate of methane formation.
- the conversion versus time profiles can be very well fitted by the following expression $df/dt = k f^a (1-f)^b$ suggesting a kinetic sequence closely related to autocatalytic steps.
- the oxygenated surface species play a major role in the methane formation, which probably takes place at the lower temperatures (625-700°C) via reaction between surface CO and chemisorbed hydrogen catalyzed by the metals. CO is the very most active of the metals at this level. At higher temperatures (>700°C), direct reaction of hydrogen with the surface carbon atoms also seems to occur.

ACKNOWLEDGMENTS

The authors express their gratitude to the Ministry of Education of Quebec, the National Research Council of Canada and the NATO fellowship program which contributed financially to the realization of this work.

REFERENCES

- 1- Blackwood, J.D. and D.J. McCarthy, *Aust. J. Chem.* **19**, 797 (1966).
- 2- Zielke, C.W. and E. Gorin, *Ind. Eng. Chem.* **47**, 820 (1955).
- 3- Gilliland, E.R. and P. Harriot, *Ind. Eng. Chem.* **46**, 2195 (1954).
- 4- Walker, P.L. jr., F. Russinko, jr. and L.G. Austin, *Adv. Catalysis* **11**, 133 (1959).
- 5- Cavalier, J.C., E. Chornet, B. Beaugard and G. Coquard, *Carbon* **16**, 21 (1978).
- 6- Tomita, A., O.P. Mahajan and P.L. Walker, jr., *Fuel* **56**, 137 (1977).
- 7- Tomita, A., N. Sato and Y. Tamai, *Carbon* **12**, 143 (1974).
- 8- Bansal, R.C., F.J. Vastola and P.L. Walker, jr., *Carbon* **8**, 443 (1970).
- 9- Tomita, A. and Y. Tamai, *J. Catal.* **27**, 293 (1972).
- 10- McKee, D.W., *Carbon* **12**, 453 (1974).
- 11- Tamai, Y., H. Watanabe and A. Tomita, *Carbon* **15**, 103 (1977).
- 12- Chornet, E., J.M. Baldasano and H.T. Tarki, *Fuel* **58**, 395 (1979).
- 13- Mahajan, O.P., R. Yarab and P.L. Walker, jr., *Fuel* **57**, 643 (1978).
- 14- Aston, B.W., V.Y. Labaton and A. Smith, *Third Conference on Industrial Carbons and Graphite*, 329 (1970).
- 15- Lewis, J.B., *Modern Aspects of Graphite Technology*, Academic Press, N.Y., pp. 168-171, (1970).
- 16- De Villelume, J., *Ann. Chem. (Paris)* **7**, 265 (1952).
- 17- Redmond, J.P. and P.L. Walker, jr., *J. Phys. Chem.* **64**, 1093 (1960).
- 18- Breisacher, P. and P.C. Marx, *J. Am. Chem. Soc.* **85**, 3518 (1963).
- 19- Rewick, R.T., P.R. Wentreck and H. Wise, *Fuel* **53**, 274 (1974).
- 20- Heintz, A. and W.E. Parker, *Carbon* **4**, 473 (1966).
- 21- Long, F.J. and K.W. Sykes, *Proc. Roy. Soc. London A* **215**, 100 (1952).
- 22- Voll, M. and H.P. Boehm, *Carbon* **9**, 481 (1970).
- 23- Boehm, H.P., E. Diehl, W. Heck and R. Sappock, *Angew. Chem.* **76**, 742 (1964).

- 24- Shaw, J.T., Fuel 56, 134 (1977).
- 25- Wender, I., Catal, Rev. Sci. Eng. 14, 97 (1976).
- 26- Ponec, V., Catal. Rev. Sci. Eng. 18, 151 (1978).
- 27- Ngongola, K. and H.A. Pulsifer, Fuel 55, 211 (1976).
- 28- Kiennemann, A. and E. Chornet, to be published and presented at 6th Canadian Symp. on Catalysis, Ottawa (1979).

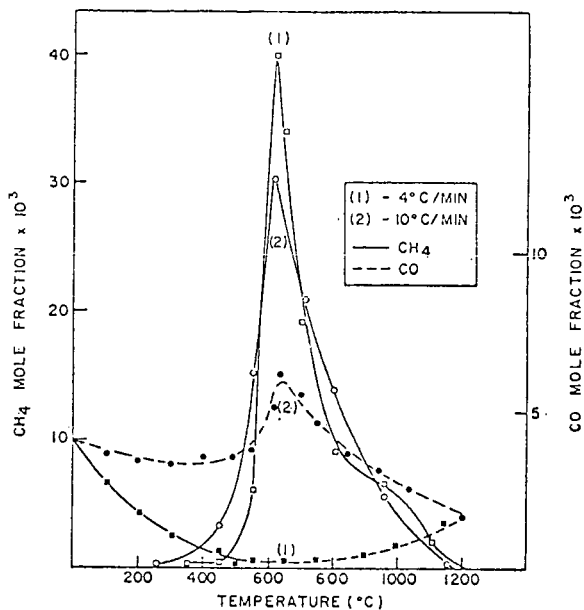


Figure 1 Heating rate effects on Ni-peat char hydrogenolysis as measured by the CH₄ mole fraction in exit gas

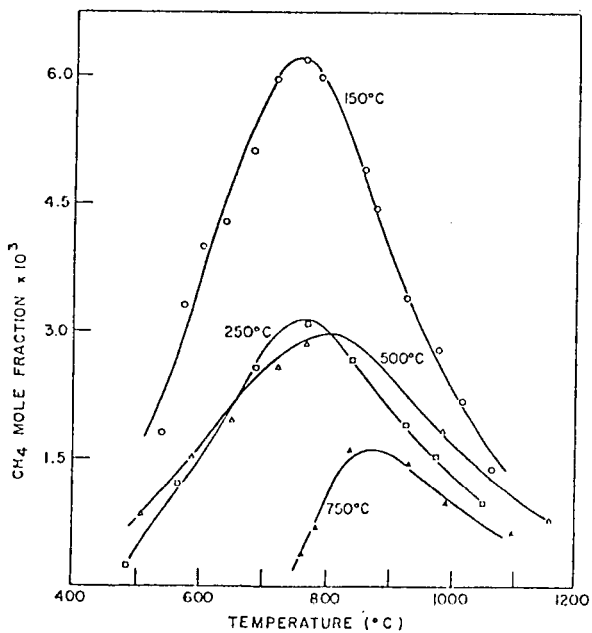


Figure 2 Methane formation during hydrogenolysis of peat char as a function of devolatilization temperature

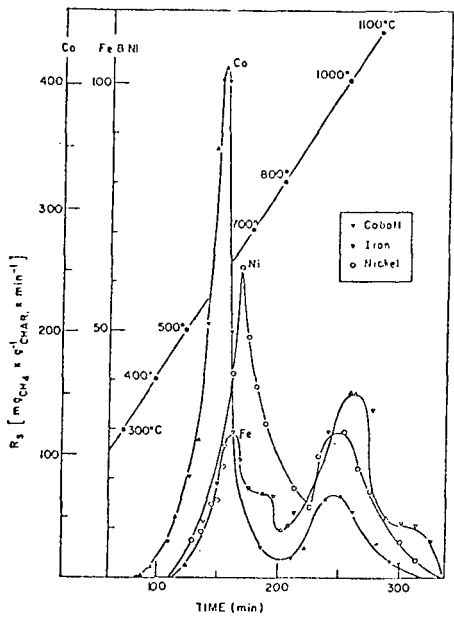


Figure 3 Hydrogen reactivity of metal impregnated peat chars as measured by CH_4 formation

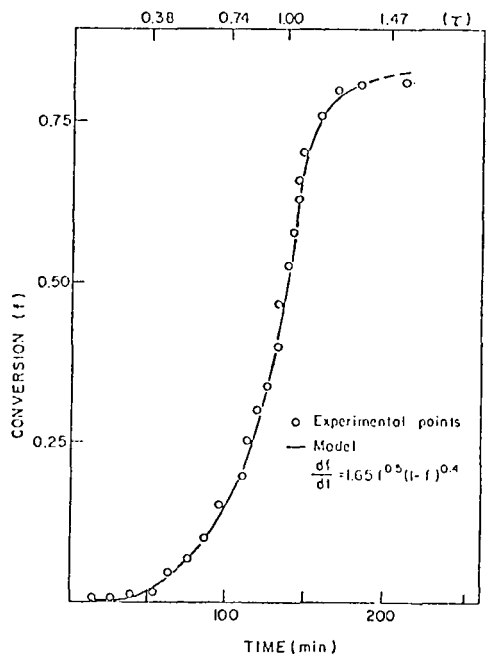


Figure 4 Conversion, f , as a function of time, t , and standardized time $\tau = t/t_{0.5}$ for the hydrogenolysis of Co-impregnated peat chars